US Army Corps of Engineers

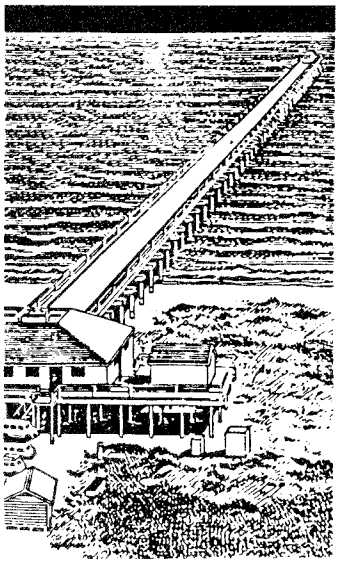

COASTAL ENGINEERING RESEARCH CENTER

MISCELLANEOUS PAPER CERC-87-18

DUCK85 PHOTOPOLE EXPERIMENT

by

Bruce A. Ebersole, Steven A. Hughes

Coastal Engineering Research Center

DEPARTMENT OF THE ARMY
Waterways Experiment Station, Corps of Engineers
PO Box 631, Vicksburg, Mississippi 39180-0631

November 1987
Final Report

Prepared for DEPARTMENT OF THE ARMY
US Army Corps of Engineers
Washington, DC 20314-1000

Under Regional Coastal Processes Numerical Modeling System
Work Unit 32240 and Wave Estimation
for Design Work Unit 31592

Steve Hughes

Unclassified

SECURITY CLASSIFICATION OF THIS PAGE

REPORT DOCUMENTATION PAGE

Form Approved
OMB No 0704-0188
Exp. Date: Jun 30, 1986

1a. REPORT SECURITY CLASSIFICATION Unclassified	1b. RESTRICTIVE MARKINGS
2a. SECURITY CLASSIFICATION AUTHORITY	3. DISTRIBUTION/AVAILABILITY OF REPORT Approved for public release; distribution unlimited.
2b. DECLASSIFICATION/DOWNGRADING SCHEDULE	
4. PERFORMING ORGANIZATION REPORT NUMBER(S) Miscellaneous Paper CERC-87-18	5. MONITORING ORGANIZATION REPORT NUMBER(S)
6a. NAME OF PERFORMING ORGANIZATION USAEWES, Coastal Engineering Research Center 6b. OFFICE SYMBOL (If applicable) WESCV	7a. NAME OF MONITORING ORGANIZATION
6c. ADDRESS (City, State, and ZIP Code) PO Box 631 Vicksburg, MS 39180-0631	7b. ADDRESS (City, State, and ZIP Code)
8a. NAME OF FUNDING/SPONSORING ORGANIZATION US Army Corps of Engineers 8b. OFFICE SYMBOL (If applicable)	9. PROCUREMENT INSTRUMENT IDENTIFICATION NUMBER
8c. ADDRESS (City, State, and ZIP Code) Washington, DC 20314-1000	10. SOURCE OF FUNDING NUMBERS PROGRAM ELEMENT NO. / PROJECT NO / TASK NO. / WORK UNIT ACCESSION NO see reverse
11. TITLE (Include Security Classification) DUCK85 Photopole Field Experiment	
12. PERSONAL AUTHOR(S) Ebersole, Bruce A.; Hughes, Steven A.	
13a. TYPE OF REPORT Final report 13b. TIME COVERED FROM Jun 1985 TO Feb 1987 14. DATE OF REPORT (Year, Month, Day) November 1987 15. PAGE COUNT 165	
16. SUPPLEMENTARY NOTATION Available from National Technical Information Service, 5285 Port Royal Road, Springfield, VA 22161.	

17. COSATI CODES		
FIELD	GROUP	SUB-GROUP

18. SUBJECT TERMS (Continue on reverse if necessary and identify by block number)

Automatic data collection systems (LC)
Duck (N.C.)
Ocean waves (LC)
Photographic interpretation (LC)
Time-series analysis (LC)

19. ABSTRACT (Continue on reverse if necessary and identify by block number)

A field study was conducted at the Coastal Engineering Research Center's Field Research Facility in Duck, North Carolina, during the fall of 1985. The photopole experiment was one component of the overall study. Synchronized 16mm movie cameras were used to film the propagation of waves past a shore-perpendicular transect of brightly painted poles. The film was developed and the photographic images were digitized to obtain the time variation of the free surface at each pole location. Time series data of free surface elevation were analyzed to compute information for characterizing the short-period incident wave field. Data collection and analysis techniques are documented as are results of the data analysis.

20. DISTRIBUTION/AVAILABILITY OF ABSTRACT ☒ UNCLASSIFIED/UNLIMITED ☐ SAME AS RPT. ☐ DTIC USERS	21. ABSTRACT SECURITY CLASSIFICATION Unclassified
22a. NAME OF RESPONSIBLE INDIVIDUAL	22b. TELEPHONE (Include Area Code) / 22c. OFFICE SYMBOL

DD FORM 1473, 84 MAR

83 APR edition may be used until exhausted.
All other editions are obsolete.

SECURITY CLASSIFICATION OF THIS PAGE

Unclassified

10. SOURCE OF FUNDING NUMBERS (Continued).

Regional Coastal Processes Numerical Modeling System Work Unit 32240 and Wave Estimation and Design Work Unit 31592.

PREFACE

The investigation described in this report was authorized as part of the Civil Works Research and Development Program by the Office, Chief of Engineers (OCE), US Army Corps of Engineers. This study was jointly conducted by the following work units: "Regional Coastal Processes Numerical Modeling System" Work Unit 32240, under the Shore Protection and Restoration Program, and "Wave Estimation for Design" Work Unit 31592, under the Coastal Flooding Program at the Coastal Engineering Research Center (CERC) of the US Army Engineer Waterways Experiment Station (WES). Messrs. John H. Lockhart, Jr., and John G. Housley were the OCE Technical Monitors. Dr. C. Linwood Vincent is CERC Program Manager.

The study, which involved planning and executing a field experiment and subsequent analysis of measured data, was conducted from 1 June 1985 through 1 February 1987 and was supervised by the authors of this report, Mr. Bruce A. Ebersole, Research Hydraulic Engineer, and Dr. Steven A. Hughes, Research Hydraulic Engineer, Coastal Processes Branch (CR-P), Research Division (CR), CERC. However, the study would not have been possible without the participation of Dr. Shintaro Hotta, Tokyo Metropolitan University. The time and expertise contributed by Dr. Hotta during the field experiment is gratefully acknowledged. Many others, too numerous to individually name, assisted during the field experiment. Their extraordinary efforts made the field experiment a success. The authors would like to particularly thank Dr. Nicholas C. Kraus, CR, CERC, for providing the impetus for initiating the study and for his advice and assistance during all study phases. We also appreciate his providing technical review of this report. The efforts of Mr. William K. Halford, who manually digitized most of the data, and others who performed this tedious task, are especially acknowledged, as are the efforts of those who participated in the preparation of this report.

The study was performed under general supervision of Dr. James R. Houston and Mr. Charles C. Calhoun, Jr., Chief and Assistant Chief, CERC, respectively; and direct supervision of Mr. H. Lee Butler, Chief, CR, Dr. Hughes, Chief, CR-P, and Dr. Edward F. Thompson, Chief, Coastal Oceanography Branch, CERC. This report was edited by Ms. Shirley A. J. Hanshaw, Information Products Division, Information Technology Laboratory, WES.

Commander and Director of WES during publication of this report was COL Dwayne G. Lee, CE. Technical Director was Dr. Robert W. Whalin.

CONTENTS

	Page
PREFACE	1
PART I: INTRODUCTION	3
Background	3
Scope	4
PART II: PHOTOGRAMMETRIC SURF ZONE OBSERVATIONS	6
Early Experiments	6
Overview of DUCK85	7
The Photopole Experiment	7
PART III: DATA COLLECTION AND PROCESSING	16
The Photopole Method	16
Description of the Photopoles	16
Description of the Camera System	19
Film Analysis	22
PART IV: DATA ANALYSIS	25
Overview	25
Data Editing	25
Spectral Analysis of Edited Data	27
Elimination of Low Frequency Oscillations	29
Analysis of the High-Passed Time Series	30
Identification of Individual Waves	31
Analysis of Individual Wave Heights and Periods	34
PART V: EXPERIMENTAL RESULTS	36
Synoptic View of Wave Transformation	36
Wave and Water Level Parameters	40
Spectral Analysis Results	50
Water Surface Elevation Distributions	52
Wave Height and Period Distributions	54
PART VI: CONCLUSIONS	59
REFERENCES	61
APPENDIX A: SELECTED WATER SURFACE ELEVATION TIME SERIES	A1
APPENDIX B: WAVE SPECTRA	B1
APPENDIX C: WATER SURFACE ELEVATION DISTRIBUTIONS	C1
APPENDIX D: WAVE HEIGHT AND PERIOD DISTRIBUTIONS	D1

DUCK85 PHOTOPOLE FIELD EXPERIMENT

PART I: INTRODUCTION

Background

1. In recent years coastal engineering has seen significant advances in the estimation of shallow-water wave properties and wave height statistics, by both theoretical considerations and empirical parameterizations. These advances have been possible because the irregularity and, in some cases, the nonlinearity of typical wave fields have been recognized; and attempts have been made to incorporate these wave characteristics into techniques which predict shallow-water wave transformation. Here, where shallow-water waves are considered, an irregular wave field is defined as one which is comprised of waves of various heights and periods and, to a lesser degree, various directions. The capability to more accurately describe the irregular wave field in shallow water has led to significant cost savings in the design, construction, and maintenance of coastal projects. Although presently available estimation techniques provide reasonable results for waves in water depths well seaward of the surf zone, our understanding of irregular wave behavior is quite limited in the regions just seaward of the surf zone, at wave breaking, and in the surf zone. In these regions waves undergo radical transformation; they become very peaked and asymmetrical and then break. Rapid generation of intense turbulence and changes in wave shape accompany the breaking process. Significant changes in wave properties in the very nearshore region can occur over a relatively short distance (a fraction of the wavelength) compared to the usual horizontal length scale associated with deeper water wave transformations (scales greater than one wavelength).

2. The quantification of irregular wave transformation in, and just outside, the surf zone remains a critical need in coastal engineering (Nath and Dean 1984). Prediction of beach evolution, changes induced by the placement of both hard and soft structures, and the effective design and construction of shore protection measures are just three of many examples of engineering problems that could be solved more accurately if more suitable methods can be found for estimating characteristics of waves in the surf zone.

3. The severe environmental conditions frequently encountered in the nearshore zone have hindered the collection of high quality field measurements of wave and water level characteristics in this area using conventional in situ instrumentation. There are also uncertainties concerning interpretation of data collected using certain conventional techniques which do not directly measure the water surface. An alternate and somewhat innovative approach to measuring surf zone water surface fluctuations is the use of synchronized movie cameras and/or video systems to film surf zone water surface fluctuations on stationary poles placed on a line perpendicular to the beach and extending out through the surf zone. The authors refer to this technique as "the photopole method."

4. During September 1985, personnel from the US Army Engineer Waterways Experiment Station's Coastal Engineering Research Center (CERC) conducted a photopole experiment as part of a larger nearshore processes field data collection project called DUCK85. The experiment was performed at the CERC Field Research Facility (FRF), located on the Outer Banks of North Carolina. Water surface variations were filmed at stationary poles placed on a line extending from the subaerial beach seaward through the surf zone. Filming was done using a system of synchronized, 16mm movie cameras actuated at a relatively rapid sampling rate.

Scope

5. The report herein presents the following results obtained from the photopole experiment: (a) analysis techniques, (b) synoptic spectra, (c) water surface elevation distributions, (d) wave height and period distributions, (e) statistical wave height and period parameters, and (f) local estimates of the mean water surface elevation. This information was computed for each pole location filmed during nine experiment runs. In Part II, previous studies involving photogrammetric surf zone observations are briefly described; an overview is given of the more comprehensive field data collection project, DUCK85; and hydrodynamic, meteorologic, and morphologic conditions which existed during the photopole experiment are discussed. Part III is a detailed description of the experimental arrangement, the camera system, and the procedure for obtaining water surface fluctuations from the photographic images. Part IV describes the procedures which were used to analyze

the water surface elevation data. Part V contains a summary of the data collected and representative results. Complete results are given in the appendices.

PART II: PHOTOGRAMMETRIC SURF ZONE OBSERVATIONS

Early Experiments

6. Many researchers have applied photogrammetric methods to measure wave properties in the surf zone. Maresca and Seibel (1976) used single and stereoscopic oblique-image analysis of film shot with 35mm cameras to monitor waves, water levels, and longshore currents in the nearshore zone. Weishar and Bryne (1978) used a 16mm movie camera to film 116 waves passing an upright plane grid placed perpendicular to the beach. The camera was used to track wave crests as they peaked and underwent breaking. Their study focused primarily on individual characteristics of breaking waves. Suhayda and Pettigrew (1977) photographed waves passing a series of poles placed in a line extending from the swash zone to beyond the break point. The 16mm movie camera followed individual waves into the nearshore zone. They measured wave crest and trough elevations from which wave heights and wave celerity could be determined. Holman and Guza (1984) used three synchronized movie cameras, which were operated at a pulse rate of one frame every 2 sec, to film the spatial (alongshore) and temporal variation in wave runup on a natural beach. The data were used to investigate infragravity wave characteristics (Holman and Bowen 1984). Carlson (1984a,b) utilized a 16mm movie camera to simultaneously record time series of the offshore incident waves and runup on the beach face. The camera was located on the beach, slightly offset from a line of reference stakes placed normal to the beach. Filming was conducted at a rate of approximately 10 frames per second; however, only every other frame was processed for analysis.

7. Perhaps the most comprehensive study of surf zone wave heights and water surface fluctuations using photographic techniques was done in Japan by Hotta and Mizuguchi (1980). They used 11 synchronized 16mm movie cameras to film synoptic water surface fluctuations on 61 poles placed on a transect through the surf zone at approximately 2-m intervals. Each camera filmed six poles. Filming runs lasted approximately 13 min, and a pulse rate of five frames per second was used. All cameras were synchronized, i.e., all cameras were actuated at the same time. Subsequent experiments served to refine the filming technique and to provide additional data (Mizuguchi 1982). Longer synoptic records, up to 5 hr in length, were obtained by using the 16mm

cameras in pairs (one camera films while the other is being reloaded). Up to eight camera pairs were used to film these longer records (Hotta, Mizuguchi, and Isobe 1981, 1982).

Overview of DUCK85

8. "During September and October 1985, a major nearshore processes experiment, DUCK85, was conducted at CERC's FRF in Duck, North Carolina. Investigators from CERC joined with several others from universities and government agencies to collect, analyze, and interpret data on waves, currents, winds, and sediment movement. The experiment was conducted in two parts to take advantage of seasonal variations in wave heights. According to Mason (1986), "experiments requiring low wave conditions were conducted between 3 and 21 September, while those focusing on storm processes took place between 15 and 25 October."

9. The major experimental objectives of DUCK85 were to

   a. Develop fundamental knowledge related to nearshore processes (wave transformation, coastal wind patterns, nearshore current generation, sediment transport, and nearshore morphological development.

   b. Collect a data set for improving numerical models of nearshore processes.

   c. Test equipment and procedures applicable to Corps projects as well as those useful in planning a second, larger, experiment during the fall of 1986 (Mason 1986).

Summaries of several DUCK85 experiments were reported in Holman (1986), Kraus (1986), Mason (1986), and Mason, Birkemeier, and Howd (1987). Preliminary results relating specifically to the photopole experiments are given by Ebersole (1987), Hughes and Borgman (1987), and Kraus and Dean (1987).

The Photopole Experiment

10. The photopole experiment, which took place in the low wave energy phase of DUCK85 during the period 2-10 September 1985, had three objectives: (a) to collect high quality water level and wave height data in, and just outside, the surf zone; (b) to collect wave data in support of the sediment trap experiments (see Kraus and Dean 1987); and (c) to determine ways to improve the photopole technique, including methods to facilitate fully automatic film

analysis. All three were successfully accomplished as described herein.

11. Equipment unloading from a truck, erection of a camera platform (scaffold), and placement of the photopole line occupied the period of 2 and 3 September. The pole array was comprised of 14 poles spaced approximately 5.9 m apart. Camera tripods were permanently affixed to the scaffold, but the camera system was installed and removed each day. The camera system consisted of six 16mm movie cameras and a battery-powered pulse generator. Data collection for the photopole experiment began on 4 September and continued through 9 September. Removal of the photopoles and packing of all equipment was completed on 10 September. A description of the data collected during runs 1-9 is given in Part V of this report.

12. Table 1 summarizes the experiments which were conducted. The following information is given for each experiment run: (a) the date, (b) starting time, (c) number of frames of film shot during the run, and (d) the pole locations for which data are available. All starting times are given relative to eastern daylight time (EDT).

Table 1

Summary of Runs Conducted During the Photopole Experiment

Run No.	Date	Start Time, EDT	No. Frames	Poles
1	09/04	1400	3,804	3, 5-6, 8-13
2	09/04	1510	3,807	3-13
3	09/05	0955	3,888	3-9, 11-14
4	09/05	1055	3,814	3-12
5	09/05	1352	3,737	3-14
6	09/05	1525	3,810	3-14
7	09/06	0915	3,807	3-5, 7-12
8	09/06	1015	3,904	3-14
9	09/06	1300	3,902	3-14
10*	09/06	1400	3,804	3-14
11*	09/07	1000	3,904	3-14
12*	09/07	1110	3,902	3-14
13*	09/09	0800	3,904	3-14
14*	09/09	1400	3,807	3-14

* Runs that have not been analyzed as of this writing.

13. Beach morphology exerts great control on wave transformation in the nearshore zone. The pole array was positioned far from the research pier to avoid effects of that structure (irregular bathymetric features) on the incident wave field. Figure 1 shows bathymetric contours in the vicinity of the FRF. The photopole line was located approximately 430 m north of the pier (at the 950-m longshore coordinate shown in Figure 1). The hatched rectangular area shown in Figure 1 is included in a region referred to as the "minigrid." The minigrid was frequently surveyed during the DUCK85 experiment. Figure 2 shows contour and three-dimensional plots of bathymetric survey data collected

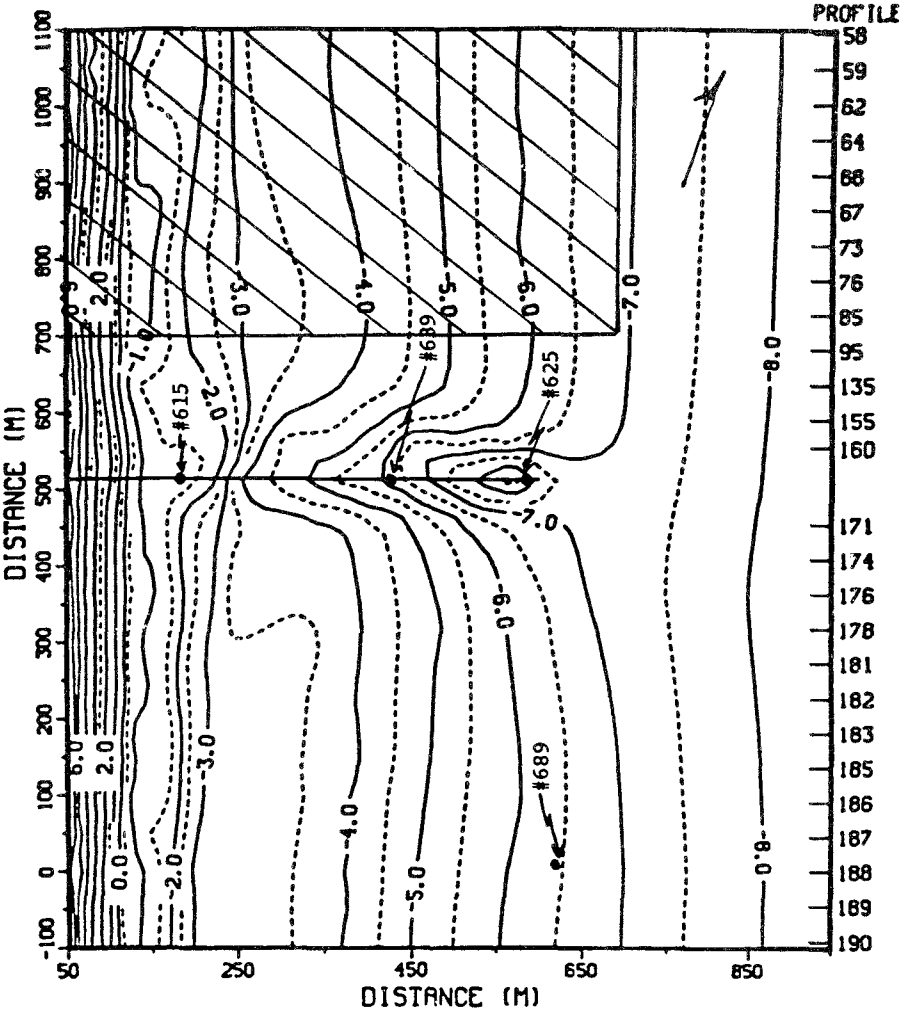

FRF BATHYMETRY 21 AUG 85
CONTOURS IN METERS

Figure 1. Bottom topography in the general vicinity of the FRF

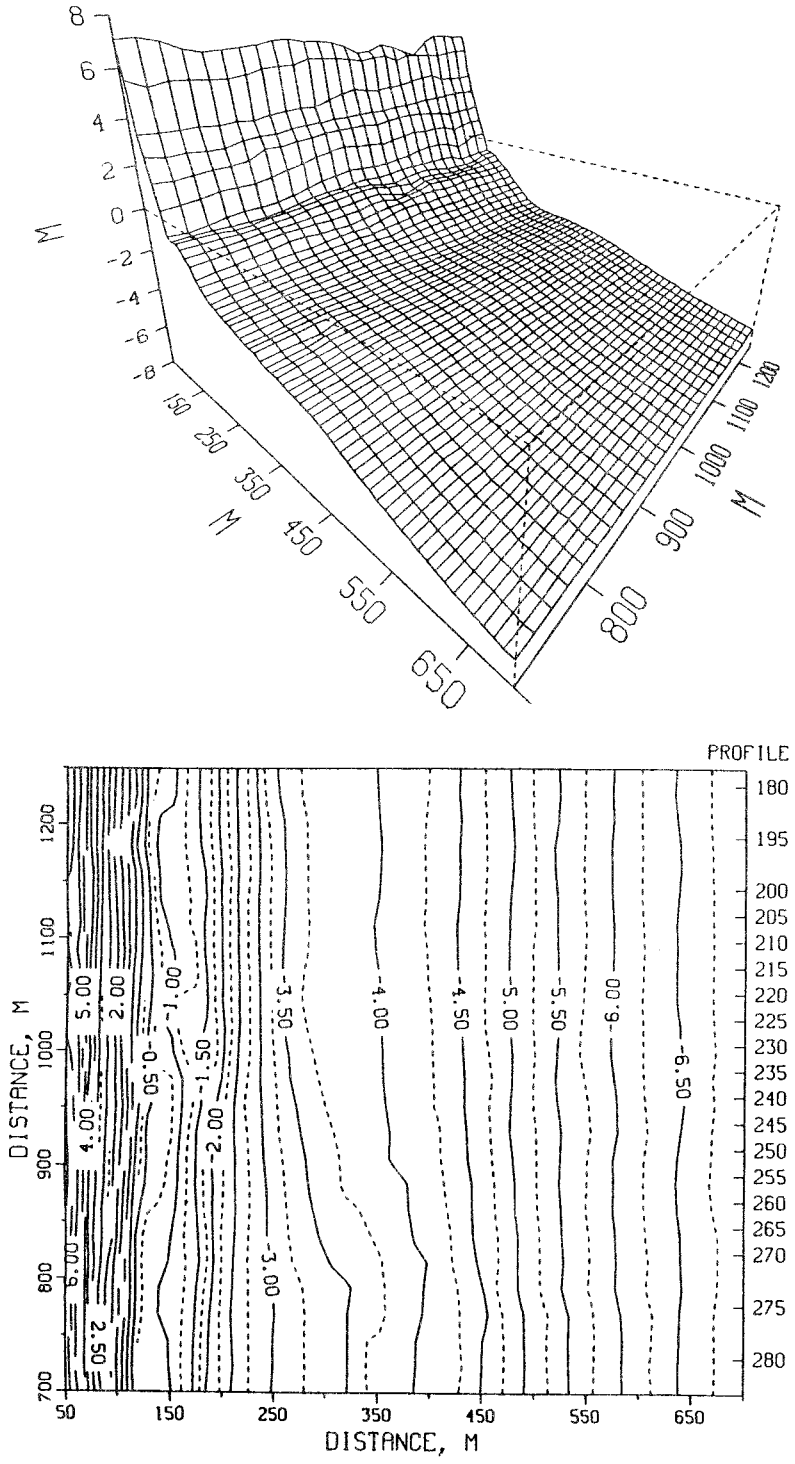

a. Minigrid bathymetry, 3 September 1985 (contours in metres)

Figure 2. Results from minigrid bathymetric surveys conducted during the photopole experiment (Continued)

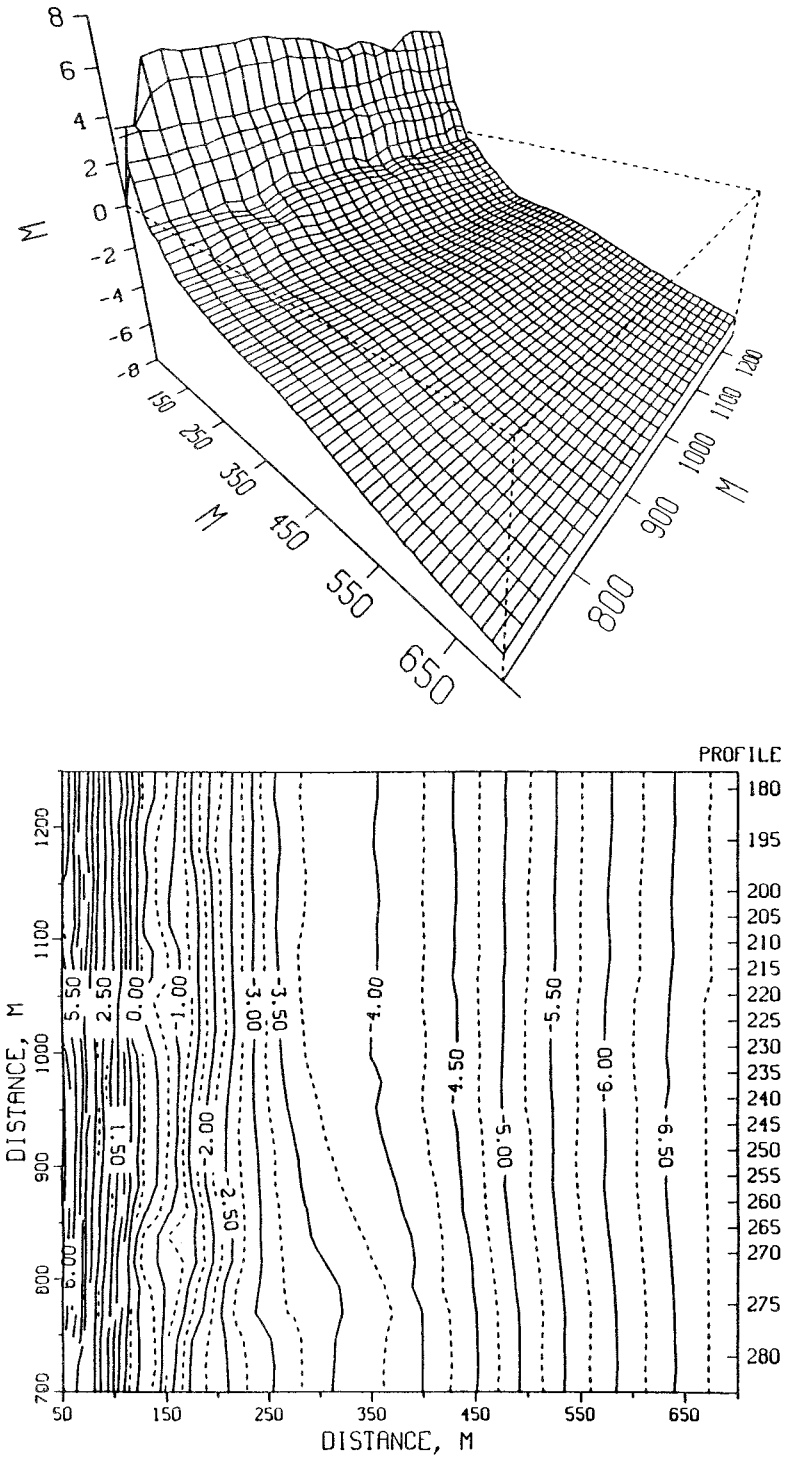

b. Minigrid bathymetry, 9 September 1985 (contours in metres)

Figure 2. (Concluded)

within the minigrid on 3 and 9 September. As seen in Figure 2, bottom contours in the general vicinity of the photopole experiment site were fairly straight and parallel throughout the duration of the experiment. Bathymetry in the immediate vicinity of the photopole line was characterized by two different slopes which met near the midpoint of the pole transect (see Figure 3). The midpoint of the transect is located near pole P07. Seaward of

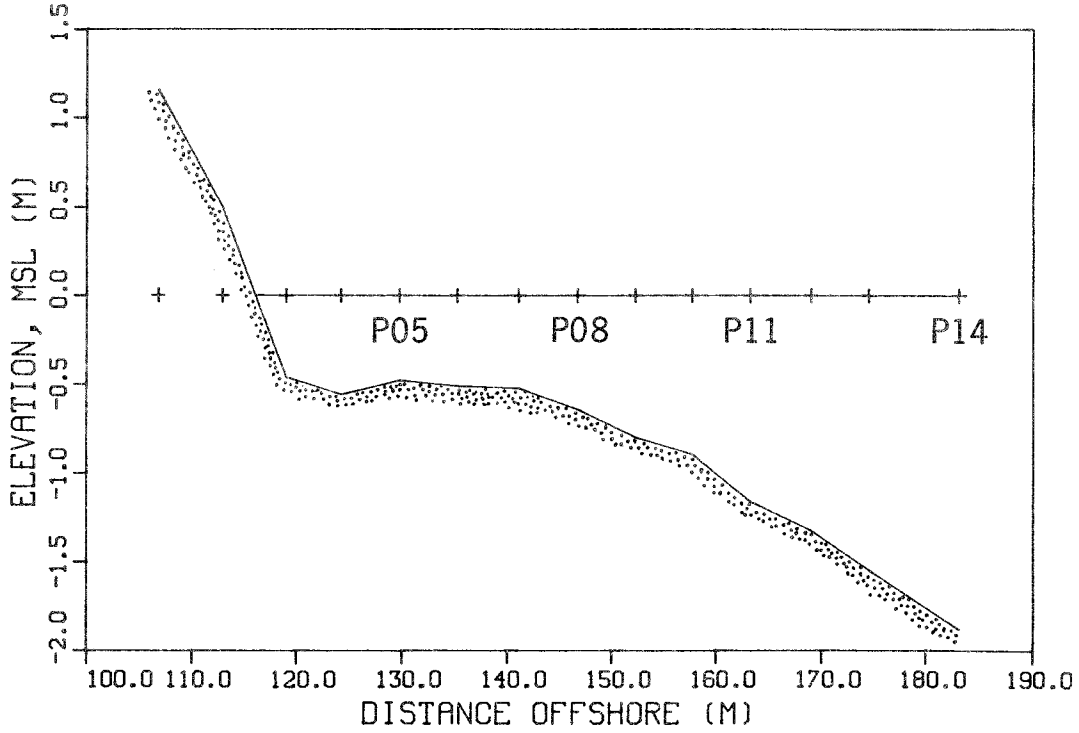

Figure 3. Seabed elevations measured along the photopole transect on 5 September 1985

this point the slope was approximately 1:30; landward of this point a terrace which was nearly flat extended to pole P03. Figure 3 shows seabed elevations along the pole transect which were measured on 5 September. In Figures 1-3, distance offshore is given in terms of the FRF coordinate system in which coordinate axes are essentially parallel and perpendicular to the local shoreline. All elevations are given relative to mean sea level (MSL), as referenced to the 1929 National Geodetic Vertical Datum (NGVD). Beach morphology in the entire study area, immediately adjacent to the pole transect and extending to the limits of the FRF survey grid, remained fairly constant during the photopole experiment. Local wave characteristics observed along the photopole transect were affected to a greater degree by the changing tide elevation and changes in incident wave conditions than by changes in bottom

bathymetry. There were no great changes in wave conditions during the experiment which significantly altered the beach shape.

14. Hydrodynamic and meteorological conditions also greatly influence the local wave climate. Figure 4 presents plots of wind speed, wind direction, and the energy-based significant wave height (H_{mo}) and peak spectral period (T_p) of the incident wave field for the period of time over which the photopole experiment was conducted. These values are also tabulated in Table 2 (time in EDT and eastern standard time (EST). The two wave parameters are computed from the energy density spectrum. Tidal elevations were obtained from a National Oceanic and Atmospheric Administration gage located at the seaward end of the research pier. The tide range during the experiment was

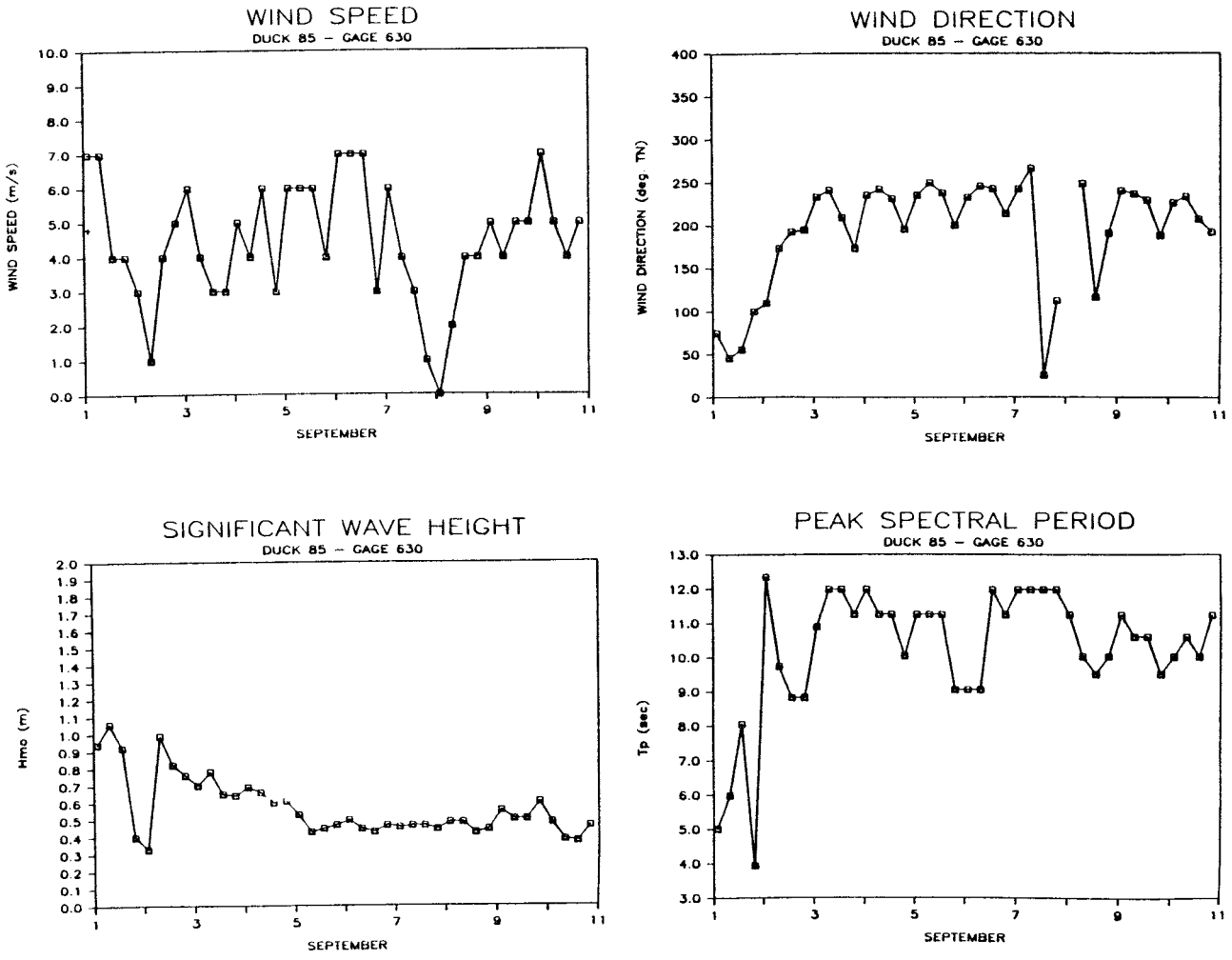

Figure 4. Wind and offshore incident wave conditions measured during the photopole experiment

approximately 1 m. The wave data shown were measured at FRF Gage 630, a Waverider buoy moored approximately 6 km from shore in approximately 18 m of water. Wave conditions experienced during the experiment consisted primarily of long-crested swell waves with energy-based significant wave heights which ranged from 0.4 to 0.7 m and peak spectral periods which ranged from 9 to 12 sec. Breaking wave heights varied between 0.8 and 2 m. Longshore currents were generally between 0.1 and 0.3 m/sec. Winds remained fairly steady, blowing almost directly offshore (250 deg relative to true north (TN)) for the majority of the experiment runs. The field team was continually subjected to brutal attacks by vicious, carnivorous flies driven from Currituck Sound by the wind. Additional environmental data can be found in the Preliminary Data Summary for September 1985 (Field Research Facility 1985).

Table 2

Summary of Wind and Incident Wave Conditions in September

Date	Time EST	Time EDT	Wind Speed m/sec	Wind Direction deg, TN	H_{mo} m	T_p sec
1	100	200	7	75	0.94	5.0
	700	800	7	46	1.06	6.0
	1300	1400	4	56	0.92	8.0
	1900	2000	4	100	0.40	4.0
2	100	200	3	110	0.33	12.3
	700	800	1	174	0.99	9.8
	1300	1400	4	193	0.82	8.8
	1900	2000	5	195	0.76	8.8
3	100	200	6	233	0.70	10.9
	700	800	4	241	0.78	12.0
	1300	1400	3	209	0.65	12.0
	1900	2000	3	173	0.64	11.3
4	100	200	5	235	0.69	12.0
	700	800	4	242	0.66	11.3
	1300	1400	6	231	0.60	11.3
	1900	2000	3	195	0.61	10.0
5	100	200	6	235	0.53	11.3
	700	800	6	250	0.43	11.3
	1300	1400	6	238	0.45	11.3
	1900	2000	4	200	0.47	9.1
6	100	200	7	233	0.50	9.1
	700	800	7	246	0.45	9.1
	1300	1400	7	243	0.43	12.0
	1900	2000	3	214	0.47	11.3
7	100	200	6	243	0.46	12.0
	700	800	4	267	0.47	12.0
	1300	1400	3	26	0.47	12.0
	1900	2000	1	113	0.45	12.0
8	100	200	0	--	0.49	11.3
	700	800	2	249	0.49	10.0
	1300	1400	4	117	0.43	9.5
	1900	2000	4	192	0.45	10.0
9	100	200	5	241	0.56	11.3
	700	800	4	237	0.51	10.6
	1300	1400	5	230	0.51	10.6
	1900	2000	5	189	0.61	9.5
10	100	200	7	227	0.49	10.0
	700	800	5	234	0.39	10.6
	1300	1400	4	208	0.38	10.0
	1900	2000	5	193	0.47	11.3

PART III: DATA COLLECTION AND PROCESSING

The Photopole Method

15. Fourteen stationary photopoles were placed on a shore-perpendicular transect across the surf zone. Water surface fluctuations at the poles were filmed using six synchronized 16mm movie cameras. Collection of water surface data using the photopole method has several advantages:

a. Equipment installation is reasonably easy.

b. No valuable equipment is placed in the water.

c. It is possible to synoptically measure waves at many locations in the surf zone.

d. It is relatively inexpensive to collect the raw data.

e. Absolute water surface variations in the surf zone are directly and accurately measured.

f. A permanent visual record is created for later referral and analysis.

The photopole method has the following disadvantages:

a. Operation of the camera system requires a fairly high level of photographic expertise.

b. Success of the experiments is not fully determined until the film is developed and viewed.

c. The digitization of water surface elevations from the photographic images is labor intensive and time consuming if done manually.

d. Filming must be done in daylight.

e. Ideally, filming should be done in such a way that the line of sight is parallel to wave crests. Unless filming is done from a pier, this optimal arrangement is difficult to achieve. If filming is done from the beach, the camera system must be placed at a high elevation and offset from the photopole line.

Description of the Photopoles

16. The majority of photopoles used in this experiment were constructed of 2-in. (50-mm) outside diameter galvanized steel pipe with a wall thickness of 0.25 in. (6 mm). Several smaller photopoles with an outside diameter of 1 in. (25 mm) and a wall thickness of 0.125 in. (3 mm) were used close to the beach and in the swash zone. To accommodate varying water depths, the larger diameter poles were fabricated in lengths of 10, 15, and 18 ft (3.2, 4.6, and

5.5 m). The smaller photopoles had lengths of 5 or 10 ft (1.5 or 3.2 m). Some of the larger diameter photopoles, in place in the surf zone, are shown in Figure 5.

Figure 5. Photograph of the photopoles

17. Horizontal rods were welded onto the upper section of each photopole (see Figure 5). Each rod was 9 in. (23 cm) long and was made of 0.75-in. (19-mm) -thick cold rolled steel. The rods were spaced 1 m apart on the larger diameter poles and 0.305 m apart on the smaller diameter poles. The rods provide in situ calibration of water surface fluctuations measured along the axis of each pole, assuming the pole is aligned in the vertical direction. However, slight departure of the pole from the vertical does not introduce significant error since the error is proportional to the cosine of the angle between the pole axis and true vertical. Angular deviations from true vertical resulting from the pole installation procedure were found to be quite small. The rods also provided an accessible location on the pole for defining an absolute vertical reference elevation. This vertical control is necessary for relating relative water surface fluctuations, observed at the pole, to a known elevation (datum). The poles were painted bright yellow to provide a sharp contrast between the pole and the water. Shortcomings of this color selection will be discussed below.

18. The photopoles were installed by air-jetting them into the bottom

using a shore-based 100-ft^3/sec (2.83-m^3/sec) air compressor. Each pole was carried out to its approximate position in the surf zone, visually aligned by an observer on shore, and then jetted into the bottom. Poles were spaced at approximately 5.9-m intervals. Pole installation in the vicinity of the breaker zone was difficult because of breaking waves with heights often reaching 2 m. Consequently, the seawardmost pole was installed in a depth of 1.9 m with the aid of the Coastal Research Amphibious Buggy as a working platform. Air-jetting of the photopoles worked well; the average bottom penetration of the poles was about 1.7 m. All poles remained in place for the duration of the experiment, and they could be rotated by hand so that the calibration rods faced the camera system.

19. The top, landward-facing calibration rod of each photopole was surveyed twice during the experiment using a total station transit situated on the roof of the FRF headquarters building, located approximately 430 m south of the photopole line. The transit provided a capability for establishing horizontal positioning as well as vertical control relative to the FRF coordinate system and the MSL datum. The coordinates of each photopole, relative to the FRF baselines, are given in Table 3. Elevations of the top calibration rods and the adjacent seabed elevations are given in Table 4; they are relative to the MSL datum. Differences between calibration rod elevation

Table 3

Horizontal Coordinates of the Photopoles

Pole No.	Offshore Coordinate Distance, m	Longshore Coordinate Distance, m
1	106.78	952.21
2	112.89	951.86
3	119.03	951.60
4	124.17	951.55
5	129.69	951.27
6	135.20	951.00
7	141.14	950.77
8	146.71	950.43
9	152.26	950.09
10	157.73	950.21
11	163.22	949.59
12	169.05	949.59
13	174.82	949.15
14	183.11	949.41

Table 4

Calibration Rod and Seabed Elevations

Pole No.	Calibration Rod Elevations, ft				Seabed Elevations, ft			
	4 Sep 85 1100 EDT	6 Sep 85 1120 EDT	Avg. ft	Avg. m	4 Sep 85 1100 EDT	5 Sep 85 1630 EDT	6 Sep 85 1120 EDT	7 Sep 85 0930 EDT
1	6.42	6.37	6.40	1.95	1.12	1.16	1.16	--
2	4.74	4.70	4.72	1.44	0.49	0.50	0.45	0.49
3	5.06	5.10	5.08	1.55	-0.41	-0.46	-0.49	-0.46
4	4.63	4.57	4.60	1.40	-0.67	-0.56	-0.47	-0.29
5	6.83	6.78	6.81	2.08	-0.53	-0.48	-0.45	-0.29
6	7.65	7.57	7.81	2.38	-0.61	-0.51	-0.52	-0.35
7	6.85	6.71	6.78	2.07	-0.70	-0.52	-0.55	-0.48
8	5.54	5.51	5.53	1.69	-0.70	-0.64	-0.66	-0.56
9	5.89	5.88	5.89	1.80	-0.83	-0.80	-0.80	-0.77
10	8.10	8.01	8.06	2.46	-0.95	-0.89	-0.98	-0.93
11	7.64	7.56	7.60	2.32	-1.17	-1.16	-1.18	-1.18
12	6.70	6.56	6.63	2.02	-1.33	-1.32	-1.40	-1.39
13	6.77	6.67	6.72	2.05	-1.44	-1.55	-1.63	-1.62
14	--	7.69	--	2.34	--	-1.88	-1.91	-1.85

measurements are attributed to the difficultly of holding the surveying prism on the calibration rod in breaking wave conditions and to possible settling of the poles which may have occurred. The average elevation is taken as the photopole reference elevation. Seabed elevations at each pole were surveyed once a day during the period of September 4-7.

Description of the Camera System

20. Filming of the water surface variations at the photopoles was conducted by Dr. Shintaro Hotta of Tokyo Metropolitan University, Japan. He provided a system of six synchronized movie cameras that had been developed and operated in Japan (Hotta and Mizuguchi 1980; Hotta, Mizuguchi, and Isobe 1982). The cameras (16mm Bolex H16 cine cameras) are controlled by a single, battery-powered, programmable control unit. This unit ensures that the cameras are fired, or pulsed, at exactly the same time. The pulse rate is variable and is selected by the camera system operator. Filming was done with a pulse rate of five frames per second (one frame every 0.2 sec) by specially modified drive motors. Since the entire camera system is battery powered, it is free of external power constraints.

21. The camera system (Figure 6) was situated on a scaffold (Figure 7) erected on the beach berm approximately 125 m south of the photopole line and

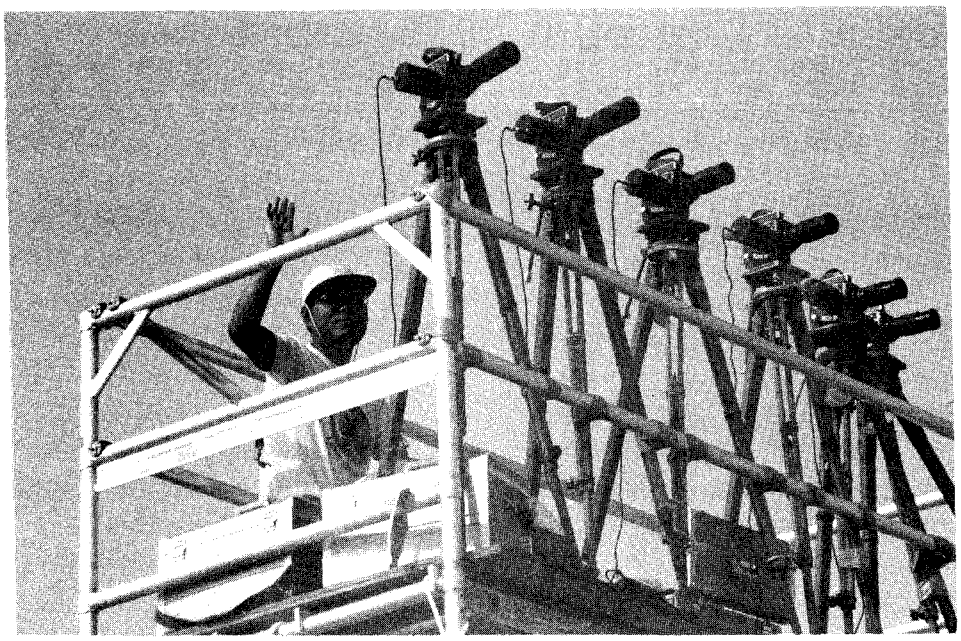

Figure 6. Photograph of the cameras and the photopole shogun

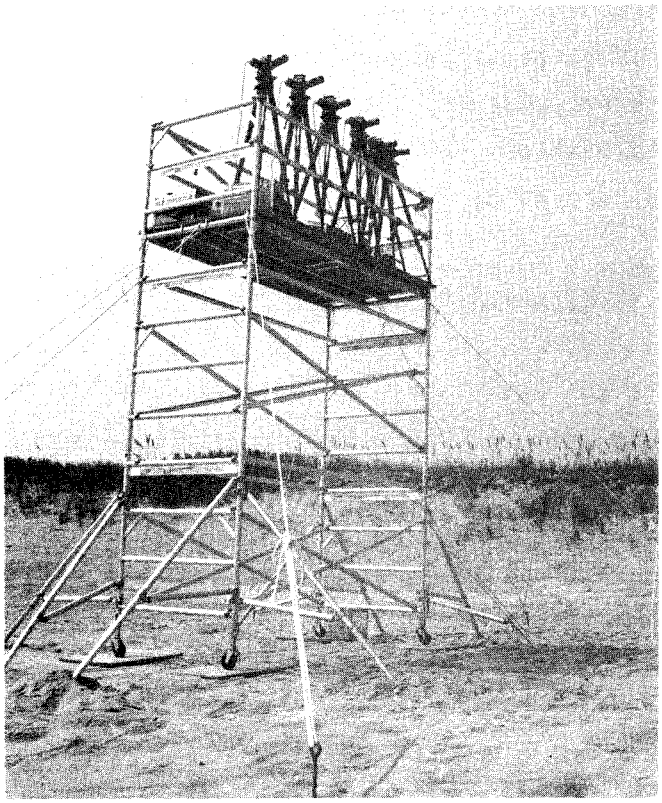

Figure 7. Photograph showing the scaffold and camera system on the beach berm

just landward of the high-water line. The approximate location of the camera system relative to the photopole line and to the sediment trap experiment line is shown in Figure 8. The height of the cameras was estimated to be 6 m above the MSL datum.

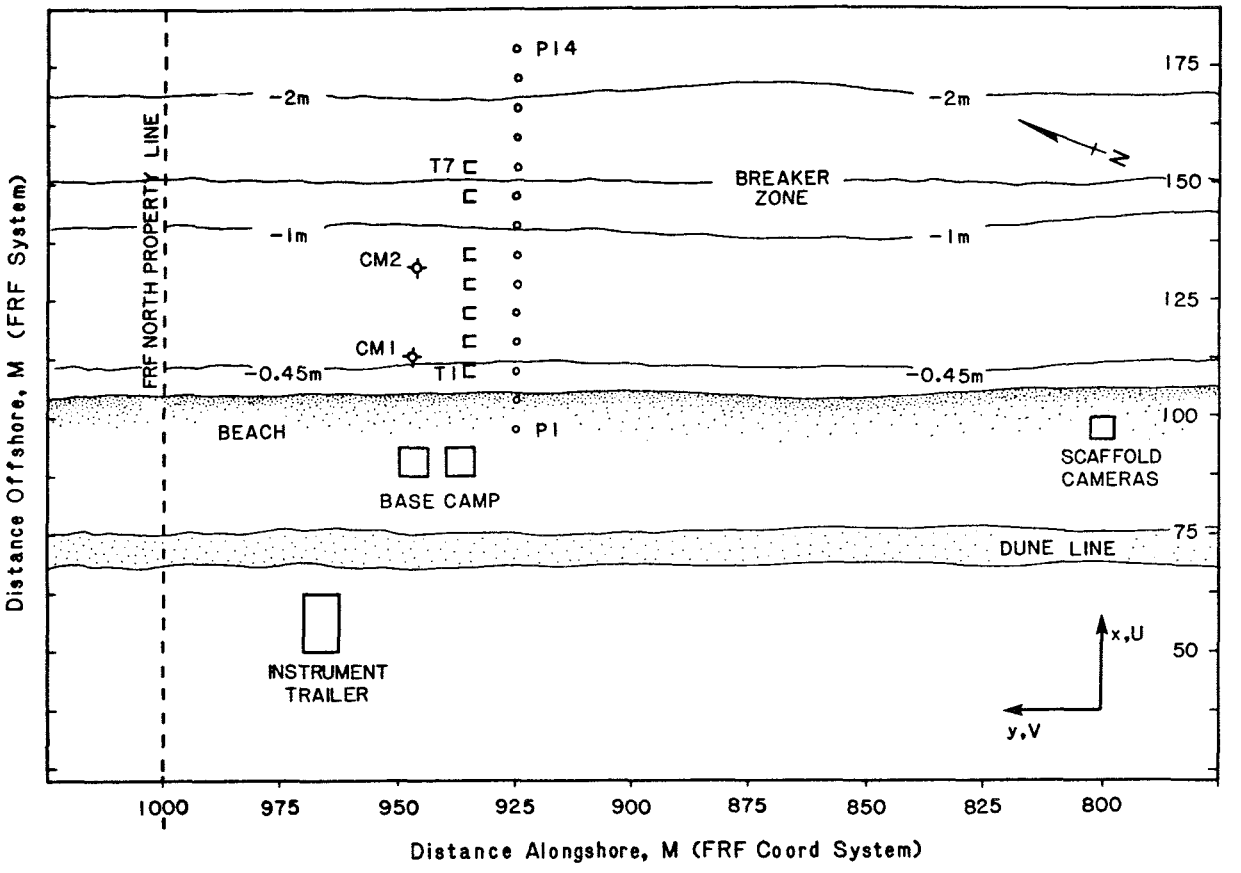

Figure 8. Map showing relative positions of the camera system and photopole transect

22. Each camera was aimed to focus on two adjacent photopoles. This configuration allowed twelve photopoles to be filmed. Poles P01 and P02 were always on the dry beach or in the runup zone and were never filmed. Each camera was fitted with an appropriate zoom lens to enlarge the pair of poles so that they filled the viewing frame, thereby maximizing the image of the water surface/photopole interface. The cameras used 100-ft (30-m) rolls of film, each roll containing approximately 4,000 frames. The film used was 160 ASA color video news film, and all runs were shot using an exposure time of 1/30 sec. Neutral density filters were used, as necessary, to obtain proper aperture settings in bright conditions. Filming runs typically lasted about 12 min, 40 sec (3,800 frames at 5 frames per second). The duration of a

filming run was completely determined by the film length and sampling rate. The sampling rate adopted for the experiment reflects that needed to accurately identify the maximum crest elevation in very asymmetrical waves and was selected based upon the experience of Dr. Hotta.

Film Analysis

23. A fully automated film analysis procedure was originally intended to be used to analyze the 16mm film images. A 16mm film digitizer was programmed for this task, but the computer program was unable to discern the water surface/pole intersection in the presence of white water because the light intensity level of the bright yellow pole and the white water were approximately the same. Since the great majority of the film contained breaking waves, extensive use of the automatic method was not possible. However, the automatic procedure was successfully applied to extract data from a limited number of films, those of a few poles seaward of the breaker zone where the yellow color contrasted well against the blue water. It is anticipated that the use of black photopoles will allow many more films to be digitized automatically. Further discussion of the automated digitization procedure is deferred until it has been fully developed and tested.

24. After photographic development, all films were screened to verify image quality and to confirm the film labeling (identification of the poles on each roll of film done in the field and etching of this information onto the film in the laboratory). Manual analysis of the film was done in a semi-automatic mode using a Numonics 1225-1 digitizer and electronic graphics calculator interfaced to a PDP 11/24 minicomputer. At the start of a roll of film, the operator entered pertinent identification information into the computer which was then written as a file header. This information included the surveyed elevation of the top calibration rod. The film was loaded onto a Lafayette Analytic Projector, and the image was reflected off a mirror onto a horizontal table. The mirror was placed at a 45-deg angle to the horizontal projector beam so that the image was turned through a 90-deg angle. In this manner, the image projected onto the horizontal table maintained the same proportion as if projected onto a vertical wall. Next, the Numonics digitizer scale factor was set by determining the distance in digitizer units between the two horizontal calibration rods on the film image. Since the distance is

100 cm for the larger diameter poles (30.5 cm for the smaller diameter poles), a factor can be determined and entered into the digitizer so that the digitizer output is given in prototype dimensions for that specific pole filmed during that particular experiment run.

25. With the initialization procedure completed, digitization of the water surface proceeded. For each frame, the operator moved the crosshairs of the digitizer to the top calibration rod and pressed a foot switch. Computer software accepted the coordinates of that position. The operator then moved the crosshairs to the water surface position on the pole and again pressed the foot switch. The computer software determined the vertical distance in centimetres between the top calibration rod and the water surface and then subtracted this distance from the known elevation of the top calibration rod. Water surface elevations were stored as elevations in centimetres relative to the MSL datum. A second foot switch advanced the film to the next frame. (An experienced operator is capable of processing a maximum of about 1,000 frames per hour using this technique.)

26. At the completion of the water surface elevation time series for a photopole, a plot of the time series was produced and visually inspected for anomalous points. (Editing procedures are discussed in Part IV.) After editing, the time series files were compressed into a more convenient form for storage and further analysis.

27. The film analysis procedure revealed potential improvements to the photopole method as implemented during this experiment. Movement of the camera because of wind and operator movement on the scaffold made it necessary to digitize both the water surface and the top calibration rod on each frame of the film because the photopole did not maintain the same relative position from frame to frame. A steady filming platform would allow manual analysis to be performed by digitizing only the water surface since the top calibration rod would remain stationary in the frame. This would increase digitizing speeds and reduce operator fatigue.

28. The small diameter pipe used for the innermost photopoles was much more difficult to see than the large diameter poles. Consequently, use of the large diameter poles is recommended for future photopole applications.

29. The absence of wind ripples on the water surface made it difficult to distinguish the brightly painted pole from its reflection on the water surface when a wave trough was passing the pole. This occurrence slowed the

digitizing process and introduced a slight amount of scatter into the time series trace in the wave troughs. The solution to this problem, as well as the problem of automatically analyzing the film in the presence of white water, is to paint the photopoles flat black.

30. On a few occasions very steep waves would pass by the photopoles, and the crests would obscure the water surface/pole interface for several frames after passage of the crest. This problem arose because the line of sight of the camera was not aligned parallel to wave crests. The operator of the digitizer was required to estimate the position of the water surface during these frames.

31. On other occasions, plunging breakers would throw up a plume of white water, momentarily obscuring the pole. This problem also arose because the line of sight of the camera was not aligned parallel to wave crests. As before, the operator had to make an estimate of the position of the water surface. The two situations decribed above occurred only rarely and during the higher wave conditions.

PART IV: DATA ANALYSIS

Overview

32. Digitization of the photographic images results in time series of water surface elevations at each photopole location. These are the raw data. Certain editing procedures are implemented to eliminate errors in the raw data prior to their analysis. Two types of analyses are performed on the edited data: (a) time series analysis of the water surface elevation fluctuations, and (b) identification of individual waves contained within the time series and subsequent analysis of their characteristics. Some aspects of the time series analysis use the edited water surface elevation data as input; others use filtered versions of the data. In addition to analyzing the entire water surface elevation signal, individual waves within the record are identified using "zero-crossing" methods. A slightly different method for identifying individual waves is implemented here. It involves the use of band-pass filtering to remove both very low and very high frequency (relative to the peak spectral frequency) oscillations in the digitized signal. This method results in a systematic procedure for identifying only the "primary individual waves" (conceptually defined by Mizuguchi (1982)). All analyses described here represent standard types of analyses which are applied to water surface elevation time series. It is important to note that these results represent a small subset of the information which can be extracted from the data.

Data Editing

33. Water surface elevation is manually digitized from the photographic images. Several types of errors can occur during this process. Data errors resulting from digitizer operator mistakes, not those involving subjective judgment, are manifested as "spikes" (anomalies existing for one or two data points) in the elevation time series. These are manually corrected by averaging water surface elevations on either side of the spike. Manual digitization also introduces subjectivity into the definition of the water surface intersection with the photopole, particularly if one of the following situations occurs: (a) the pole is surrounded by "white water," (b) the pole's reflection on a "glassy" water surface in the wave trough makes the intersection

difficult to discern, or (c) the splash from a plunging wave obscures the pole. Subjectivity results in the introduction of artificial variability to the data in the form of point-to-point oscillations. These oscillations are removed with a simple filter; however, this filtering procedure is only applied to points which lie within plus or minus one standard deviation of the mean. Consequently, water surface elevations comprising the wave crests are not affected.

34. Figure 9 shows the effect of the point-to-point filtering on data collected in the inner surf zone. At this location, frequent occurrences of white water rendered definition of the water surface/pole intersection difficult. Point-to-point oscillations are effectively removed.

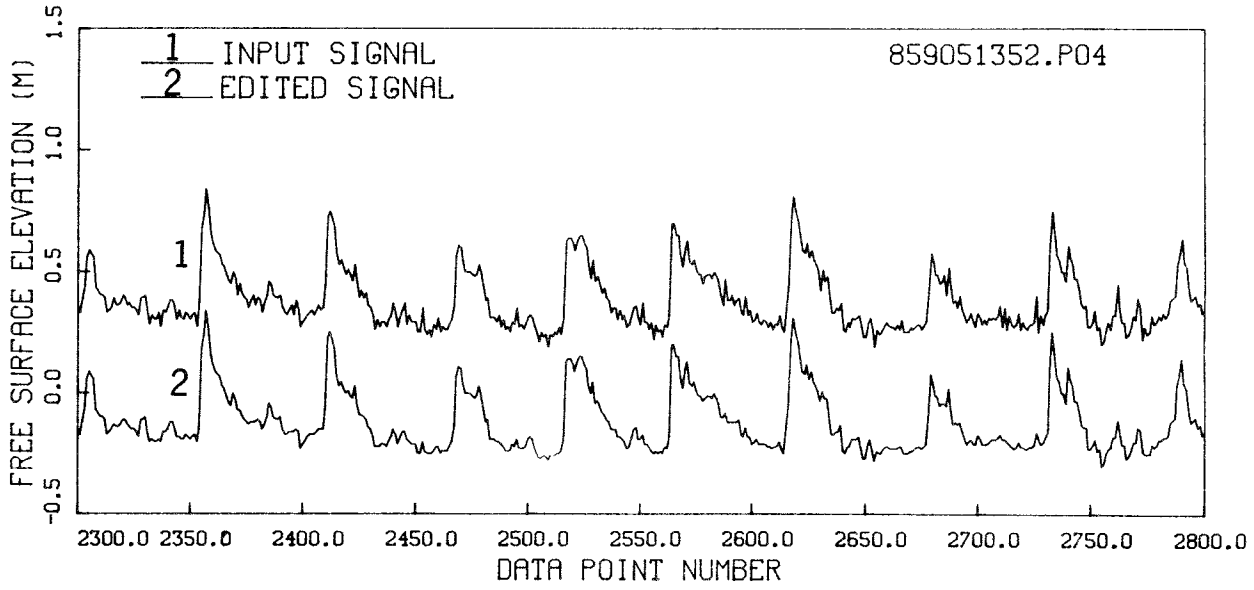

Figure 9. Effect of the point-to-point filter on data digitized from images of waves in the inner surf zone

35. Figure 10 illustrates the variability caused by difficulties in definitively locating the water surface intersection with the photopole when the water surface is "glassy" in appearance and the pole image is reflected onto the water surface. The artificial variability is demonstrated via a comparison between data digitized manually and data digitized automatically. In the automated procedure, a consistent criterion is implemented for defining the position of the water surface; therefore, less variability in the digitized signal is expected. Variability should not be confused with accuracy. A comparison between the accuracy of the manual and automatic digitizing procedures has not been made. The example shows data signals measured at the

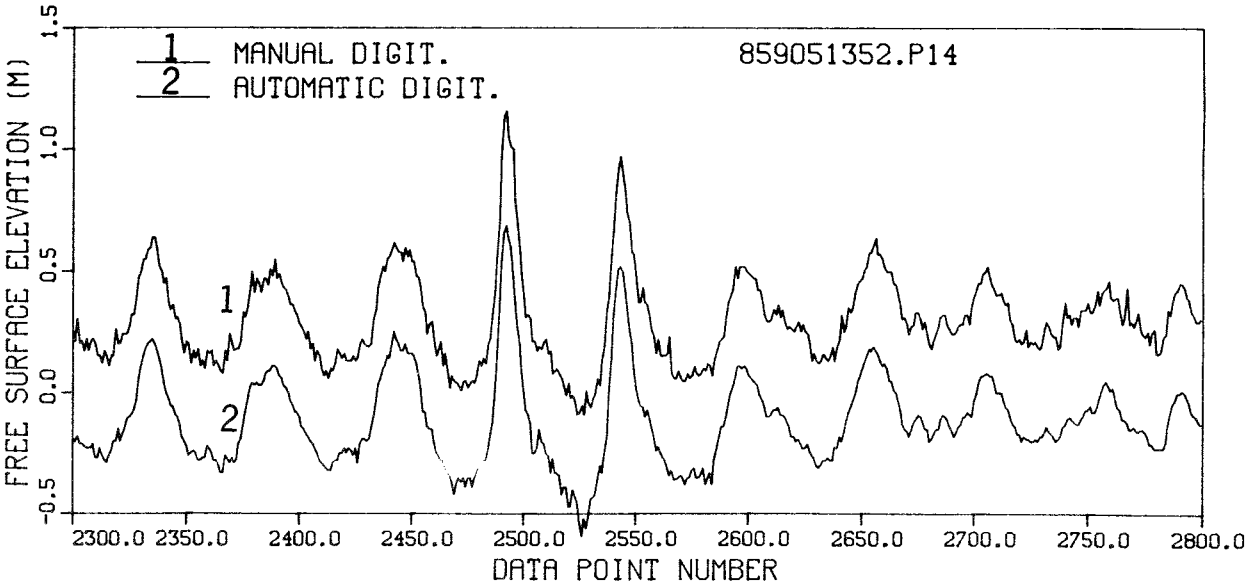

Figure 10. Comparison between manually and automatically digitized data obtained at poles outside the breaker zone

seawardmost end of the photopole transect. The reflection problem is usually encountered seaward of the breaker zone.

36. The third source of error, also introduced as a result of subjective judgment, is associated with the camera position. This error is caused by the inability of the cameras to "see" behind the crests of some of the larger waves, and it usually occurs at the breaking point where wave asymmetry is greatest. Subjective judgment in these instances results in errors in defining water surface elevations during frames which immediately follow the crest. Errors of this nature cannot be corrected with complete certainty. However, since the highest point on the wave crest is always visible, correct heights can always be obtained.

37. Suspected errors that might potentially affect calculations of wave height are manually checked and corrected. The edited water surface elevation signals comprise the data base used in both the time series and individual wave analyses.

Spectral Analysis of Edited Data

38. Spectral analysis of each edited time series is performed to investigate the energy levels associated with oscillations of various frequencies present in the data signal. Prior to analysis, any linear trend existing in

the data is removed. Removal of the linear trend effectively eliminates the water surface variation caused by the astronomical tide during the course of the filming run. Since the semidiurnal component of the tide changes from a maximum to a minimum over a 6-hr period (360 min), tidal fluctuations experienced during a 12.5-min filming run can be assumed to have a linear variation.

39. The spectral analysis routine given by Brenner (1967) is used to compute the energy density spectra. This algorithm performs the Cooley-Tukey transform and was selected because it requires only that the number of data points in the input signal be evenly divisible by 2. The number of data points need not be a power of 2, as is required in common spectral analysis procedures. Consequently, the number of data points which can be utilized is maximized. Prior to application of the Cooley-Tukey transform, the time series is cosine-tapered at each end to reduce side band leakage in computing the spectral estimates (Otnes and Enochson 1972). Raw spectral estimates are then scaled to account for the variance reduction caused by the cosine taper and band-averaged in such a way that the spectral bandwidth associated with each spectral estimate is approximately 0.01 Hz. Band-averaging results in spectral estimates which are statistically more stable than those comprising the raw spectrum. The 0.01-Hz bandwidth is a typical bandwidth selected for displaying sea state spectra.

40. An example of results obtained from a spectral analysis of data collected at the seaward end of the pole transect is shown in Figure 11.

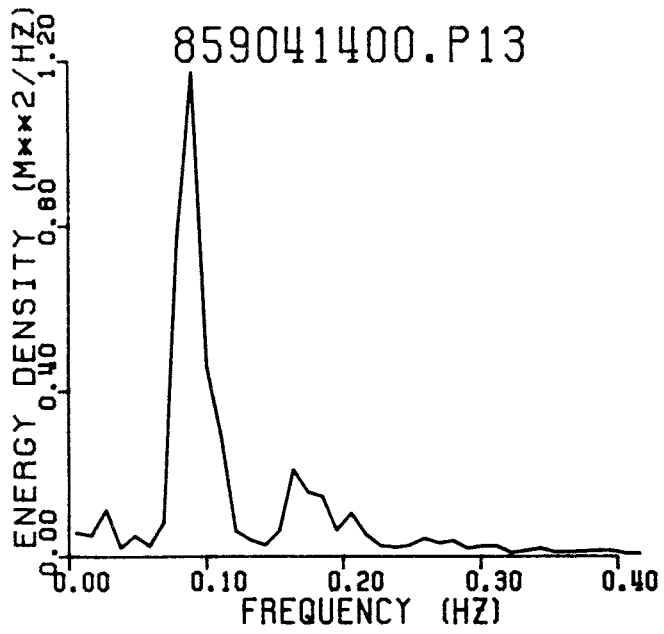

Figure 11. Sea state spectrum measured at photopole P13

Pole P13 was located outside the breaker zone during this experimental run. The example illustrates two aspects of the wave conditions which generally existed during the DUCK85 experiment. First, the wave spectrum is "narrow-banded" about the peak frequency (the frequency associated with the spectral band containing the maximum energy density) which is characteristic of swell-like wave trains where a majority of the waves have periods which fall within a very narrow range. Incident waves were characterized by long periods relative to periods most frequently encountered along the eastern coast of the United States. They were usually between 10 and 12 sec. The waves also had very long crests. A second feature visible in the spectrum is the existence of energy at much longer periods (with frequencies between 0.02 and 0.03 Hz). As evidenced by Figure 11, these long period oscillations existed not only inside the surf zone (see Appendix B) but also seaward of the breaker zone.

41. Spectral analysis of the complete water surface elevation time series does provide useful information. However, two points should be remembered. First, spectral analysis inherently treats the wave forms as a superposition of linear waves with different frequencies. Results, shown in Part V of this report, show that the measured waves in the very nearshore zone do not have linear forms. The energy density near 0.16 Hz (see Figure 11) should not be misinterpreted to represent incident waves with periods of approximately 6 sec. The interpretation of this feature is discussed in Part V. Secondly, caution should be exercised in describing the incident wave field using parameters computed from the complete spectrum. For example, if interest lies in the shorter period incident waves and significant energy exists at much longer periods, energy-based significant wave heights computed using the complete spectrum may provide misleading information in the nearshore zone. Methods for isolating the variations resulting from the long-period fluctuations and procedures for removing them from the data record are discussed below.

Elimination of Low Frequency Oscillations

42. The primary thrust of the DUCK85 photopole experiment was to measure the shorter period wave field, i.e., the surface waves which are clearly visible. The low frequency fluctuations which were mentioned above are treated as a time varying mean water surface upon which the shorter waves propagate. A low-pass filter is used to isolate them, and then they are

removed from the time series. The shape of the low-pass filter is dependent upon the cutoff frequency and the number of points sacrificed in constructing the filter; the number of points which are sacrificed determines the "sharpness" of the filter. The shape of the filter which was adopted is shown in Figure 12.

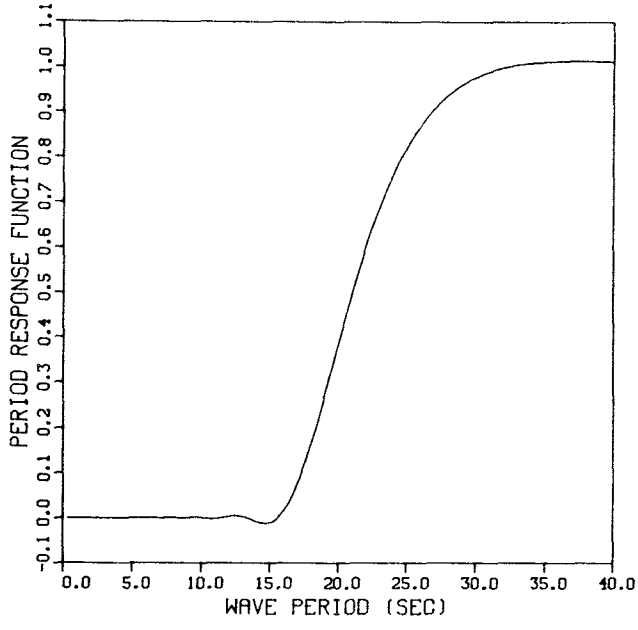

Figure 12. Period response function of the low-pass filter

The filter represents a compromise between sharpness and the minimization of the loss of data points. Two hundred points were lost from both ends of each time series by application of this filter. A cutoff period of 21 sec was chosen. This filter effectively eliminates oscillations with periods greater than 30 sec and preserves oscillations with periods less than 16 sec.

43. The effectiveness of the filter is demonstrated in Figure 13. The original, unedited data (without point-to-point oscillations removed), the low-passed signal, and the high-passed signal which remains after low frequency oscillations are removed, are shown for pole P14. The data presented were obtained during the run initiated on 5 September at 1352 EDT. The horizontal axis in the figure represents the time scale; 50 data points are equivalent to 10 sec. The high-passed signals are assumed to represent the incident short wave field.

Analysis of the High-Passed Time Series

44. The high-passed data signals contain 400 fewer points than the

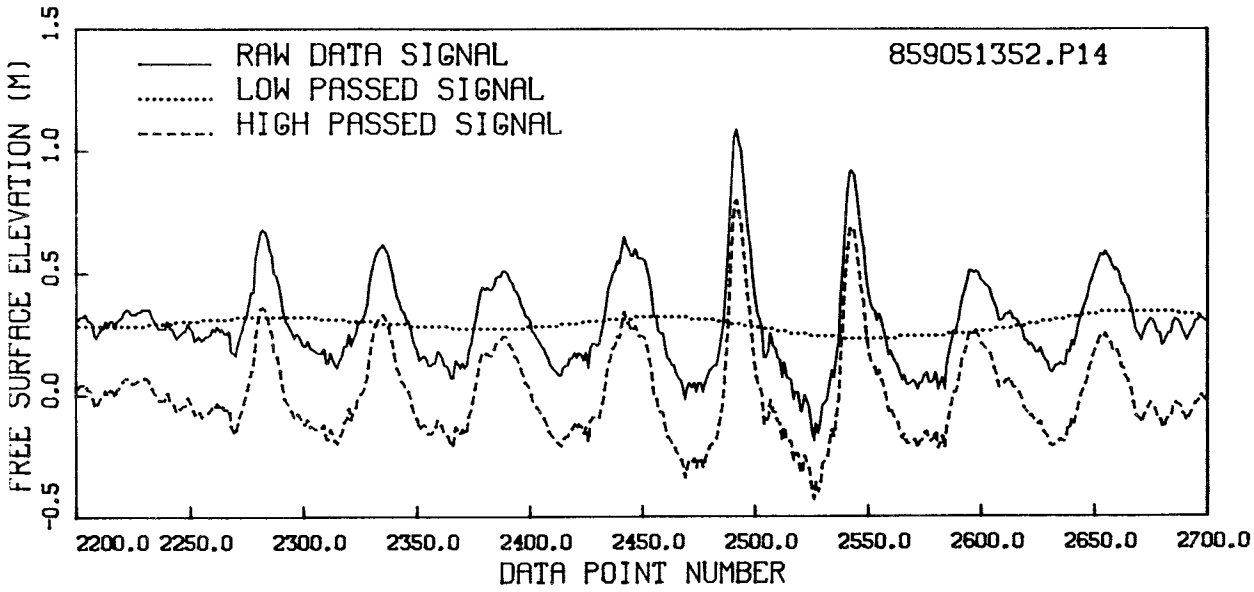

Figure 13. An example showing the effect of the low-pass filter and removal of longer period oscillations

original time series because of the low-pass filter. The high-passed data are used to identify the maximum and minimum water surface elevations. They are used also to compute the mean, variance, standard deviation, skewness, and kurtosis for the entire record. The frequency of occurrence of water surface elevations, relative to the mean and nondimensionalized by the standard deviation, are calculated and displayed in histogram form. A spectral analysis of the high-passed data record, using cosine-tapering and band-averaging identical to that discussed previously, is performed. The band-averaged spectral estimates are used to compute the energy-based significant wave height and to determine the peak spectral period of the incident wave field.

Identification of Individual Waves

45. A zero-crossing method could be directly applied to the edited, high-passed data signal to identify individual waves. However, the resulting time series frequently contains short period oscillations, typically with small amplitudes (see Figures 9 and 10). These are referred to as secondary waves. If these small waves occur near the mean water surface elevation of the data record, they cause an increase in the number of waves which are identified by the zero-crossing method. The number of these smaller waves increases in the surf zone. Only the larger, well-defined waves are of interest since their influence on nearshore processes is expected to be much greater

than that of the smaller secondary waves. Primary individual waves are conceptually defined such that the number of waves is constant across the surf zone. Hotta and Mizuguchi (1980) and Mizuguchi (1982) integrate the smaller, or secondary, waves in the preceding primary wave by adding the period of the secondary wave to the period of the primary wave. They define secondary waves as waves with crest or trough elevations within an "error band" (on the order of 3 to 5 cm) on either side of the data mean. If the error bandwidth is decreased, more secondary waves are interpreted as being primary waves. If the bandwidth is continually increased, fewer secondary waves will be identified as primary waves. The choice of the error bandwidth is selected in such a way that statistical parameters defining characteristic wave heights and periods do not significantly change with additional increases in the error bandwidth; the parameters become stable because the total number of primary waves identified becomes stable.

46. A different method for identifying individual waves is implemented in the present study; a filtering technique is used to identify them. The edited, but unfiltered, data are subjected to a band-pass filter with period cutoffs at 3 and 21 sec. The amplitude response of this filter, as a function of wave period, is shown in Figure 14.

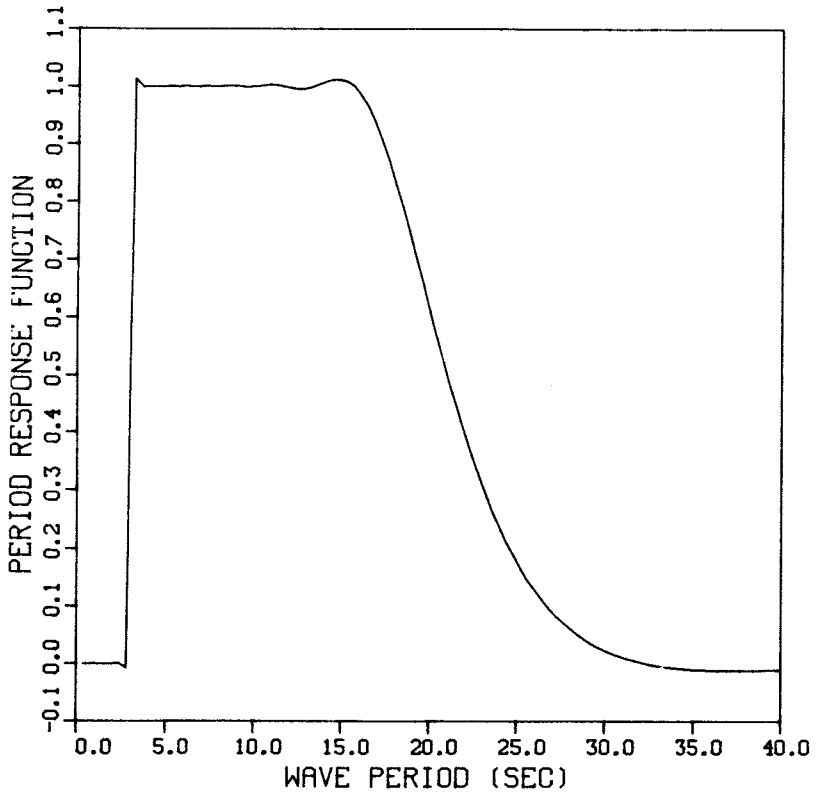

Figure 14. Period response function of the band-pass filter

47. Again, 200 data points are sacrificed from each end of the time series in order to construct the filter. At the 21-sec cutoff period, the band-pass filter has response properties similiar to the low-pass filter shown in Figure 12. At the 3-sec cutoff period, the response function is much "sharper." Filter sharpness is highly desirable and is achieved at this frequency because of the large number of points used to construct the filter relative to the 3-sec period. This filter removes both lower frequency and very high frequency oscillations; consequently, most of the secondary waves are removed.

48. The effect of the filter is demonstrated in Figure 15 for

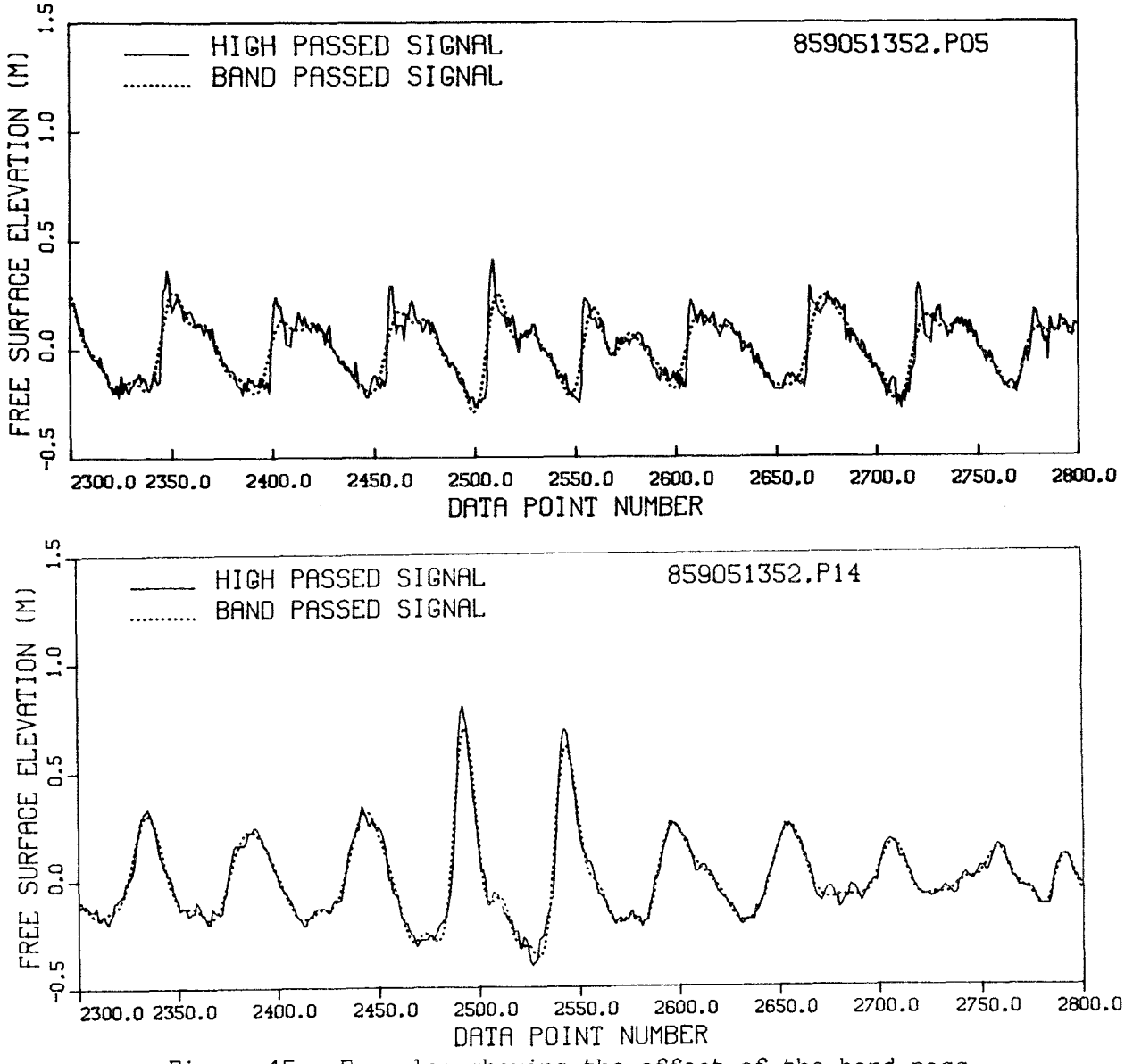

Figure 15. Examples showing the effect of the band-pass filter inside and outside the surf zone

photopoles P05 and P14. Pole P05 was located well inside the surf zone, and pole P14 was seaward of the breaker zone. The filter completely eliminates fluctuations with periods less than 3 sec. There is a smoothing effect of the filter on the forward faces of the wave crests measured at P05. The effect is less severe for the pole located outside the surf zone. Smoothing of the forward face of the wave is undesirable if a zero-upcrossing method is used to identify individual waves; however, it appears that the smoothing effect on all waves is quite similar and systematic. Therefore, consecutive wave periods are probably changed by approximately the same amount.

49. Use of the zero-downcrossing method appears to be a better choice for two reasons: (a) it is more physically appealing to include the drawdown of water in the wave trough with the subsequent wave crest rather than with the preceding crest, and (b) effects of the band-pass filter on waves in the surf zone are less severe at the rear face of the wave crest (where downcrossings occur) than on the forward face where the elevation increases rapidly and upcrossings would be identified. Results obtained using both methods are presented in this report.

50. Finally, an error band criterion similar to that described previously is applied to the band-passed data. Oscillations with crest or trough elevations less than 3 cm are integrated into the preceding primary wave, i.e., the period of the small wave is added to the period of the primary wave. This error band is equal to an estimate of the overall accuracy of the procedure for obtaining water surface elevations from the photographic image.

51. It is emphasized that only the sequence of waves and individual wave periods are defined using the band-pass filtered data. As evidenced in Figure 15, band-pass filtering reduces maximum values of the crest and trough elevations and would result in the computation of smaller wave heights. Therefore, the original, high-passed data are used to compute wave heights for each of the waves identified by application of the downcrossing method to the band-passed data.

Analysis of Individual Wave Heights and Periods

52. The following parameters are computed from the population of individual wave heights: the mean, the root-mean-squared value, the highest one-third and highest one-tenth values, and the maximum. Histograms showing

the frequency of occurrence of individual wave heights, nondimensionalized by the mean wave height, are computed. An average wave period is calculated. Frequency of occurrence estimates of individual wave periods are computed. The wave periods also are nondimensionalized by their mean value. Results are displayed in histogram form. This information is computed for wave heights and periods determined by using both the zero-up- and downcrossing methods.

PART V: EXPERIMENTAL RESULTS

Synoptic View of Wave Transformation

53. Figure 16 illustrates the transformation of a group of eight waves as they passed each photopole. It is included to show general characteristics of the waves which were observed and the transformation process which is being investigated. The indivdual plots show the temporal variation of water surface elevations measured during the experiment run initiated at 1352 EDT on 5 September. The plot showing the waves passing pole P14 reveals characteristics of the wave conditions which were observed during the entire photopole experiment. There are four waves with heights of approximately 0.5 m followed by two with heights approaching 1 m and then two more waves with heights nearly equal to 0.5 m. The incident wave field was comprised of wave groups throughout the course of the experiment. This feature is most clearly visible in the figures given in Appendix A. The plots in Appendix A show the entire time series of water surface elevation measured at the seawardmost photopole available during each experiment run. The appearance of well-defined groups diminished over the duration of the photopole experiments. The periods of each of the waves shown in Figure 16 are nearly equal to one another. This feature is indicative of swell waves.

54. There is greater asymmetry of the higher waves compared to that of smaller waves and an increasing asymmetry of all the waves as they propagate past poles P13, P12, and P11. Asymmetry, as used here, refers to the increase in peakedness of the wave crest and the broadening of the wave trough. There is also some asymmetry in the wave form about the wave crest. Elevation changes on the forward faces occur rapidly; whereas elevations defining the rear face change more gradually with time. The plots show water surface fluctuations as a function of time at one point in space; but since the waves are nearly nondispersive in these water depths and all parts of the wave travel with nearly the same speed, wave forms observed in the time domain are indicative of those which occur in the spatial domain. Increasing asymmetry clearly illustrates the effects of the nonlinear processes operating in the very nearshore zone.

55. Near pole P10 the two larger waves break; the remaining waves in the group break in the vicinity of poles P07 and P08. After breaking, the

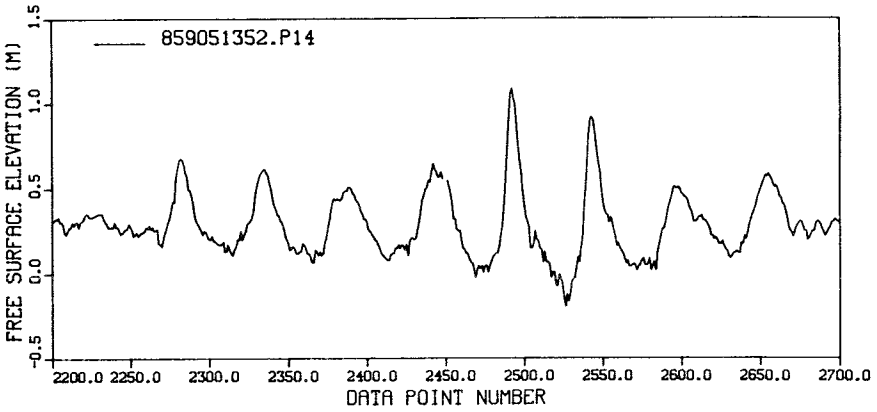

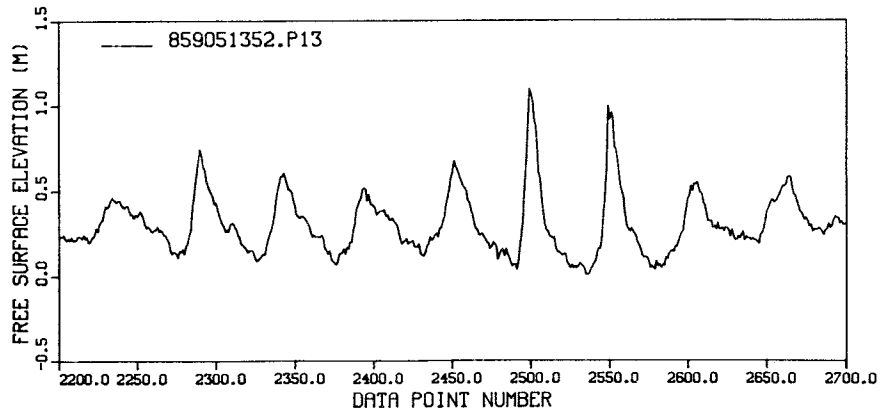

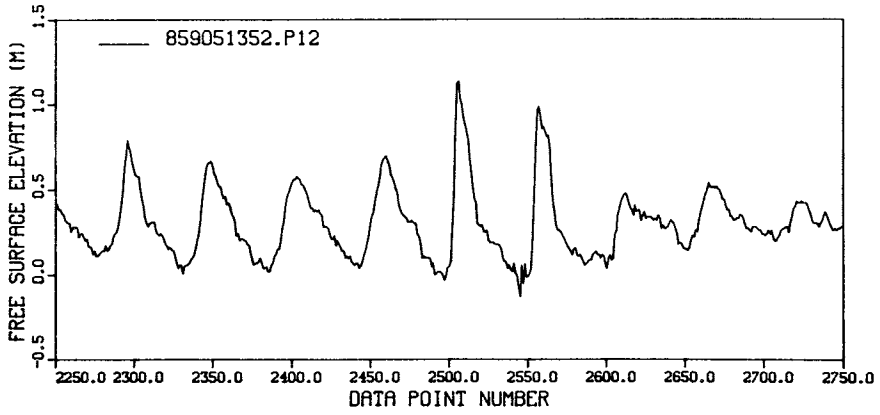

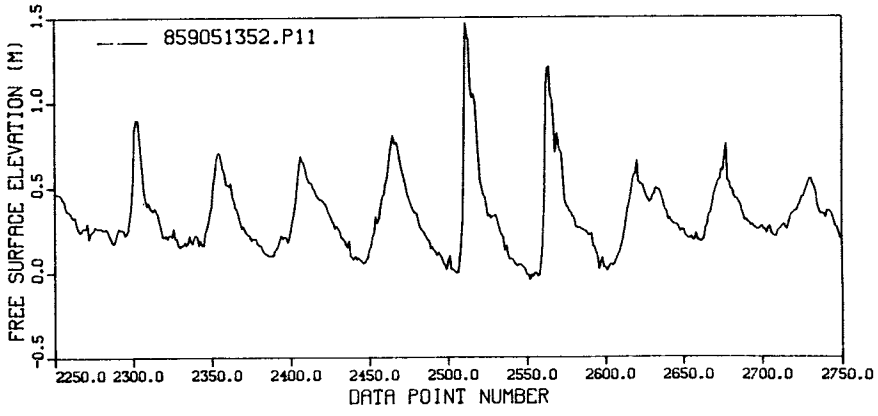

Figure 16. Nearshore transformation of a wave group
(Sheet 1 of 3)

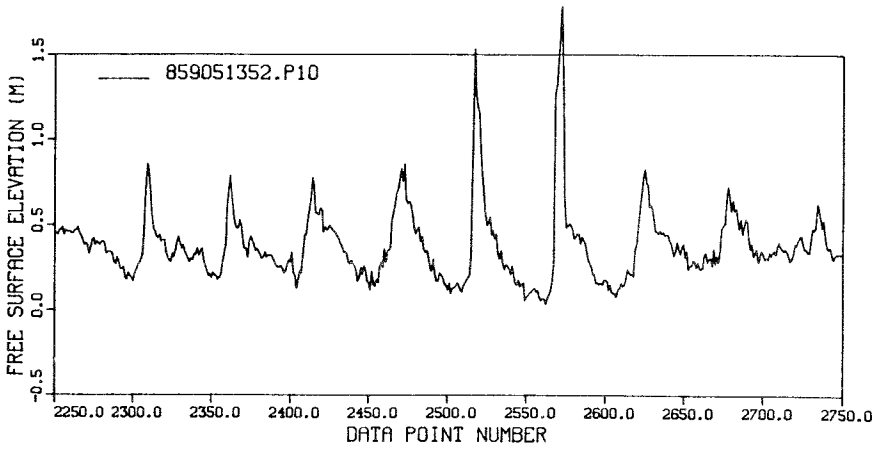

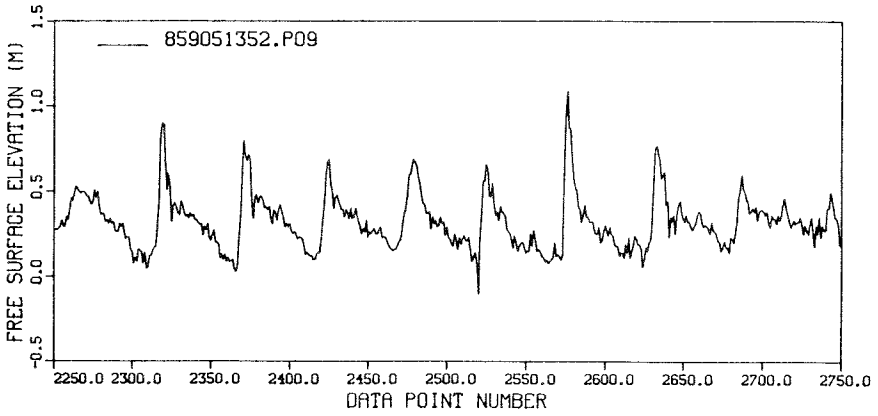

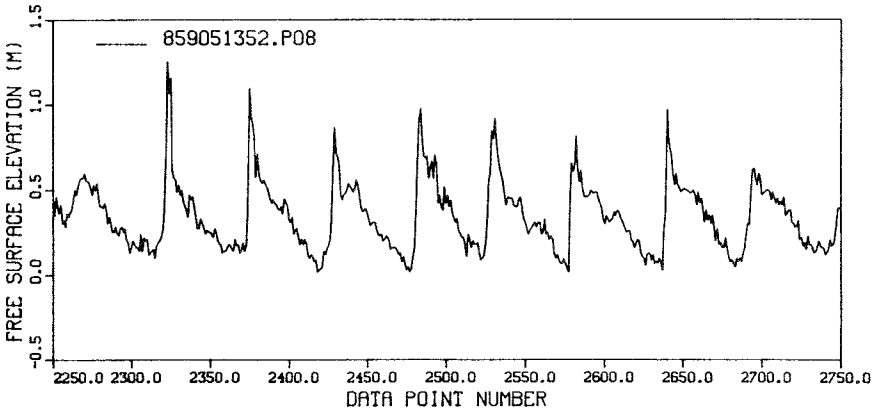

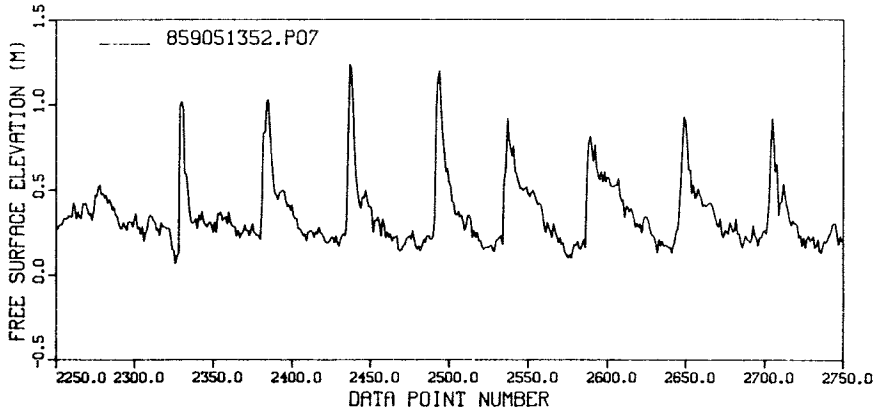

Figure 16. (Sheet 2 of 3)

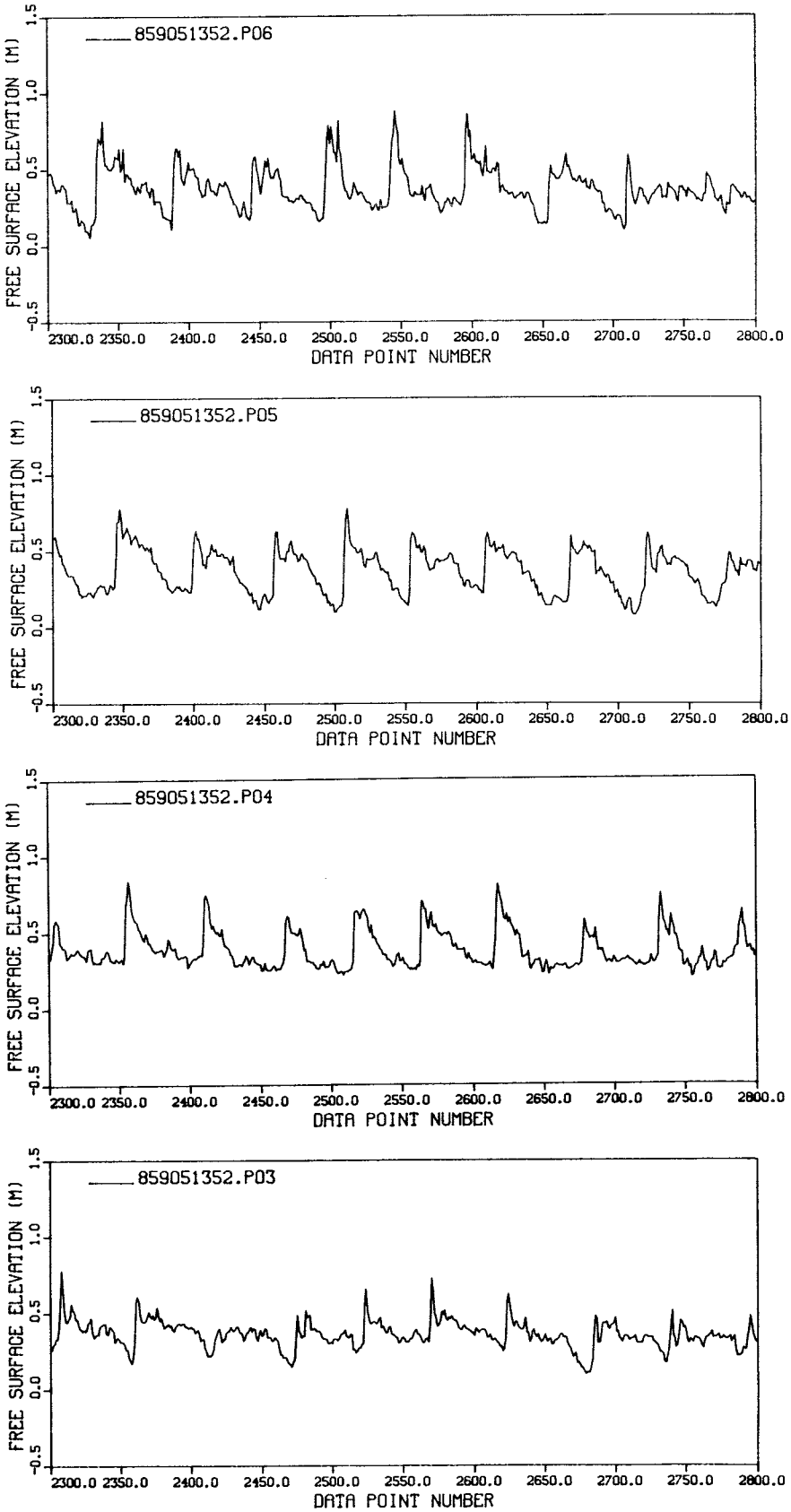

Figure 16. (Sheet 3 of 3)

wave forms resemble those of periodic bores; they are saw-toothed in appearance with very steep forward faces and gradual slopes on the rear face of the crest. Also there is the creation of secondary peaks within some wave crests and the formation of small oscillations, or secondary waves, within the wave forms. At poles P04 and P05, the similarity in wave form for all waves in the group is apparent. The heights of these waves are also approximately equal to one another. This property is characteristic of the inner surf zone, as evidenced in some of the other results which are presented.

Wave and Water Level Parameters

56. A summary of all experimental runs was given in Table 1, and those runs for which data were analyzed were noted. A summary of the wave and water level parameters computed from these data is given in Table 5. The headings in the table are defined as follows:

Run ID - a concatenation of information which identifies results obtained at a particular photopole during a particular experiment run

Example - 859041400.A03

85	denotes the year 1985
9	denotes the month, September 1985
04	denotes the day, 4 September 1985
1400	denotes the time, 1400 EDT
A03	denotes results from analysis of data from photopole P03 (the "A" stands for analysis)

DEPTH - seabed elevation below the MSL datum (in metres)

ELEV mean - mean water surface elevation, measured during the experimental run, above (+) or below (-) the MSL datum (in metres)

TOTAL DEPTH - total mean water depth equal to the sum of the seabed elevation, below the MSL datum, and the mean water surface elevation (in metres)

ELEV max - maximum water surface elevation relative to the mean (in metres)

ELEV min - minimum water surface elevation relative to the mean (in metres)

ELEV skewness - skewness of the water surface elevations relative to the mean

ELEV kurtosis - kurtosis of the water surface elevations relative to the mean

Table 5

Summary of Wave and Water Level Parameters

RUN ID	DEPTH (m)	ELEV mean (m)	TOTAL DEPTH (m)	ELEV max (m)	ELEV min (m)	ELEV skewness	ELEV kurtosis	Hmo (m)	Tp (sec)	WAVES UP	WAVES DOWN	Havg UP (m)	Havg DOWN (m)	Tavg UP (sec)	Tavg DOWN (sec)	Hrms UP (m)	Hrms DOWN (m)	H1/3 UP (m)	H1/3 DOWN (m)	H1/10 UP (m)	H1/10 DOWN (m)	Hmax UP (m)	Hmax DOWN (m)
859041400.A03	0.41	0.317	0.73	0.49	-0.25	0.688	5.34	0.38	13.0	65	66	0.36	0.39	10.2	10.1	0.38	0.41	0.49	0.51	0.57	0.60	0.63	0.62
859041400.A05	0.53	0.353	0.88	0.65	-0.27	0.603	2.86	0.58	11.2	62	62	0.53	0.53	10.6	10.8	0.54	0.54	0.66	0.66	0.74	0.75	0.78	0.86
859041400.A06	0.61	0.332	0.94	0.74	-0.35	0.566	4.33	0.52	13.0	68	68	0.45	0.49	9.8	9.9	0.49	0.52	0.67	0.68	0.87	0.82	0.96	0.94
859041400.A08	0.70	0.329	1.30	1.11	-0.34	1.388	5.46	0.82	11.2	66	66	0.73	0.73	10.2	10.2	0.78	0.79	1.03	1.03	1.18	1.18	1.33	1.37
859041400.A09	0.83	0.333	1.16	1.21	-0.40	1.487	6.42	0.84	11.2	69	68	0.72	0.71	9.7	9.7	0.80	0.81	1.11	1.13	1.31	1.31	1.53	1.50
859041400.A10	0.95	0.325	1.28	1.16	-0.41	1.844	7.90	0.84	11.2	66	67	0.71	0.70	10.3	10.0	0.80	0.81	1.19	1.21	1.37	1.35	1.47	1.47
859041400.A11	1.17	0.283	1.40	1.42	-0.39	1.880	8.21	0.90	11.2	61	64	0.75	0.73	10.9	10.5	0.85	0.84	1.24	1.24	1.56	1.56	1.75	1.80
859041400.A12	1.33	0.289	1.52	1.25	-0.39	1.566	6.87	0.88	11.2	60	60	0.68	0.69	11.1	11.3	0.77	0.77	1.09	1.10	1.40	1.38	1.61	1.62
859041400.A13	1.44	0.306	1.75	1.47	-0.44	1.403	6.75	0.85	11.5	61	60	0.65	0.66	10.9	11.3	0.72	0.74	1.01	1.03	1.31	1.31	1.80	1.91
859041510.A03	0.44	0.103	0.54	0.42	-0.23	-0.001	3.40	0.32	12.5	52	54	0.32	0.34	12.6	12.0	0.33	0.35	0.42	0.43	0.51	0.49	0.58	0.58
859041510.A04	0.67	0.093	0.76	0.44	-0.19	1.401	6.05	0.30	8.8	67	66	0.31	0.31	9.9	10.0	0.32	0.33	0.42	0.43	0.52	0.51	0.59	0.63
859041510.A05	0.50	0.132	0.63	0.49	-0.32	0.436	2.71	0.52	13.0	62	61	0.47	0.47	10.7	11.0	0.48	0.48	0.59	0.59	0.68	0.64	0.72	0.69
859041510.A06	0.60	0.106	0.70	0.53	-0.31	0.562	3.16	0.51	13.0	62	67	0.48	0.48	10.7	10.1	0.49	0.49	0.59	0.58	0.63	0.63	0.66	0.67
859041510.A07	0.70	0.118	0.72	0.60	-0.31	0.914	3.71	0.56	11.2	62	63	0.53	0.55	10.8	10.7	0.55	0.56	0.68	0.68	0.78	0.77	0.82	0.85
859041510.A08	0.70	0.099	0.80	0.79	-0.33	0.989	3.97	0.70	13.0	67	63	0.65	0.67	9.9	10.5	0.68	0.69	0.83	0.82	0.95	0.93	1.10	1.10
859041510.A09	0.80	0.096	0.89	0.93	-0.34	1.342	5.03	0.77	11.2	67	66	0.73	0.75	10.0	10.2	0.77	0.78	0.95	0.95	1.07	1.09	1.23	1.24
859041510.A10	0.95	0.099	1.04	1.27	-0.47	1.640	6.21	0.92	11.2	66	63	0.87	0.90	10.0	10.7	0.92	0.95	1.22	1.22	1.40	1.40	1.62	1.65
859041510.A11	1.17	0.098	1.26	1.37	-0.37	1.824	7.08	1.00	11.2	67	63	0.88	0.94	10.1	10.7	0.95	1.00	1.30	1.34	1.56	1.57	1.72	1.74
859041510.A12	1.32	0.049	1.36	1.13	-0.44	1.683	6.08	1.01	11.2	65	62	0.84	0.87	10.4	10.7	0.93	0.94	1.29	1.31	1.41	1.41	1.48	1.45
859041510.A13	1.44	0.054	1.49	1.32	-0.41	1.687	6.51	1.00	11.2	62	63	0.82	0.82	10.9	10.7	0.90	0.91	1.27	1.29	1.52	1.53	1.65	1.71
359050955.A03	0.46	0.293	0.75	0.45	-0.25	0.776	5.48	0.34	11.4	62	69	0.35	0.38	10.9	10.0	0.37	0.39	0.48	0.49	0.56	0.57	0.64	0.64
359050955.A04	0.56	0.284	0.84	0.50	-0.21	1.241	4.67	0.43	11.4	65	66	0.43	0.44	10.3	10.2	0.44	0.45	0.54	0.52	0.60	0.58	0.65	0.66
359050955.A05	0.49	0.278	0.77	0.62	-0.33	0.561	3.18	0.54	11.4	60	63	0.49	0.49	11.5	10.7	0.51	0.50	0.64	0.61	0.75	0.71	0.80	0.79
859050955.A06	0.51	0.307	0.82	0.68	-0.29	0.826	4.75	0.51	13.1	65	65	0.52	0.51	10.4	10.4	0.54	0.54	0.70	0.67	0.80	0.75	0.93	0.85
859050955.A07	0.52	0.289	0.81	1.12	-0.33	1.528	7.02	0.60	11.4	68	69	0.57	0.58	10.0	10.0	0.62	0.61	0.83	0.81	0.98	0.97	1.36	1.39
859050955.A08	0.64	0.287	0.93	1.28	-0.41	1.565	6.79	0.79	11.4	72	69	0.66	0.68	9.3	9.8	0.73	0.76	1.02	1.03	1.21	1.26	1.42	1.56
859050955.A09	0.80	0.323	1.12	1.32	-0.37	1.815	8.46	0.76	11.4	72	71	0.64	0.65	9.5	9.6	0.73	0.74	1.05	1.06	1.29	1.29	1.56	1.57
859050955.A11	1.16	0.284	1.44	0.83	-0.37	1.357	5.66	0.70	11.4	63	65	0.57	0.57	10.8	10.5	0.63	0.62	0.87	0.87	1.03	1.04	1.11	1.15
859050955.A12	1.32	0.262	1.58	0.82	-0.28	1.091	4.67	0.65	11.4	64	65	0.53	0.52	10.6	10.5	0.56	0.57	0.76	0.78	0.93	0.92	1.09	1.06
859050955.A13	1.55	0.256	1.81	0.68	-0.31	1.002	4.29	0.61	11.4	67	64	0.46	0.47	10.2	10.6	0.50	0.51	0.68	0.70	0.80	0.83	0.89	0.87
859050955.A14	1.88	0.259	2.14	0.59	-0.30	0.936	3.89	0.61	11.4	65	64	0.47	0.49	10.5	10.7	0.50	0.52	0.68	0.71	0.78	0.81	0.82	0.88
859051055.A03	0.46	0.513	0.97	0.64	-0.23	1.693	8.74	0.37	15.3	65	70	0.39	0.39	10.1	9.6	0.41	0.42	0.55	0.55	0.69	0.68	0.82	0.78
859051055.A04	0.56	0.511	1.07	0.67	-0.24	1.413	5.54	0.48	11.2	66	67	0.46	0.47	10.2	10.0	0.49	0.50	0.61	0.63	0.72	0.74	0.80	0.82
859051055.A05	0.49	0.510	1.00	0.72	-0.28	0.825	3.92	0.59	11.2	68	68	0.52	0.53	9.9	9.9	0.56	0.56	0.73	0.73	0.83	0.82	0.93	0.87
859051055.A06	0.51	0.495	1.01	0.76	-0.36	1.018	5.32	0.56	15.3	64	65	0.54	0.56	10.3	10.3	0.58	0.60	0.78	0.78	0.88	0.91	0.93	0.96
859051055.A07	0.52	0.505	1.03	0.94	-0.25	1.930	8.64	0.60	11.2	70	70	0.55	0.55	9.6	9.6	0.61	0.62	0.86	0.87	0.98	0.99	1.14	1.16
859051055.A08	0.64	0.502	1.14	1.10	-0.36	1.494	7.65	0.67	11.2	66	66	0.59	0.61	10.1	10.1	0.66	0.68	0.92	0.97	1.22	1.24	1.44	1.45
859051055.A09	0.80	0.493	1.29	1.13	-0.39	1.462	8.90	0.55	11.2	68	68	0.48	0.48	9.8	9.8	0.55	0.56	0.76	0.79	1.14	1.16	1.47	1.51
859051055.A10	0.89	0.489	1.38	0.89	-0.32	1.337	6.84	0.51	10.0	64	69	0.44	0.43	10.4	9.7	0.47	0.47	0.62	0.64	0.81	0.88	1.12	1.21
859051055.A11	1.16	0.488	1.65	0.93	-0.28	1.274	6.58	0.53	11.2	61	62	0.45	0.44	11.0	10.8	0.50	0.48	0.66	0.64	0.91	0.87	1.15	1.18
359051055.A12	1.32	0.477	1.80	0.83	-0.32	1.022	5.76	0.50	11.3	61	63	0.42	0.42	10.8	10.6	0.46	0.46	0.61	0.61	0.82	0.84	1.11	1.15
859051352.A03	0.46	0.368	0.83	0.52	-0.24	0.616	5.05	0.36	12.6	49	62	0.36	0.40	13.2	10.4	0.37	0.41	0.47	0.50	0.53	0.56	0.58	0.64
359051352.A04	0.56	0.381	0.94	0.49	-0.21	1.307	4.56	0.44	10.9	60	61	0.45	0.45	10.8	10.6	0.46	0.46	0.53	0.53	0.58	0.57	0.65	0.62
859051352.A05	0.49	0.375	0.87	0.61	-0.27	0.477	2.66	0.56	12.6	63	62	0.49	0.49	10.3	10.5	0.51	0.50	0.62	0.60	0.69	0.66	0.74	0.73
859051352.A06	0.51	0.374	0.88	0.72	-0.33	0.702	4.00	0.56	12.6	64	61	0.52	0.55	10.1	10.6	0.55	0.58	0.70	0.70	0.80	0.81	0.90	0.97
859051352.A07	0.52	0.355	0.88	1.22	-0.28	1.817	7.87	0.69	10.9	66	68	0.65	0.64	9.8	9.6	0.70	0.70	0.95	0.93	1.12	1.11	1.40	1.42
859051352.A08	0.64	0.356	1.00	1.32	-0.38	1.711	7.76	0.83	12.6	64	64	0.76	0.78	10.1	10.1	0.84	0.86	1.16	1.19	1.39	1.40	1.60	1.70
859051352.A09	0.80	0.341	1.14	1.06	-0.32	1.631	7.47	0.72	12.6	66	68	0.63	0.64	9.7	9.6	0.70	0.72	1.00	1.03	1.21	1.21	1.32	1.32
859051352.A10	0.89	0.382	1.28	1.47	-0.38	1.932	9.43	0.79	10.9	69	72	0.63	0.61	9.4	9.1	0.71	0.71	1.02	1.03	1.38	1.38	1.75	1.79
859051352.A11	1.16	0.340	1.50	1.10	-0.37	1.633	7.14	0.78	10.9	62	64	0.62	0.63	10.5	10.1	0.71	0.72	1.05	1.06	1.25	1.24	1.43	1.47
859051352.A12	1.32	0.313	1.63	0.81	-0.42	1.089	4.52	0.71	10.9	59	60	0.58	0.59	11.0	10.8	0.63	0.63	0.88	0.87	1.03	1.03	1.23	1.16
859051352.A13	1.55	0.321	1.87	0.79	-0.31	1.021	4.46	0.66	10.9	60	60	0.54	0.55	10.9	10.9	0.58	0.59	0.78	0.80	0.93	0.95	1.06	1.05
859051352.A14	1.88	0.308	2.19	0.80	-0.40	0.988	4.46	0.64	10.9	62	64	0.49	0.48	10.4	10.2	0.54	0.53	0.73	0.74	0.91	0.92	1.20	1.11

(Continued)

Table 5 (Concluded)

RUN ID	DEPTH (m)	ELEV mean (m)	TOTAL DEPTH (m)	ELEV max (m)	ELEV min (m)	ELEV skewness	ELEV kurtosis	Hmo (m)	Tp (sec)	WAVES UP	WAVES DOWN	Havg UP (m)	Havg DOWN (m)	Tavg UP (sec)	Tavg DOWN (sec)	Hrms UP (m)	Hrms DOWN (m)	H1/3 UP (m)	H1/3 DOWN (m)	H1/10 UP (m)	H1/10 DOWN (m)	Hmax UP (m)	Hmax DOWN (m)
859051525.A03	0.46	0.129	0.59	0.28	-0.21	0.027	2.86	0.30	12.8	54	55	0.29	0.30	12.2	11.9	0.30	0.31	0.37	0.37	0.44	0.42	0.47	0.43
859051525.A04	0.56	0.108	0.67	0.39	-0.18	1.145	5.08	0.28	11.1	58	64	0.28	0.29	11.4	10.4	0.30	0.30	0.37	0.38	0.45	0.43	0.53	0.47
859051525.A05	0.49	0.097	0.59	0.58	-0.23	0.507	3.11	0.44	12.8	55	57	0.40	0.41	12.0	11.7	0.41	0.42	0.52	0.50	0.61	0.61	0.71	0.77
859051525.A06	0.51	0.077	0.59	0.53	-0.29	0.592	3.68	0.45	12.8	60	63	0.41	0.45	10.9	10.6	0.44	0.46	0.58	0.58	0.70	0.65	0.77	0.68
859051525.A07	0.52	0.096	0.62	0.57	-0.29	0.830	3.72	0.51	11.1	61	65	0.47	0.47	10.8	10.2	0.49	0.49	0.61	0.62	0.68	0.70	0.81	0.79
859051525.A08	0.64	0.079	0.72	0.66	-0.38	0.909	4.06	0.60	12.8	64	63	0.56	0.57	10.4	10.4	0.59	0.60	0.77	0.75	0.89	0.84	1.02	0.91
859051525.A09	0.80	0.085	0.85	0.89	-0.32	1.623	7.58	0.58	9.8	62	65	0.55	0.55	10.7	10.2	0.61	0.61	0.86	0.85	1.00	1.00	1.13	1.08
859051525.A10	0.89	0.077	0.97	1.05	-0.39	1.650	7.56	0.69	11.1	61	66	0.59	0.60	10.8	10.1	0.66	0.68	0.96	0.96	1.13	1.20	1.32	1.44
859051525.A11	1.16	0.057	1.22	0.83	-0.31	1.343	6.24	0.66	11.1	62	64	0.52	0.54	10.7	10.3	0.57	0.60	0.80	0.85	0.99	1.03	1.14	1.13
859051525.A12	1.32	0.044	1.36	0.96	-0.32	1.273	6.26	0.60	11.1	61	62	0.48	0.50	10.7	10.6	0.54	0.55	0.76	0.78	0.95	0.96	1.23	1.24
859051525.A13	1.55	0.051	1.60	0.85	-0.34	1.223	6.33	0.56	11.1	62	61	0.44	0.46	10.7	10.8	0.49	0.50	0.67	0.71	0.85	0.87	1.16	1.19
859051525.A14	1.88	0.062	1.94	0.74	-0.36	0.886	4.65	0.53	11.1	59	59	0.45	0.45	11.3	11.1	0.48	0.48	0.65	0.64	0.85	0.83	0.99	1.03
859060915.A03	0.49	0.033	0.52	0.19	-0.17	-0.198	2.67	0.23	12.8	43	50	0.23	0.24	14.8	13.1	0.23	0.24	0.28	0.28	0.31	0.31	0.34	0.35
859060915.A04	0.47	0.051	0.52	0.32	-0.13	1.132	5.03	0.21	11.1	49	55	0.24	0.24	13.5	12.2	0.24	0.24	0.28	0.30	0.32	0.33	0.34	0.40
859060915.A05	0.45	0.035	0.49	0.40	-0.18	0.522	3.18	0.33	12.8	52	59	0.32	0.30	12.6	11.0	0.33	0.31	0.41	0.39	0.50	0.45	0.55	0.47
859060915.A07	0.55	0.071	0.62	0.57	-0.24	0.952	4.49	0.43	12.8	63	62	0.42	0.42	10.5	10.7	0.44	0.44	0.57	0.56	0.66	0.67	0.76	0.76
859060915.A08	0.66	0.039	0.70	0.88	-0.28	1.334	6.51	0.52	12.8	62	62	0.52	0.53	10.7	10.7	0.55	0.57	0.73	0.75	0.84	0.89	0.91	1.13
859060915.A09	0.80	0.045	0.85	1.02	-0.28	1.935	9.45	0.57	9.8	69	69	0.52	0.53	9.6	9.6	0.58	0.60	0.83	0.86	1.02	1.04	1.22	1.26
859060915.A10	0.98	0.032	1.01	1.10	-0.32	1.953	10.27	0.57	9.8	66	68	0.47	0.49	10.0	9.7	0.55	0.58	0.80	0.86	1.09	1.14	1.37	1.42
859060915.A11	1.18	0.002	1.18	0.92	-0.28	1.625	8.06	0.54	12.8	61	62	0.44	0.47	10.7	10.7	0.49	0.53	0.70	0.76	0.92	0.98	1.05	1.16
859060915.A12	1.40	-0.005	1.40	1.05	-0.27	1.390	7.74	0.51	12.8	64	62	0.42	0.43	10.4	10.7	0.48	0.50	0.69	0.74	0.98	1.00	1.26	1.32
859061015.A03	0.49	0.282	0.77	0.42	-0.22	0.363	3.89	0.32	13.1	59	64	0.31	0.32	11.6	10.7	0.32	0.33	0.40	0.43	0.45	0.50	0.47	0.59
859061015.A04	0.47	0.255	0.73	0.39	-0.17	1.083	4.80	0.33	10.1	66	70	0.33	0.33	10.2	9.7	0.34	0.35	0.43	0.44	0.48	0.50	0.51	0.54
859061015.A05	0.45	0.231	0.68	0.53	-0.25	0.675	3.31	0.45	13.1	56	59	0.44	0.43	12.2	11.6	0.45	0.44	0.55	0.53	0.64	0.62	0.75	0.69
859061015.A06	0.52	0.238	0.76	0.88	-0.29	0.600	4.33	0.47	13.1	64	63	0.44	0.43	10.7	10.8	0.46	0.46	0.60	0.59	0.75	0.75	1.06	1.13
859061015.A07	0.55	0.218	0.77	0.71	-0.27	1.515	7.02	0.51	10.1	68	66	0.49	0.51	10.0	10.3	0.54	0.55	0.73	0.73	0.84	0.84	0.86	0.87
859061015.A08	0.66	0.245	0.91	0.99	-0.27	1.641	8.26	0.58	13.1	74	76	0.52	0.50	9.3	8.9	0.58	0.57	0.83	0.83	1.00	0.99	1.20	1.22
859061015.A09	0.80	0.228	1.03	1.11	-0.29	1.558	8.20	0.57	13.1	68	68	0.49	0.51	9.9	9.9	0.56	0.58	0.80	0.83	1.08	1.07	1.35	1.35
859061015.A10	0.98	0.212	1.19	0.95	-0.30	1.379	7.95	0.53	10.1	65	70	0.43	0.43	10.4	9.7	0.48	0.49	0.68	0.68	0.91	0.92	1.20	1.24
859061015.A11	1.18	0.231	1.41	0.77	-0.28	1.110	5.62	0.52	13.1	67	67	0.42	0.42	10.2	10.2	0.45	0.46	0.61	0.62	0.80	0.81	0.97	0.99
859061015.A12	1.40	0.211	1.61	0.63	-0.27	0.849	4.40	0.49	13.1	64	65	0.39	0.39	10.6	10.4	0.42	0.42	0.58	0.58	0.70	0.71	0.85	0.78
859061015.A13	1.63	0.236	1.87	0.61	-0.25	0.811	4.16	0.44	13.1	63	65	0.35	0.35	10.7	10.5	0.38	0.38	0.50	0.51	0.59	0.61	0.80	0.81
859061015.A14	1.91	0.234	2.14	0.46	-0.28	0.686	3.77	0.42	9.0	67	67	0.34	0.35	10.1	10.1	0.36	0.37	0.47	0.49	0.56	0.62	0.61	0.69
859061300.A03	0.49	0.502	0.99	0.53	-0.21	1.742	7.46	0.40	9.0	61	67	0.41	0.45	11.2	10.1	0.44	0.47	0.56	0.57	0.60	0.61	0.65	0.65
859061300.A04	0.47	0.508	0.98	0.60	-0.24	1.202	4.82	0.50	10.1	74	74	0.48	0.48	9.3	9.2	0.50	0.51	0.63	0.64	0.70	0.73	0.77	0.79
859061300.A05	0.45	0.510	0.96	0.94	-0.30	1.298	6.55	0.54	11.4	68	69	0.54	0.56	10.1	9.9	0.58	0.59	0.78	0.76	0.96	0.93	1.17	1.15
859061300.A06	0.52	0.524	1.04	0.80	-0.46	1.303	6.15	0.55	9.0	66	71	0.57	0.54	10.3	9.7	0.60	0.59	0.78	0.79	0.90	0.91	0.96	1.03
859061300.A07	0.55	0.497	1.05	1.15	-0.34	1.721	9.45	0.59	10.1	68	66	0.54	0.56	10.0	10.3	0.61	0.62	0.88	0.88	1.13	1.13	1.46	1.48
859061300.A08	0.66	0.526	1.19	0.83	-0.34	1.220	6.73	0.57	11.4	76	74	0.47	0.49	8.9	9.2	0.51	0.54	0.71	0.77	0.95	1.01	1.10	1.15
859061300.A09	0.80	0.502	1.30	0.83	-0.28	1.247	6.36	0.52	9.0	71	72	0.44	0.44	9.6	9.4	0.48	0.49	0.66	0.67	0.84	0.87	1.00	1.03
859061300.A10	0.98	0.504	1.48	0.69	-0.28	0.906	4.38	0.54	10.1	65	65	0.46	0.46	10.5	10.4	0.49	0.49	0.64	0.66	0.79	0.80	0.91	0.92
859061300.A11	1.18	0.519	1.70	0.64	-0.29	0.659	3.70	0.51	11.4	68	67	0.41	0.42	10.0	10.1	0.44	0.45	0.58	0.59	0.75	0.76	0.86	0.89
859061300.A12	1.40	0.489	1.89	0.53	-0.28	0.655	3.78	0.47	9.0	75	73	0.36	0.36	9.1	9.3	0.39	0.40	0.53	0.54	0.66	0.67	0.70	0.77
859061300.A13	1.63	0.519	2.15	0.52	-0.27	0.761	4.10	0.44	9.0	69	70	0.35	0.35	9.9	9.7	0.37	0.38	0.50	0.51	0.63	0.61	0.76	0.69
859061300.A14	1.91	0.518	2.43	0.61	-0.30	0.630	3.51	0.49	10.1	67	67	0.40	0.39	10.2	10.2	0.42	0.42	0.54	0.56	0.67	0.69	0.83	0.80

H_{mo} - energy-based significant wave height computed as four times the square root of the area under the energy density spectrum, as determined from the high-passed water surface elevation time series (in metres)

T_p - peak spectral period, computed from the central frequency associated with the spectral band containing the greatest energy density (in sec)

WAVES UP - number of primary, individual waves identified using the zero-upcrossing method

WAVES DOWN - number of primary, individual waves identified using the zero-downcrossing method

Havg UP - average wave height using upcrossing results (in metres)

Havg DOWN - average wave height using downcrossing results (in metres)

Tavg UP - average wave period using upcrossing results (in sec)

Tavg DOWN - average wave period using downcrossing results (in sec)

Hrms UP - root-mean-squared wave height using upcrossing results (in metres)

Hrms DOWN - root-mean-squared wave height using downcrossing results (in metres)

H1/3 UP - average of the highest one-third wave heights using upcrossing results (in metres)

H1/3 DOWN - average of the highest one-third wave heights using downcrossing results (in metres)

H1/10 UP - average of the highest one-tenth wave heights using upcrossing results (in metres)

H1/10 DOWN - average of the highest one-tenth wave heights using downcrossing results (in metres)

Hmax UP - maximum wave height using upcrossing results (in metres)

Hmax DOWN - maximum wave height using downcrossing results (in metres)

For each experiment run, the landwardmost pole is at the top of the group, and the seawardmost pole is at the bottom.

57. The mean water surface elevation measurements, relative to the MSL datum, include both the effects of tide and wave setup. The tidally induced mean elevation is assumed to be constant across the surf zone; therefore, the variation in the mean can be assumed to represent changes resulting from the incident wave field. All experiments, with the exception of 859061300, show a

general trend of increasing mean water surface elevation from the breaker zone toward the inner surf zone. The magnitude of the wave setup (defined here as the difference between the maximum and minimum mean elevations along the pole transect) ranges from 3 to 8 cm during those eight experiments; setup is essentially nonexistent during 859061300.

58. A method for estimating wave setup for monochromatic incident waves is given in the Shore Protection Manual(SPM) (1984). Since waves measured during the photopole experiment closely resembled monochromatic conditions, measured wave setup can be compared to estimates obtained using the SPM method. A plane beach with an average beach slope between 1:30 and 1:50 will be assumed to represent the beach morphology in the surf zone. The SPM method is not very sensitive to the choice of beach slope for slopes in this range. A wave period of 11 sec is assumed to be representative of all waves measured during the experimental runs and is used in the computations. The SPM method recommends the use of the significant wave height (the statistical wave height parameter H1/3) at breaking. Measured values of this breaking wave height varied between 0.8 and 1.3 m. Using these wave and beach slope parameters, calculations result in wave setup estimates which vary from 10 to 17 cm. These are a factor of 2 greater than the measurements. Hotta and Mizuguchi (1980) report measurements of wave setup that are also much smaller than those which would be calculated using the observed breaking wave properties and the SPM method.

59. The measured setup is much smaller than the changes associated with the longer period oscillations described earlier, i.e., those with periods between 30 and 50 sec. The magnitude of these fluctuations increases from approximately 10 cm at the seawardmost poles to 20 cm at the landwardmost poles.

60. Table 5 shows the number of waves identified at each pole by the upcrossing and downcrossing methods. The results demonstrate the effectiveness of the zero-crossing method, as implemented here, in identifying the primary waves. The number of waves is nearly constant across the surf zone, and the average wave periods are quite close to the peak spectral period. This result is expected considering the swell-type wave conditions which existed. Exceptions to this result appear at the innermost poles, where the combination of the band-pass filter and crest/trough cutoff value sometimes underestimated the number of primary waves. However, at these locations, most of the primary waves have heights which are approximately equal in magnitude, i.e., a narrow

wave height distribution. The authors feel that an underestimation of the number of primary waves will have less impact on statistical wave height parameters than would an overestimate. Some of the primary waves would be missed in an underestimation, but these would not significantly affect the already narrow wave height distribution. However, overestimation of the number of waves would probably result in the inclusion of some much smaller secondary waves in the distribution. Consequently, any statistical wave parameters computed from the distribution which contains numerous small waves would be underestimated.

61. The upcrossing and downcrossing methods result in statistical wave parameter estimates which are nearly equal. This occurrence is to be expected since an effort was made in the individual wave identification procedure to eliminate any effects of secondary waves. Results presented by Hotta, Mizuguchi, and Isobe (1982) also indicate that the up- and downcrossing methods produce similar estimates. Figure 17 shows plots of the variation of the statistical wave height parameters along the photopole transect from each experiment run. The parameters Havg, Hrms, H1/3, H1/10, and Hmax are those obtained using the downcrossing method. The statistical parameters are

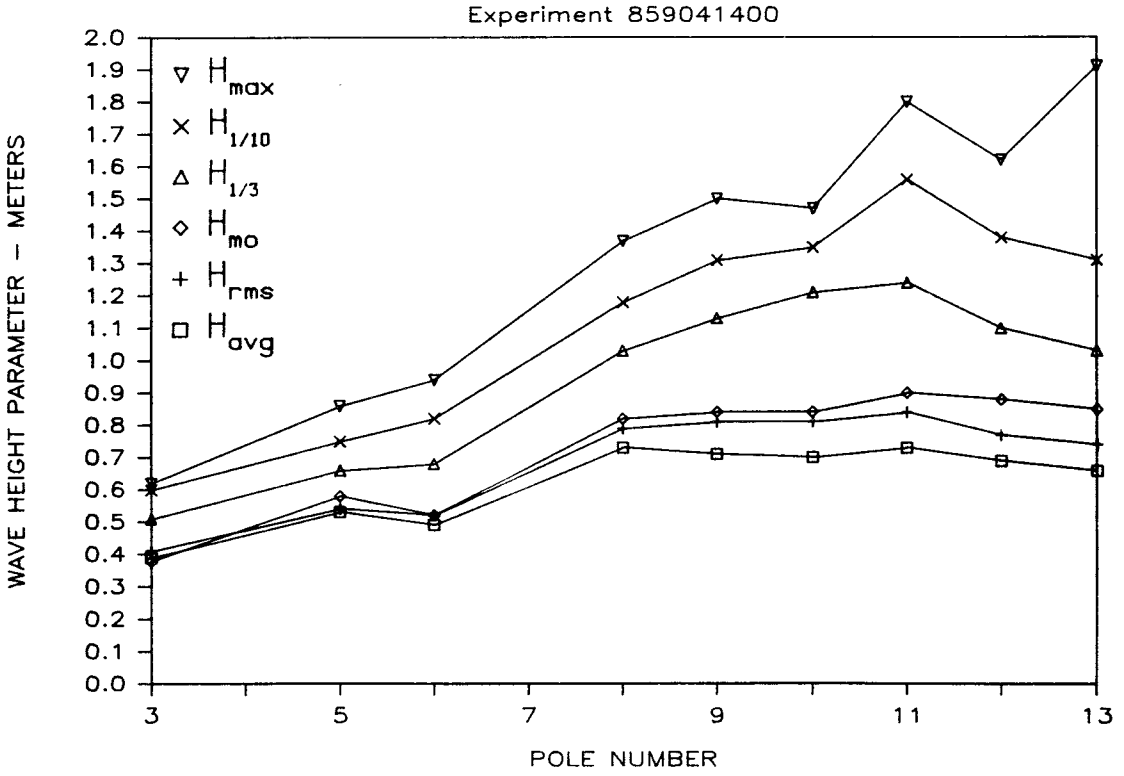

Figure 17. Variation of statistical wave height parameters along the photopole transect (Sheet 1 of 5)

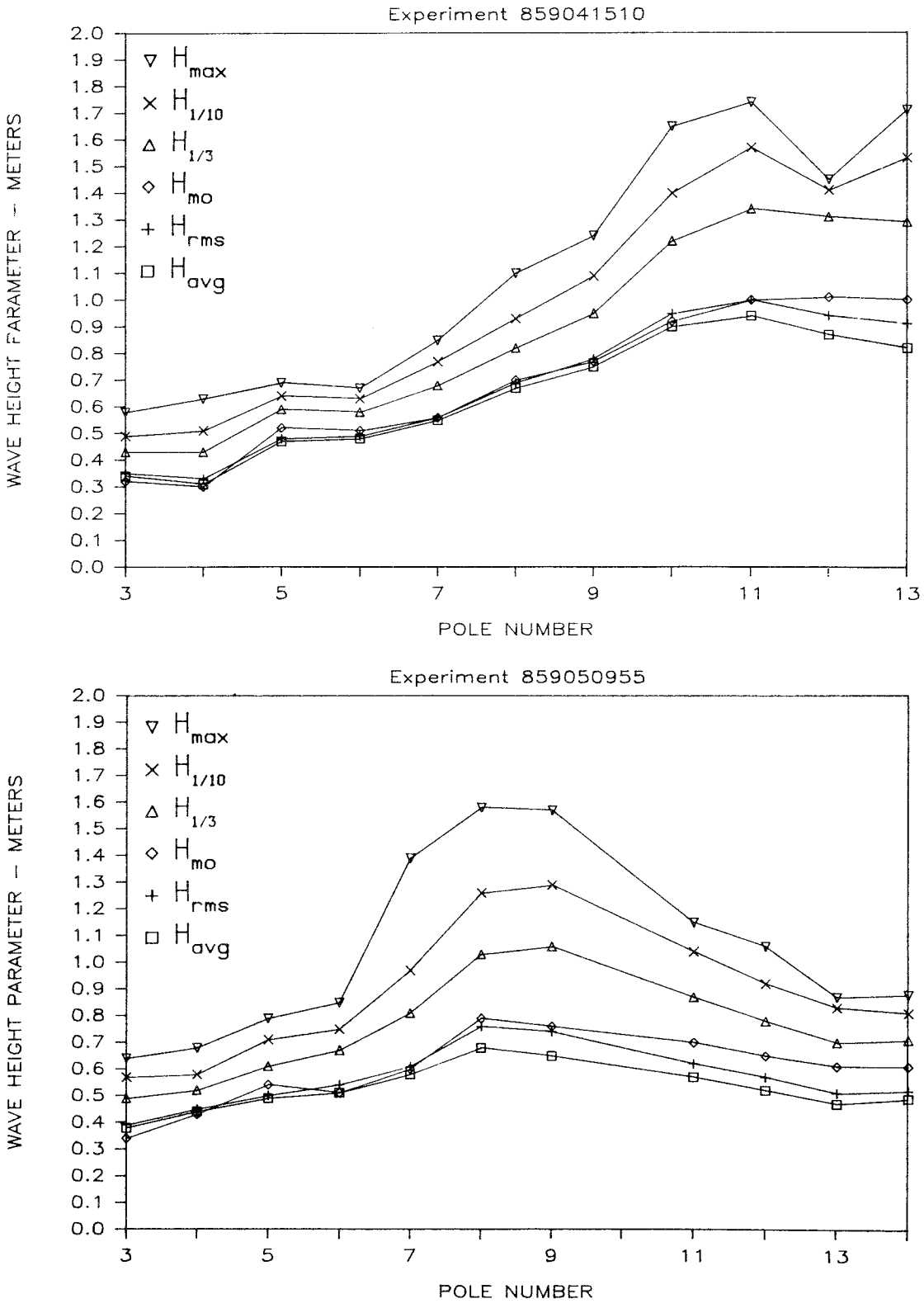

Figure 17. (Sheet 2 of 5)

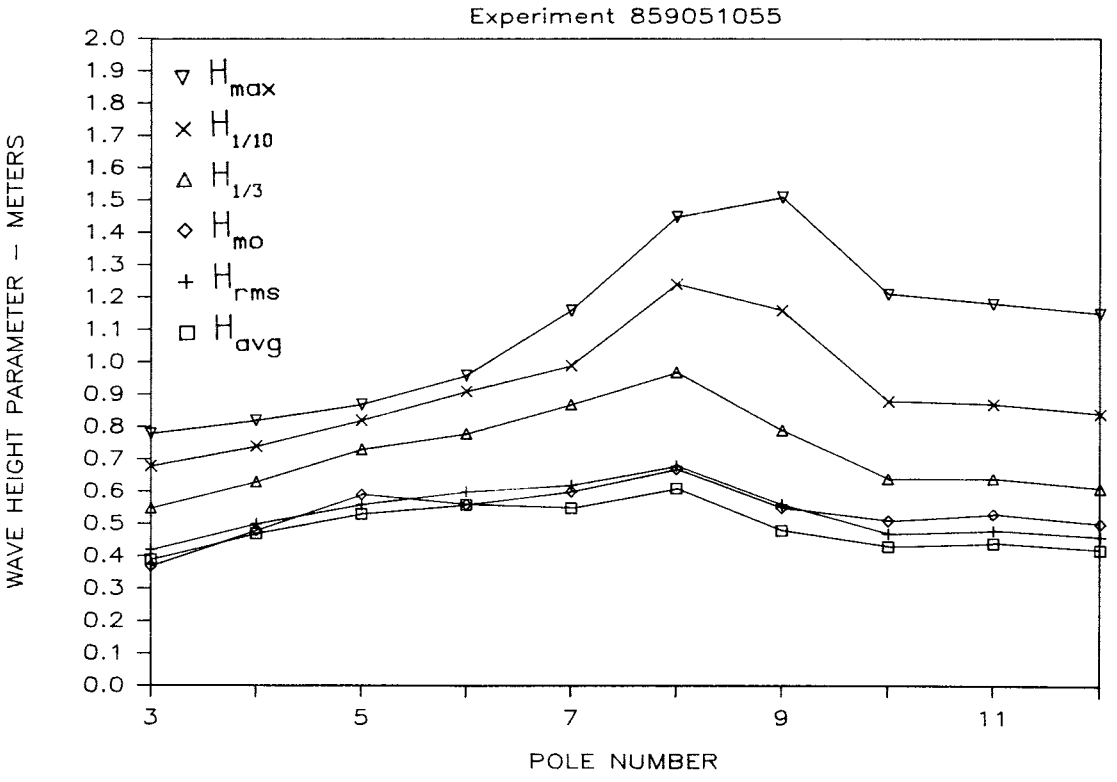

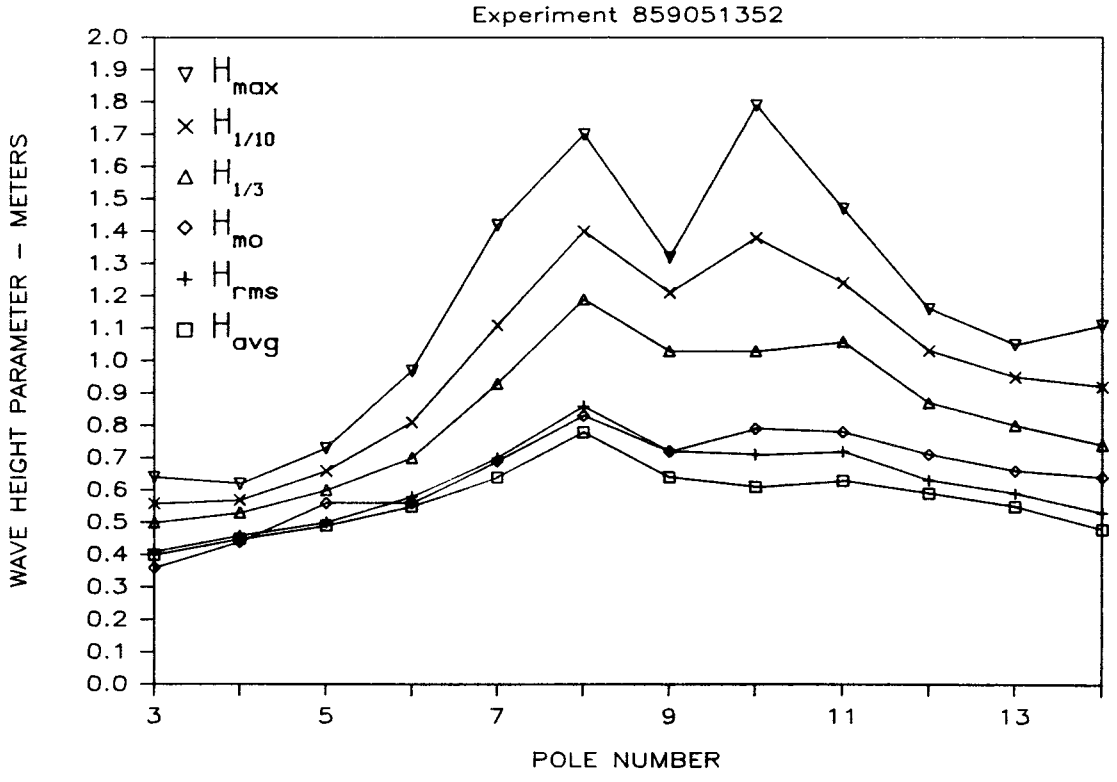

Figure 17. (Sheet 3 of 5)

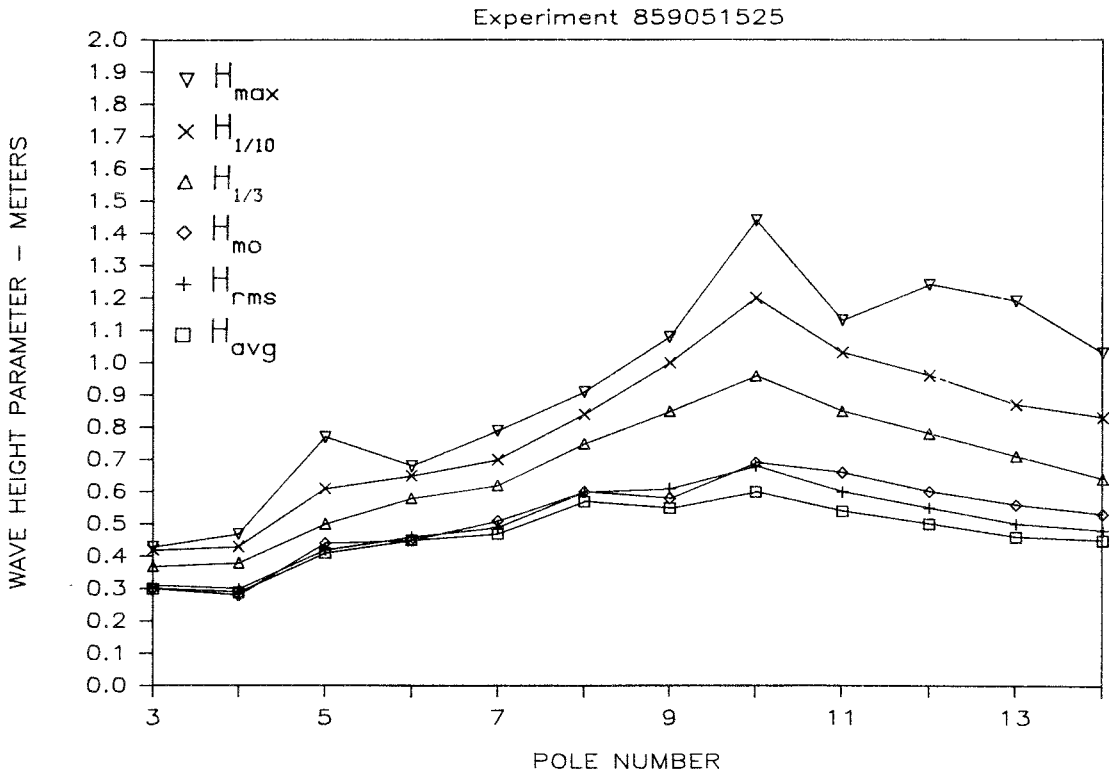

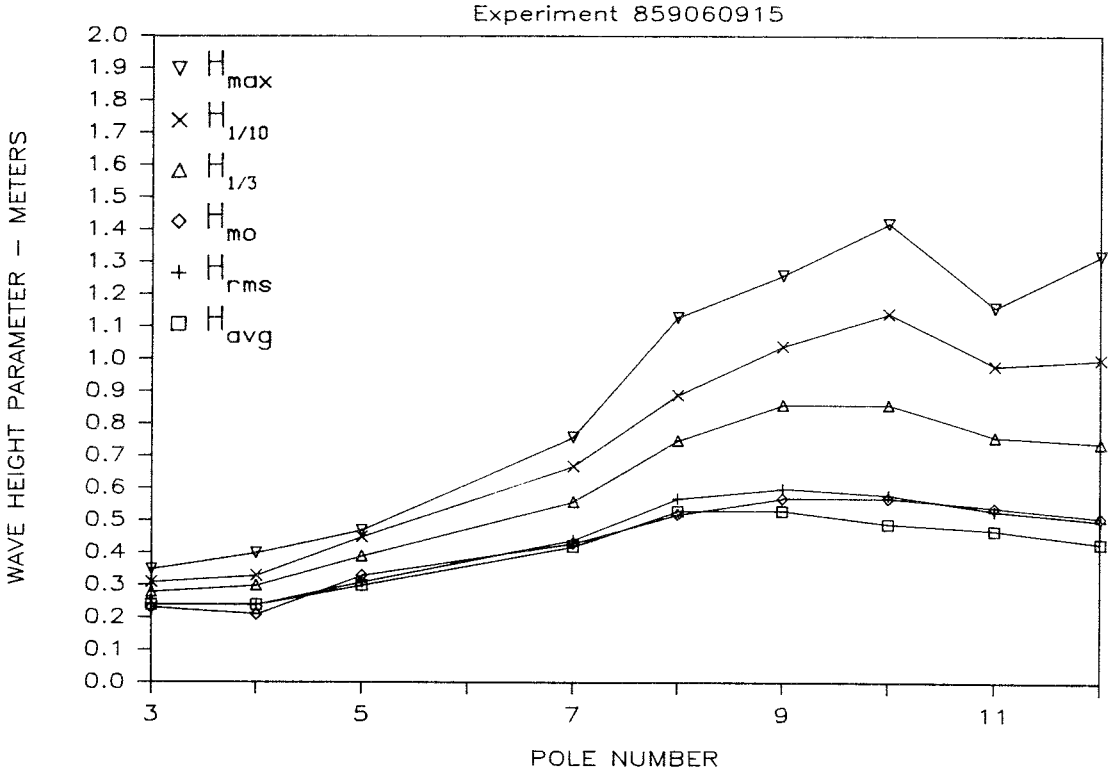

Figure 17. (Sheet 4 of 5)

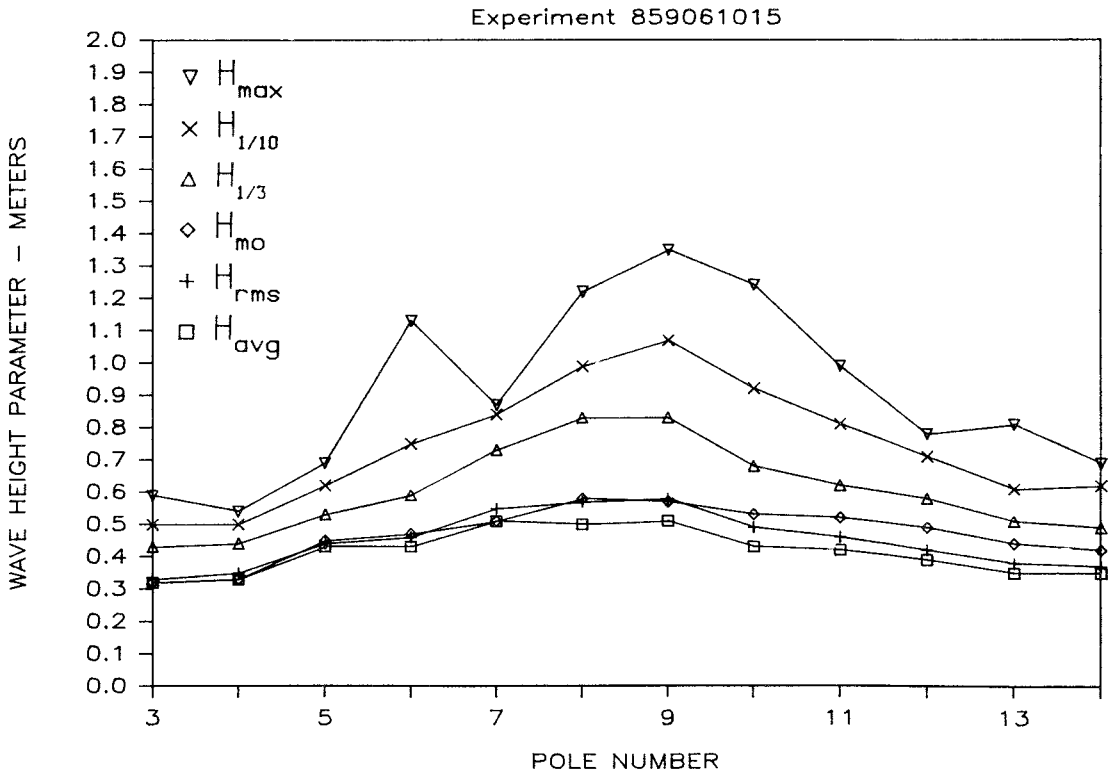

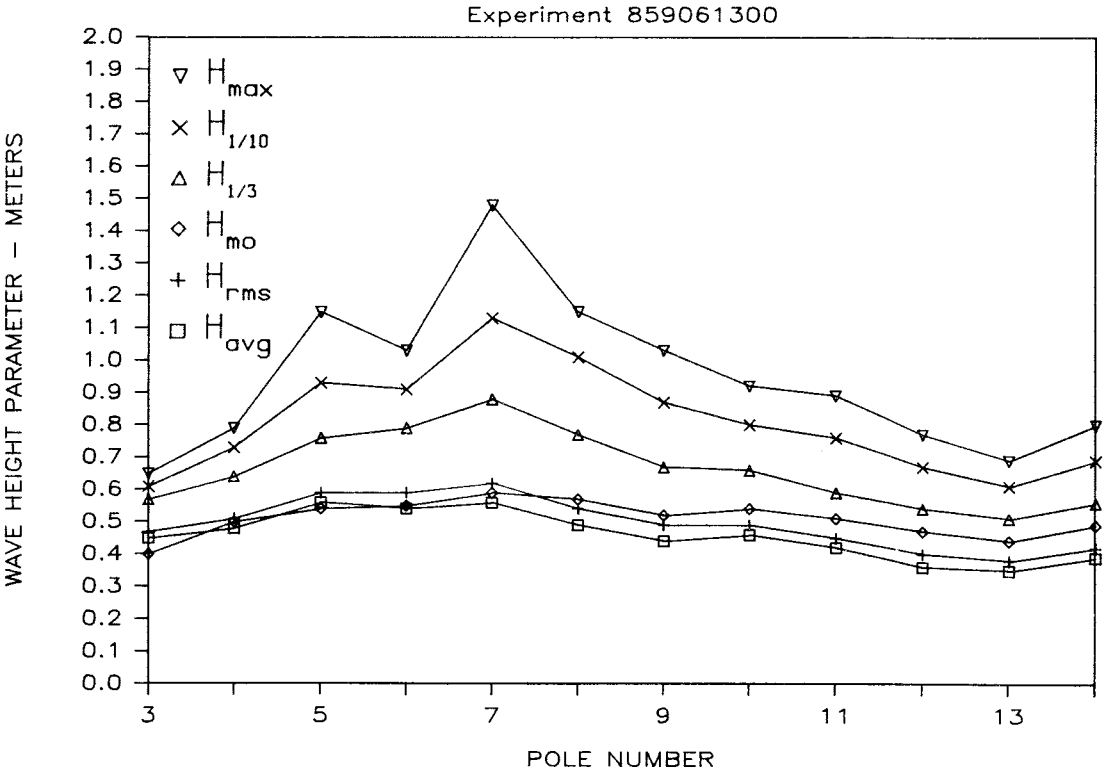

Figure 17. (Sheet 5 of 5)

reasonably stable during shoaling with the exception of H1/10 and Hmax. These two parameters exhibit more pronounced fluctuations because of their dependence upon a single wave or a very small number of the highest waves. The breaking position of these larger waves greatly influences local values of Hmax and H1/10, whereas the more stable parameters are less affected by the behavior of individual waves. For this reason, empirical methods for predicting irregular wave transformation in the surf zone should be formulated in terms of the more stable parameters.

62. Values of the energy-based significant wave heights, H_{mo}, were computed from the high-passed data signals; the effects of long period oscillations were removed. The longer period oscillations are also absent from the data used to identify individual waves and, subsequently, to compute the statistical wave height parameters.

Spectral Analysis Results

63. Wave spectra computed from data collected at each photopole during each experiment run are given in Appendix B. These spectra were computed from the edited data signals with the linear trend removed but with the longer period oscillations still present. An example of the synoptic spectra are given in Figure 18 for the experiment run initiated on 4 September at 1510 EDT. In the figure, spectral results are given for every other pole location. (A complete set is given in Appendix B.) The plots illustrate spectral features observed during all the runs, and they show changes that occur in the spectrum during the shoaling and breaking processes.

64. Results for pole P13 show three very typical features which are representative of the incident wave conditions measured during the experiment. First, the spectrum is narrow banded; this is characteristic of swell wave trains. Second, significant energy exists at a frequency equal to twice the peak frequency. This occurrence does not indicate the presence of incident waves with much shorter periods; rather, it reflects the nonlinearity of the waves. The energy density at these frequencies is associated with the higher harmonics of the peak frequency. There is even some energy density apparent at frequencies near the third harmonic. The third feature is the existence of appreciable energy at very low frequencies.

65. The larger waves during this run broke at poles P13, P12, and P11. Figure 18 shows the decreasing contribution of the higher harmonics after

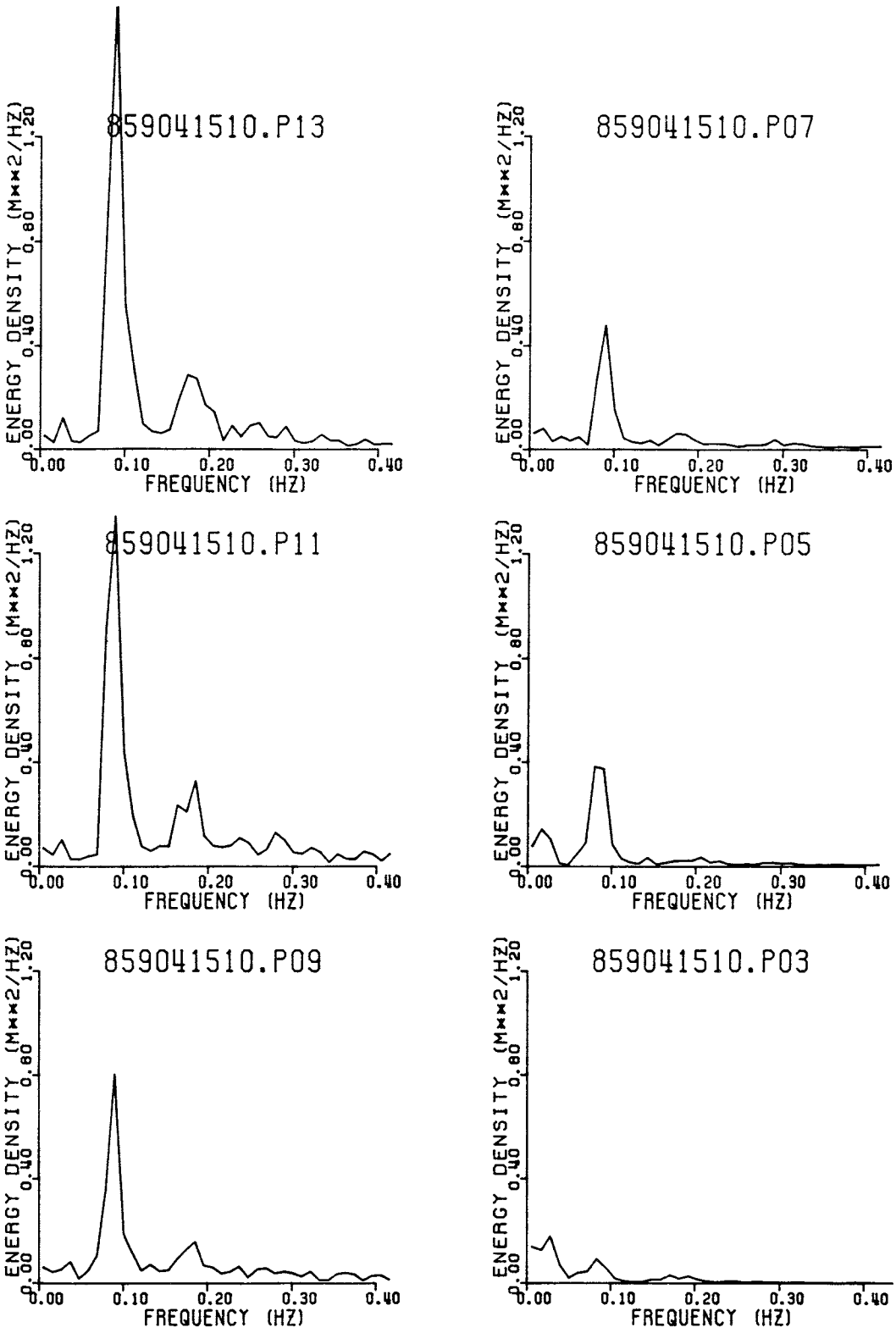

Figure 18. Changes in wave spectra along the photopole transect

pole P11 which results from the changes in wave form occurring after breaking. However, despite these changes, there is some energy density at the second harmonic apparent at each photopole. This energy probably results from smaller, but still nonlinear, unbroken waves. The energy contained in frequencies near the peak frequency steadily decreases across the surf zone due to dissipative processes.

66. Examination of the spectra shown in Figure 18 also indicates changes in the lower frequency component of the spectrum. Energy density associated with these oscillations remains fairly constant from poles P13 to P07 then continues to increase in very shallow water. At pole P03, where it reaches its maximum, its energy density is greater than that associated with frequencies near the peak frequency of the incident wave field. Given the very low frequency of this component, the potential energy associated with these oscillations is much greater than the energy contained in the shorter period incident waves.

Water Surface Elevation Distributions

67. Water surface elevation distributions computed from data collected at each photopole during each experiment run (examples of which are presented in Figure 19) are given in Appendix C. These distributions were computed from the edited, high-passed data; hence the influence of longer waves (those with periods over 21 sec) is not present in the plotted distributions. The water surface elevation distribution plots were constructed by first normalizing each water surface elevation by the standard deviation of all elevations in the time series (the mean being previously removed during the low-pass filtering procedure) and then grouping the normalized elevations into bands. The number of normalized elevations in each band was expressed as a percentage of the total elevations in the record, and the percentages for each band were plotted as a histogram, as shown in Figure 19. The solid curve on the plots represents the Gaussian (or normal) distribution having the same area under the curve as the area contained in the histogram.

68. The water surface elevation distributions given in Figure 19 illustrate the changes that occur as waves shoal and break in the surf zone. This particular set of plots, shown for every other pole, corresponds to the experiment run initiated at 1510 EDT on 4 September. Histograms at the locations

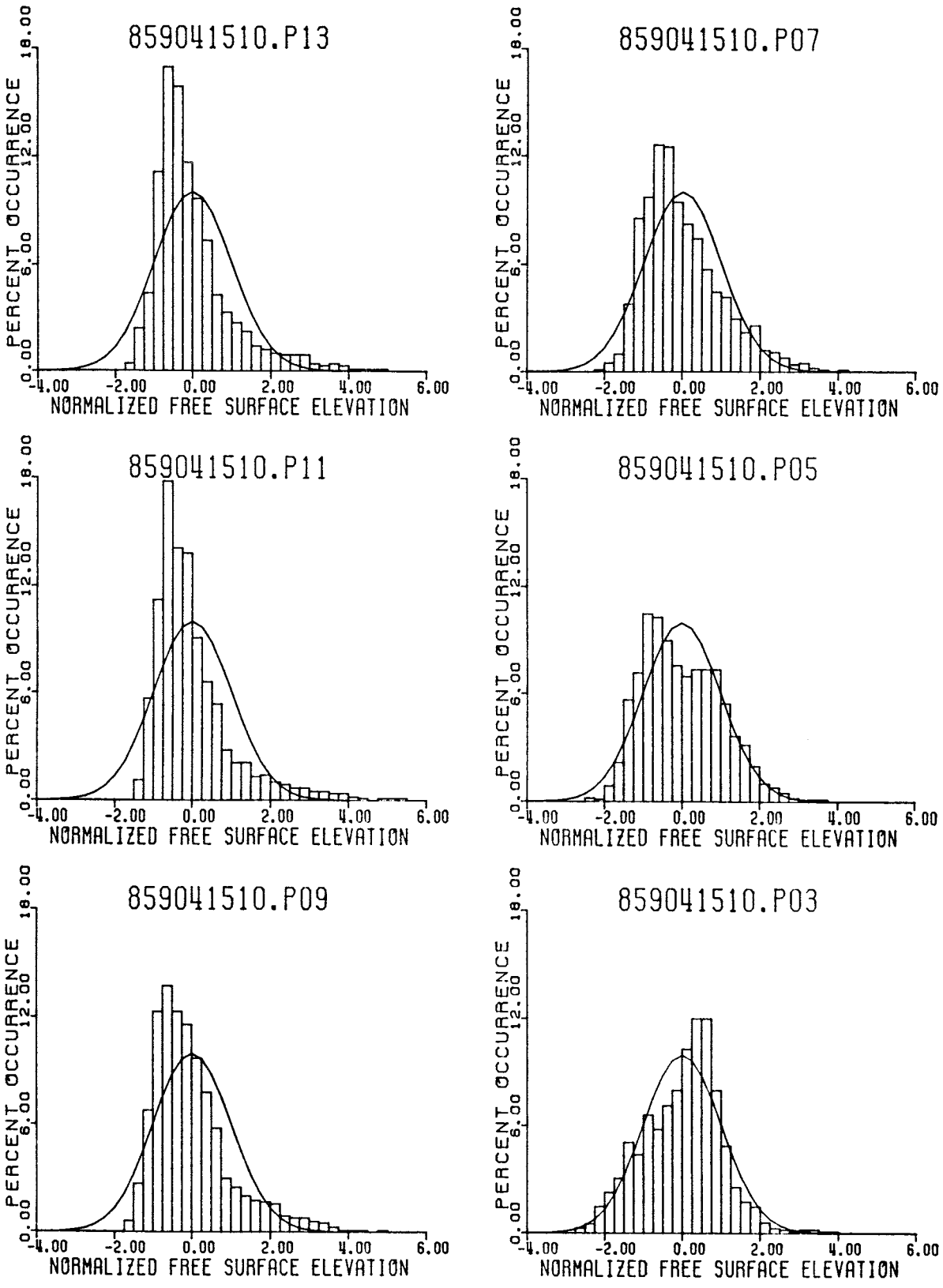

Figure 19. Changes in water surface elevation distributions along the photopole transect

of poles P13 and P11 exhibit a very noticeable deviation from the Gaussian distribution, which is primarily because of the nonsinusoidal wave shapes. Actual shapes are characterized by short, steep crests and long, shallow troughs. (See Figure 16, for example.) The deviation of the observed histogram from the Gaussian distribution is reflected by the value of the skewness parameter, which is a measure of asymmetry about the mean elevation. The skewness for a Gaussian distribution is equal to zero. Examination of Table 5 indicates that a maximum skewness of 1.824 occurs at pole P11 for this run. A decrease in the value of skewness, which reflects a trend in the histogram toward a more Gaussian shape, is evident at poles P09 and P07. The change in shape of the distribution is caused primarily by the breaking of the steep, narrow-crested waves.

69. As the waves reach the inner surf zone (poles P05 and P03), almost all primary waves have undergone initial breaking, and many are propagating as periodic bores. The measured water surface elevations for these waves have distributions which are nearly Gaussian in shape. Apparently, the continual large-scale dissipation of energy through turbulence maintains the symmetry of sea surface elevations about the mean elevation as typified by the characteristic saw-tooth wave forms. Although not shown in Figure 19, results from data measured at pole P04 of this run show a significant increase in sea surface skewness, as seen in Table 5 and in the full set of plots contained in Appendix C. The increase in skewness is thought to be linked to the reformation of broken waves and the steepening of the smallest waves which have yet to break. At pole P03, even the reformed waves have broken, and the water surface elevation distribution is once again nearly Gaussian in shape.

70. Table 5 also lists values of the kurtosis, which is a measure of the fourth moment of the water surface elevation about the mean. The kurtosis for a Gaussian distribution is 3.0. Computed values for all the experiment runs are typically greater than this value throughout the nearshore zone. Only in the inner surf zone do kurtosis values approach 3.0.

71. In general, the water surface elevation distributions for the other experimental runs presented in Appendix C exhibit similar trends to those discussed above.

Wave Height and Period Distributions

72. Wave height and wave period distributions computed from the data

obtained at all photopoles for all experiment runs are given in Appendix D. The wave height histograms for a particular experiment run were constructed by first normalizing the individual wave heights by the average wave height Havg computed for that run (see Table 5 for values of Havg). The normalized wave heights were then grouped into bands, with each band, or interval, representing a small range of normalized wave heights. The number of normalized wave heights in each band was expressed as a percentage of the total number of waves identified during the run. Wave period histograms were computed in a similar manner; individual wave periods were also normalized using the average period. Distributions computed from results obtained using both the up- and downcrossing methods are presented in Appendix D.

73. Figure 20 shows wave height and period distributions at selected locations along the photopole transect (poles P14, P10, P07, and P04). The histograms were computed from data obtained during the experiment run initiated on 5 September at 1352 EDT. Results at pole P14 typify data measured outside the surf zone; results at pole P10 represent conditions near breaking of the higher waves; results at pole P07 represent a location where most of the waves have broken; and results at pole P04 represent inner surf zone wave conditions. Both zero-crossing methods yield similar results at all locations across the surf zone. Hotta and Mizuguchi (1980) reported greater differences between histograms computed from results obtained using the different zero-crossing methods. In that particular study, however, the authors did not eliminate the effects of secondary waves as they did in subsequent studies, i.e., they strictly applied the zero-crossing methods.

74. The wave height distributions at pole P14 are rather widely distributed about the mean height and skewed toward the higher wave heights. These features are similar to those which are characteristic of the Rayleigh distribution for wave heights. Wave period distributions at this location are very narrowly banded about the mean period. This narrow bandedness is indicative of the swell-like wave conditions which existed.

75. At pole P10 the wave height distributions are more widely distributed about the mean. The largest waves broke in the vicinity of this point. Broken waves are apparent as very low normalized wave heights and shoaled waves, near breaking, are apparent as very large normalized wave heights. Consequently the normalized wave heights vary over a much wider range at this point. Figure 20 shows the presence of low wave periods in the wave period

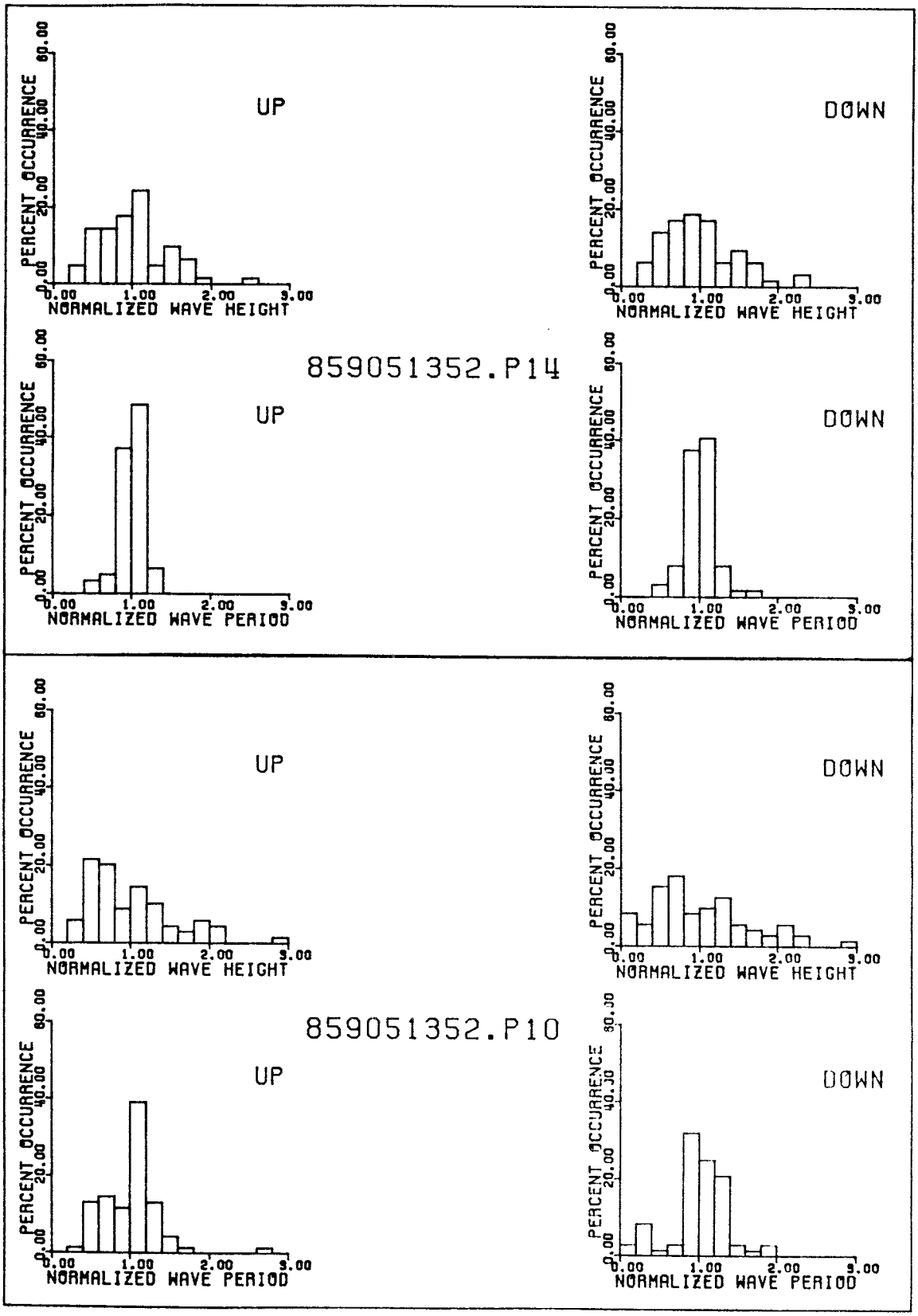

Figure 20. Changes in wave height and wave period distributions along the photopole transect (Continued)

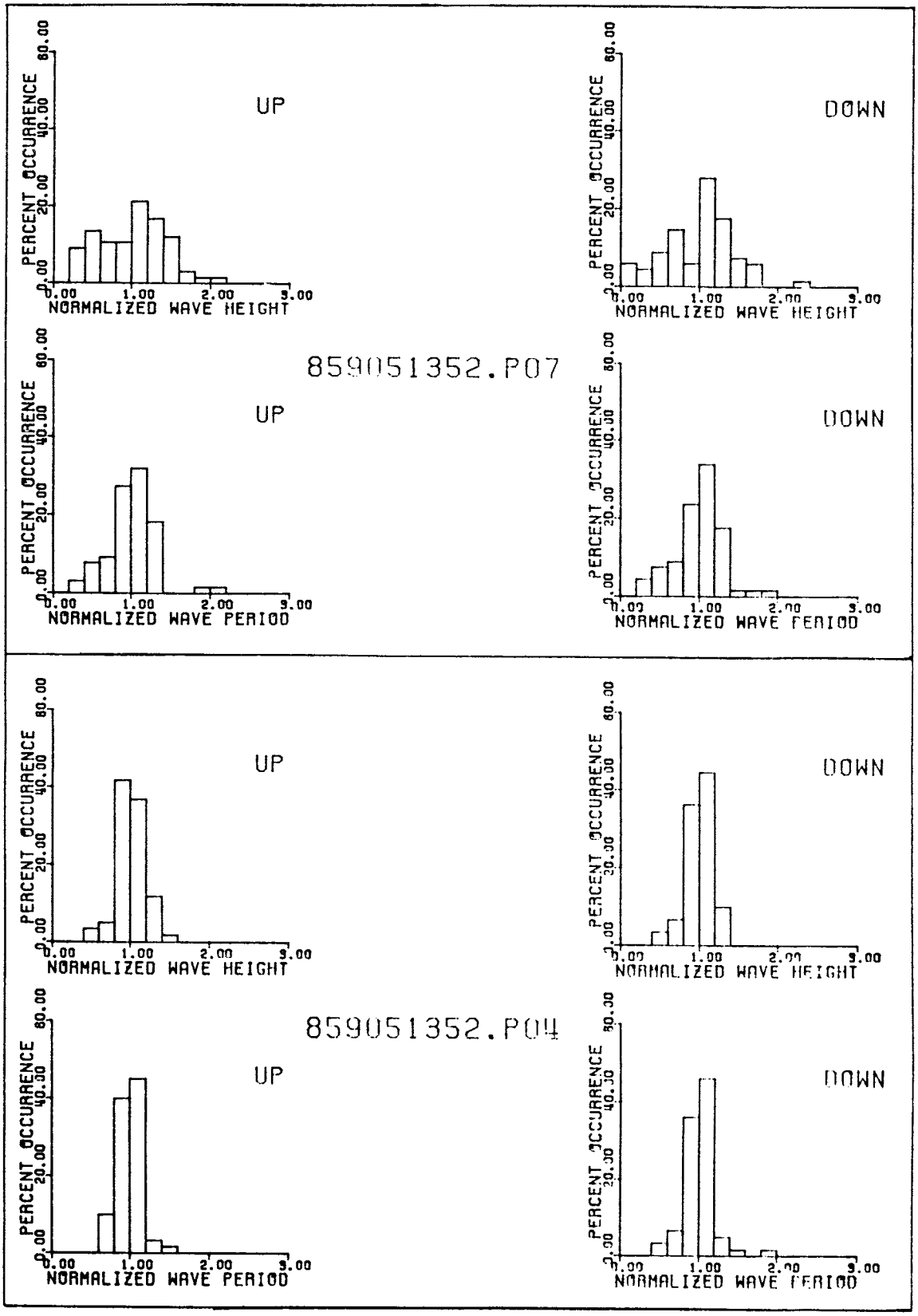

Figure 20. (Concluded)

distribution. These periods result from the existence of multiple crests in some wave forms; the multiple crests are sometimes identified as individual waves. If a wave with two crests is identified as two waves, the heights of these two waves are, most likely, each smaller than the height of the composite wave. This occurrence also would result in the computation of smaller wave heights. An increase in the number of waves identified near the breaker zone was computed for all the experiment runs.

76. Figure 20 shows the occurrence of a very long wave in results from the upcrossing method. This phenomenon probably indicates that the zero-crossing method was unable to detect one of the primary waves because of a very shallow trough relative to the zero-level of the high-passed data signal. Consequently, two waves were treated as one.

77. At pole P07, most of the waves had broken. Figure 20 shows the decrease in the number of higher wave heights, an indication that breaking has greatly reduced the heights of the majority of the waves. The wave height histograms are becoming more narrowly distributed about the mean. The wave period histograms at this location are quite similar to those computed at pole P10. They remain rather closely distributed about the mean.

78. Distributions of wave height become very narrowly banded at pole P04. This trend also was apparent in the individual wave forms shown in Figure 16, where the periodic bores exhibited nearly identical heights. The average wave height at this location is approximately 0.45 m, and the total water depth is approximately 0.9 m. The average height-to-depth ratio at this point in the inner surf zone is, therefore, 0.5. This value is much less than the value of 0.78 which is typically used to estimate surf zone wave heights. Values for the average wave height-to-depth ratio of approximately 0.5 were found during all experiment runs. Values for individual wave height-to-depth ratios of approximately 0.5 were also typically found in the inner surf zone. The wave period distributions at this location are nearly identical to those measured at pole P14; i.e., they remain narrowly banded about the mean wave period.

PART VI: CONCLUSIONS

79. The DUCK85 photopole experiment had three objectives: (a) to collect high quality water level and wave height data in, and just seaward of, the surf zone (to be used to improve methods for estimating wave conditions in the very nearshore zone), (b) to collect wave data in support of the sediment trap experiments, and (c) to determine ways to improve the photopole technique, including methods to facilitate fully automatic film analysis. The experiment was successful; all three goals were accomplished as described herein.

80. The first two objectives are quite similar. High quality data collection is needed for both nearshore wave estimation and for relating sediment transport rates to wave and current properties. An accurate method for directly measuring water surface elevation fluctuations was applied during the DUCK85 field project, and a high quality data set was obtained. Data were collected at a spatial and temporal resolution which adequately addressed the needs of both types of experiments.

81. Scientific procedures were used to analyze the water surface elevation data and to extract individual wave information from these data. Filtering techniques were successfully used to isolate longer period fluctuations. These water surface changes were removed from the measured data and, as a result, variations in elevation because of the shorter period and incident wave field were easily identified. The method used to identify only the primary, individual waves, those which were of interest to the investigators, was highly successful. Again, filtering techniques were used to eliminate effects of smaller, secondary waves.

82. Standard types of time series and individual wave analyses were applied to the data. The results presented in this report illustrate many features of the nearshore wave transformation process. However, the data contain much more information than was presented. Results given here reflect the immediate interests of the authors and the principal investigators of the sediment transport experiments.

83. The DUCK85 photopole experiment was a highly successful study in itself, but was also useful in testing the adequacy of the photopole method for application during a larger, follow-up field data collection project called SUPERDUCK. A great deal was learned concerning potential improvements

to the equipment arrangement used during the DUCK85 photopole experiment and to the film analysis procedures which were used to extract the water surface elevation data.

84. Analysis of film taken during the experiment revealed three ways in which the photopole method, as it was applied in this study, could be improved. The time required to manually digitize the film can be halved if movement of the cameras is eliminated, thereby eliminating the need to digitize the calibration rod in each photographic image because the rod position would not change. Secondly, the photopoles should be painted a color which contrasts with both the white water in the surf zone and the ambient water outside the breaker zone. The contrast between the bright yellow poles, used during DUCK85, and the white water was insufficient. Black would be a logical choice for the pole color. This second improvement should allow more film images to be digitized automatically. An automated procedure would greatly reduce the amount of person-hours required to digitize the film. The third improvement is the elimination of the smaller diameter poles from the pole transect. These poles were much more difficult to detect in the film images than were the larger diameter poles. The remainder of the camera system and operating procedures worked exceptionally well; no modifications are anticipated.

REFERENCES

Brenner, N. M. 1967. "Three FORTRAN Programs that Perform the Cooley-Tukey Transform," Technical Note 1967-2, Massachusetts Institute of Technology, Lincoln Laboratories, Lexington, Mass.

Carlson, C. T. 1984a. "Field Studies of Run-Up Generated by Wind Waves on Dissipative Beaches," Standard Research Institute International, Menlo Park, Calif.

_____. 1984b. "Field Studies of Run-Up on Dissipative Beaches," Nineteenth Coastal Engineering Conference, Proceedings of the International Conference, American Society of Civil Engineers, Vol 2, pp 399-414.

Ebersole, B. A. 1987. "Measurement and Prediction of Wave Height Decay in the Surf Zone," Proceedings of the Specialty Conference on Coastal Hydrodynamics, American Society of Civil Engineers, pp 1-16.

Field Research Facility. 1985 (Sep). "Preliminary Data Summary," Monthly Series, Coastal Engineering Research Center, US Army Engineer Waterways Experiment Station, Vicksburg, Miss.

Holman, R. A. 1986. "The Fall 1985 Nearshore Processes Experiment, Part III: Wave Runup and Nearshore Morphology," Proceedings of the 44th Meeting of the Coastal Engineering Research Board, Coastal Engineering Research Center, US Army Engineer Waterways Experiment Station, pp 95-99.

Holman, R. A., and Bowen, A. J. 1984. "Longshore Structure of Infragravity Motions," Journal of Geophysical Research, Vol 89, No. C4, pp 6446-6452.

Holman, R. A., and Guza, R. T. 1984. "Measuring Runup on Natural Beaches," Coastal Engineering, Vol 8, pp 129-140.

Hotta, S., and Mizuguchi, M. 1980. "A Field Study of Waves in the Surf Zone," Coastal Engineering in Japan, Vol 23, pp 59-79.

Hotta, S., Mizuguchi, M., and Isobe, M. 1981. "Observations of Long Period Waves in the Nearshore Zone," Coastal Engineering in Japan, pp 41-76.

_____. 1982. "A Field Study of Waves in the Nearshore Zone," Proceedings of the Eighteenth Coastal Engineering Conference, American Society of Civil Engineers, Vol 1, pp 38-57.

Hughes, S. A., and Borgman L. E. 1987. "Beta-Rayleigh Distribution for Shallow Water Wave Heights," Proceedings of the Specialty Conference on Coastal Hydrodynamics, American Society of Civil Engineers, pp 17-31.

Kraus, N. C. 1986. "The Fall 1985 Nearshore Processes Experiment, Part III: Surf Zone Sediment Transport and Wave Transformation Experiments," Proceedings of the 44th Meeting of the Coastal Engineering Research Board, Coastal Engineering Research Center, US Army Engineer Waterways Experiment Station, pp 82-95.

Kraus, N. C., and Dean, J. L. 1987. "Longshore Sand Transport Rate Distributions Measured by Trap," Proceedings, Coastal Sediments '87, pp 881-896.

Maresca, J. W., Jr., and Seibel, E. 1976. "Terrestrial Photogrammetric Measurements of Breaking Waves and Longshore Currents in the Nearshore Zone," Proceedings of the Fifteenth Coastal Engineering Conference, American Society of Civil Engineers, Vol 1, pp 681-700.

Mason, C. 1986. "The Fall 1985 Nearshore Processes Experiment, Part I: An Overview of the Experiment," Proceedings of the 44th Meeting of the Coastal Engineering Research Board, Coastal Engineering Research Center, US Army Engineer Waterways Experiment Station, pp 72-82.

Mason, C., Birkemeier, W. A., and Howd, P. A. 1987. "An Overview of DUCK85, A Nearshore Processes Experiment," Proceedings, Coastal Sediments '87, American Society of Civil Engineers, pp 818-833.

Mizuguchi, M. 1982. "Individual Wave Analysis of Irregular Wave Deformation in the Nearshore Zone," Proceedings of the Eighteenth Coastal Engineering Conference, American Society of Civil Engineers, Vol 1, pp 485-504.

Nath, J. H., and Dean, R. G. 1984. "Natural Hazards and Research Needs in Coastal and Ocean Engineering," Summary and Recommendations to the National Science Foundation and the Office of Naval Research, Civil and Environmental Engineering Division, National Science Foundation, Oregon State University, Corvallis, Oregon.

Otnes, R. K., and Enochson, L. 1972. Digital Time Series Analysis, John Wiley & Sons, New York, pp 281-285.

Shore Protection Manual. 1984. 4th ed., 2 vols, US Army Engineer Waterways Experiment Station, Coastal Engineering Research Center, US Government Printing Office, Washington, DC.

Suhayda, N. J., and Pettigrew, J. R. 1977. "Observation of Wave Height and Wave Celerity in the Surf Zone," Journal of Geophysical Research, Vol 82, No. 9, pp 1419-1424.

Weishar, L. L., and Byrne, R. J. 1978. "Field Study of Breaking Wave Characteristics," Proceedings of the Sixteenth Coastal Engineering Conference, American Society of Civil Engineers, Vol 1, pp 487-506.

APPENDIX A: SELECTED WATER SURFACE ELEVATION TIME SERIES

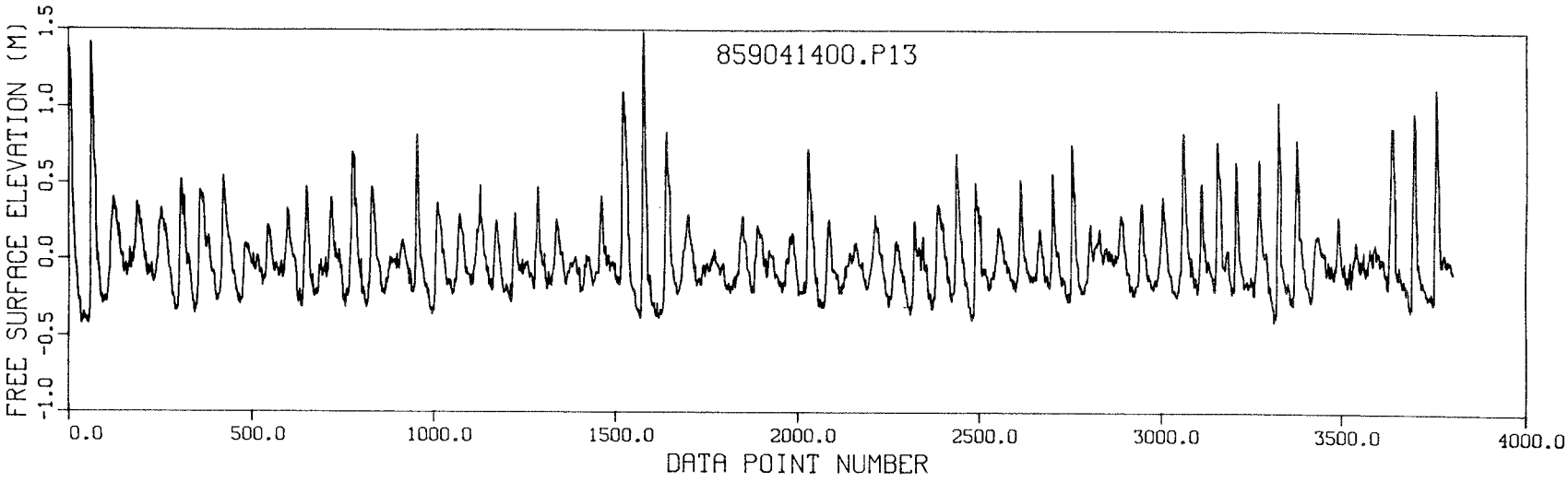
859041400.P13
FREE SURFACE ELEVATION (M)
1.5
1.0
0.5
0.0
-0.5
-1.0
0.0
500.0
1000.0
1500.0
2000.0
2500.0
3000.0
3500.0
4000.0
DATA POINT NUMBER

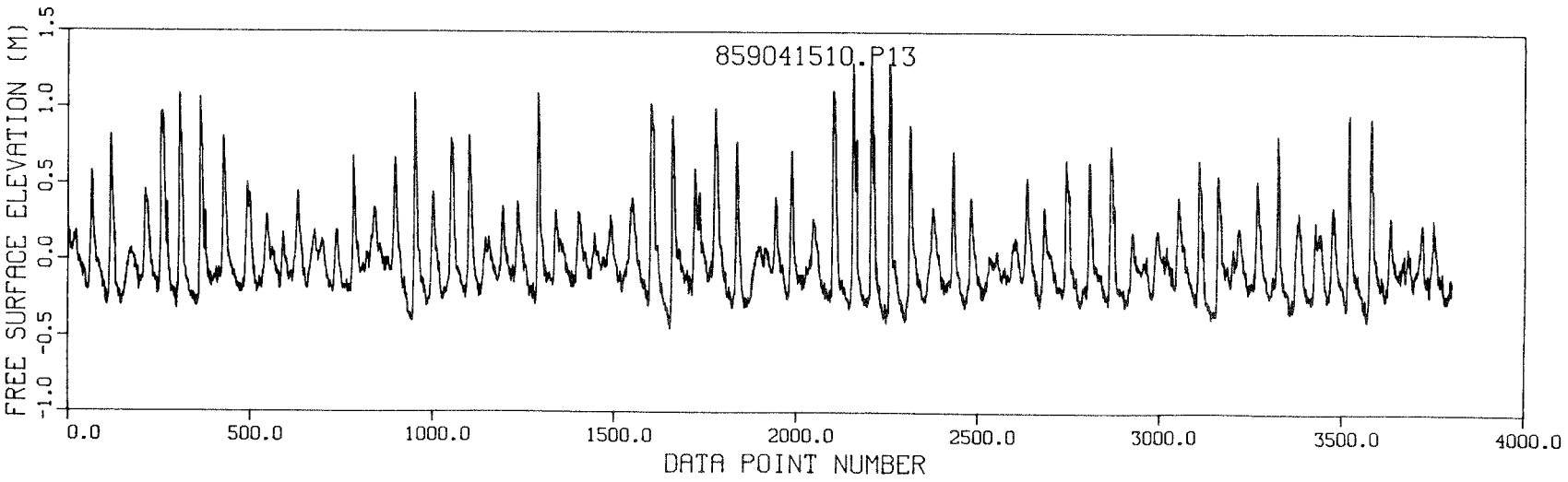
859041510.P13
FREE SURFACE ELEVATION (M)
1.5
1.0
0.5
0.0
-0.5
-1.0
0.0
500.0
1000.0
1500.0
2000.0
2500.0
3000.0
3500.0
4000.0
DATA POINT NUMBER

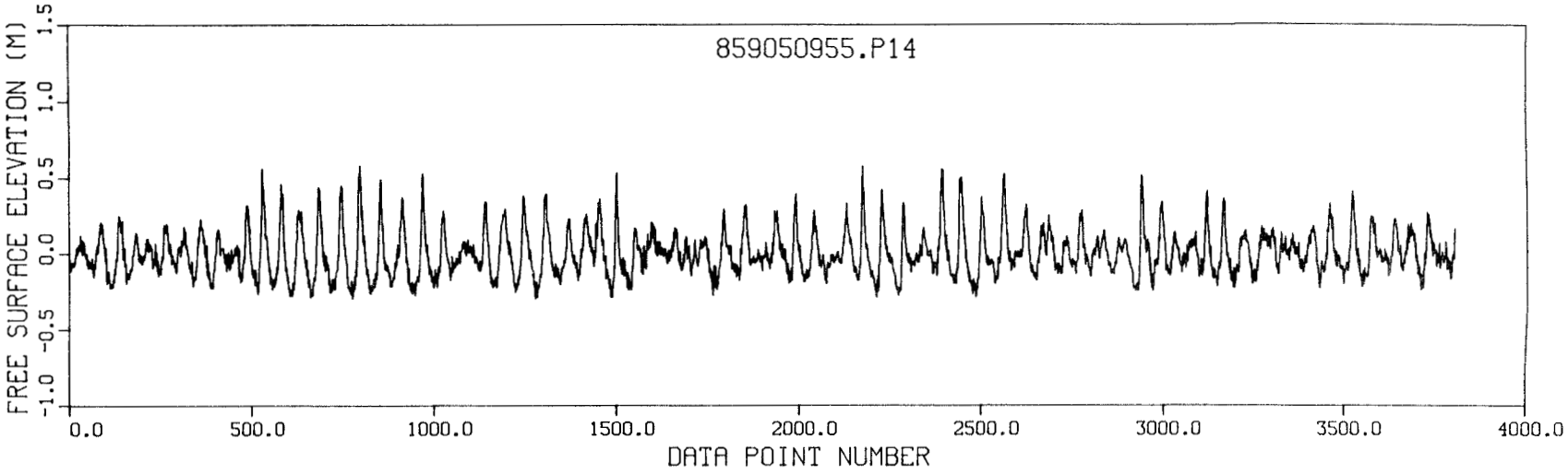
859050955.P14
FREE SURFACE ELEVATION (M)
1.5
1.0
0.5
0.0
-0.5
-1.0
0.0
500.0
1000.0
1500.0
2000.0
2500.0
3000.0
3500.0
4000.0
DATA POINT NUMBER

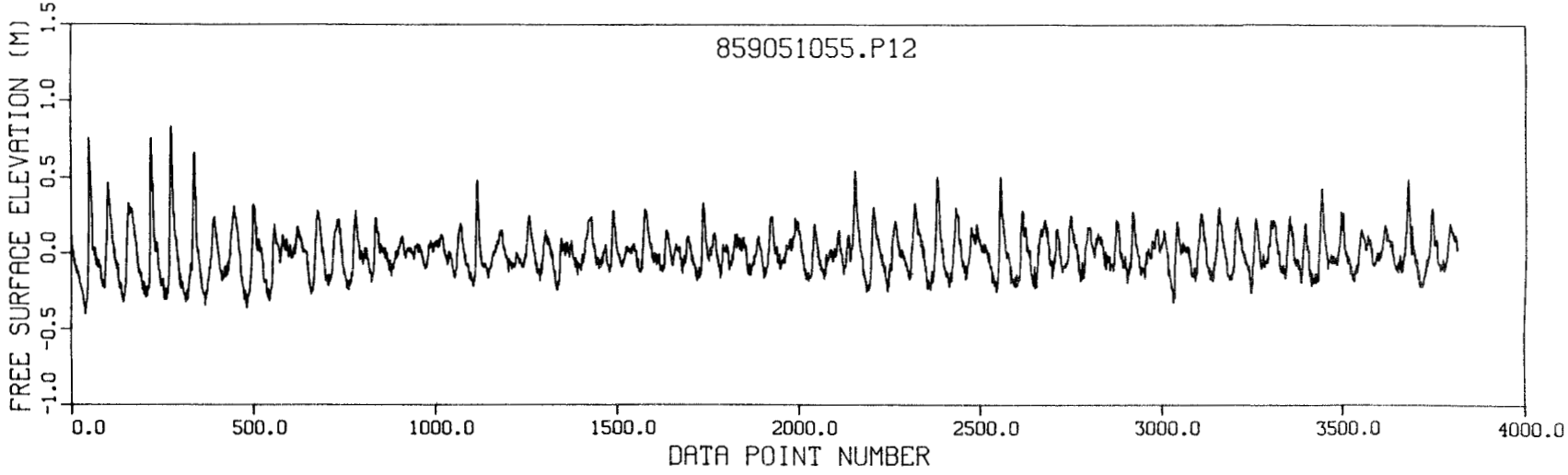
859051055.P12
FREE SURFACE ELEVATION (M)
1.5
1.0
0.5
0.0
-0.5
-1.0
0.0
500.0
1000.0
1500.0
2000.0
2500.0
3000.0
3500.0
4000.0
DATA POINT NUMBER

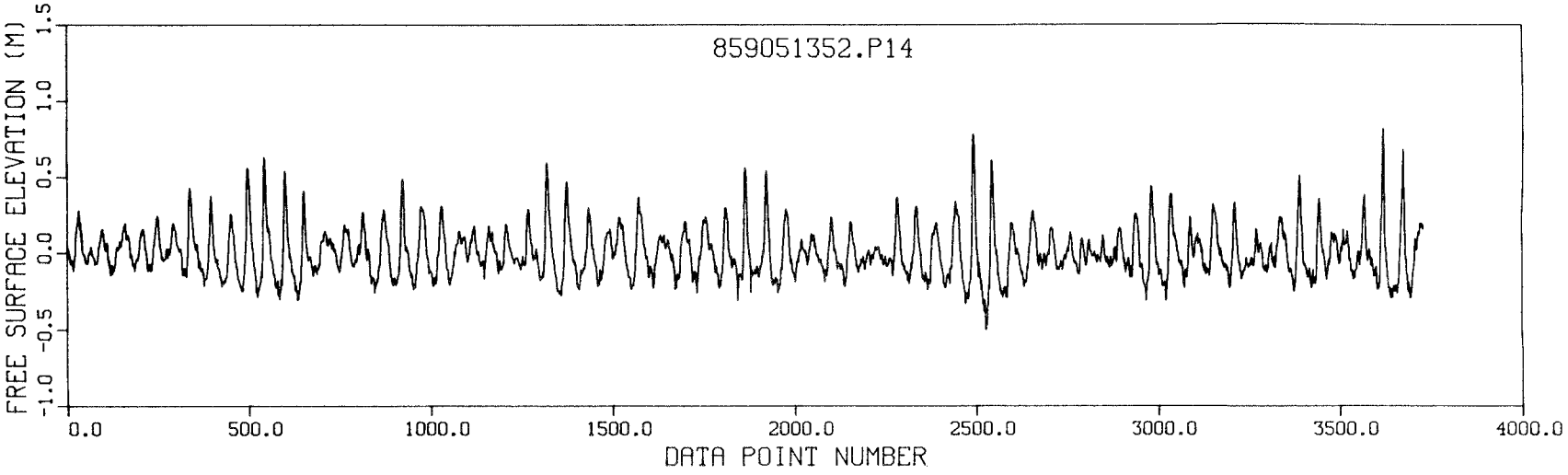
859051352.P14
FREE SURFACE ELEVATION (M)
1.5
1.0
0.5
0.0
-0.5
-1.0
0.0
500.0
1000.0
1500.0
2000.0
2500.0
3000.0
3500.0
4000.0
DATA POINT NUMBER

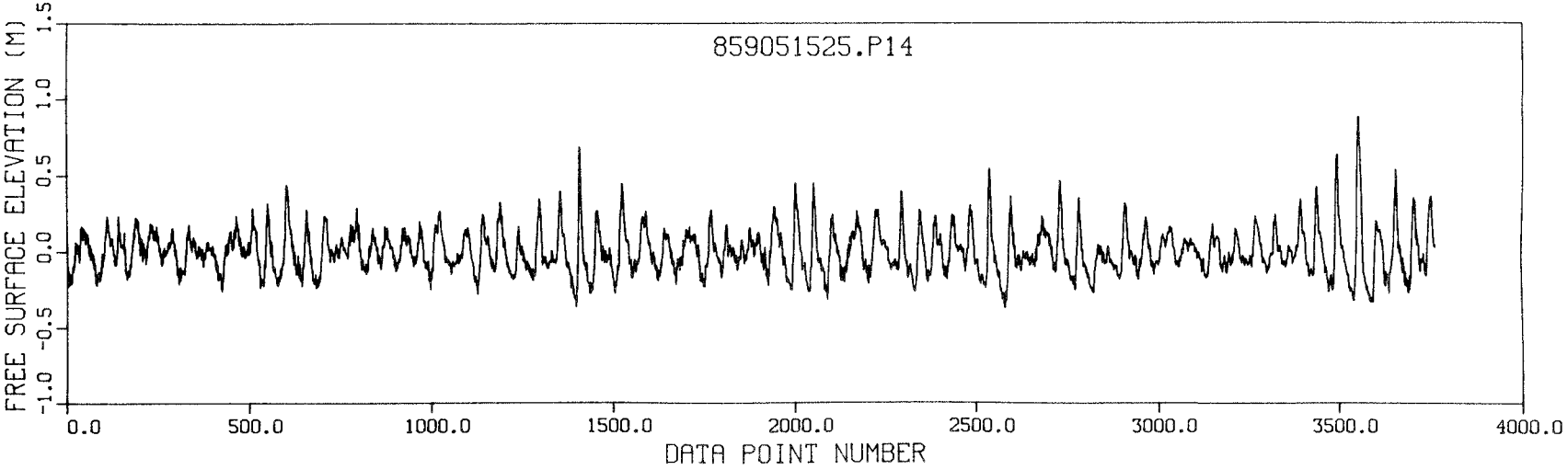
859051525.P14
FREE SURFACE ELEVATION (M)
1.5
1.0
0.5
0.0
-0.5
-1.0
0.0
500.0
1000.0
1500.0
2000.0
2500.0
3000.0
3500.0
4000.0
DATA POINT NUMBER

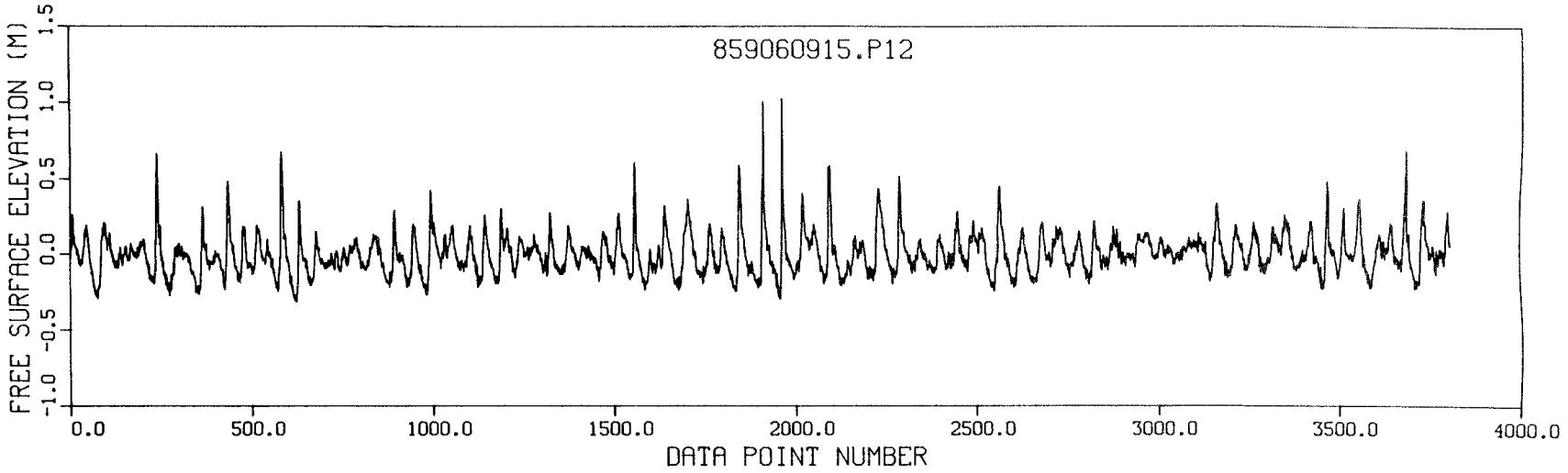
859060915.P12
FREE SURFACE ELEVATION (M)
1.5
1.0
0.5
0.0
-0.5
-1.0
0.0
500.0
1000.0
1500.0
2000.0
2500.0
3000.0
3500.0
4000.0
DATA POINT NUMBER

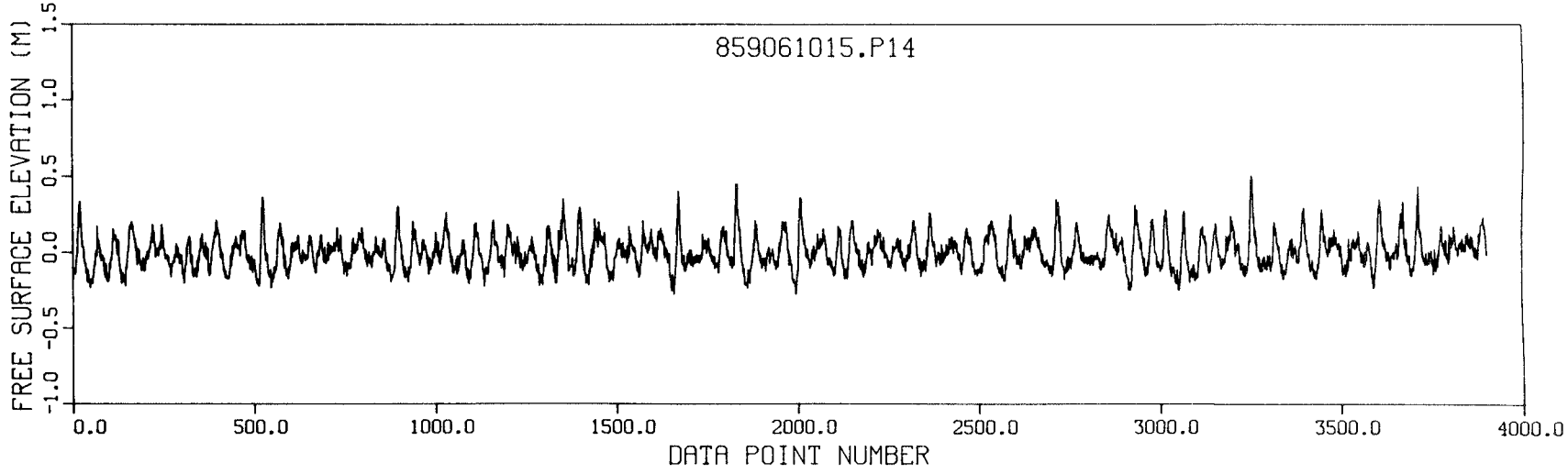
859061015.P14
FREE SURFACE ELEVATION (M)
1.5
1.0
0.5
0.0
-0.5
-1.0
0.0
500.0
1000.0
1500.0
2000.0
2500.0
3000.0
3500.0
4000.0
DATA POINT NUMBER

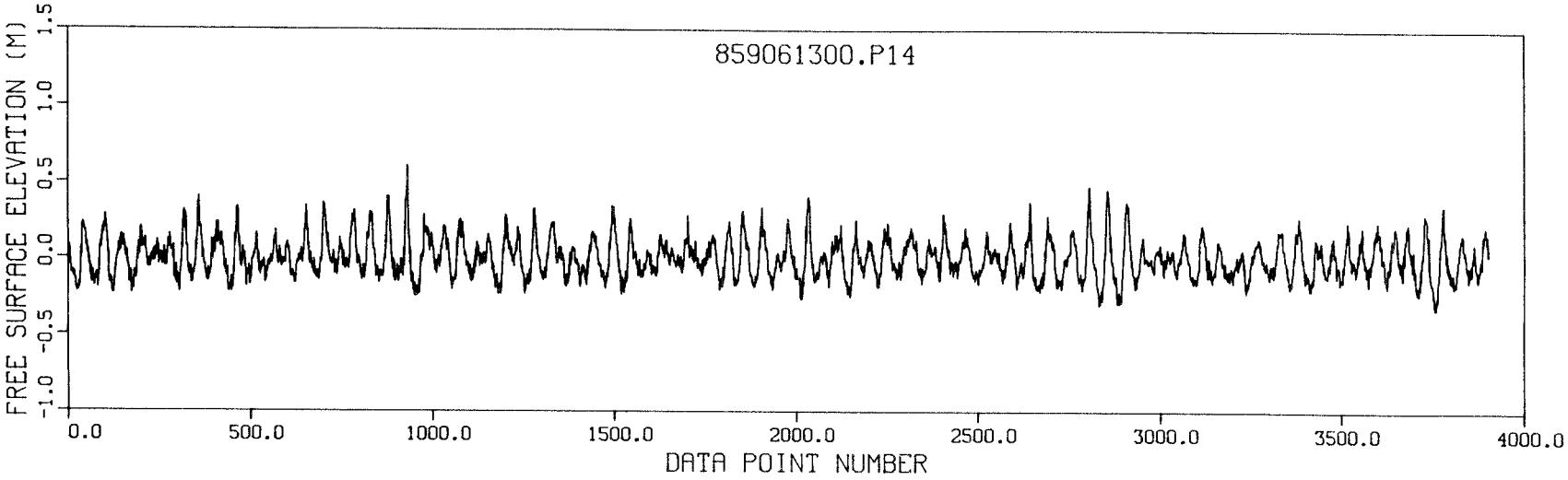
859061300.P14
FREE SURFACE ELEVATION (M)
1.5
1.0
0.5
0.0
-0.5
-1.0
0.0
500.0
1000.0
1500.0
2000.0
2500.0
3000.0
3500.0
4000.0
DATA POINT NUMBER

APPENDIX B: WAVE SPECTRA

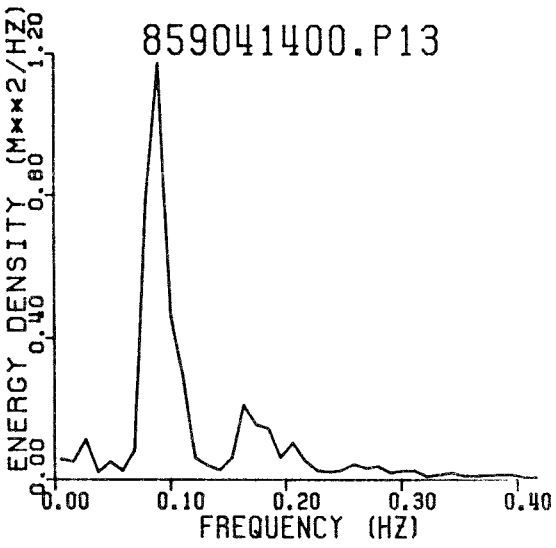
859041400.P13
ENERGY DENSITY (M**2/HZ)
0.00
0.40
0.80
1.20
0.00
0.10
0.20
0.30
0.40
FREQUENCY (HZ)

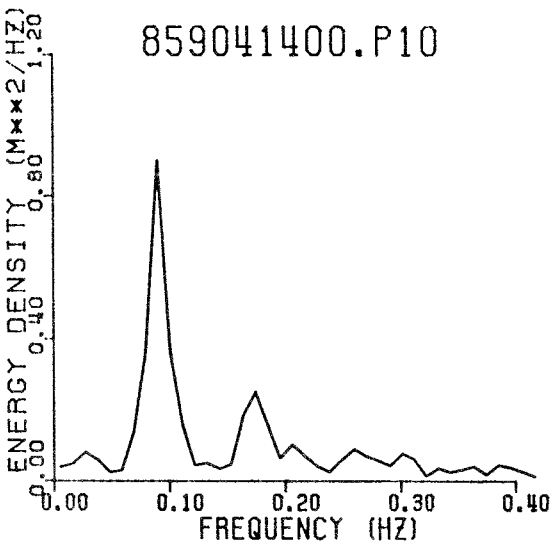
859041400.P10
ENERGY DENSITY (M**2/HZ)
0.00
0.40
0.80
1.20
0.00
0.10
0.20
0.30
0.40
FREQUENCY (HZ)

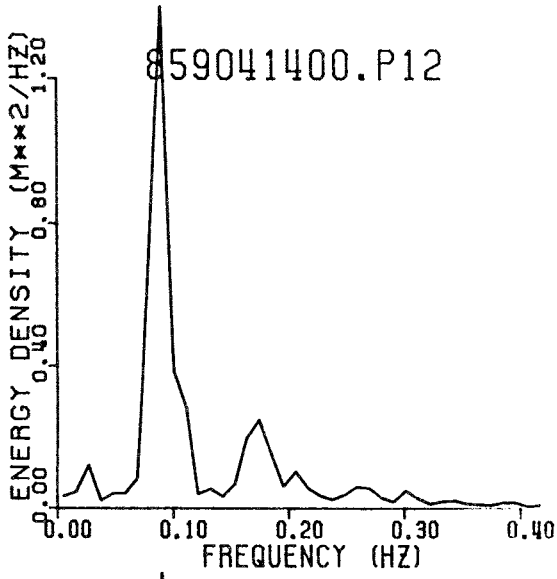
859041400.P12
ENERGY DENSITY (M**2/HZ)
0.00
0.40
0.80
1.20
0.00
0.10
0.20
0.30
0.40
FREQUENCY (HZ)

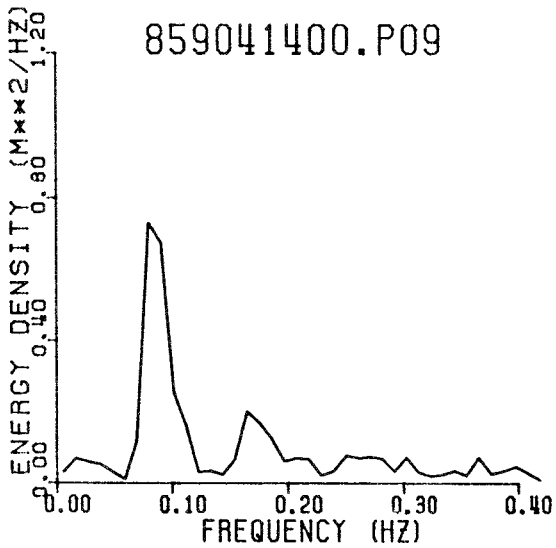
859041400.P09
ENERGY DENSITY (M**2/HZ)
0.00
0.40
0.80
1.20
0.00
0.10
0.20
0.30
0.40
FREQUENCY (HZ)

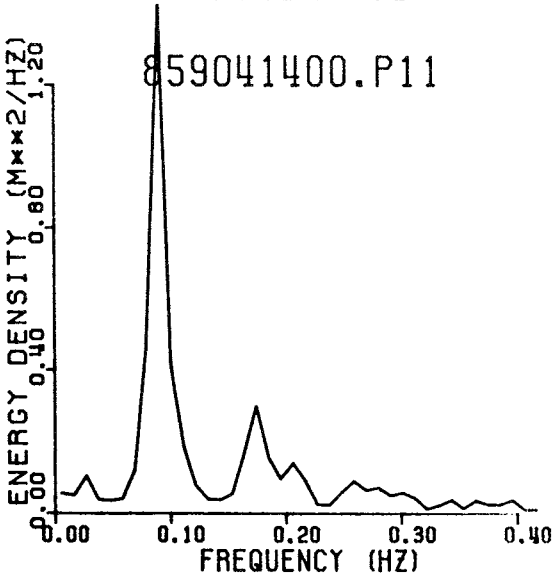
859041400.P11
ENERGY DENSITY (M**2/HZ)
0.00
0.40
0.80
1.20
0.00
0.10
0.20
0.30
0.40
FREQUENCY (HZ)

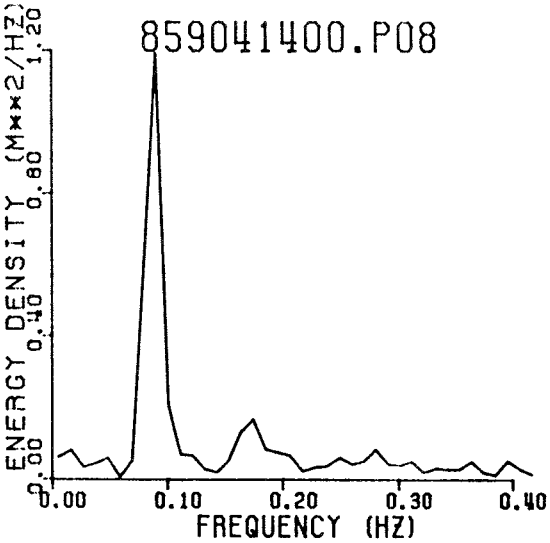
859041400.P08
ENERGY DENSITY (M**2/HZ)
0.00
0.40
0.80
1.20
0.00
0.10
0.20
0.30
0.40
FREQUENCY (HZ)

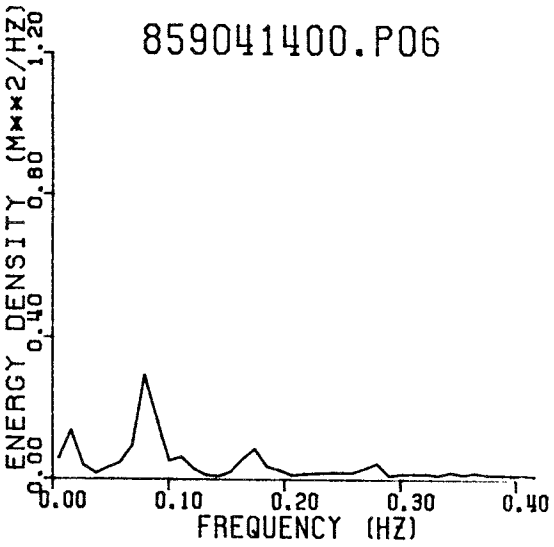
859041400.P06
ENERGY DENSITY (M**2/HZ)
0.00
0.40
0.80
1.20
0.00
0.10
0.20
0.30
0.40
FREQUENCY (HZ)

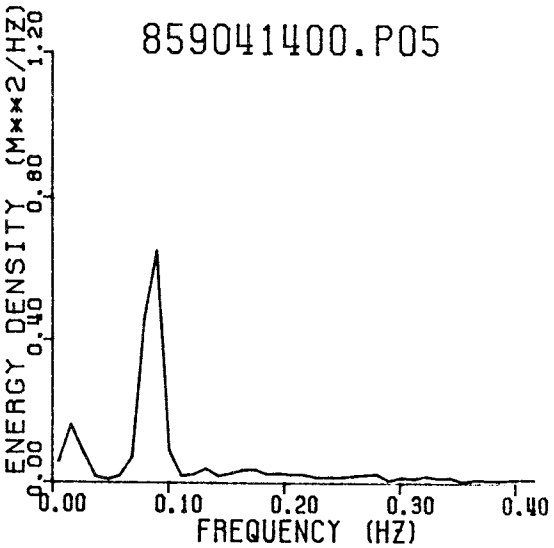
859041400.P05
ENERGY DENSITY (M**2/HZ)
0.00
0.40
0.80
1.20
0.00
0.10
0.20
0.30
0.40
FREQUENCY (HZ)

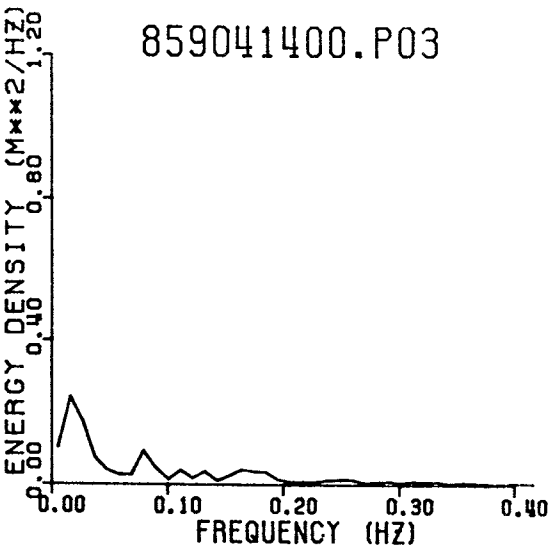
859041400.P03
ENERGY DENSITY (M**2/HZ)
0.00
0.40
0.80
1.20
0.00
0.10
0.20
0.30
0.40
FREQUENCY (HZ)

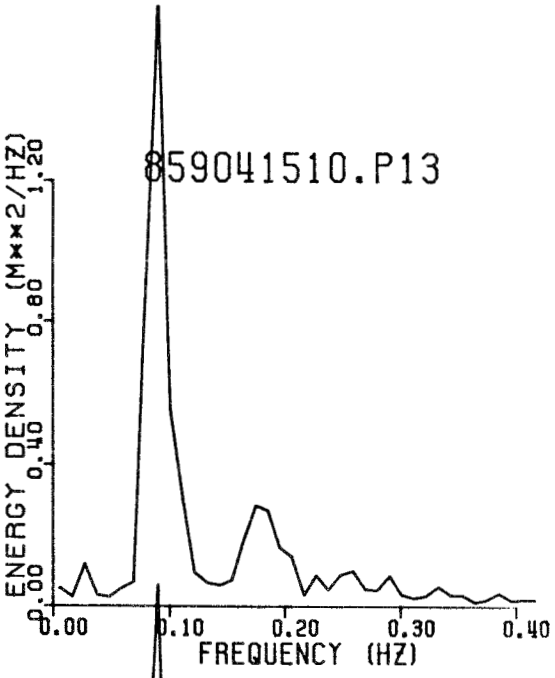
859041510.P13
ENERGY DENSITY (M**2/HZ)
0.00
0.40
0.80
1.20
0.00
0.10
0.20
0.30
0.40
FREQUENCY (HZ)

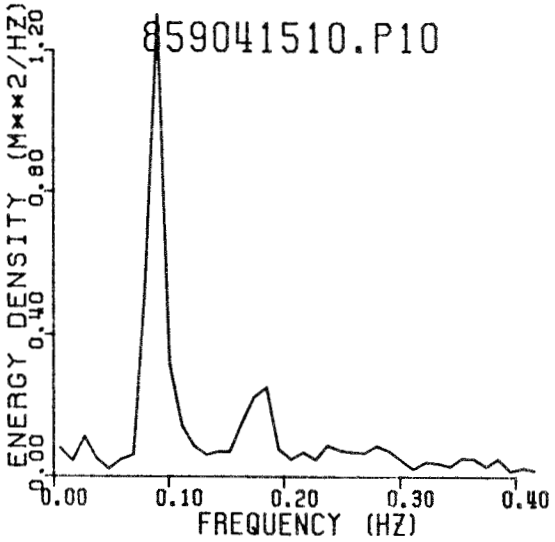
859041510.P10
ENERGY DENSITY (M**2/HZ)
0.00
0.40
0.80
1.20
0.00
0.10
0.20
0.30
0.40
FREQUENCY (HZ)

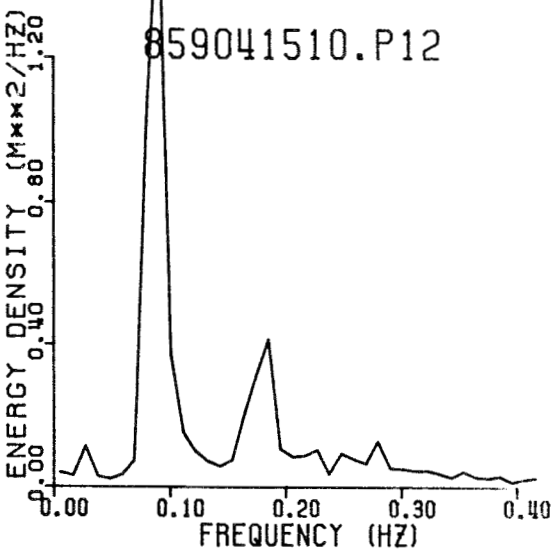
859041510.P12
ENERGY DENSITY (M**2/HZ)
0.00
0.40
0.80
1.20
0.00
0.10
0.20
0.30
0.40
FREQUENCY (HZ)

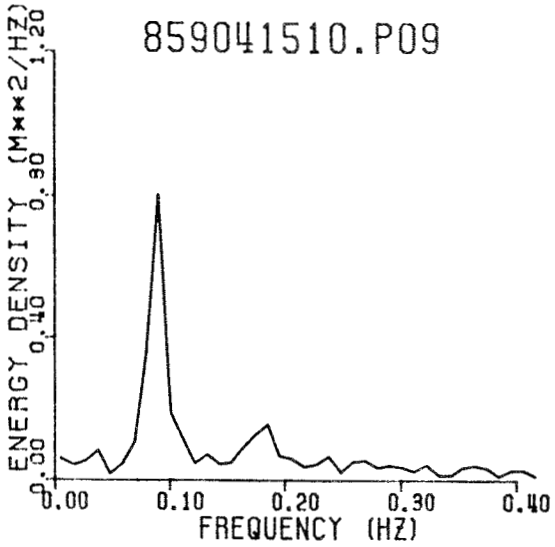
859041510.P09
ENERGY DENSITY (M**2/HZ)
0.00
0.40
0.80
1.20
0.00
0.10
0.20
0.30
0.40
FREQUENCY (HZ)

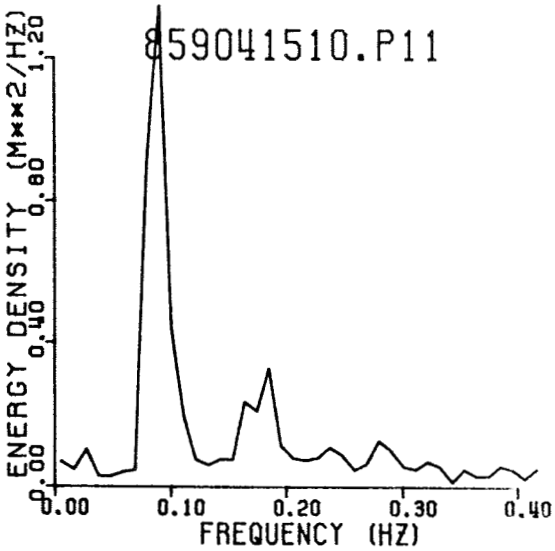
859041510.P11
ENERGY DENSITY (M**2/HZ)
0.00
0.40
0.80
1.20
0.00
0.10
0.20
0.30
0.40
FREQUENCY (HZ)

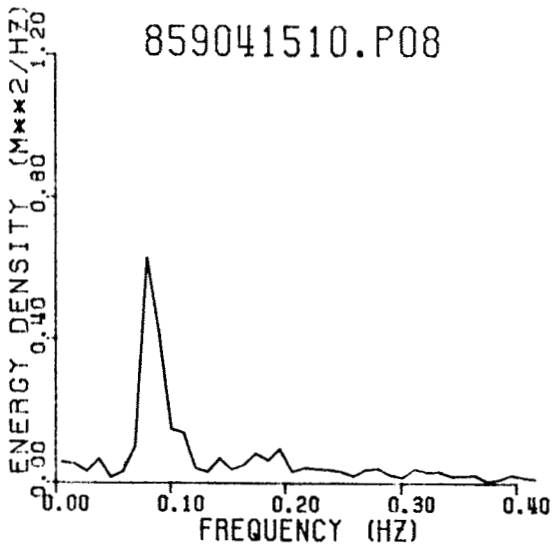
859041510.P08
ENERGY DENSITY (M**2/HZ)
0.00
0.40
0.80
1.20
0.00
0.10
0.20
0.30
0.40
FREQUENCY (HZ)

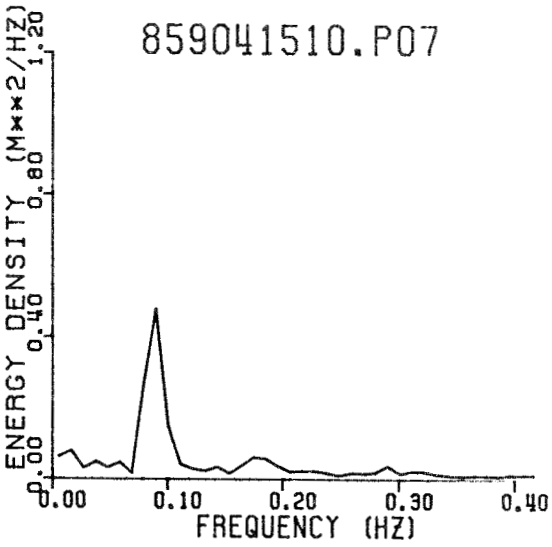
859041510.P07
ENERGY DENSITY (M**2/HZ)
0.00
0.40
0.80
1.20
0.00
0.10
0.20
0.30
0.40
FREQUENCY (HZ)

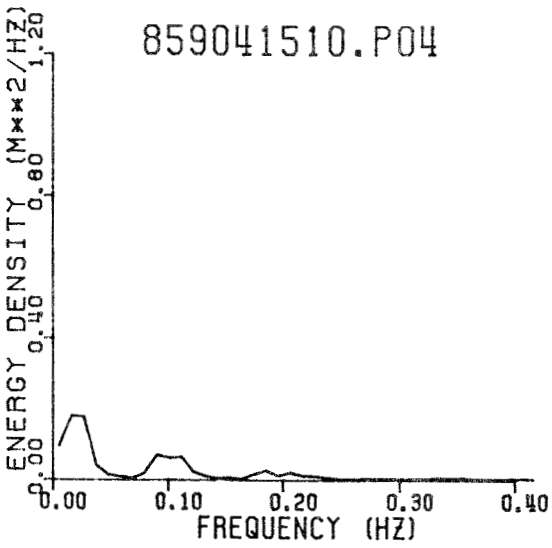
859041510.P04
ENERGY DENSITY (M**2/HZ)
0.00
0.40
0.80
1.20
0.00
0.10
0.20
0.30
0.40
FREQUENCY (HZ)

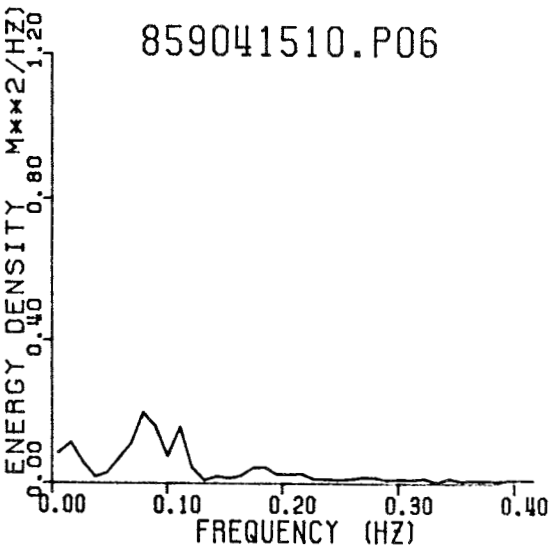
859041510.P06
ENERGY DENSITY M**2/HZ)
0.00
0.40
0.80
1.20
0.00
0.10
0.20
0.30
0.40
FREQUENCY (HZ)

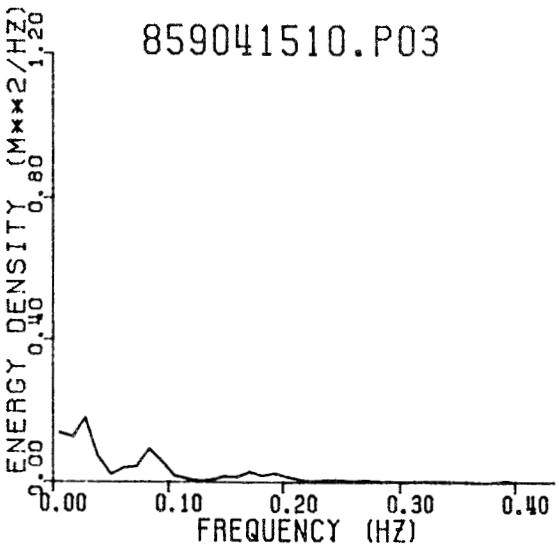
859041510.P03
ENERGY DENSITY (M**2/HZ)
0.00
0.40
0.80
1.20
0.00
0.10
0.20
0.30
0.40
FREQUENCY (HZ)

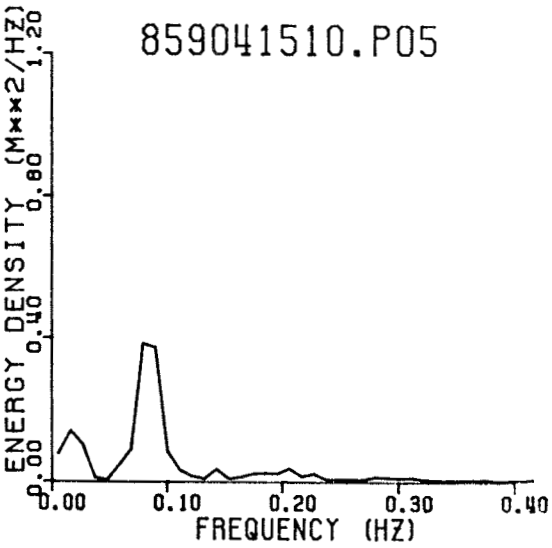
859041510.P05
ENERGY DENSITY (M**2/HZ)
0.00
0.40
0.80
1.20
0.00
0.10
0.20
0.30
0.40
FREQUENCY (HZ)

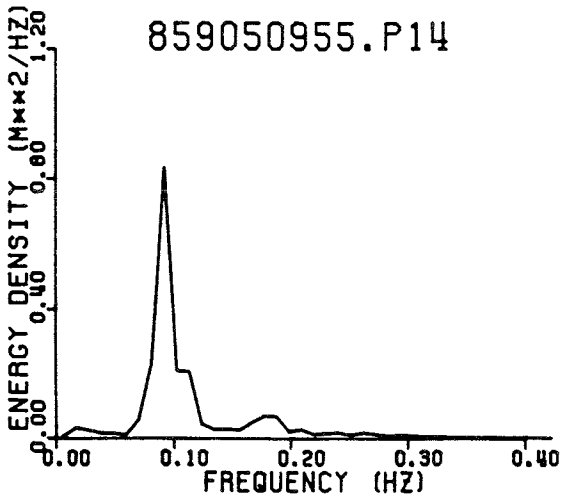
859050955.P14
ENERGY DENSITY (M**2/HZ)
0.00
0.40
0.80
1.20
0.00
0.10
0.20
0.30
0.40
FREQUENCY (HZ)

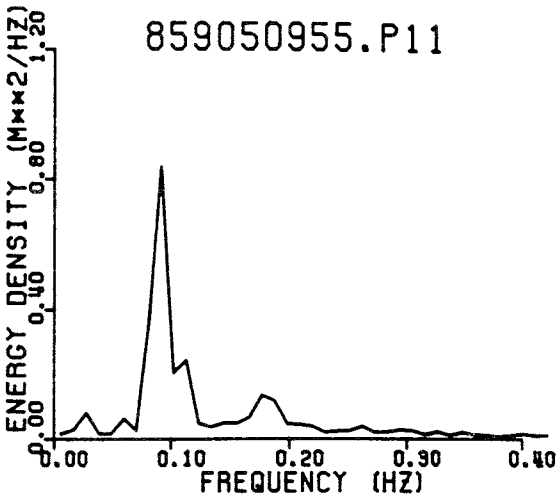
859050955.P11
ENERGY DENSITY (M**2/HZ)
0.00
0.40
0.80
1.20
0.00
0.10
0.20
0.30
0.40
FREQUENCY (HZ)

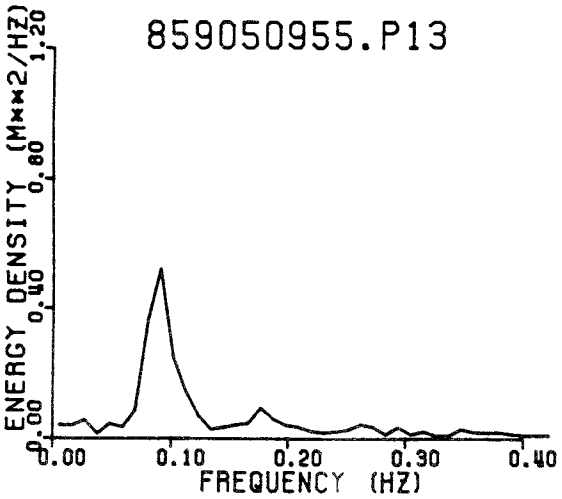
859050955.P13
ENERGY DENSITY (M**2/HZ)
0.00
0.40
0.80
1.20
0.00
0.10
0.20
0.30
0.40
FREQUENCY (HZ)

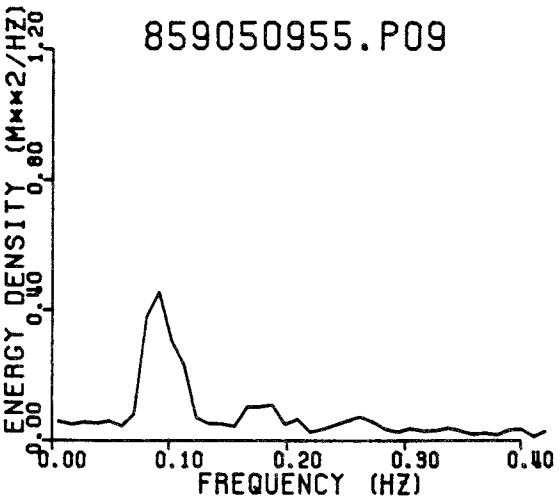
859050955.P09
ENERGY DENSITY (M**2/HZ)
0.00
0.40
0.80
1.20
0.00
0.10
0.20
0.30
0.40
FREQUENCY (HZ)

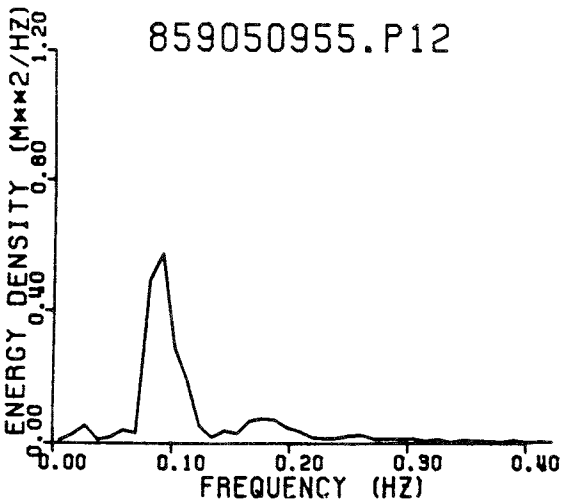
859050955.P12
ENERGY DENSITY (M**2/HZ)
0.00
0.40
0.80
1.20
0.00
0.10
0.20
0.30
0.40
FREQUENCY (HZ)

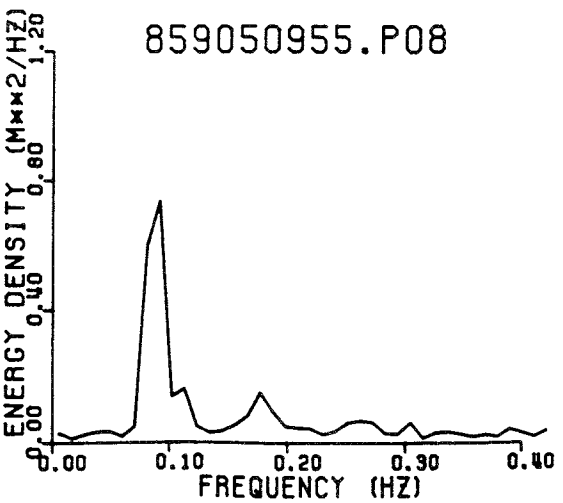
859050955.P08
ENERGY DENSITY (M**2/HZ)
0.00
0.40
0.80
1.20
0.00
0.10
0.20
0.30
0.40
FREQUENCY (HZ)

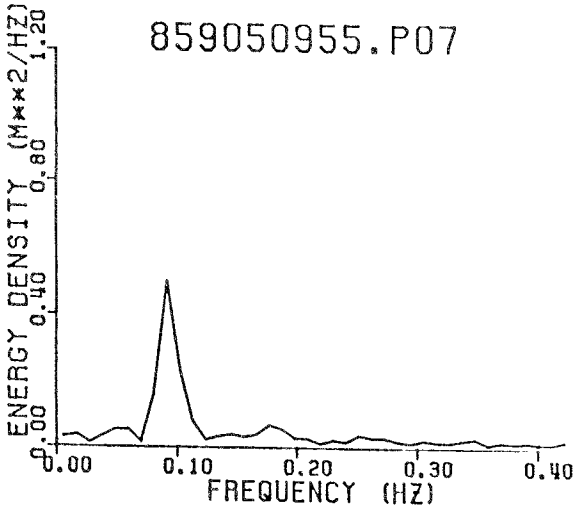
859050955.P07
ENERGY DENSITY (M**2/HZ)
0.00
0.40
0.80
1.20
0.00
0.10
0.20
0.30
0.40
FREQUENCY (HZ)

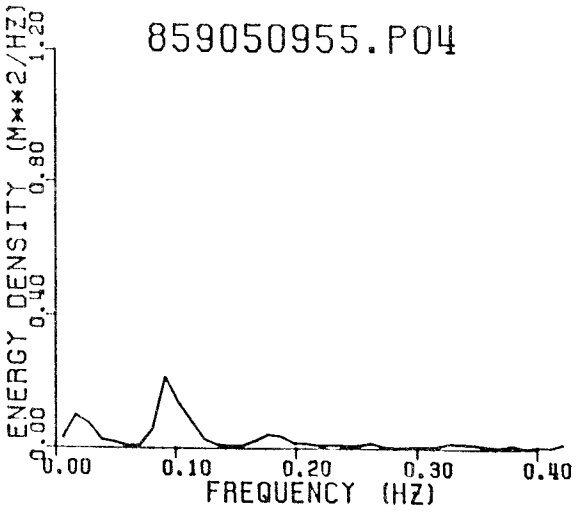
859050955.P04
ENERGY DENSITY (M**2/HZ)
0.00
0.40
0.80
1.20
0.00
0.10
0.20
0.30
0.40
FREQUENCY (HZ)

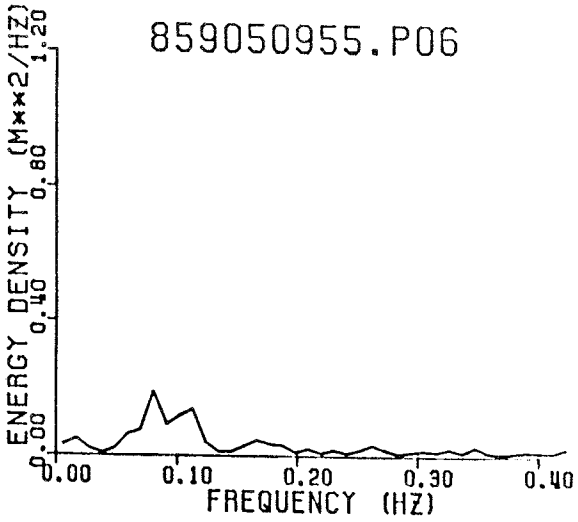
859050955.P06
ENERGY DENSITY (M**2/HZ)
0.00
0.40
0.80
1.20
0.00
0.10
0.20
0.30
0.40
FREQUENCY (HZ)

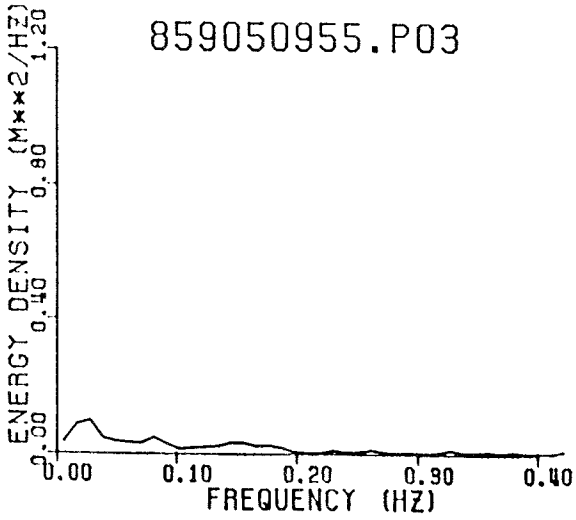
859050955.P03
ENERGY DENSITY (M**2/HZ)
0.00
0.40
0.80
1.20
0.00
0.10
0.20
0.30
0.40
FREQUENCY (HZ)

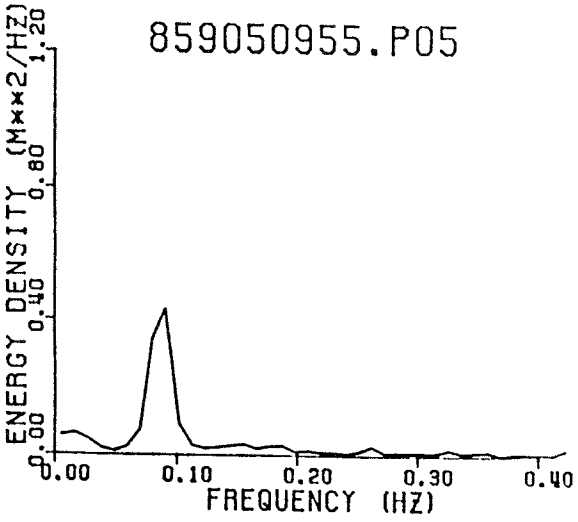
859050955.P05
ENERGY DENSITY (M**2/HZ)
0.00
0.40
0.80
1.20
0.00
0.10
0.20
0.30
0.40
FREQUENCY (HZ)

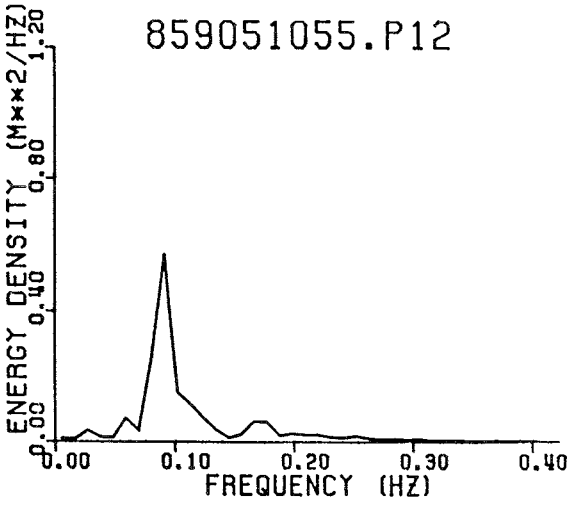
859051055.P12
ENERGY DENSITY (M**2/HZ)
0.00
0.40
0.80
1.20
0.00
0.10
0.20
0.30
0.40
FREQUENCY (HZ)

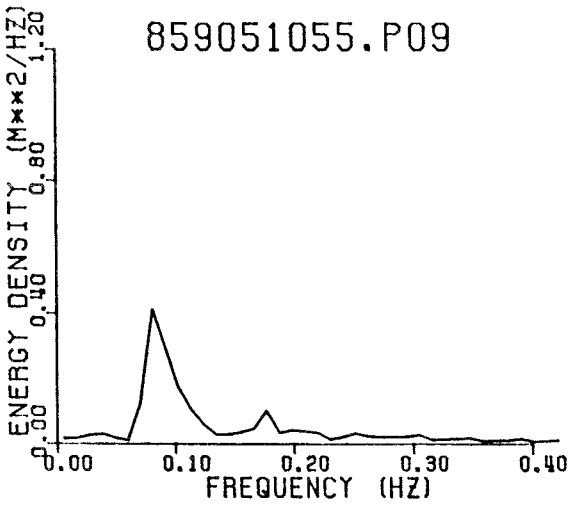
859051055.P09
ENERGY DENSITY (M**2/HZ)
0.00
0.40
0.80
1.20
0.00
0.10
0.20
0.30
0.40
FREQUENCY (HZ)

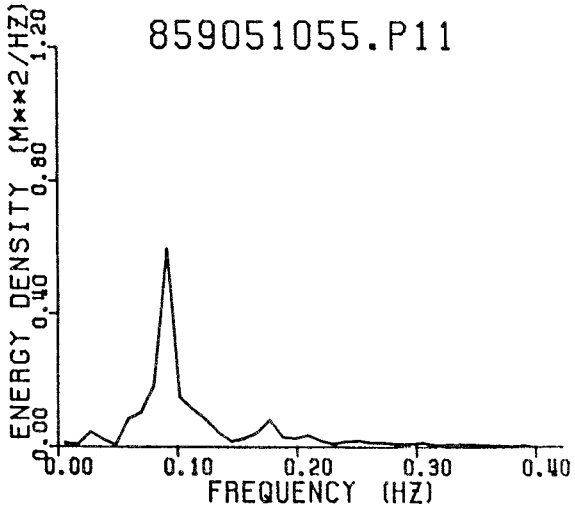
859051055.P11
ENERGY DENSITY (M**2/HZ)
0.00
0.40
0.80
1.20
0.00
0.10
0.20
0.30
0.40
FREQUENCY (HZ)

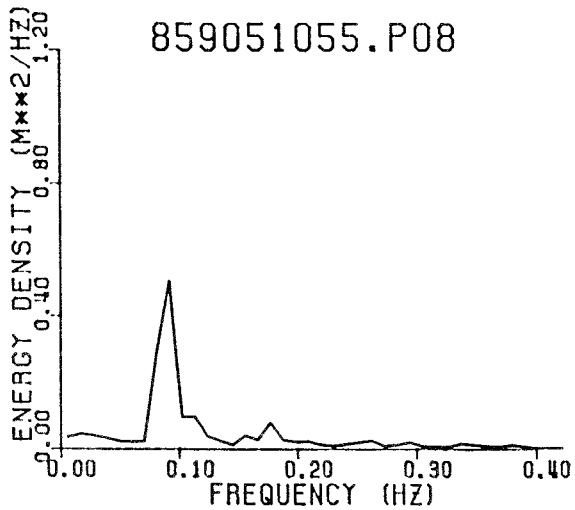
859051055.P08
ENERGY DENSITY (M**2/HZ)
0.00
0.40
0.80
1.20
0.00
0.10
0.20
0.30
0.40
FREQUENCY (HZ)

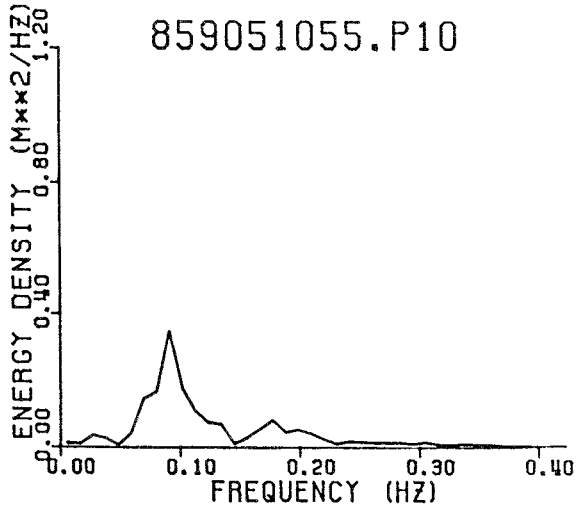
859051055.P10
ENERGY DENSITY (M**2/HZ)
0.00
0.40
0.80
1.20
0.00
0.10
0.20
0.30
0.40
FREQUENCY (HZ)

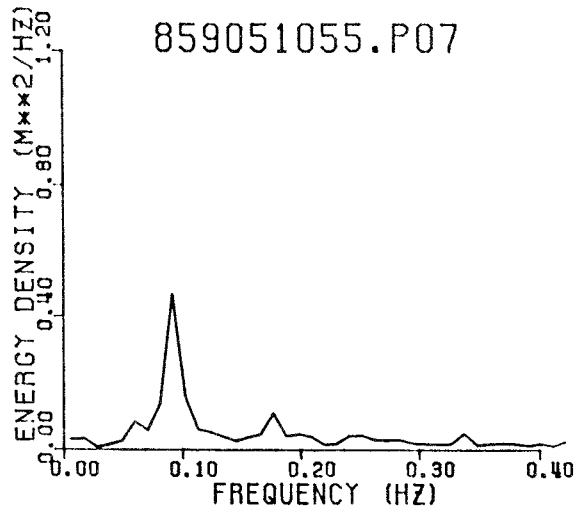
859051055.P07
ENERGY DENSITY (M**2/HZ)
0.00
0.40
0.80
1.20
0.00
0.10
0.20
0.30
0.40
FREQUENCY (HZ)

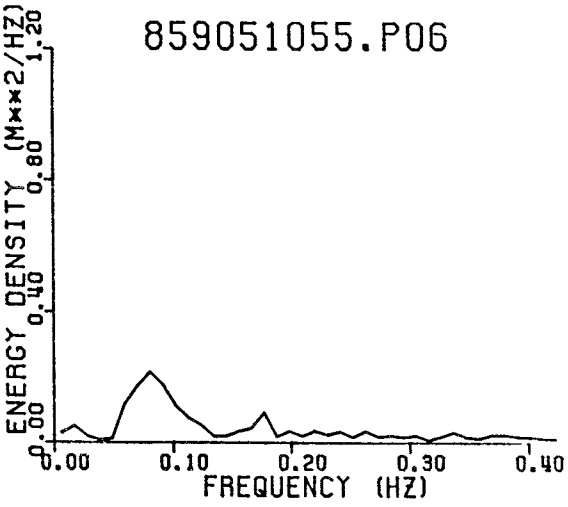
859051055.P06
ENERGY DENSITY (M**2/HZ)
0.00
0.40
0.80
1.20
0.00
0.10
0.20
0.30
0.40
FREQUENCY (HZ)

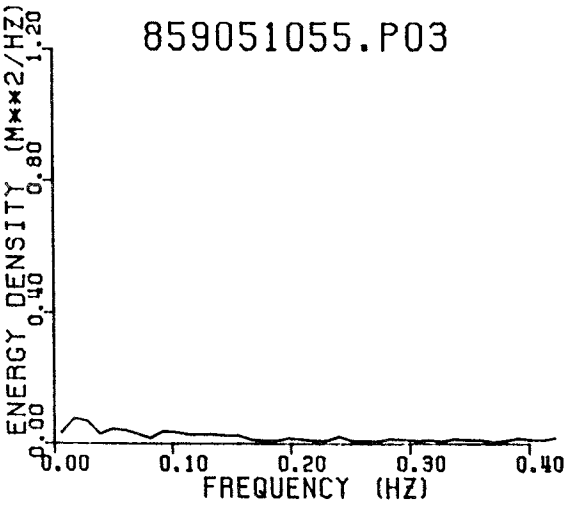
859051055.P03
ENERGY DENSITY (M**2/HZ)
0.00
0.40
0.80
1.20
0.00
0.10
0.20
0.30
0.40
FREQUENCY (HZ)

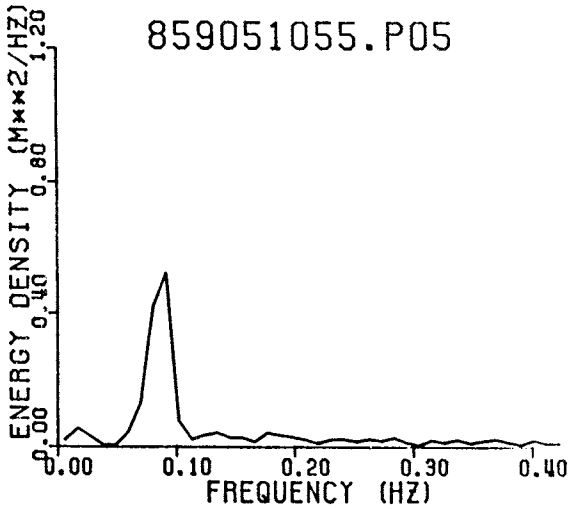
859051055.P05
ENERGY DENSITY (M**2/HZ)
0.00
0.40
0.80
1.20
0.00
0.10
0.20
0.30
0.40
FREQUENCY (HZ)

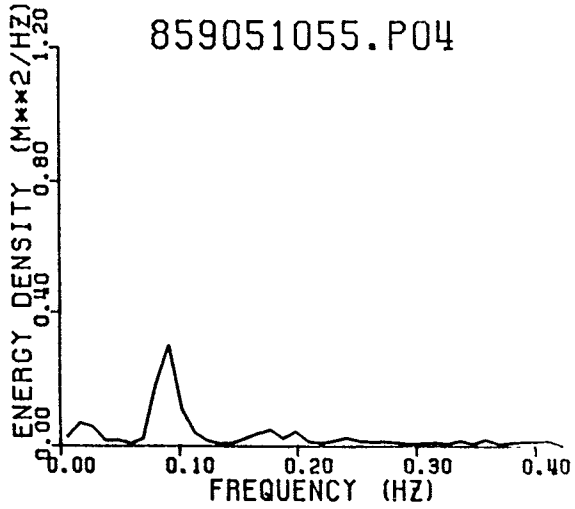
859051055.P04
ENERGY DENSITY (M**2/HZ)
0.00
0.40
0.80
1.20
0.00
0.10
0.20
0.30
0.40
FREQUENCY (HZ)

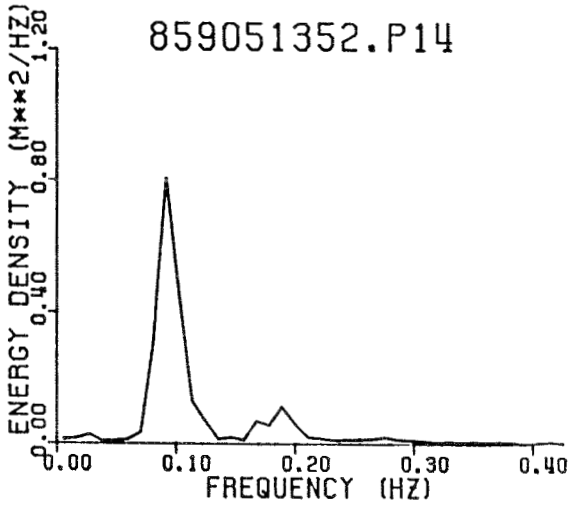
859051352.P14
ENERGY DENSITY (M**2/HZ)
0.00
0.40
0.80
1.20
0.00
0.10
0.20
0.30
0.40
FREQUENCY (HZ)

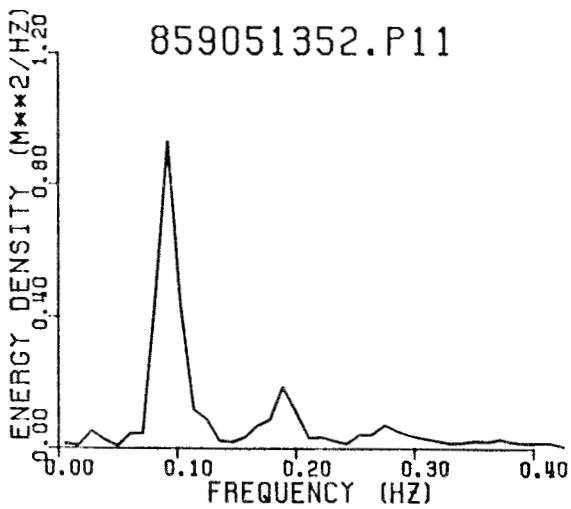
859051352.P11
ENERGY DENSITY (M**2/HZ)
0.00
0.40
0.80
1.20
0.00
0.10
0.20
0.30
0.40
FREQUENCY (HZ)

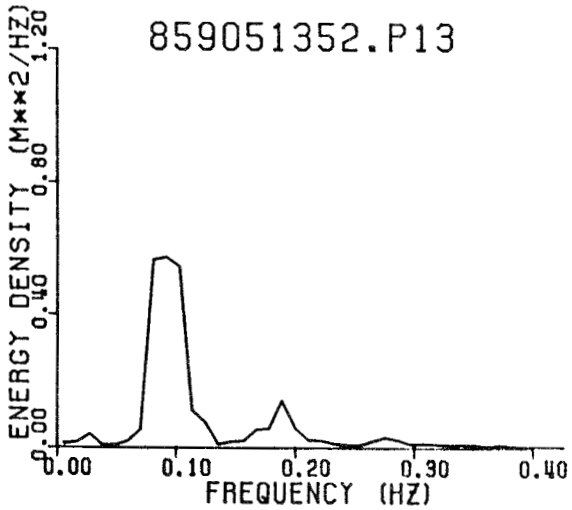
859051352.P13
ENERGY DENSITY (M**2/HZ)
0.00
0.40
0.80
1.20
0.00
0.10
0.20
0.30
0.40
FREQUENCY (HZ)

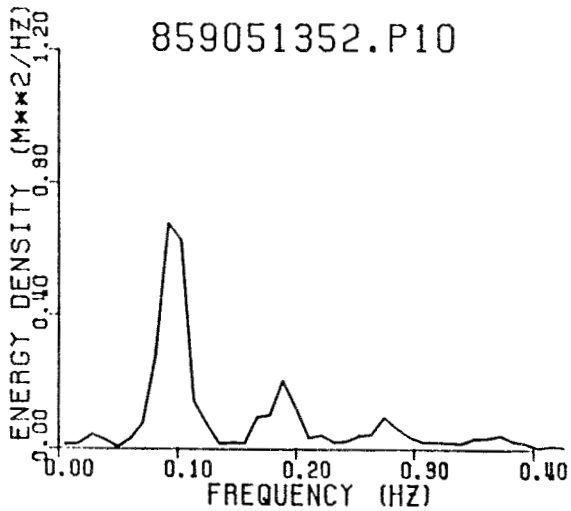
859051352.P10
ENERGY DENSITY (M**2/HZ)
0.00
0.40
0.80
1.20
0.00
0.10
0.20
0.30
0.40
FREQUENCY (HZ)

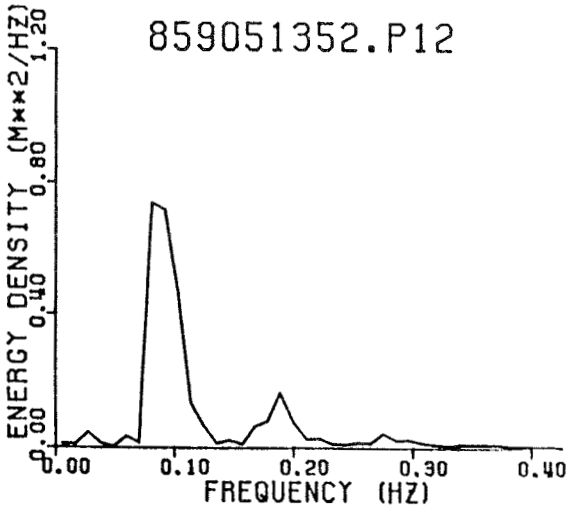
859051352.P12
ENERGY DENSITY (M**2/HZ)
0.00
0.40
0.80
1.20
0.00
0.10
0.20
0.30
0.40
FREQUENCY (HZ)

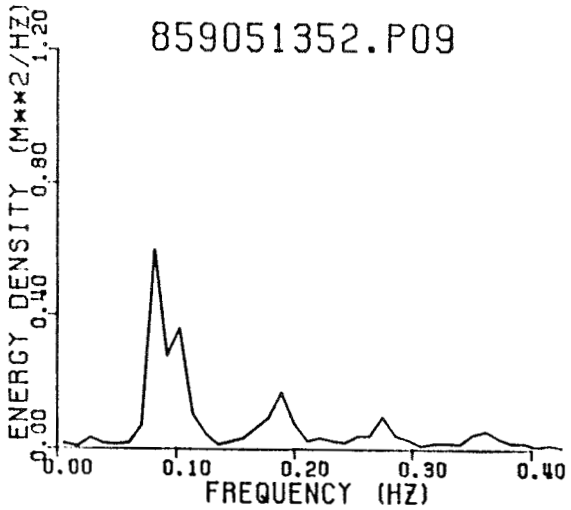
859051352.P09
ENERGY DENSITY (M**2/HZ)
0.00
0.40
0.80
1.20
0.00
0.10
0.20
0.30
0.40
FREQUENCY (HZ)

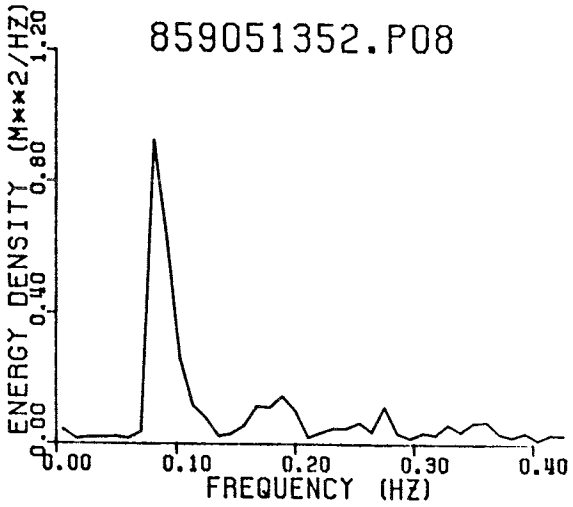
859051352.P08
ENERGY DENSITY (M**2/HZ)
0.00
0.40
0.80
1.20
0.00
0.10
0.20
0.30
0.40
FREQUENCY (HZ)

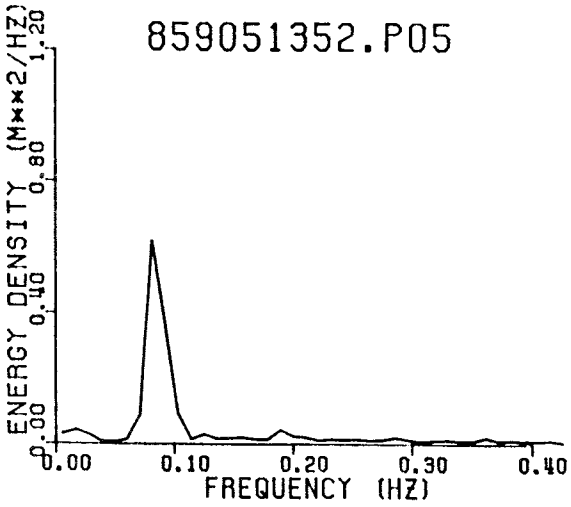
859051352.P05
ENERGY DENSITY (M**2/HZ)
0.00
0.40
0.80
1.20
0.00
0.10
0.20
0.30
0.40
FREQUENCY (HZ)

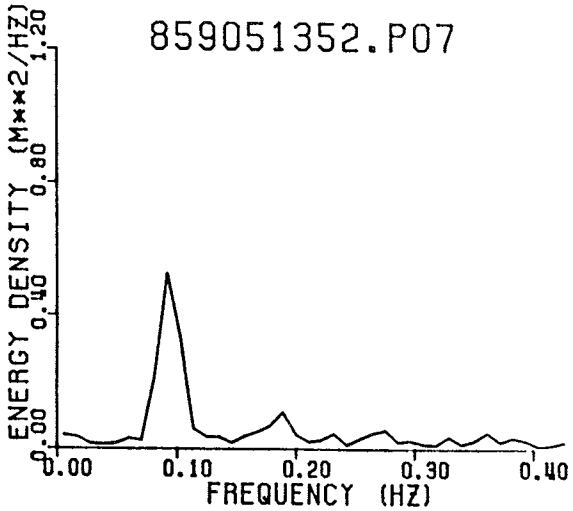
859051352.P07
ENERGY DENSITY (M**2/HZ)
0.00
0.40
0.80
1.20
0.00
0.10
0.20
0.30
0.40
FREQUENCY (HZ)

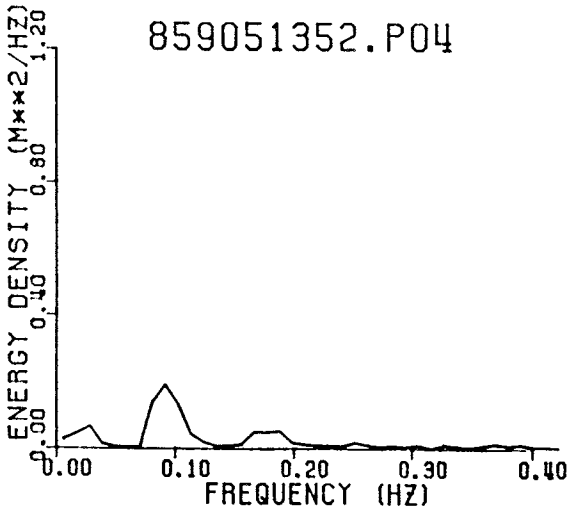
859051352.P04
ENERGY DENSITY (M**2/HZ)
0.00
0.40
0.80
1.20
0.00
0.10
0.20
0.30
0.40
FREQUENCY (HZ)

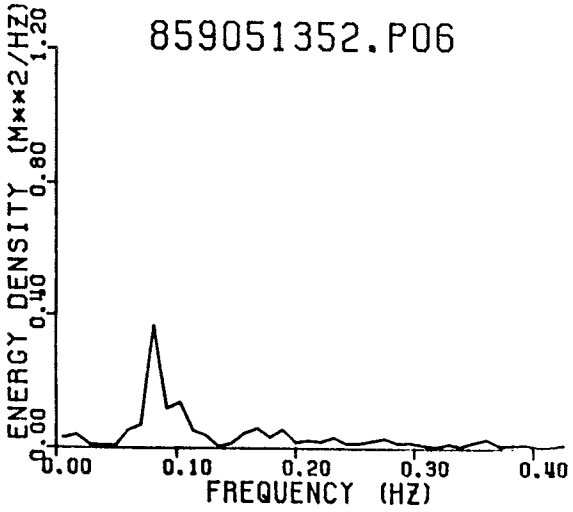
859051352.P06
ENERGY DENSITY (M**2/HZ)
0.00
0.40
0.80
1.20
0.00
0.10
0.20
0.30
0.40
FREQUENCY (HZ)

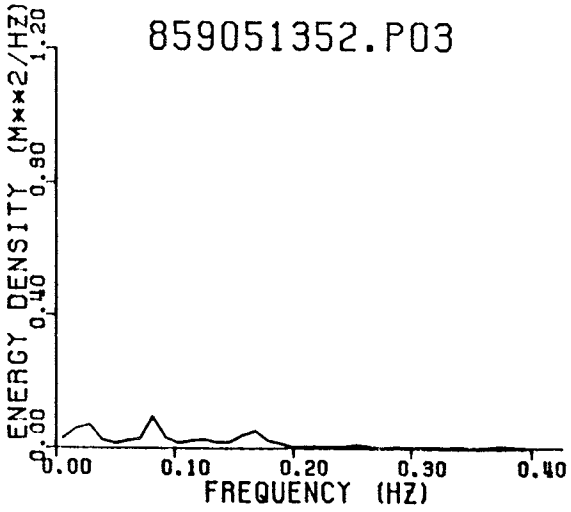
859051352.P03
ENERGY DENSITY (M**2/HZ)
0.00
0.40
0.80
1.20
0.00
0.10
0.20
0.30
0.40
FREQUENCY (HZ)

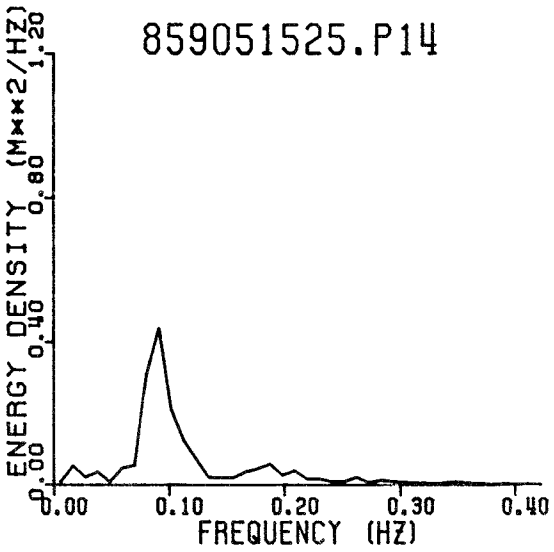
859051525.P14
ENERGY DENSITY (M**2/HZ)
0.00
0.40
0.80
1.20
0.00
0.10
0.20
0.30
0.40
FREQUENCY (HZ)

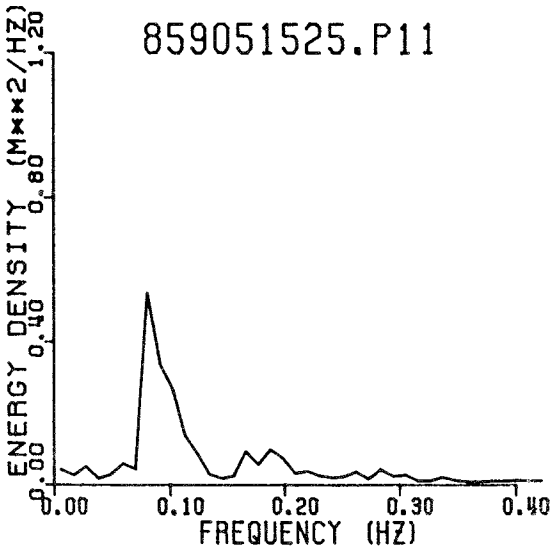
859051525.P11
ENERGY DENSITY (M**2/HZ)
0.00
0.40
0.80
1.20
0.00
0.10
0.20
0.30
0.40
FREQUENCY (HZ)

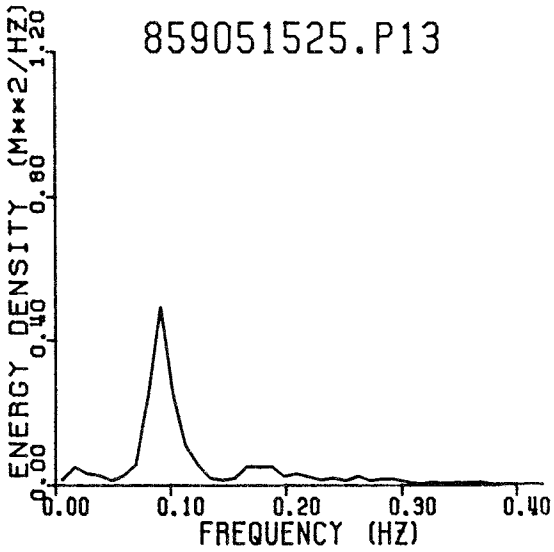
859051525.P13
ENERGY DENSITY (M**2/HZ)
0.00
0.40
0.80
1.20
0.00
0.10
0.20
0.30
0.40
FREQUENCY (HZ)

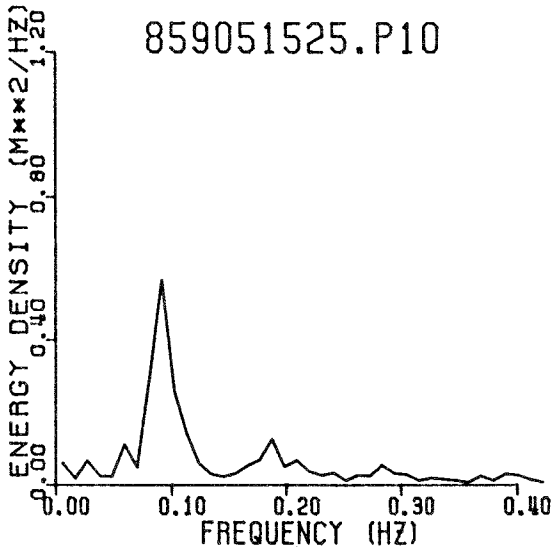
859051525.P10
ENERGY DENSITY (M**2/HZ)
0.00
0.40
0.80
1.20
0.00
0.10
0.20
0.30
0.40
FREQUENCY (HZ)

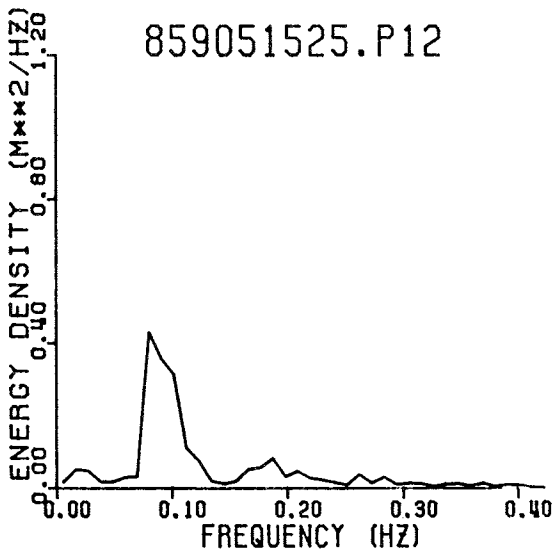
859051525.P12
ENERGY DENSITY (M**2/HZ)
0.00
0.40
0.80
1.20
0.00
0.10
0.20
0.30
0.40
FREQUENCY (HZ)

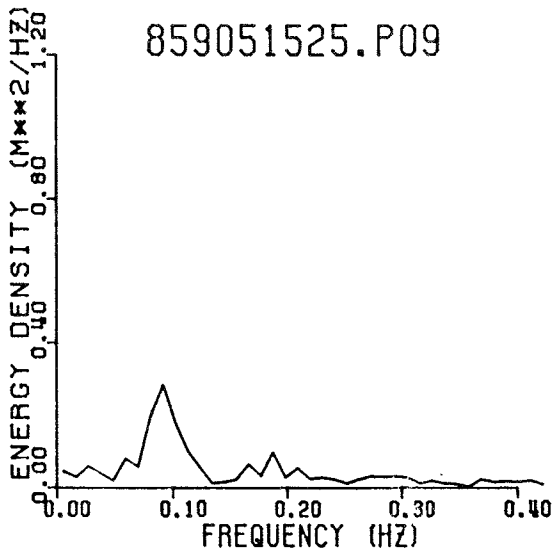
859051525.P09
ENERGY DENSITY (M**2/HZ)
0.00
0.40
0.80
1.20
0.00
0.10
0.20
0.30
0.40
FREQUENCY (HZ)

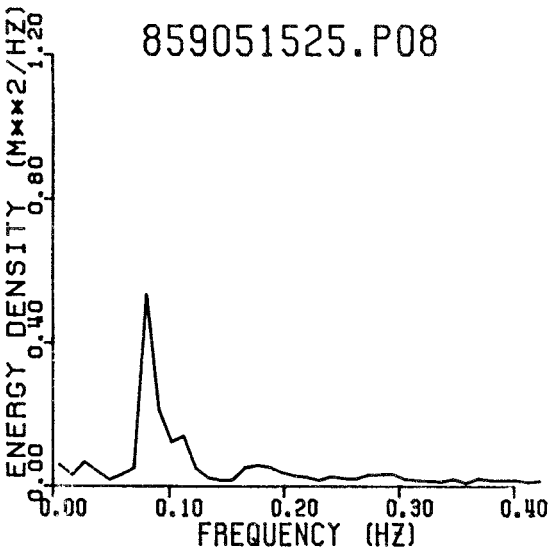
859051525.P08
ENERGY DENSITY (M**2/HZ)
0.00
0.40
0.80
1.20
0.00
0.10
0.20
0.30
0.40
FREQUENCY (HZ)

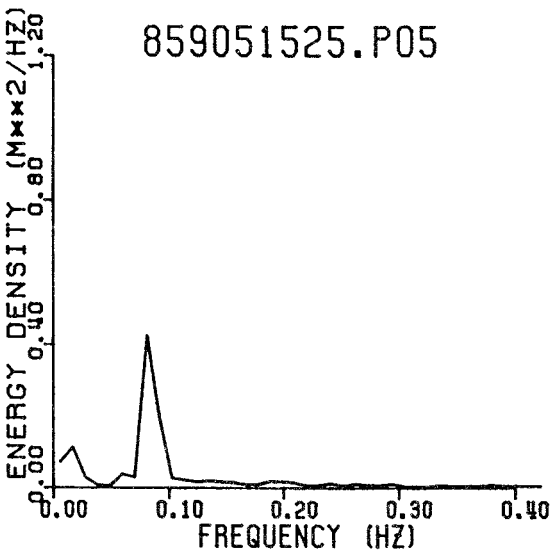
859051525.P05
ENERGY DENSITY (M**2/HZ)
0.00
0.40
0.80
1.20
0.00
0.10
0.20
0.30
0.40
FREQUENCY (HZ)

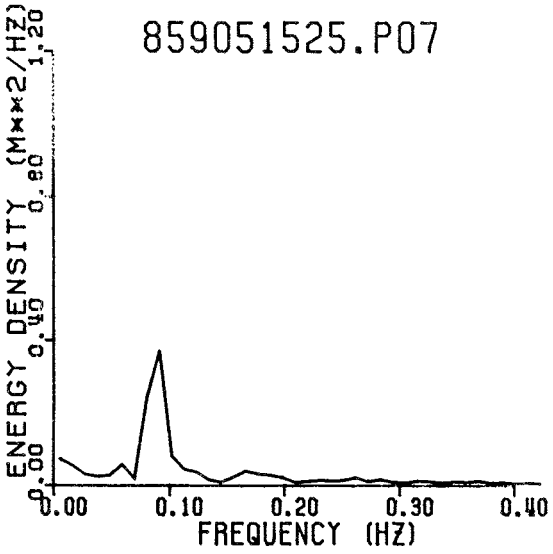
859051525.P07
ENERGY DENSITY (M**2/HZ)
0.00
0.40
0.80
1.20
0.00
0.10
0.20
0.30
0.40
FREQUENCY (HZ)

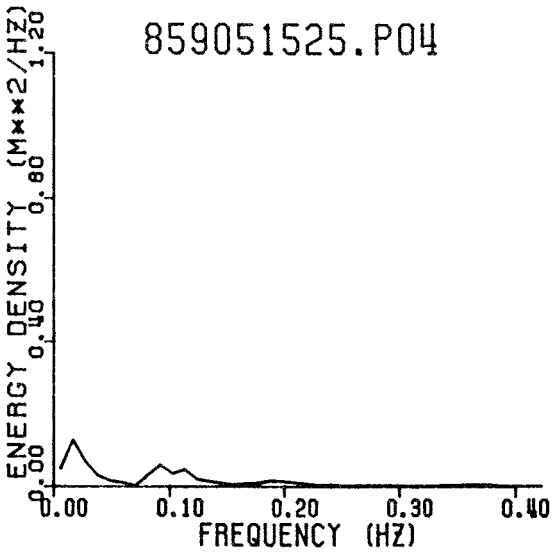
859051525.P04
ENERGY DENSITY (M**2/HZ)
0.00
0.40
0.80
1.20
0.00
0.10
0.20
0.30
0.40
FREQUENCY (HZ)

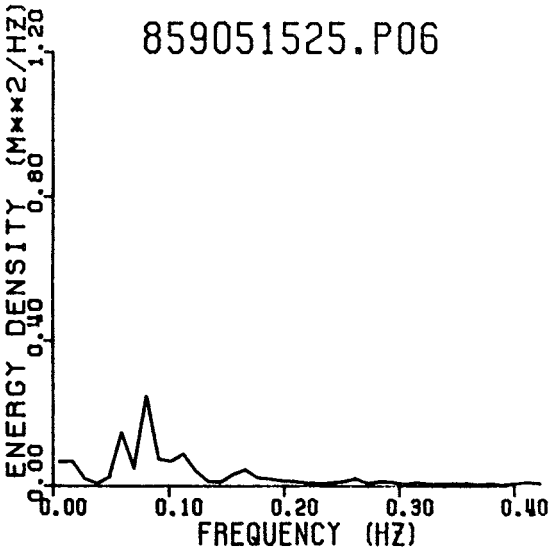
859051525.P06
ENERGY DENSITY (M**2/HZ)
0.00
0.40
0.80
1.20
0.00
0.10
0.20
0.30
0.40
FREQUENCY (HZ)

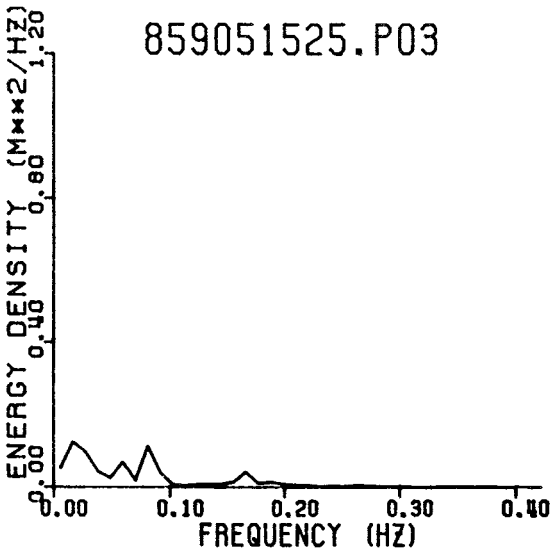
859051525.P03
ENERGY DENSITY (M**2/HZ)
0.00
0.40
0.80
1.20
0.00
0.10
0.20
0.30
0.40
FREQUENCY (HZ)

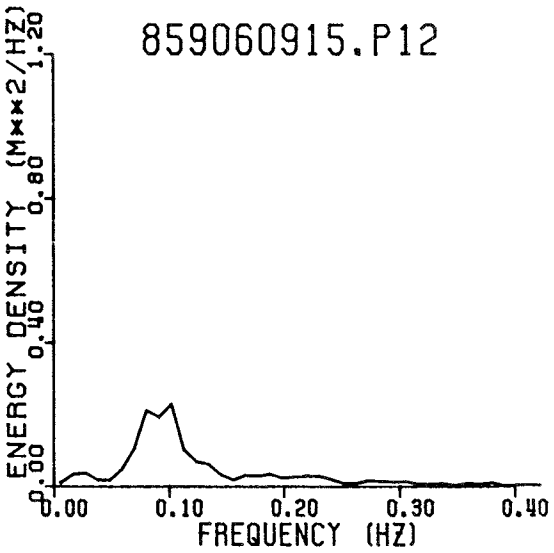
859060915.P12
ENERGY DENSITY (M**2/HZ)
0.00
0.40
0.80
1.20
0.00
0.10
0.20
0.30
0.40
FREQUENCY (HZ)

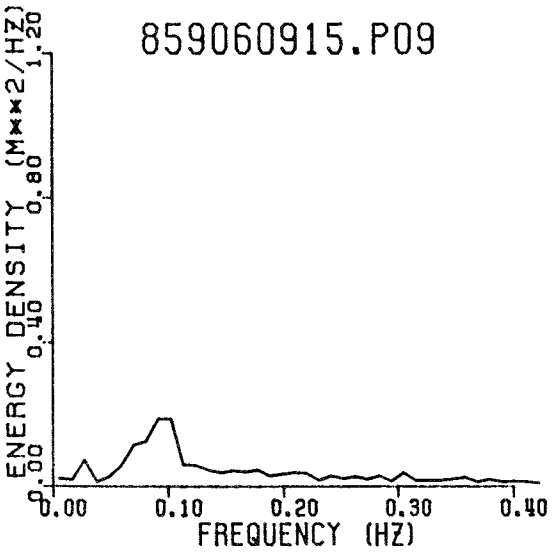
859060915.P09
ENERGY DENSITY (M**2/HZ)
0.00
0.40
0.80
1.20
0.00
0.10
0.20
0.30
0.40
FREQUENCY (HZ)

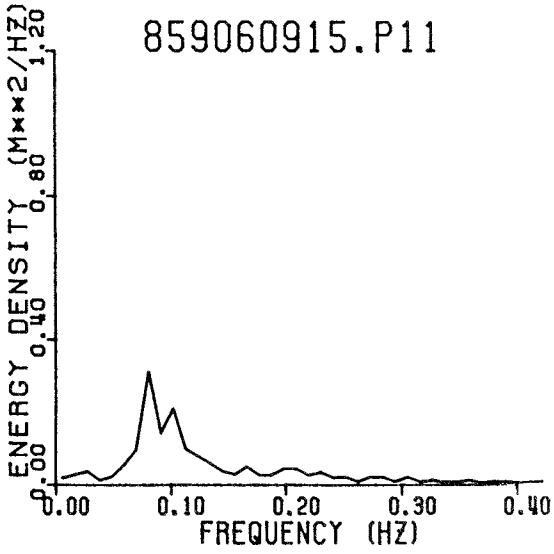
859060915.P11
ENERGY DENSITY (M**2/HZ)
0.00
0.40
0.80
1.20
0.00
0.10
0.20
0.30
0.40
FREQUENCY (HZ)

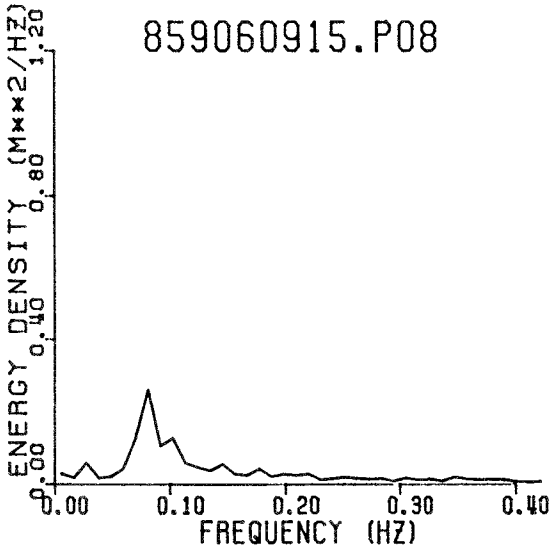
859060915.P08
ENERGY DENSITY (M**2/HZ)
0.00
0.40
0.80
1.20
0.00
0.10
0.20
0.30
0.40
FREQUENCY (HZ)

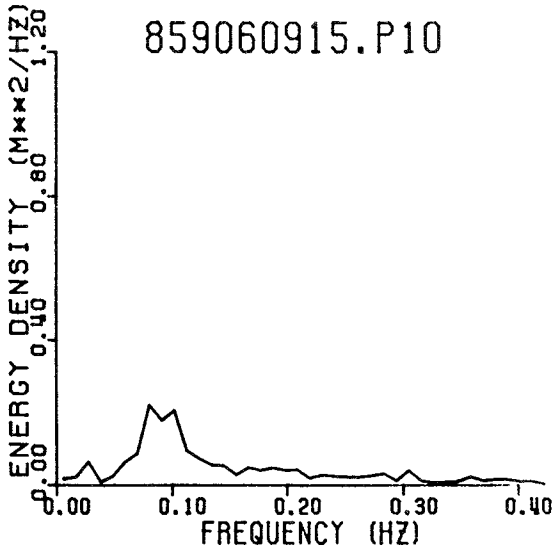
859060915.P10
ENERGY DENSITY (M**2/HZ)
0.00
0.40
0.80
1.20
0.00
0.10
0.20
0.30
0.40
FREQUENCY (HZ)

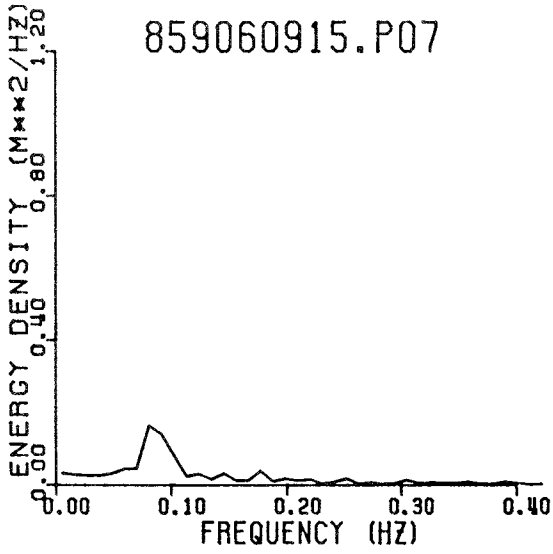
859060915.P07
ENERGY DENSITY (M**2/HZ)
0.00
0.40
0.80
1.20
0.00
0.10
0.20
0.30
0.40
FREQUENCY (HZ)

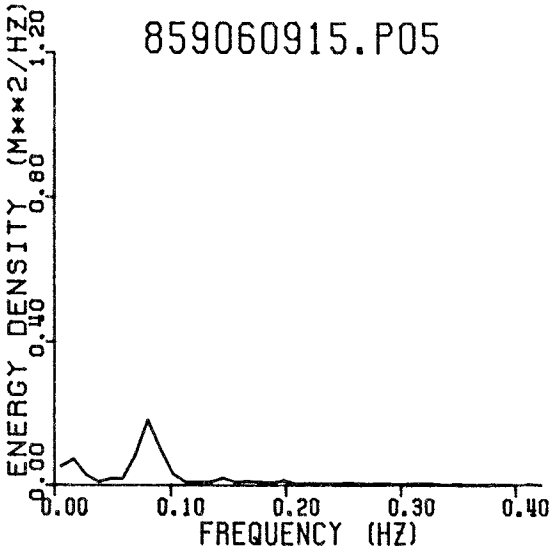
859060915.P05
ENERGY DENSITY (M**2/HZ)
1.20
0.80
0.40
0.00
0.00
0.10
0.20
0.30
0.40
FREQUENCY (HZ)

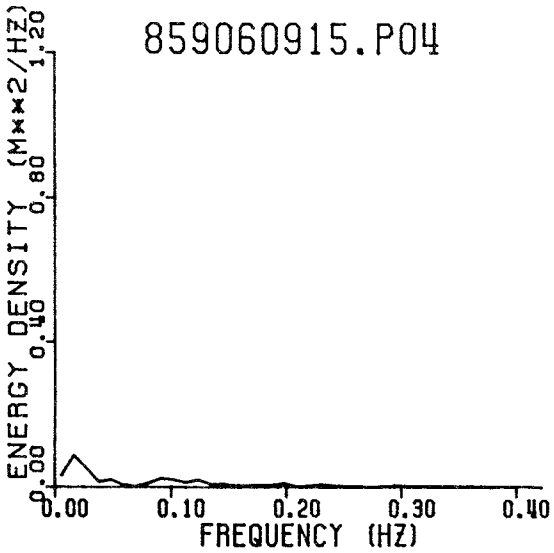
859060915.P04
ENERGY DENSITY (M**2/HZ)
1.20
0.80
0.40
0.00
0.00
0.10
0.20
0.30
0.40
FREQUENCY (HZ)

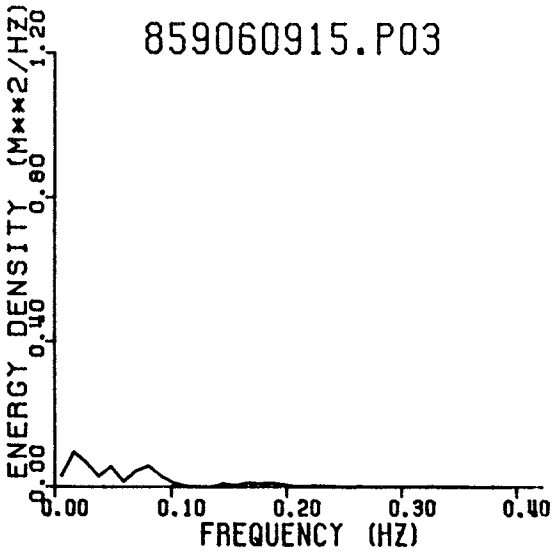
859060915.P03
ENERGY DENSITY (M**2/HZ)
1.20
0.80
0.40
0.00
0.00
0.10
0.20
0.30
0.40
FREQUENCY (HZ)

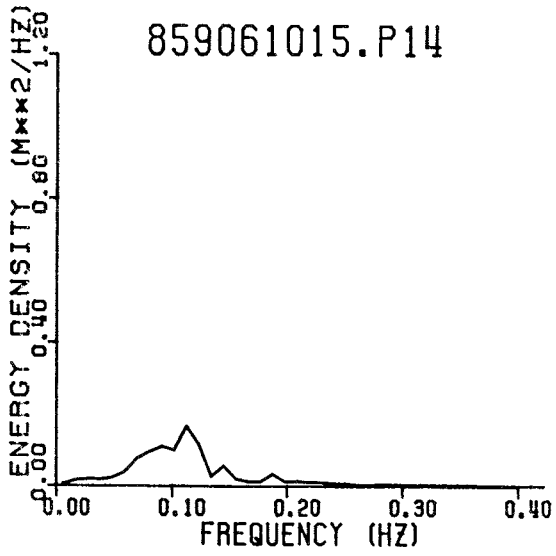
859061015.P14
ENERGY DENSITY (M**2/HZ)
0.00
0.40
0.80
1.20
0.00
0.10
0.20
0.30
0.40
FREQUENCY (HZ)

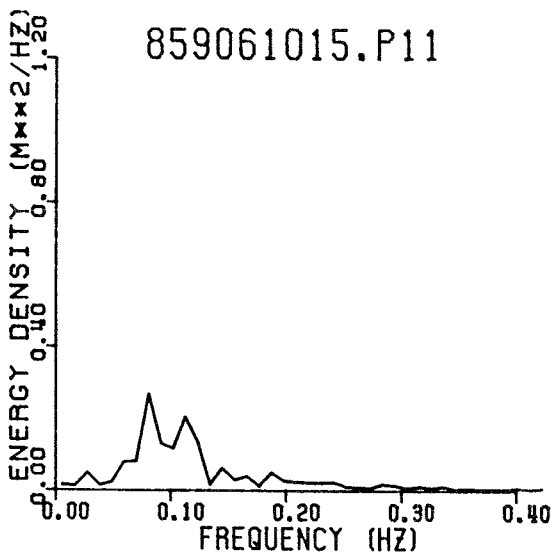
859061015.P11
ENERGY DENSITY (M**2/HZ)
0.00
0.40
0.80
1.20
0.00
0.10
0.20
0.30
0.40
FREQUENCY (HZ)

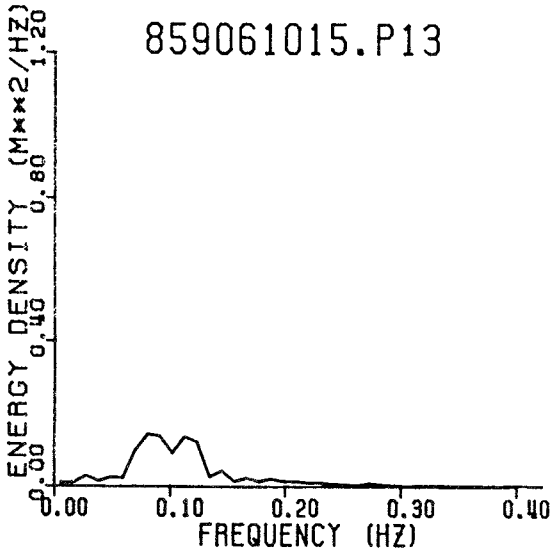
859061015.P13
ENERGY DENSITY (M**2/HZ)
0.00
0.40
0.80
1.20
0.00
0.10
0.20
0.30
0.40
FREQUENCY (HZ)

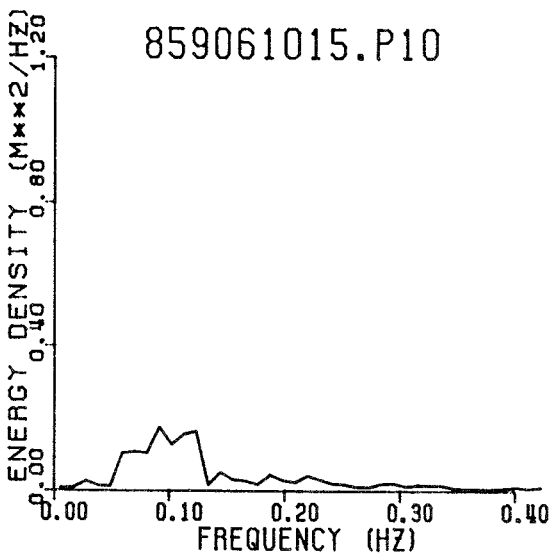
859061015.P10
ENERGY DENSITY (M**2/HZ)
0.00
0.40
0.80
1.20
0.00
0.10
0.20
0.30
0.40
FREQUENCY (HZ)

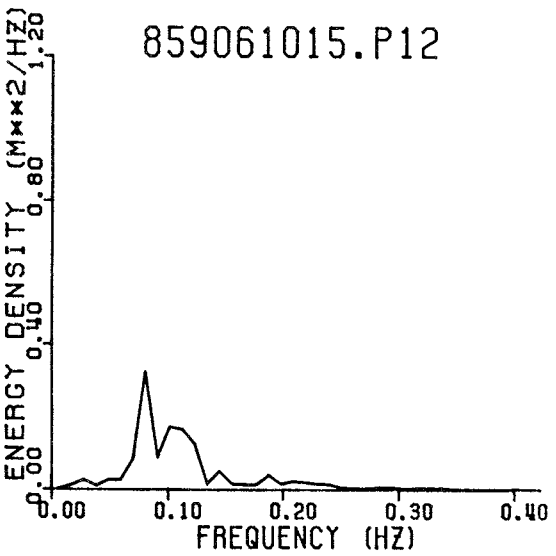
859061015.P12
ENERGY DENSITY (M**2/HZ)
0.00
0.40
0.80
1.20
0.00
0.10
0.20
0.30
0.40
FREQUENCY (HZ)

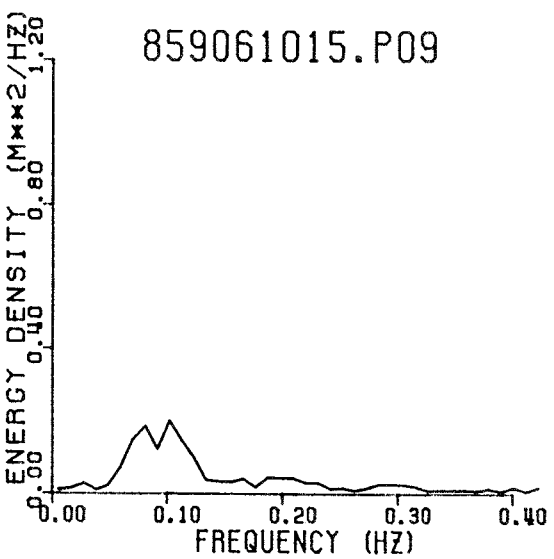
859061015.P09
ENERGY DENSITY (M**2/HZ)
0.00
0.40
0.80
1.20
0.00
0.10
0.20
0.30
0.40
FREQUENCY (HZ)

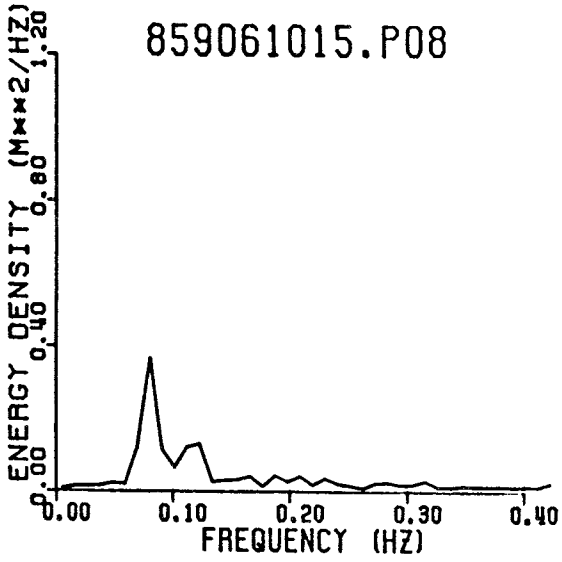
859061015.P08
ENERGY DENSITY (M**2/HZ)
0.00
0.40
0.80
1.20
0.00
0.10
0.20
0.30
0.40
FREQUENCY (HZ)

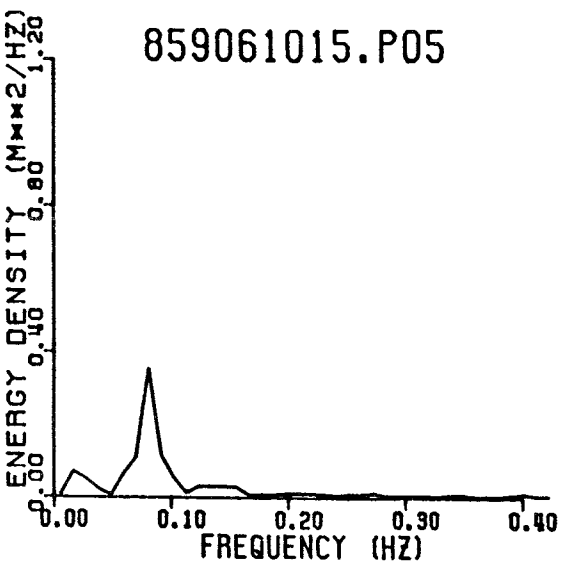
859061015.P05
ENERGY DENSITY (M**2/HZ)
0.00
0.40
0.80
1.20
0.00
0.10
0.20
0.30
0.40
FREQUENCY (HZ)

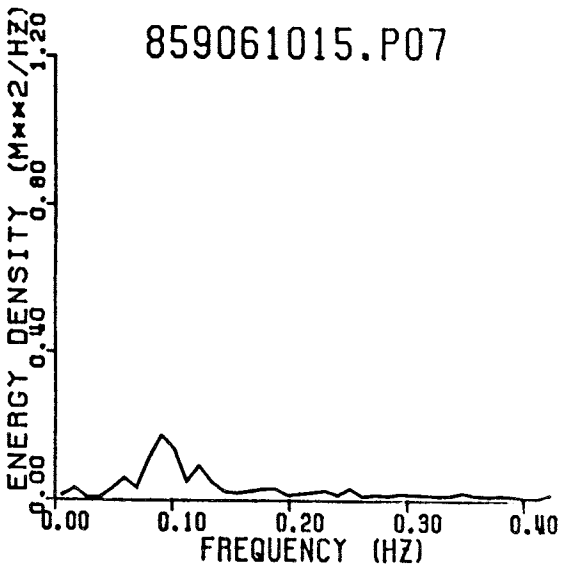
859061015.P07
ENERGY DENSITY (M**2/HZ)
0.00
0.40
0.80
1.20
0.00
0.10
0.20
0.30
0.40
FREQUENCY (HZ)

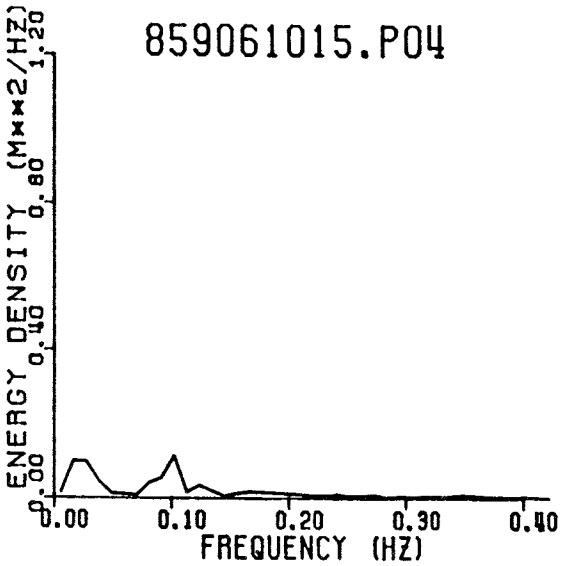
859061015.P04
ENERGY DENSITY (M**2/HZ)
0.00
0.40
0.80
1.20
0.00
0.10
0.20
0.30
0.40
FREQUENCY (HZ)

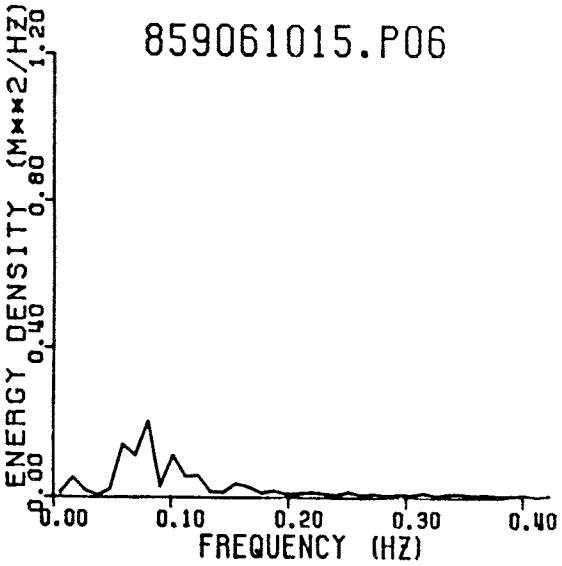
859061015.P06
ENERGY DENSITY (M**2/HZ)
0.00
0.40
0.80
1.20
0.00
0.10
0.20
0.30
0.40
FREQUENCY (HZ)

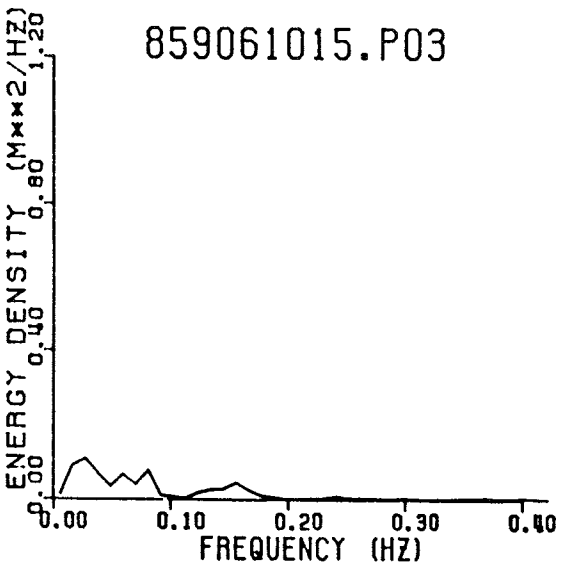
859061015.P03
ENERGY DENSITY (M**2/HZ)
0.00
0.40
0.80
1.20
0.00
0.10
0.20
0.30
0.40
FREQUENCY (HZ)

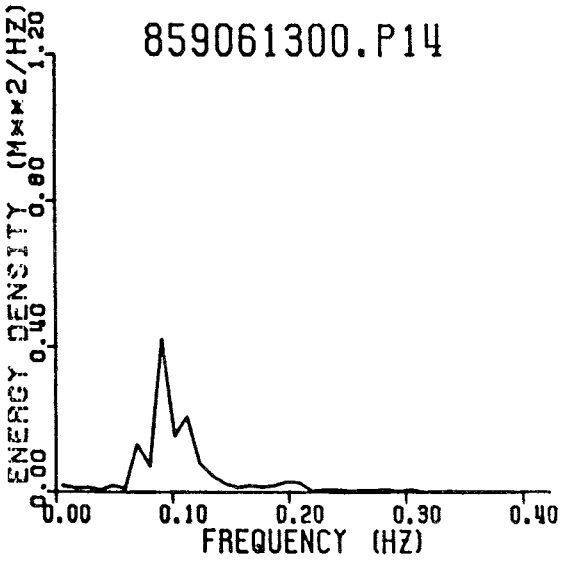
859061300.P14
ENERGY DENSITY (M**2/HZ)
0.00
0.40
0.80
1.20
0.00
0.10
0.20
0.30
0.40
FREQUENCY (HZ)

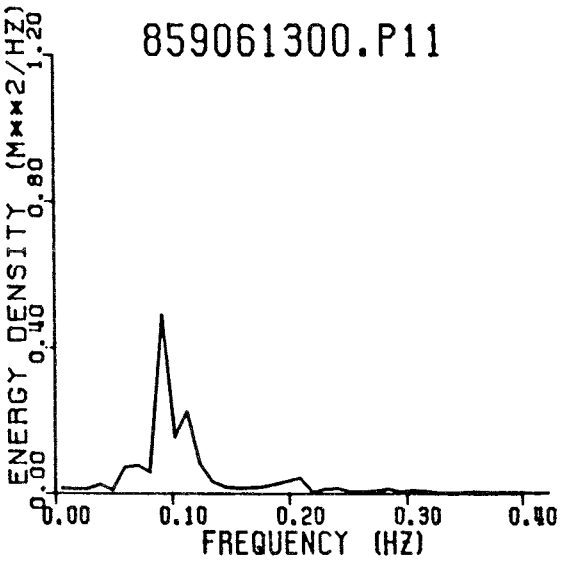
859061300.P11
ENERGY DENSITY (M**2/HZ)
0.00
0.40
0.80
1.20
0.00
0.10
0.20
0.30
0.40
FREQUENCY (HZ)

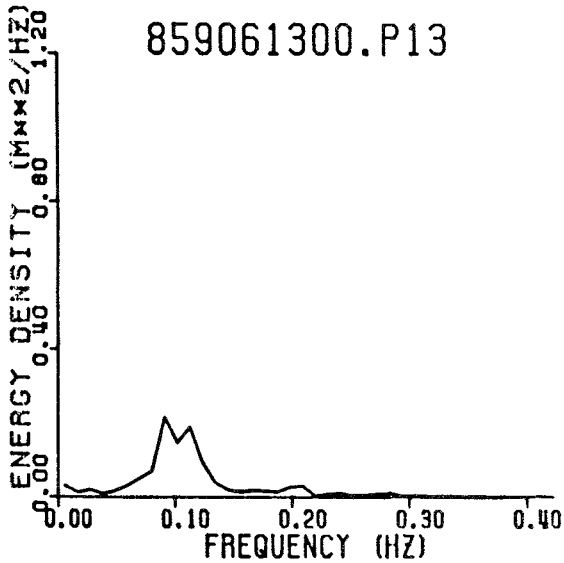
859061300.P13
ENERGY DENSITY (M**2/HZ)
0.00
0.40
0.80
1.20
0.00
0.10
0.20
0.30
0.40
FREQUENCY (HZ)

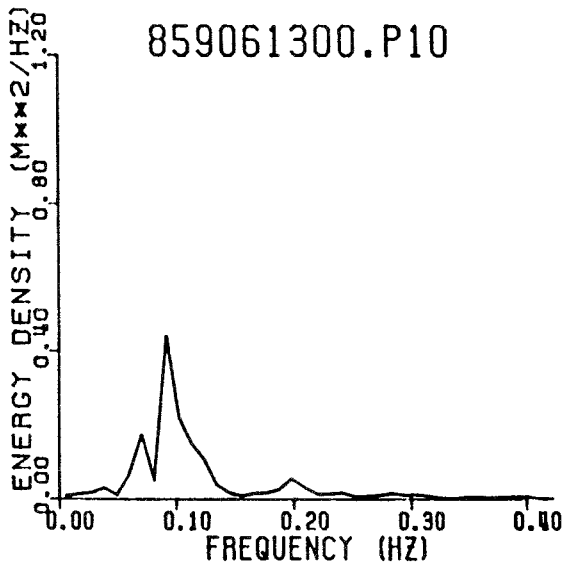
859061300.P10
ENERGY DENSITY (M**2/HZ)
0.00
0.40
0.80
1.20
0.00
0.10
0.20
0.30
0.40
FREQUENCY (HZ)

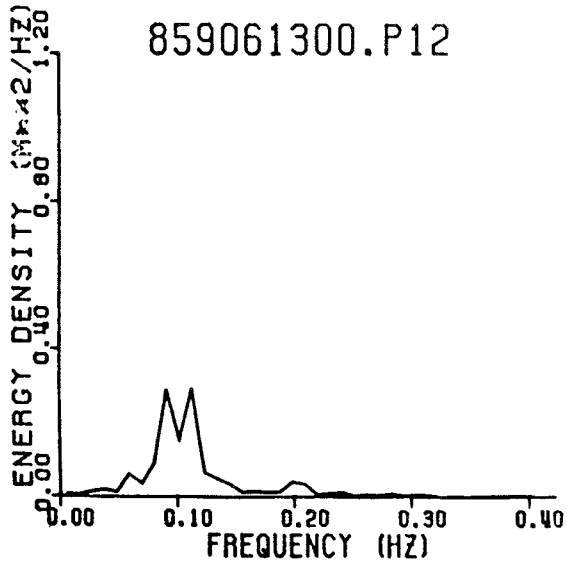
859061300.P12
ENERGY DENSITY (M**2/HZ)
0.00
0.40
0.80
1.20
0.00
0.10
0.20
0.30
0.40
FREQUENCY (HZ)

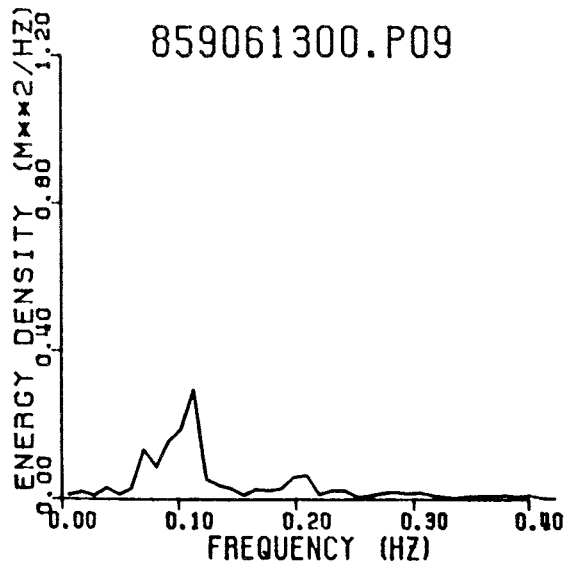
859061300.P09
ENERGY DENSITY (M**2/HZ)
0.00
0.40
0.80
1.20
0.00
0.10
0.20
0.30
0.40
FREQUENCY (HZ)

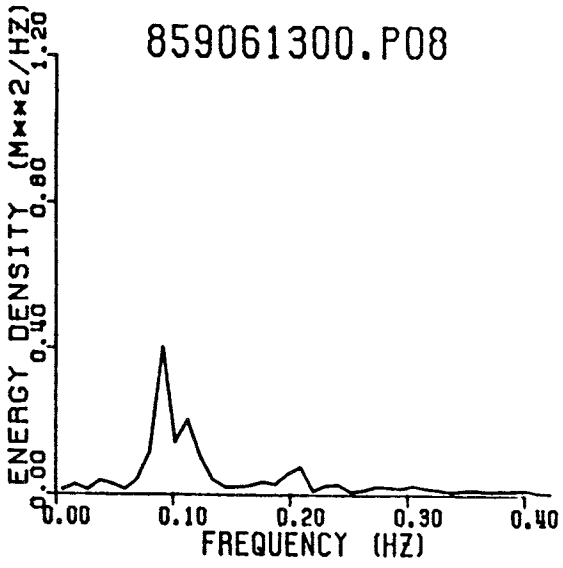
859061300.P08
ENERGY DENSITY (M**2/HZ)
0.00
0.40
0.80
1.20
0.00
0.10
0.20
0.30
0.40
FREQUENCY (HZ)

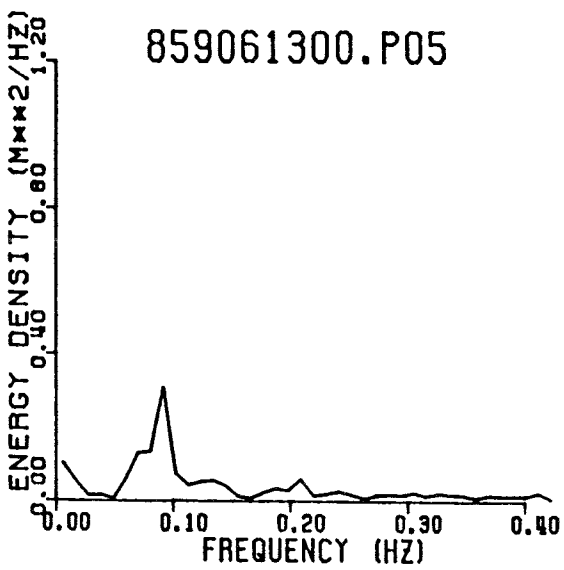
859061300.P05
ENERGY DENSITY (M**2/HZ)
0.00
0.40
0.80
1.20
0.00
0.10
0.20
0.30
0.40
FREQUENCY (HZ)

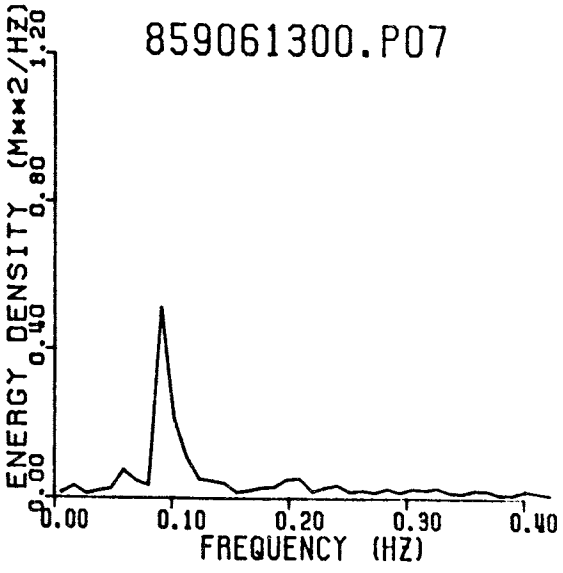
859061300.P07
ENERGY DENSITY (M**2/HZ)
0.00
0.40
0.80
1.20
0.00
0.10
0.20
0.30
0.40
FREQUENCY (HZ)

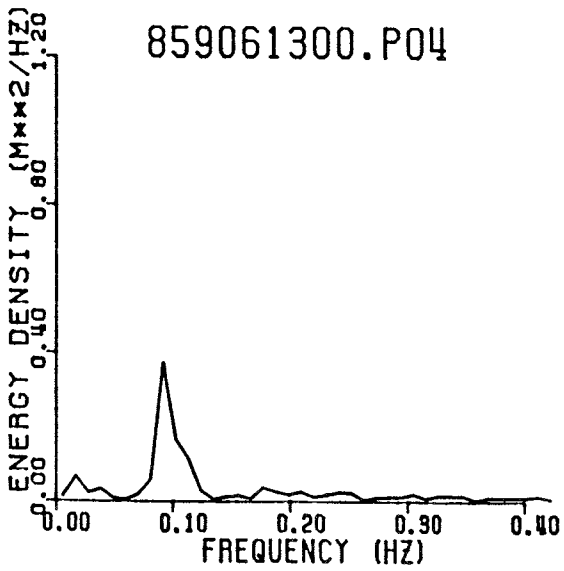
859061300.P04
ENERGY DENSITY (M**2/HZ)
0.00
0.40
0.80
1.20
0.00
0.10
0.20
0.30
0.40
FREQUENCY (HZ)

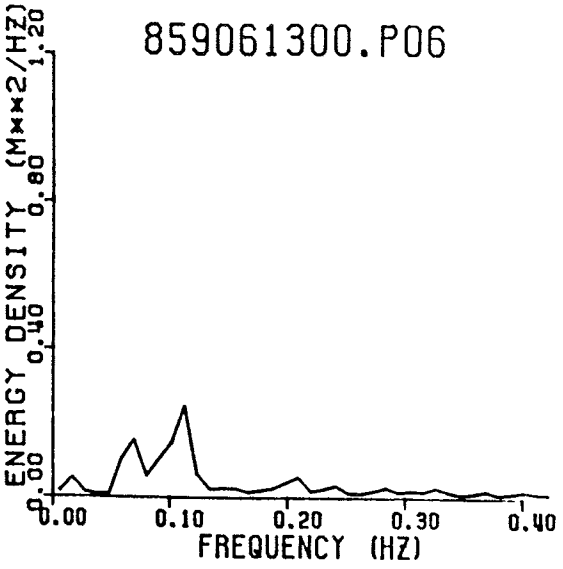
859061300.P06
ENERGY DENSITY (M**2/HZ)
0.00
0.40
0.80
1.20
0.00
0.10
0.20
0.30
0.40
FREQUENCY (HZ)

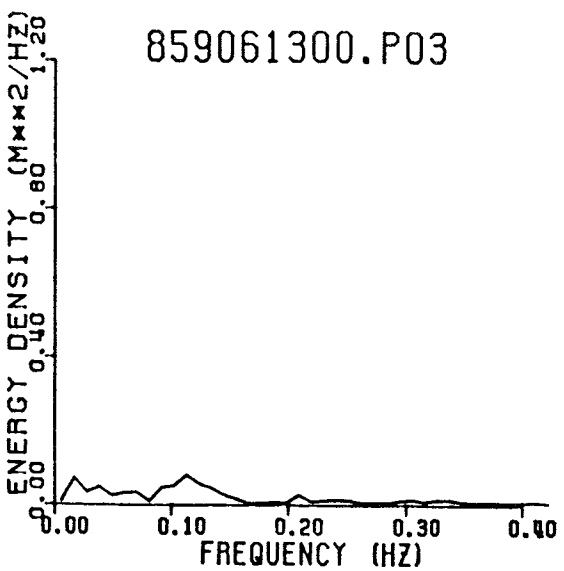
859061300.P03
ENERGY DENSITY (M**2/HZ)
0.00
0.40
0.80
1.20
0.00
0.10
0.20
0.30
0.40
FREQUENCY (HZ)

APPENDIX C: WATER SURFACE ELEVATION DISTRIBUTIONS

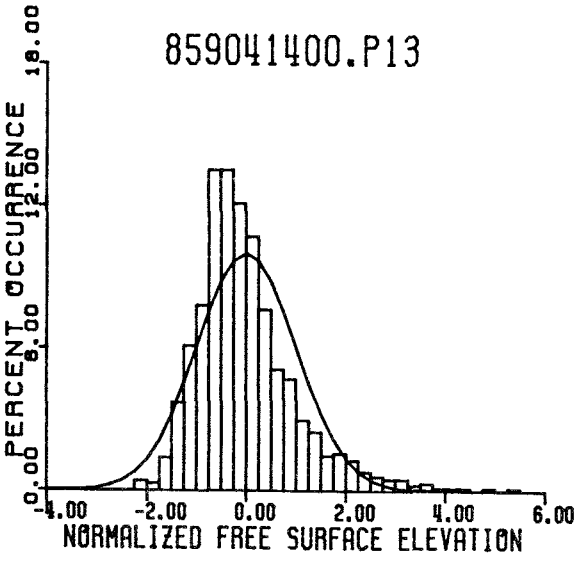
859041400.P13
PERCENT OCCURRENCE
0.00
4.00
8.00
12.00
16.00
-4.00
-2.00
0.00
2.00
4.00
6.00
NORMALIZED FREE SURFACE ELEVATION

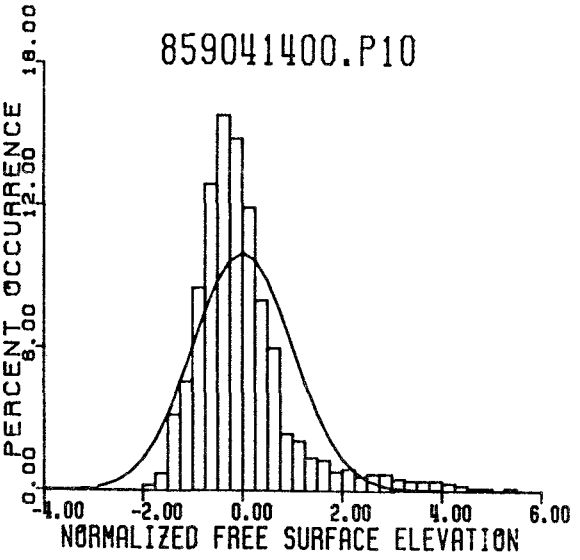
859041400.P10
PERCENT OCCURRENCE
0.00
4.00
8.00
12.00
16.00
-4.00
-2.00
0.00
2.00
4.00
6.00
NORMALIZED FREE SURFACE ELEVATION

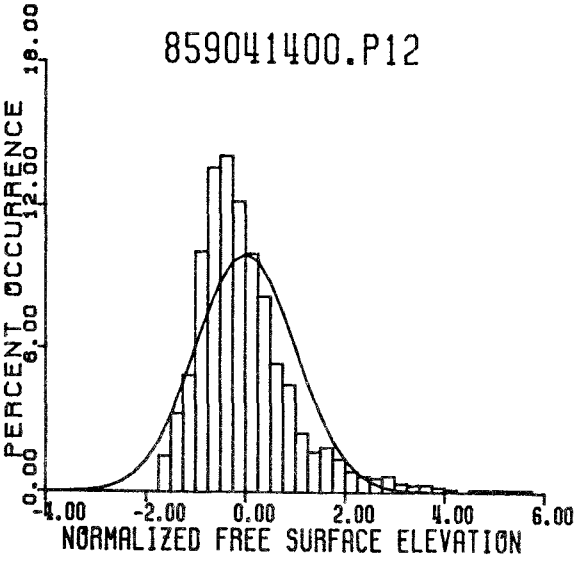
859041400.P12
PERCENT OCCURRENCE
0.00
4.00
8.00
12.00
16.00
-4.00
-2.00
0.00
2.00
4.00
6.00
NORMALIZED FREE SURFACE ELEVATION

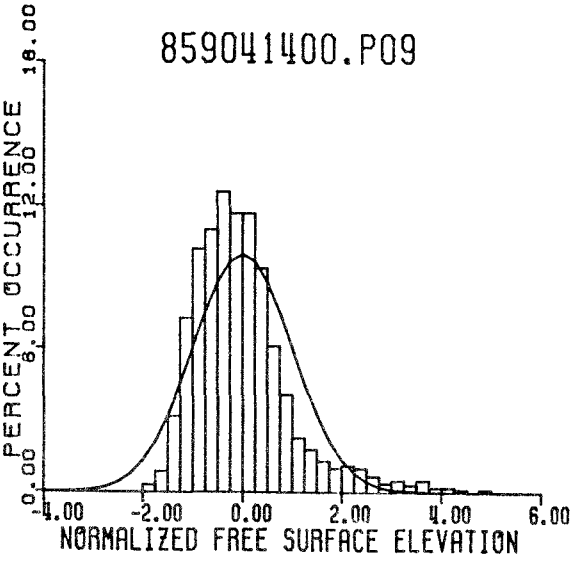
859041400.P09
PERCENT OCCURRENCE
0.00
4.00
8.00
12.00
16.00
-4.00
-2.00
0.00
2.00
4.00
6.00
NORMALIZED FREE SURFACE ELEVATION

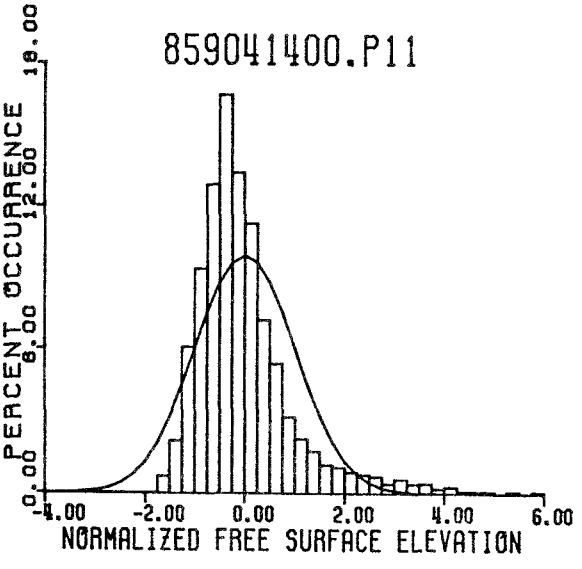
859041400.P11
PERCENT OCCURRENCE
0.00
4.00
8.00
12.00
16.00
-4.00
-2.00
0.00
2.00
4.00
6.00
NORMALIZED FREE SURFACE ELEVATION

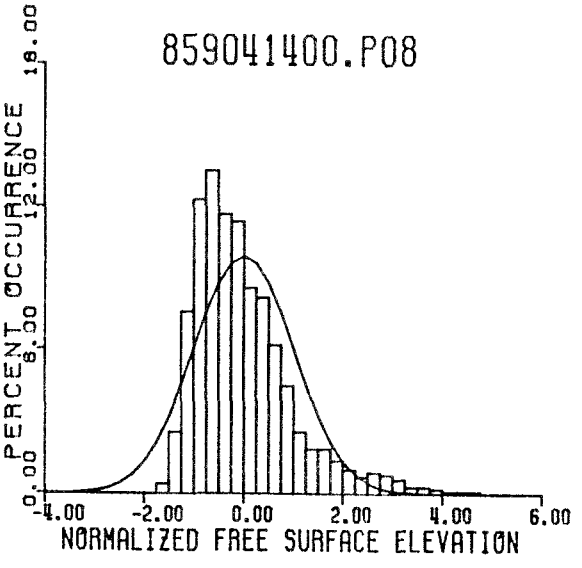
859041400.P08
PERCENT OCCURRENCE
0.00
4.00
8.00
12.00
16.00
-4.00
-2.00
0.00
2.00
4.00
6.00
NORMALIZED FREE SURFACE ELEVATION

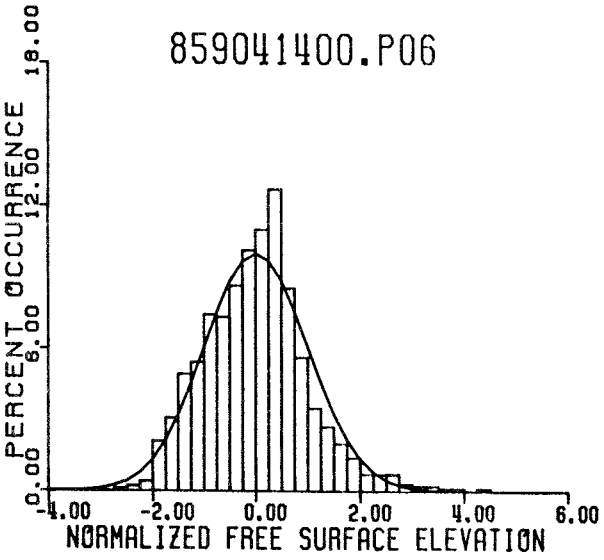
859041400.P06
PERCENT OCCURRENCE
0.00
6.00
12.00
18.00
-4.00
-2.00
0.00
2.00
4.00
6.00
NORMALIZED FREE SURFACE ELEVATION

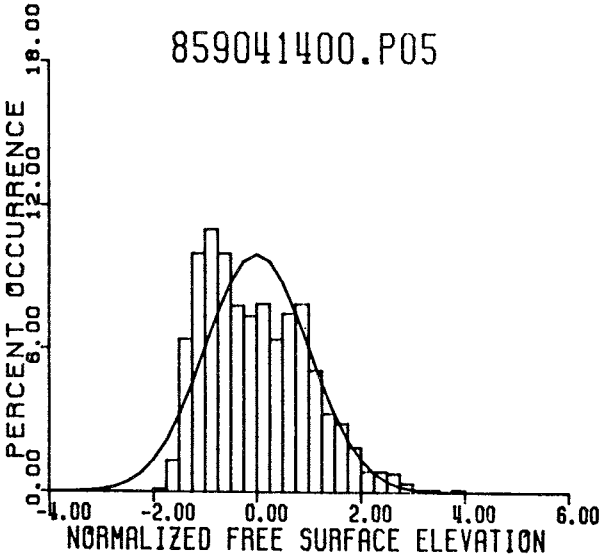
859041400.P05
PERCENT OCCURRENCE
0.00
6.00
12.00
18.00
-4.00
-2.00
0.00
2.00
4.00
6.00
NORMALIZED FREE SURFACE ELEVATION

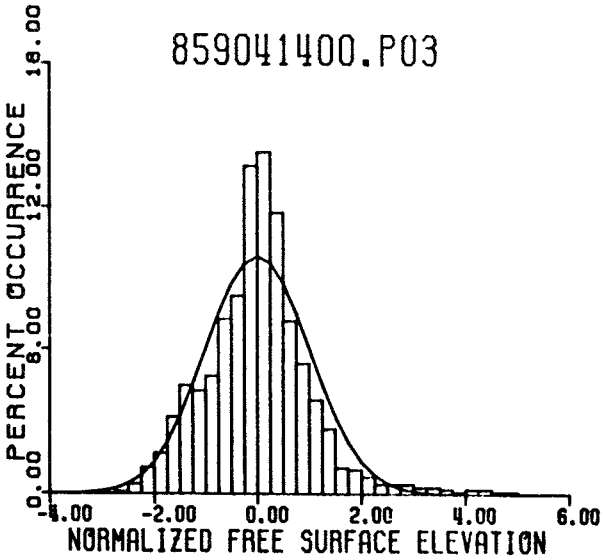
859041400.P03
PERCENT OCCURRENCE
0.00
6.00
12.00
18.00
-4.00
-2.00
0.00
2.00
4.00
6.00
NORMALIZED FREE SURFACE ELEVATION

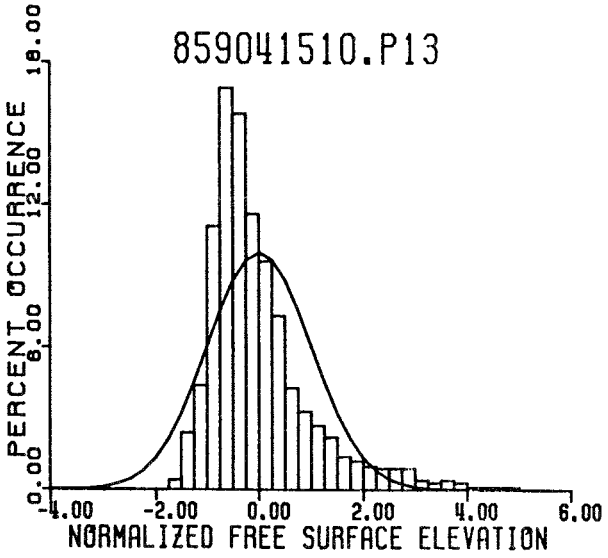
859041510.P13
PERCENT OCCURRENCE
0.00
8.00
12.00
16.00
-4.00
-2.00
0.00
2.00
4.00
6.00
NORMALIZED FREE SURFACE ELEVATION

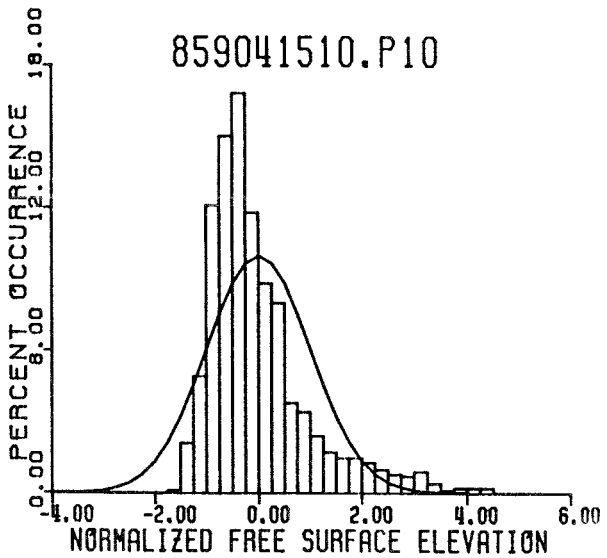
859041510.P10
PERCENT OCCURRENCE
0.00
8.00
12.00
16.00
-4.00
-2.00
0.00
2.00
4.00
6.00
NORMALIZED FREE SURFACE ELEVATION

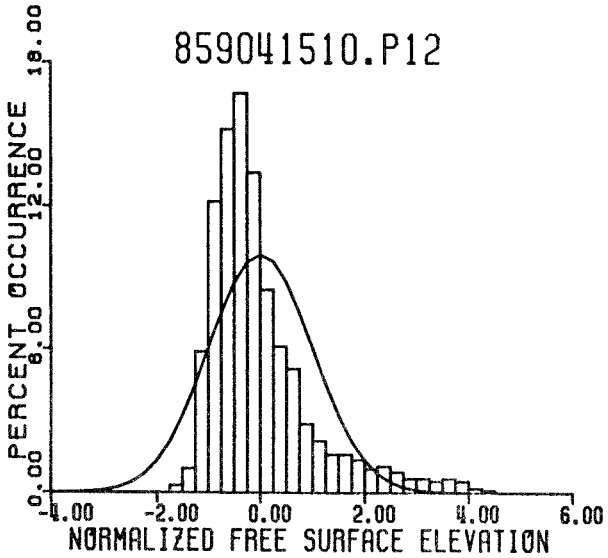
859041510.P12
PERCENT OCCURRENCE
0.00
8.00
12.00
16.00
-4.00
-2.00
0.00
2.00
4.00
6.00
NORMALIZED FREE SURFACE ELEVATION

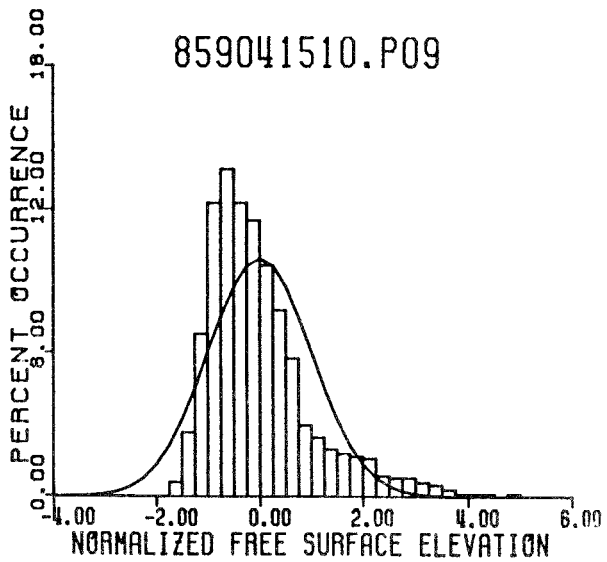
859041510.P09
PERCENT OCCURRENCE
0.00
8.00
12.00
16.00
-4.00
-2.00
0.00
2.00
4.00
6.00
NORMALIZED FREE SURFACE ELEVATION

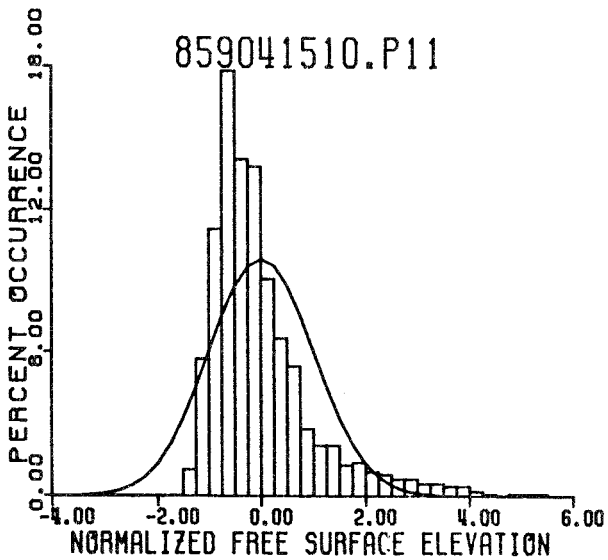
859041510.P11
PERCENT OCCURRENCE
0.00
8.00
12.00
16.00
-4.00
-2.00
0.00
2.00
4.00
6.00
NORMALIZED FREE SURFACE ELEVATION

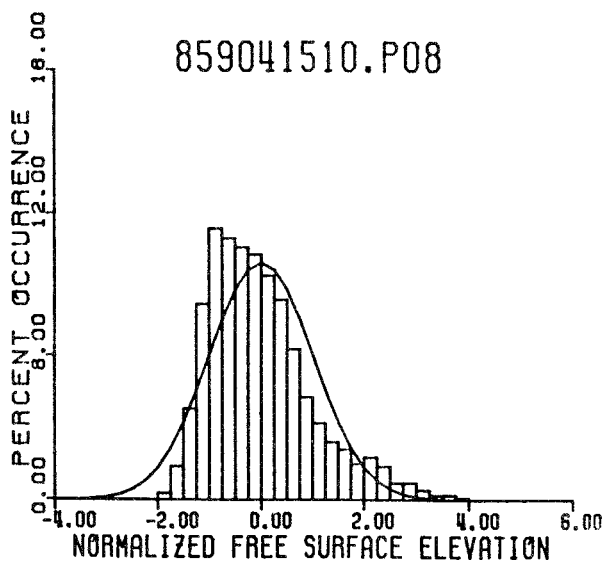
859041510.P08
PERCENT OCCURRENCE
0.00
8.00
12.00
16.00
-4.00
-2.00
0.00
2.00
4.00
6.00
NORMALIZED FREE SURFACE ELEVATION

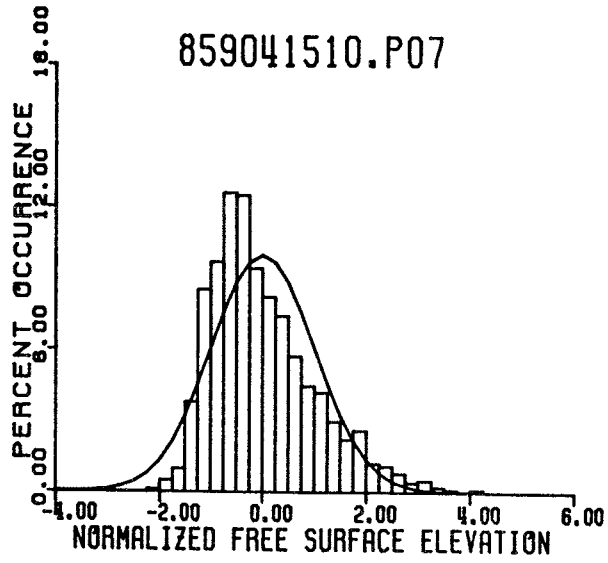
859041510.P07
PERCENT OCCURRENCE
0.00
6.00
12.00
18.00
-4.00
-2.00
0.00
2.00
4.00
6.00
NORMALIZED FREE SURFACE ELEVATION

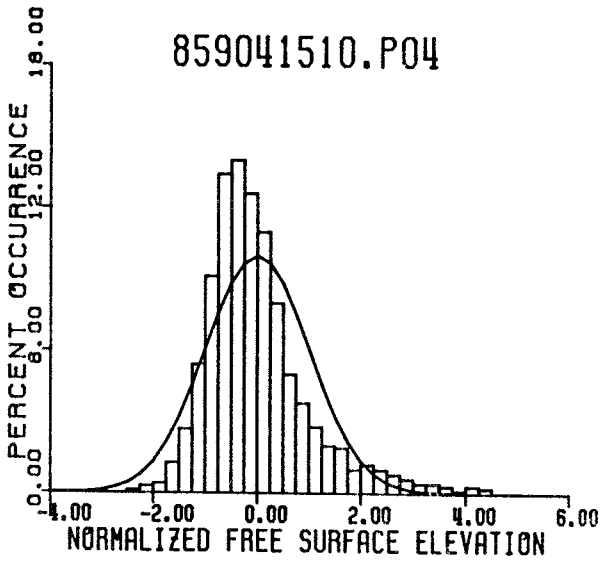
859041510.P04
PERCENT OCCURRENCE
0.00
6.00
12.00
18.00
-4.00
-2.00
0.00
2.00
4.00
6.00
NORMALIZED FREE SURFACE ELEVATION

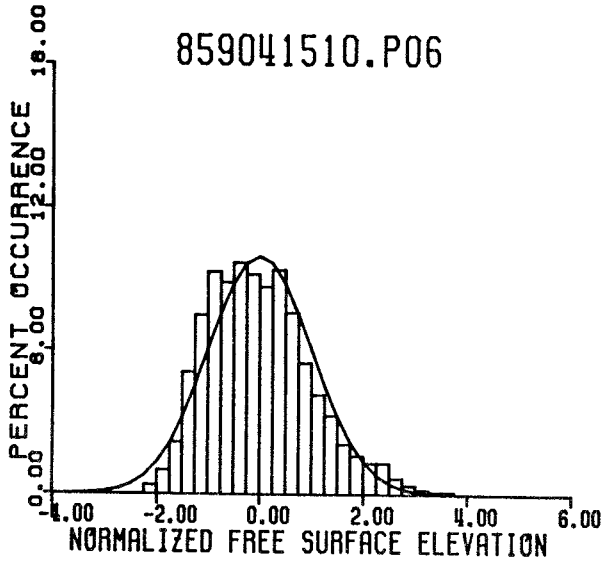
859041510.P06
PERCENT OCCURRENCE
0.00
6.00
12.00
18.00
-4.00
-2.00
0.00
2.00
4.00
6.00
NORMALIZED FREE SURFACE ELEVATION

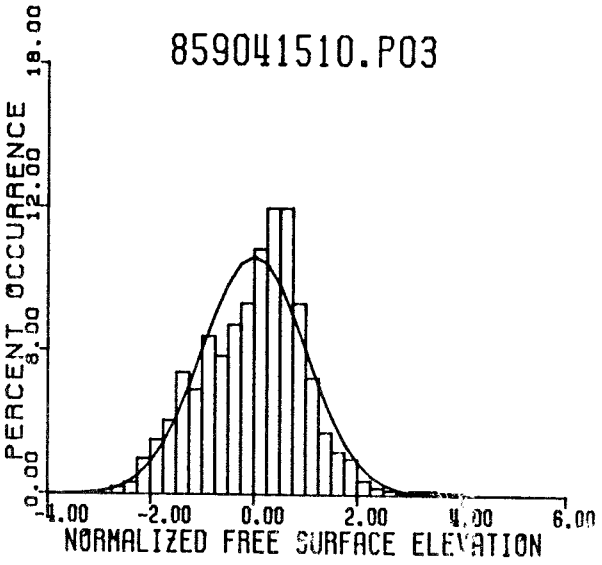
859041510.P03
PERCENT OCCURRENCE
0.00
6.00
12.00
18.00
-4.00
-2.00
0.00
2.00
4.00
6.00
NORMALIZED FREE SURFACE ELEVATION

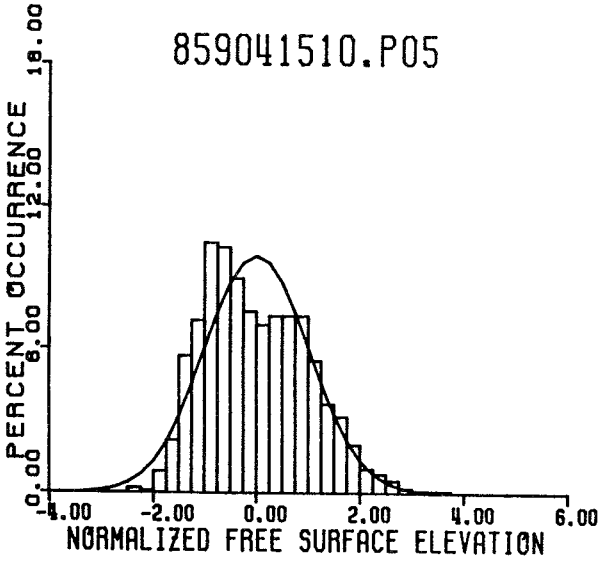
859041510.P05
PERCENT OCCURRENCE
0.00
6.00
12.00
18.00
-4.00
-2.00
0.00
2.00
4.00
6.00
NORMALIZED FREE SURFACE ELEVATION

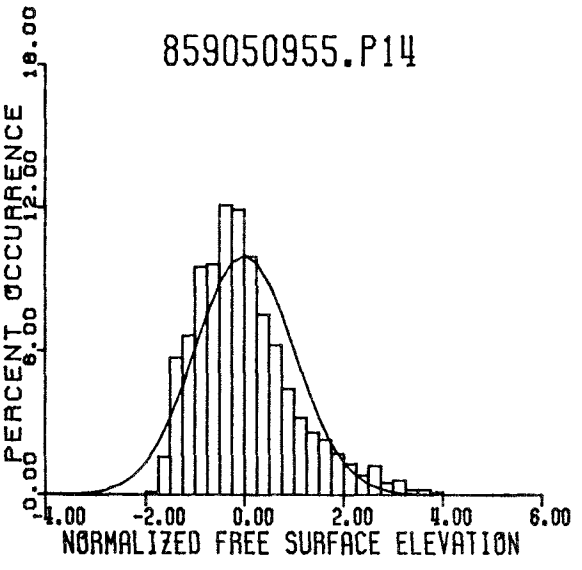
859050955.P14
PERCENT OCCURRENCE
0.00
8.00
12.00
16.00
-4.00
-2.00
0.00
2.00
4.00
6.00
NORMALIZED FREE SURFACE ELEVATION

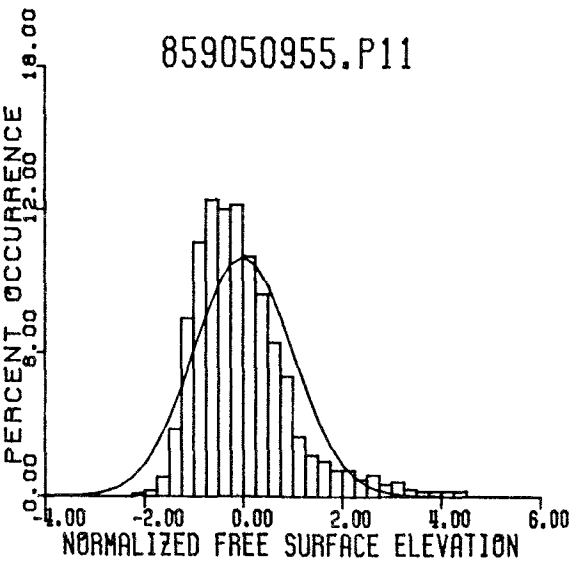
859050955.P11
PERCENT OCCURRENCE
0.00
8.00
12.00
16.00
-4.00
-2.00
0.00
2.00
4.00
6.00
NORMALIZED FREE SURFACE ELEVATION

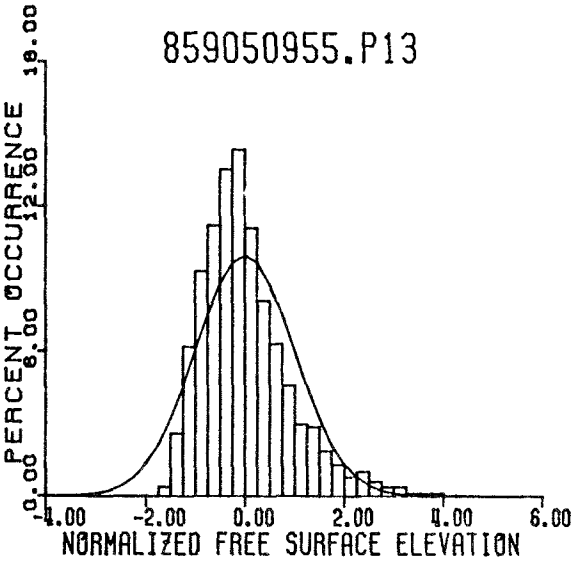
859050955.P13
PERCENT OCCURRENCE
0.00
8.00
12.00
16.00
-4.00
-2.00
0.00
2.00
4.00
6.00
NORMALIZED FREE SURFACE ELEVATION

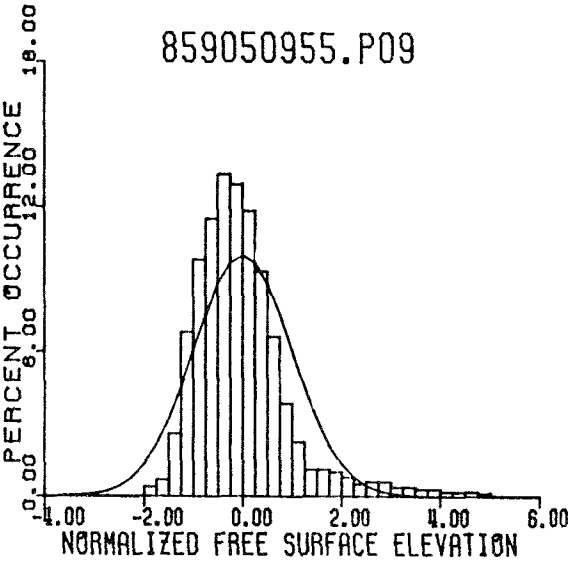
859050955.P09
PERCENT OCCURRENCE
0.00
8.00
12.00
16.00
-4.00
-2.00
0.00
2.00
4.00
6.00
NORMALIZED FREE SURFACE ELEVATION

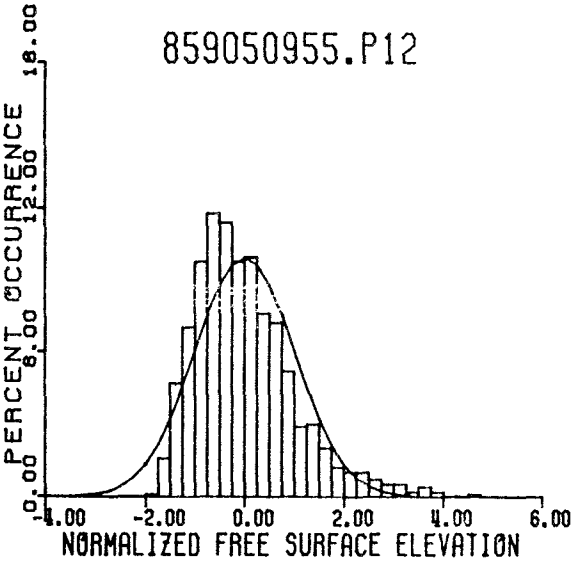
859050955.P12
PERCENT OCCURRENCE
0.00
8.00
12.00
16.00
-4.00
-2.00
0.00
2.00
4.00
6.00
NORMALIZED FREE SURFACE ELEVATION

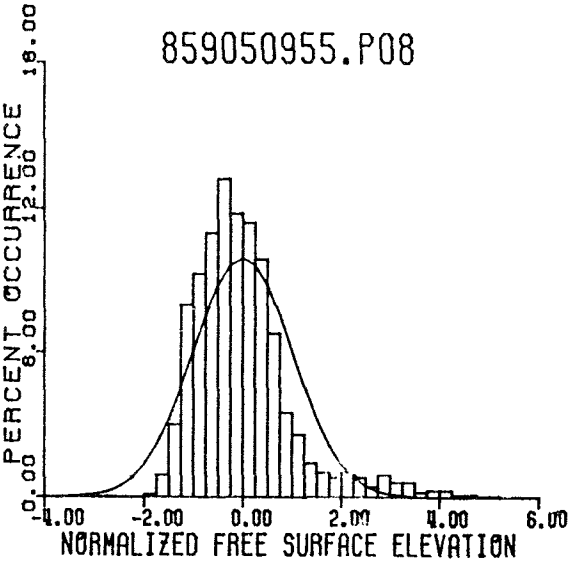
859050955.P08
PERCENT OCCURRENCE
0.00
8.00
12.00
16.00
-4.00
-2.00
0.00
2.00
4.00
6.00
NORMALIZED FREE SURFACE ELEVATION

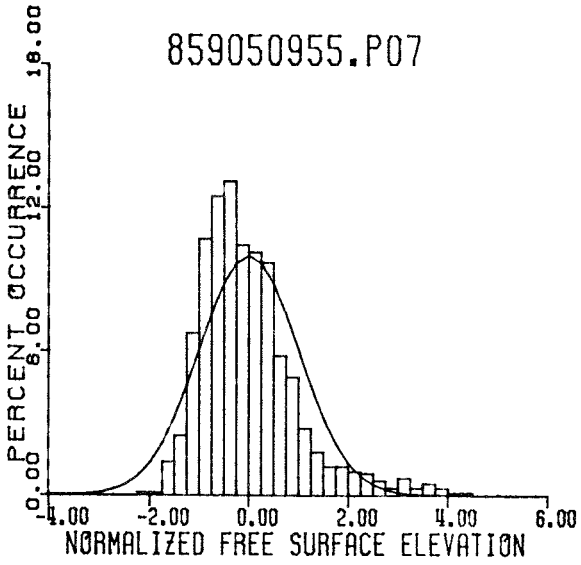
859050955.P07
PERCENT OCCURRENCE
0.00
6.00
12.00
18.00
-4.00
-2.00
0.00
2.00
4.00
6.00
NORMALIZED FREE SURFACE ELEVATION

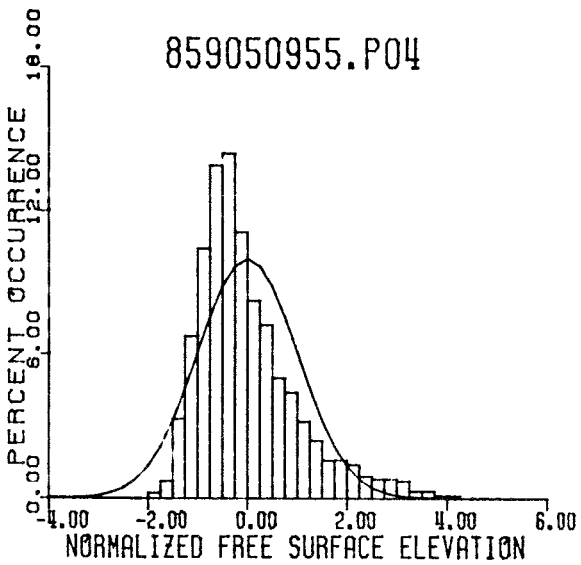
859050955.P04
PERCENT OCCURRENCE
0.00
6.00
12.00
18.00
-4.00
-2.00
0.00
2.00
4.00
6.00
NORMALIZED FREE SURFACE ELEVATION

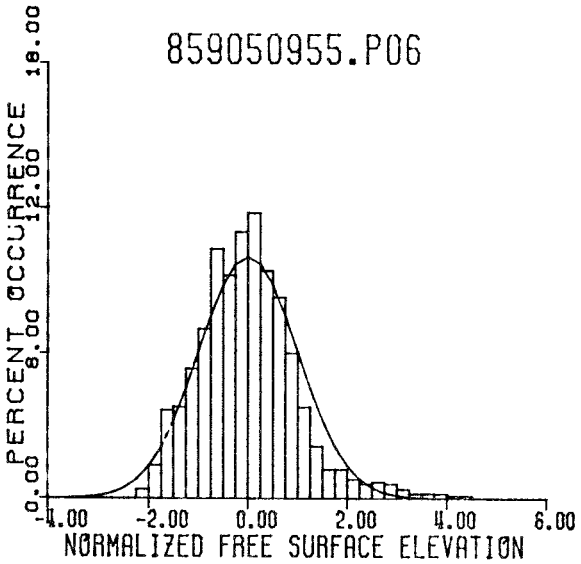
859050955.P06
PERCENT OCCURRENCE
0.00
6.00
12.00
18.00
-4.00
-2.00
0.00
2.00
4.00
6.00
NORMALIZED FREE SURFACE ELEVATION

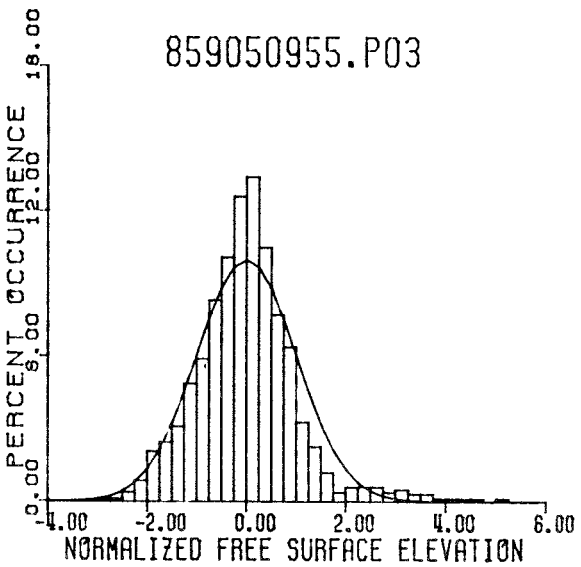
859050955.P03
PERCENT OCCURRENCE
0.00
6.00
12.00
18.00
-4.00
-2.00
0.00
2.00
4.00
6.00
NORMALIZED FREE SURFACE ELEVATION

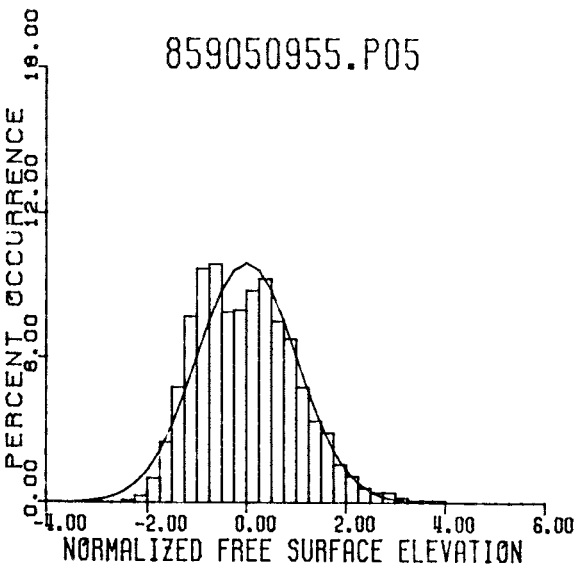
859050955.P05
PERCENT OCCURRENCE
0.00
6.00
12.00
18.00
-4.00
-2.00
0.00
2.00
4.00
6.00
NORMALIZED FREE SURFACE ELEVATION

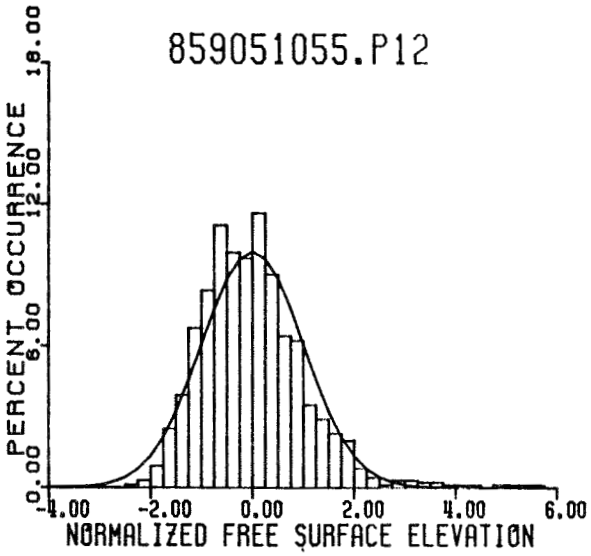
859051055.P12
PERCENT OCCURRENCE
0.00
6.00
12.00
18.00
-4.00
-2.00
0.00
2.00
4.00
6.00
NORMALIZED FREE SURFACE ELEVATION

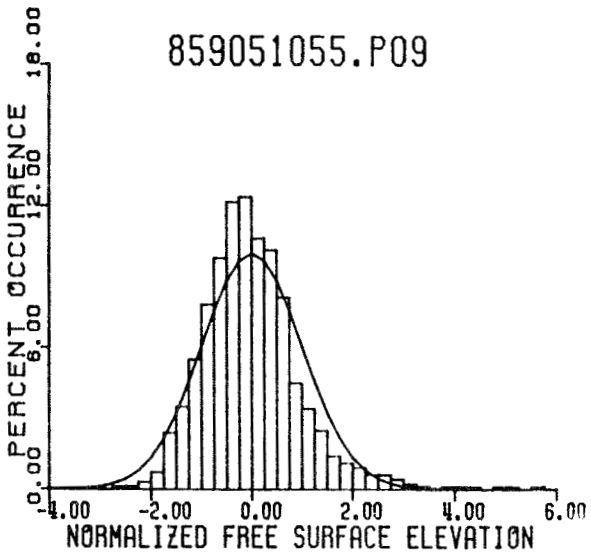
859051055.P09
PERCENT OCCURRENCE
0.00
6.00
12.00
18.00
-4.00
-2.00
0.00
2.00
4.00
6.00
NORMALIZED FREE SURFACE ELEVATION

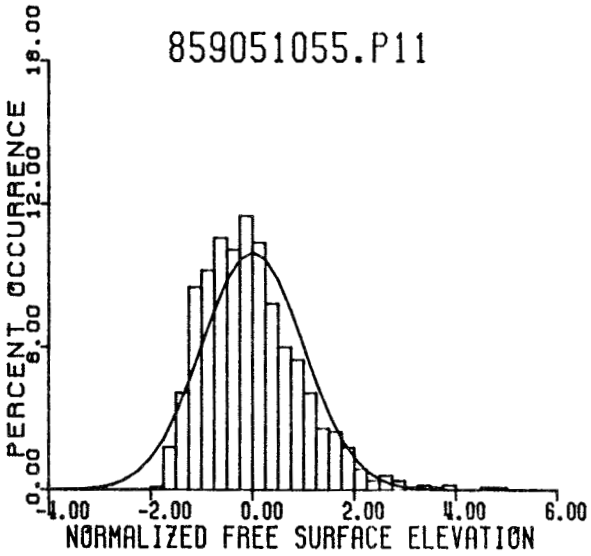
859051055.P11
PERCENT OCCURRENCE
0.00
6.00
12.00
18.00
-4.00
-2.00
0.00
2.00
4.00
6.00
NORMALIZED FREE SURFACE ELEVATION

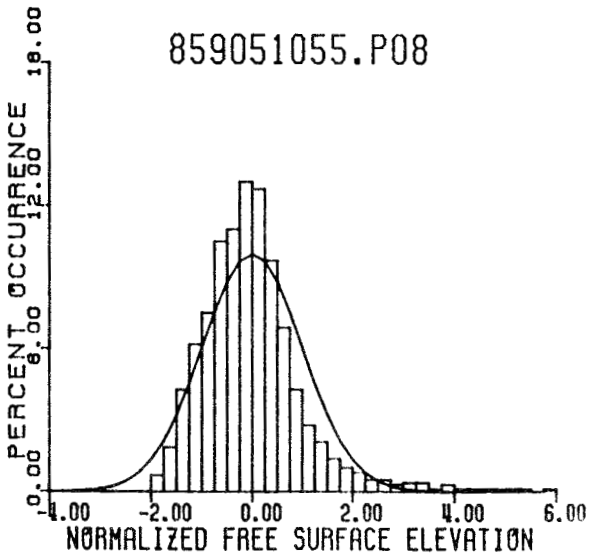
859051055.P08
PERCENT OCCURRENCE
0.00
6.00
12.00
18.00
-4.00
-2.00
0.00
2.00
4.00
6.00
NORMALIZED FREE SURFACE ELEVATION

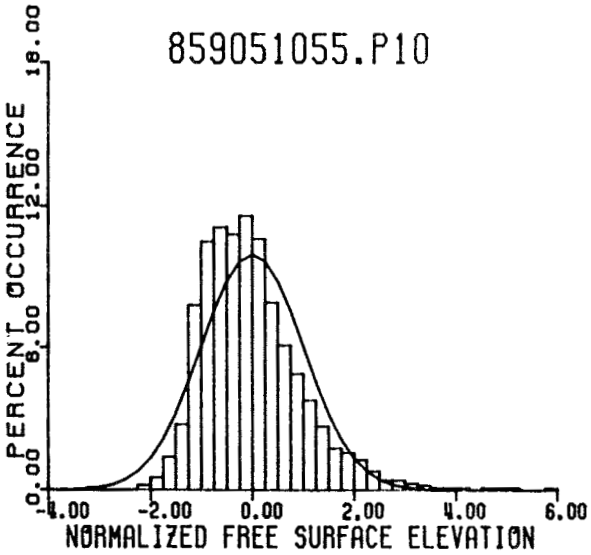
859051055.P10
PERCENT OCCURRENCE
0.00
6.00
12.00
18.00
-4.00
-2.00
0.00
2.00
4.00
6.00
NORMALIZED FREE SURFACE ELEVATION

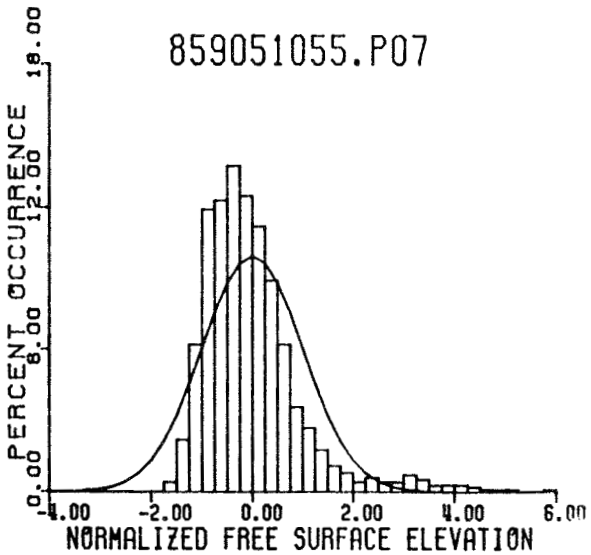
859051055.P07
PERCENT OCCURRENCE
0.00
6.00
12.00
18.00
-4.00
-2.00
0.00
2.00
4.00
6.00
NORMALIZED FREE SURFACE ELEVATION

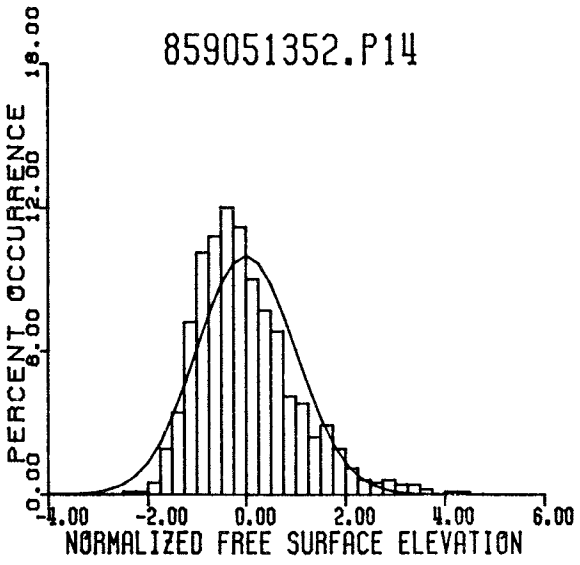
859051352.P14
PERCENT OCCURRENCE
0.00
6.00
12.00
18.00
-4.00
-2.00
0.00
2.00
4.00
6.00
NORMALIZED FREE SURFACE ELEVATION

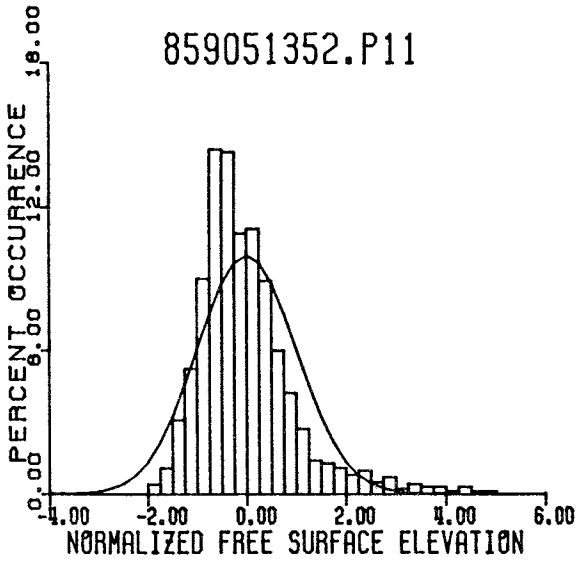
859051352.P11
PERCENT OCCURRENCE
0.00
6.00
12.00
18.00
-4.00
-2.00
0.00
2.00
4.00
6.00
NORMALIZED FREE SURFACE ELEVATION

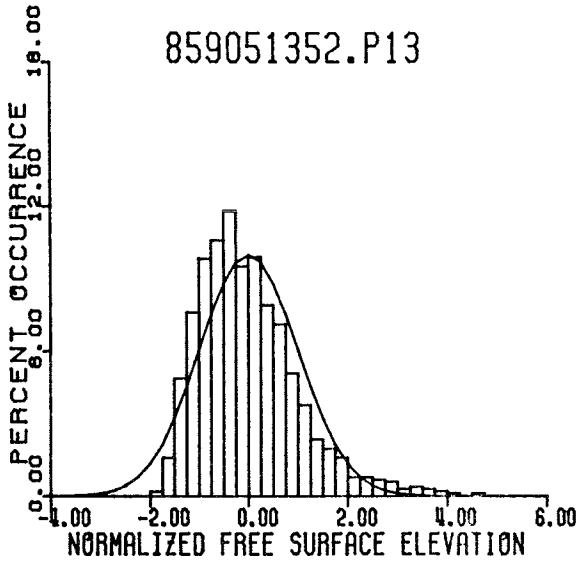
859051352.P13
PERCENT OCCURRENCE
0.00
6.00
12.00
18.00
-4.00
-2.00
0.00
2.00
4.00
6.00
NORMALIZED FREE SURFACE ELEVATION

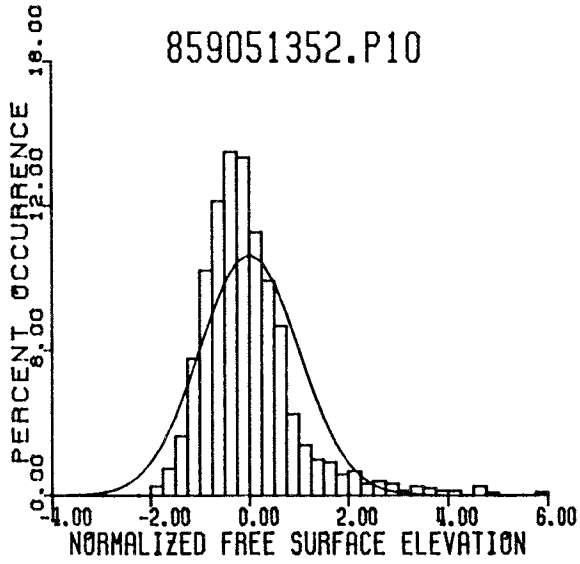
859051352.P10
PERCENT OCCURRENCE
0.00
6.00
12.00
18.00
-4.00
-2.00
0.00
2.00
4.00
6.00
NORMALIZED FREE SURFACE ELEVATION

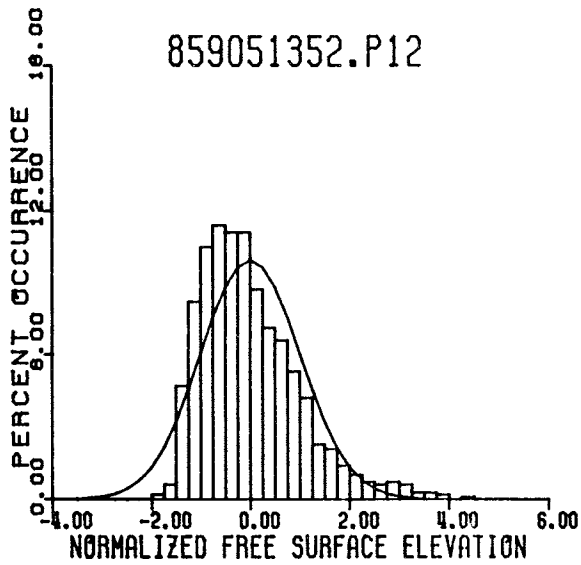
859051352.P12
PERCENT OCCURRENCE
0.00
6.00
12.00
18.00
-4.00
-2.00
0.00
2.00
4.00
6.00
NORMALIZED FREE SURFACE ELEVATION

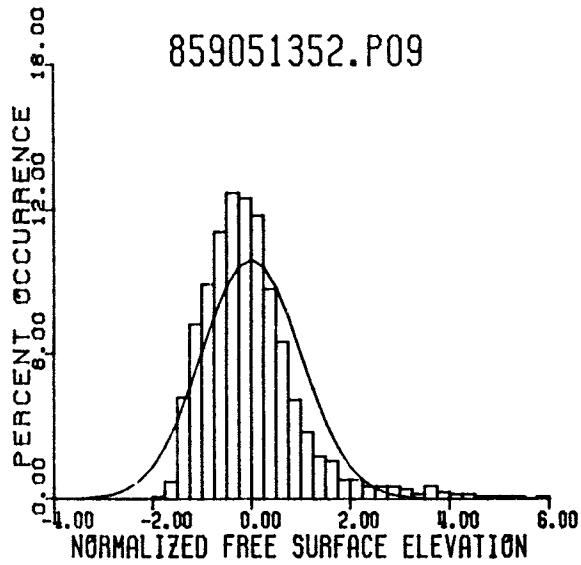
859051352.P09
PERCENT OCCURRENCE
0.00
6.00
12.00
18.00
-4.00
-2.00
0.00
2.00
4.00
6.00
NORMALIZED FREE SURFACE ELEVATION

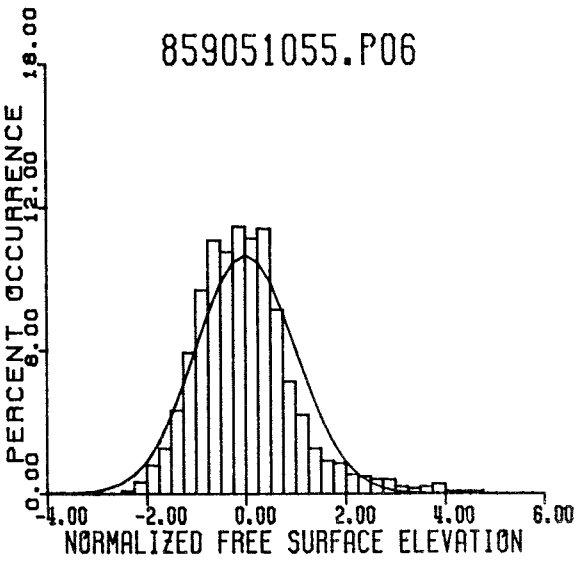
859051055.P06
PERCENT OCCURRENCE
0.00
6.00
12.00
18.00
-4.00
-2.00
0.00
2.00
4.00
6.00
NORMALIZED FREE SURFACE ELEVATION

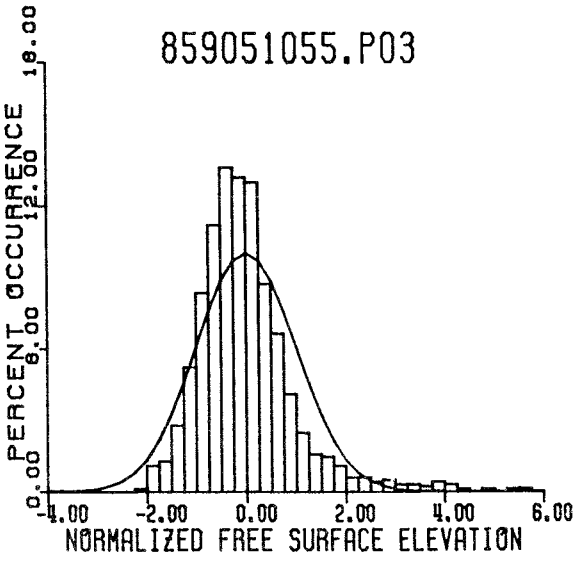
859051055.P03
PERCENT OCCURRENCE
0.00
6.00
12.00
18.00
-4.00
-2.00
0.00
2.00
4.00
6.00
NORMALIZED FREE SURFACE ELEVATION

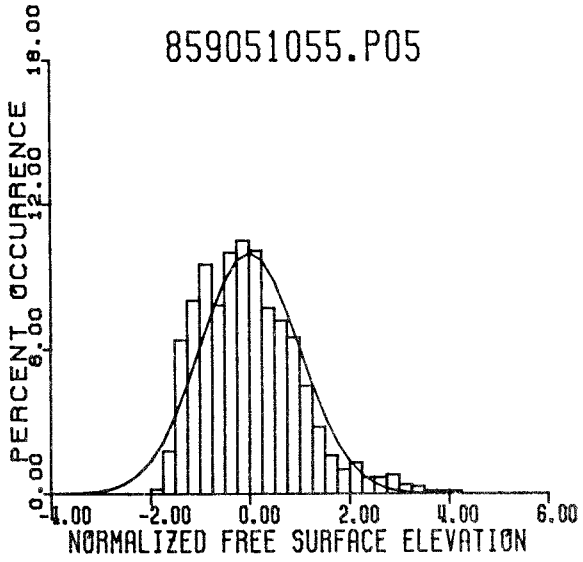
859051055.P05
PERCENT OCCURRENCE
0.00
6.00
12.00
18.00
-4.00
-2.00
0.00
2.00
4.00
6.00
NORMALIZED FREE SURFACE ELEVATION

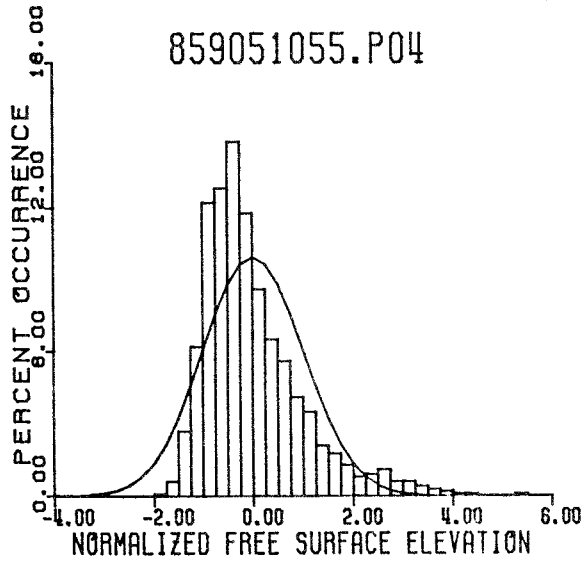
859051055.P04
PERCENT OCCURRENCE
0.00
6.00
12.00
18.00
-4.00
-2.00
0.00
2.00
4.00
6.00
NORMALIZED FREE SURFACE ELEVATION

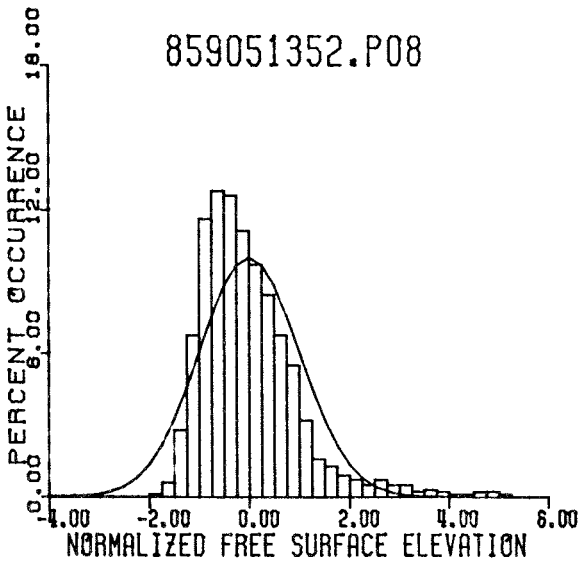
859051352.P08
PERCENT OCCURRENCE
0.00
6.00
12.00
18.00
-4.00
-2.00
0.00
2.00
4.00
6.00
NORMALIZED FREE SURFACE ELEVATION

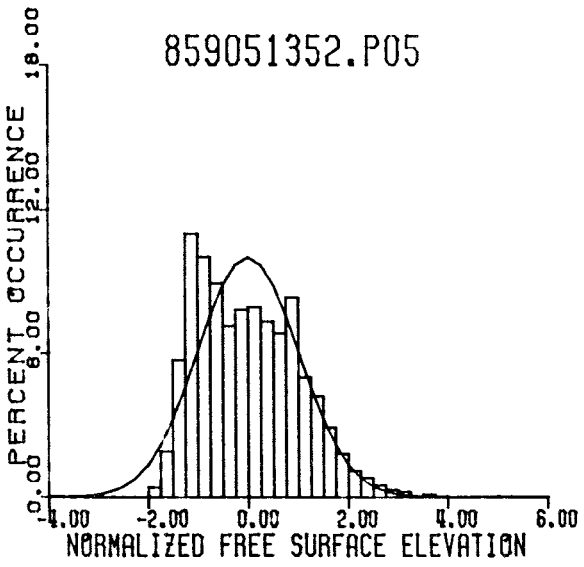
859051352.P05
PERCENT OCCURRENCE
0.00
6.00
12.00
18.00
-4.00
-2.00
0.00
2.00
4.00
6.00
NORMALIZED FREE SURFACE ELEVATION

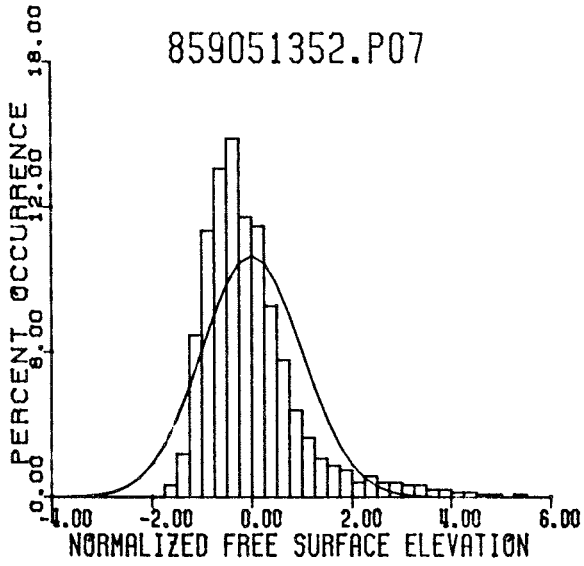
859051352.P07
PERCENT OCCURRENCE
0.00
6.00
12.00
18.00
-4.00
-2.00
0.00
2.00
4.00
6.00
NORMALIZED FREE SURFACE ELEVATION

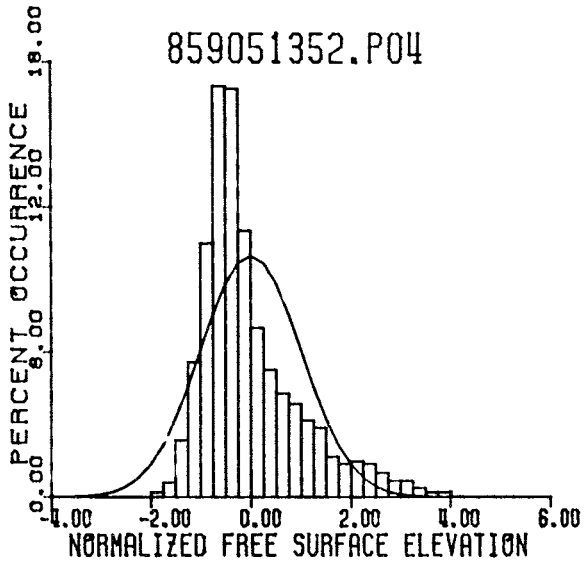
859051352.P04
PERCENT OCCURRENCE
0.00
6.00
12.00
18.00
-4.00
-2.00
0.00
2.00
4.00
6.00
NORMALIZED FREE SURFACE ELEVATION

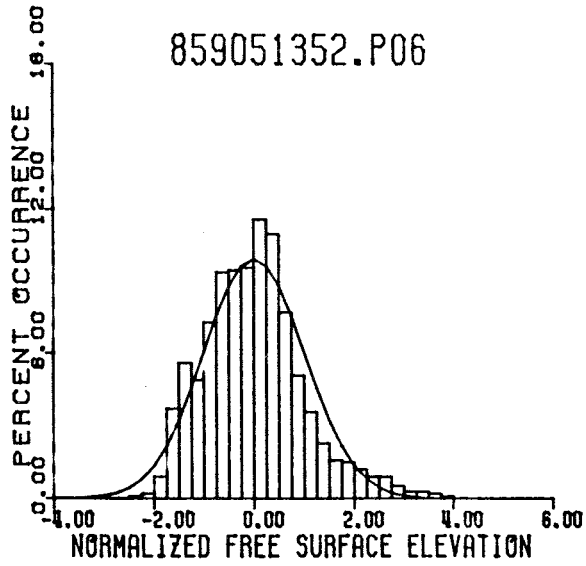
859051352.P06
PERCENT OCCURRENCE
0.00
6.00
12.00
18.00
-4.00
-2.00
0.00
2.00
4.00
6.00
NORMALIZED FREE SURFACE ELEVATION

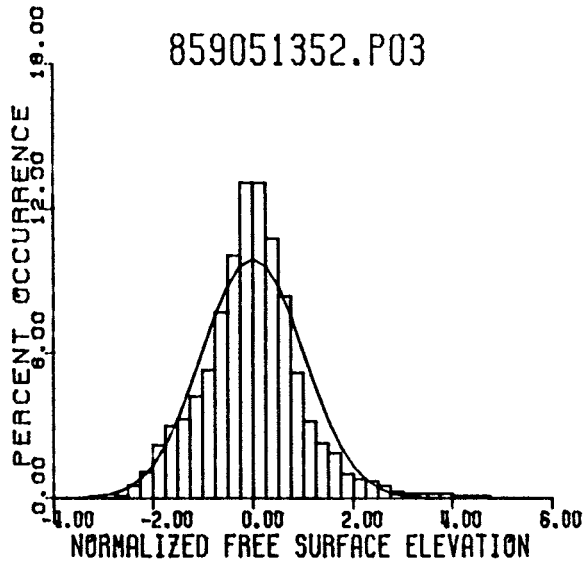
859051352.P03
PERCENT OCCURRENCE
0.00
6.00
12.50
18.00
-4.00
-2.00
0.00
2.00
4.00
6.00
NORMALIZED FREE SURFACE ELEVATION

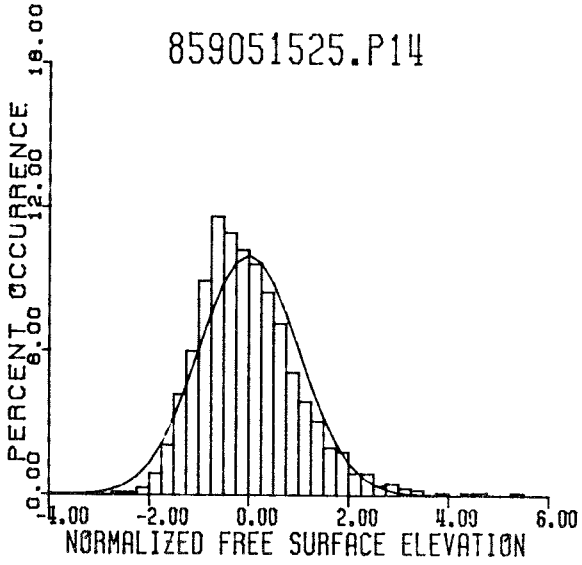
859051525.P14
PERCENT OCCURRENCE
0.00
6.00
12.00
18.00
-4.00
-2.00
0.00
2.00
4.00
6.00
NORMALIZED FREE SURFACE ELEVATION

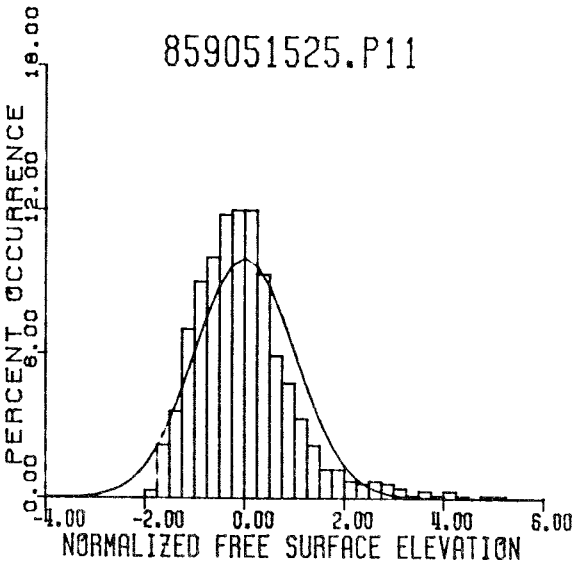
859051525.P11
PERCENT OCCURRENCE
0.00
6.00
12.00
18.00
-4.00
-2.00
0.00
2.00
4.00
6.00
NORMALIZED FREE SURFACE ELEVATION

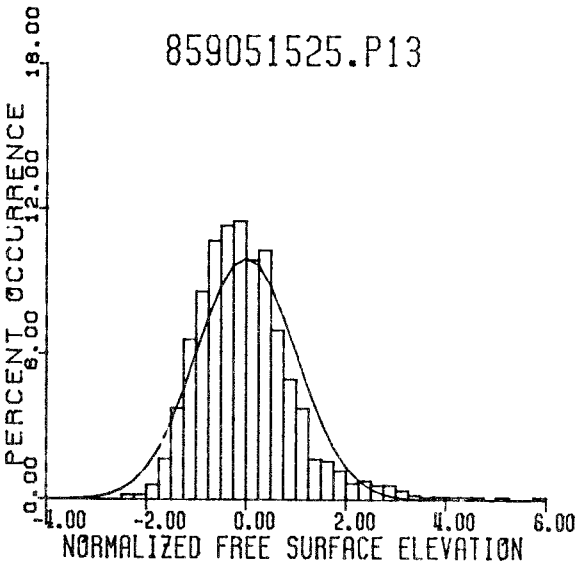
859051525.P13
PERCENT OCCURRENCE
0.00
6.00
12.00
18.00
-4.00
-2.00
0.00
2.00
4.00
6.00
NORMALIZED FREE SURFACE ELEVATION

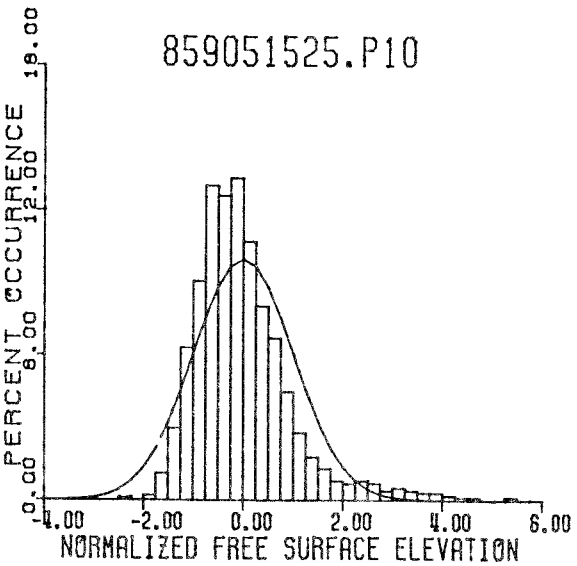
859051525.P10
PERCENT OCCURRENCE
0.00
6.00
12.00
18.00
-4.00
-2.00
0.00
2.00
4.00
6.00
NORMALIZED FREE SURFACE ELEVATION

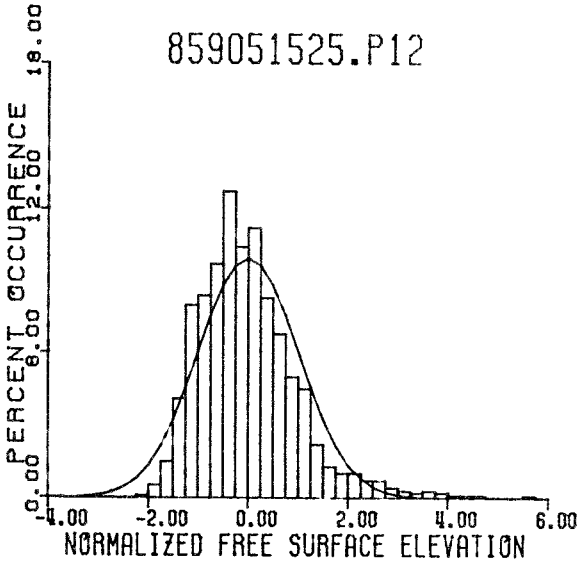
859051525.P12
PERCENT OCCURRENCE
0.00
6.00
12.00
18.00
-4.00
-2.00
0.00
2.00
4.00
6.00
NORMALIZED FREE SURFACE ELEVATION

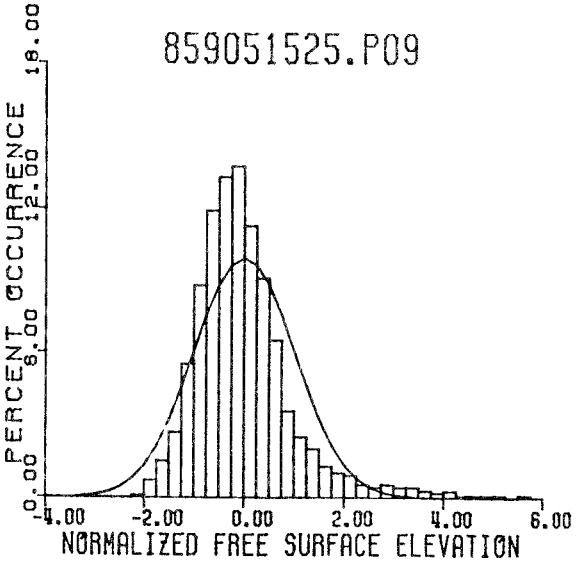
859051525.P09
PERCENT OCCURRENCE
0.00
6.00
12.00
18.00
-4.00
-2.00
0.00
2.00
4.00
6.00
NORMALIZED FREE SURFACE ELEVATION

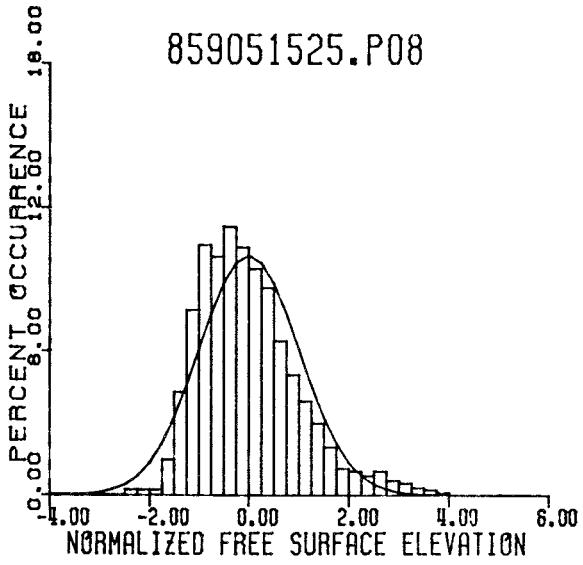
859051525.P08
PERCENT OCCURRENCE
0.00
6.00
12.00
18.00
-4.00
-2.00
0.00
2.00
4.00
6.00
NORMALIZED FREE SURFACE ELEVATION

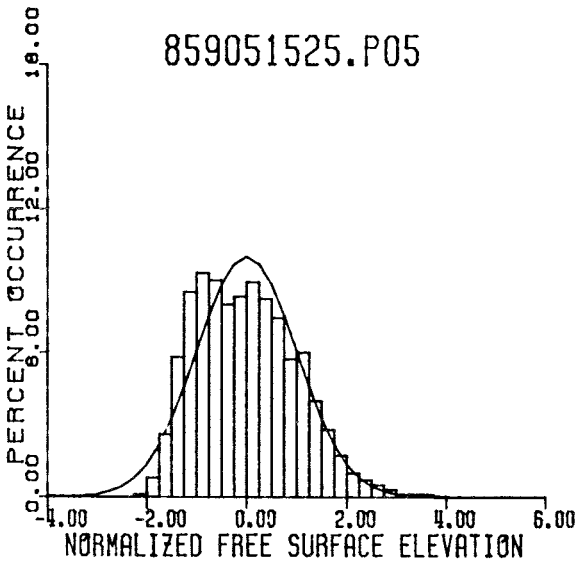
859051525.P05
PERCENT OCCURRENCE
0.00
6.00
12.00
18.00
-4.00
-2.00
0.00
2.00
4.00
6.00
NORMALIZED FREE SURFACE ELEVATION

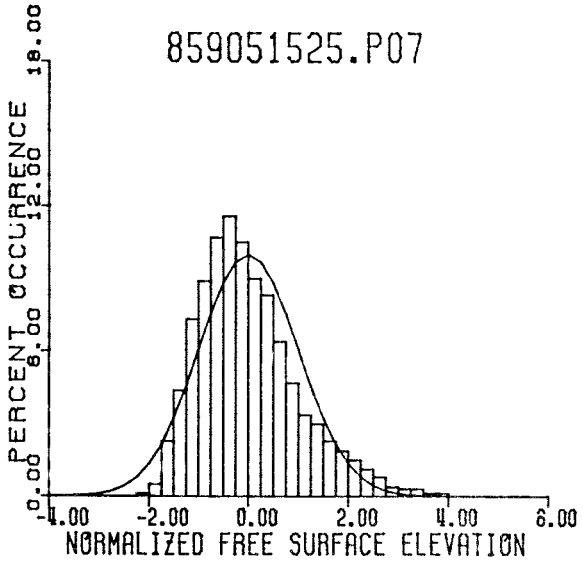
859051525.P07
PERCENT OCCURRENCE
0.00
6.00
12.00
18.00
-4.00
-2.00
0.00
2.00
4.00
6.00
NORMALIZED FREE SURFACE ELEVATION

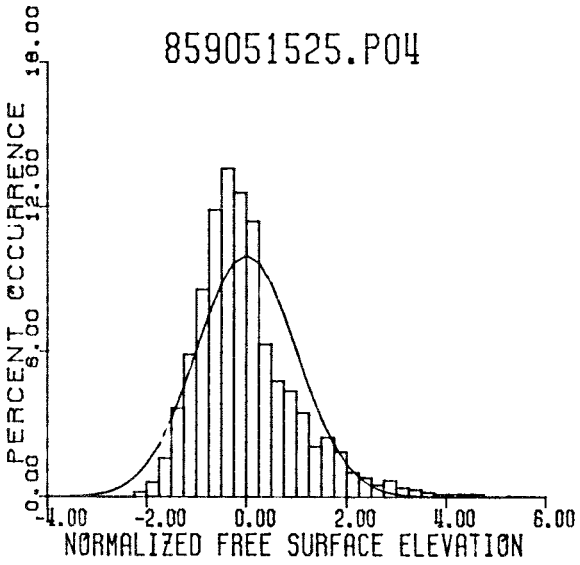
859051525.P04
PERCENT OCCURRENCE
0.00
6.00
12.00
18.00
-4.00
-2.00
0.00
2.00
4.00
6.00
NORMALIZED FREE SURFACE ELEVATION

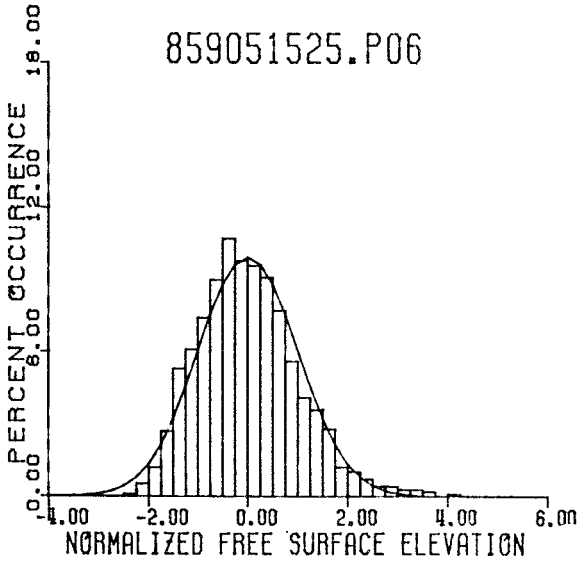
859051525.P06
PERCENT OCCURRENCE
0.00
6.00
12.00
18.00
-4.00
-2.00
0.00
2.00
4.00
6.00
NORMALIZED FREE SURFACE ELEVATION

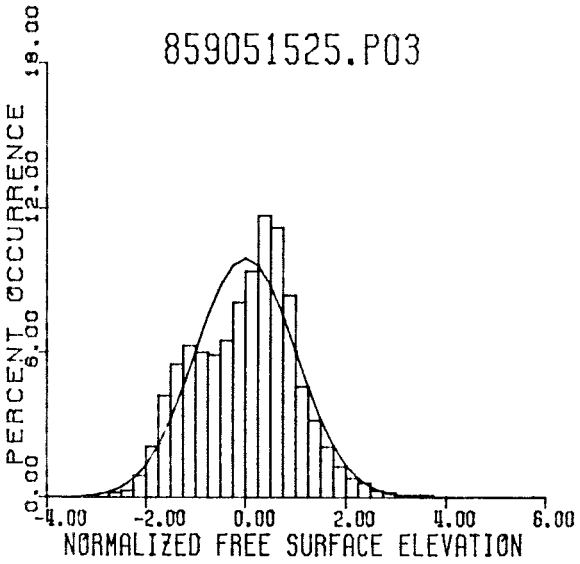
859051525.P03
PERCENT OCCURRENCE
0.00
6.00
12.00
18.00
-4.00
-2.00
0.00
2.00
4.00
6.00
NORMALIZED FREE SURFACE ELEVATION

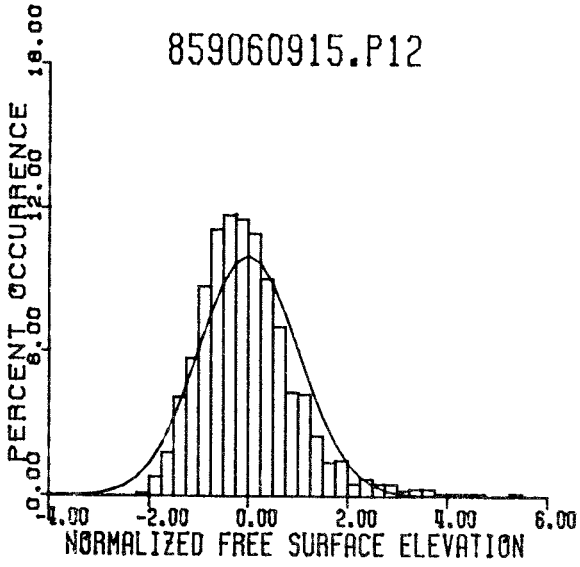
859060915.P12
PERCENT OCCURRENCE
0.00
6.00
12.00
18.00
-4.00
-2.00
0.00
2.00
4.00
6.00
NORMALIZED FREE SURFACE ELEVATION

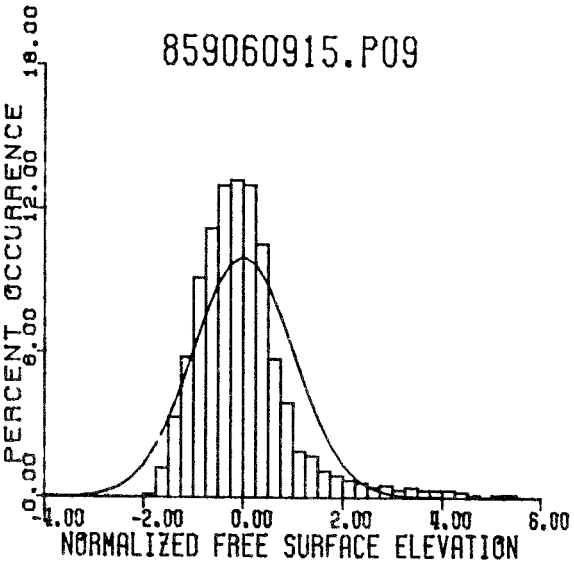
859060915.P09
PERCENT OCCURRENCE
0.00
6.00
12.00
18.00
-4.00
-2.00
0.00
2.00
4.00
6.00
NORMALIZED FREE SURFACE ELEVATION

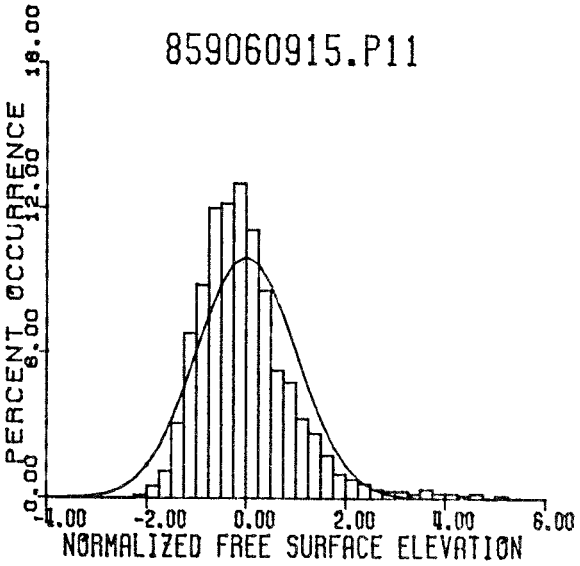
859060915.P11
PERCENT OCCURRENCE
0.00
6.00
12.00
18.00
-4.00
-2.00
0.00
2.00
4.00
6.00
NORMALIZED FREE SURFACE ELEVATION

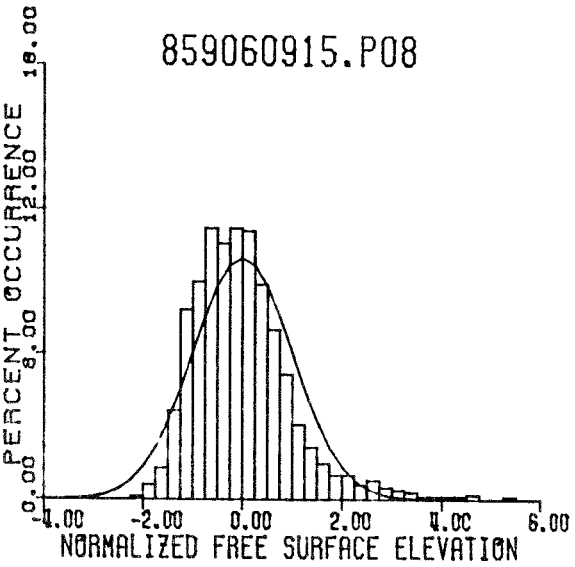
859060915.P08
PERCENT OCCURRENCE
0.00
6.00
12.00
18.00
-4.00
-2.00
0.00
2.00
4.00
6.00
NORMALIZED FREE SURFACE ELEVATION

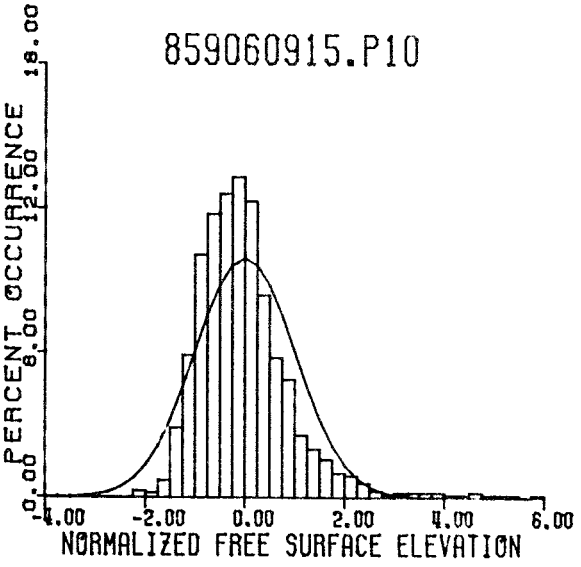
859060915.P10
PERCENT OCCURRENCE
0.00
6.00
12.00
18.00
-4.00
-2.00
0.00
2.00
4.00
6.00
NORMALIZED FREE SURFACE ELEVATION

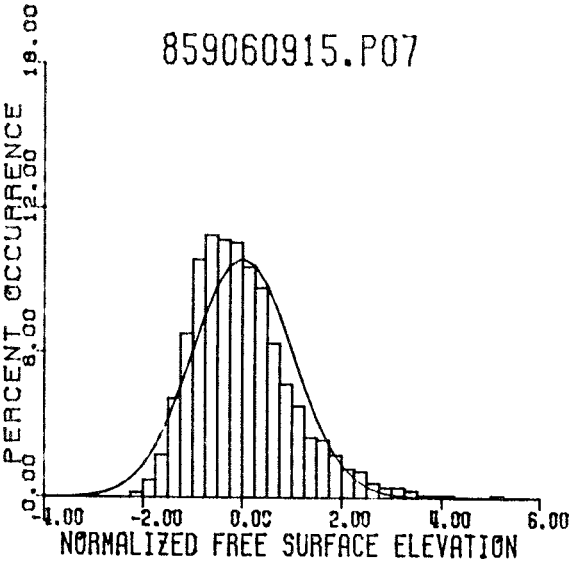
859060915.P07
PERCENT OCCURRENCE
0.00
6.00
12.00
18.00
-4.00
-2.00
0.00
2.00
4.00
6.00
NORMALIZED FREE SURFACE ELEVATION

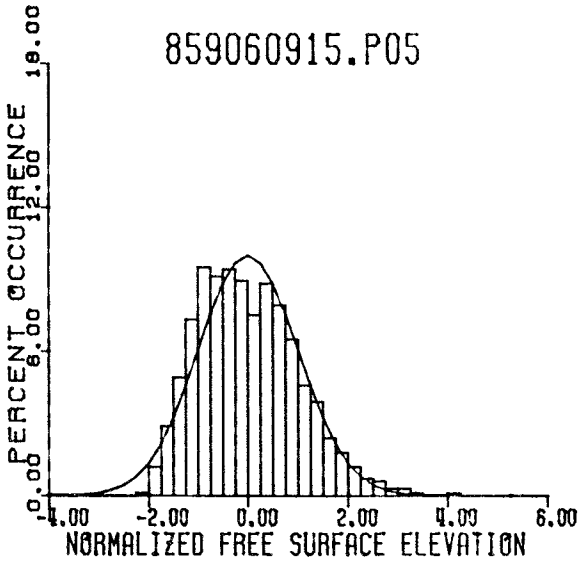
859060915.P05
PERCENT OCCURRENCE
0.00
6.00
12.00
18.00
-4.00
-2.00
0.00
2.00
4.00
6.00
NORMALIZED FREE SURFACE ELEVATION

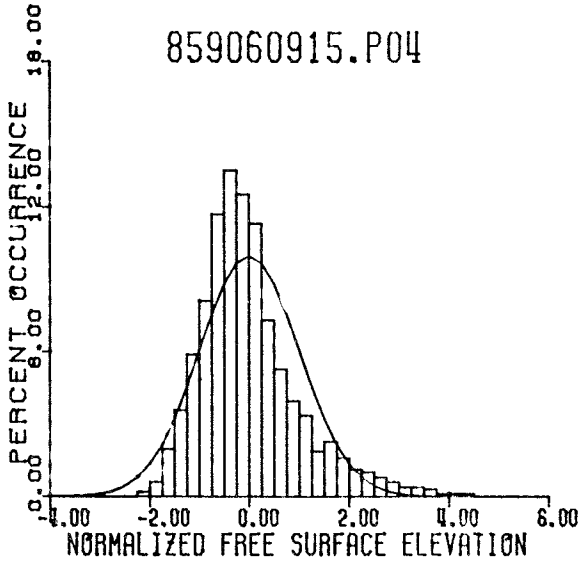
859060915.P04
PERCENT OCCURRENCE
0.00
6.00
12.00
18.00
-4.00
-2.00
0.00
2.00
4.00
6.00
NORMALIZED FREE SURFACE ELEVATION

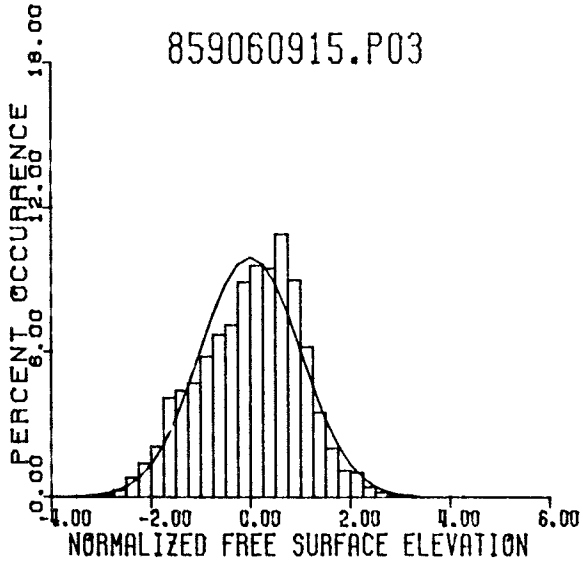
859060915.P03
PERCENT OCCURRENCE
0.00
6.00
12.00
18.00
-4.00
-2.00
0.00
2.00
4.00
6.00
NORMALIZED FREE SURFACE ELEVATION

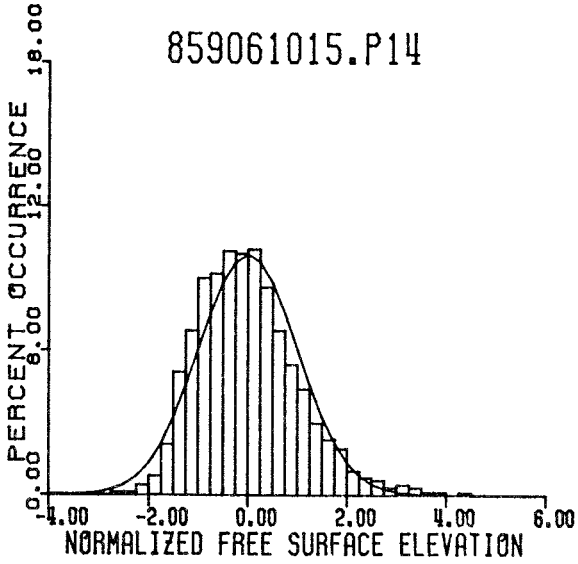
859061015.P14
PERCENT OCCURRENCE
0.00
6.00
12.00
18.00
-4.00
-2.00
0.00
2.00
4.00
6.00
NORMALIZED FREE SURFACE ELEVATION

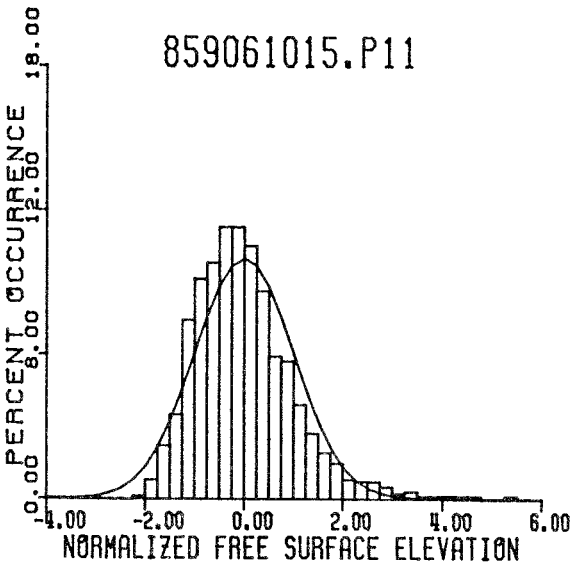
859061015.P11
PERCENT OCCURRENCE
0.00
6.00
12.00
18.00
-4.00
-2.00
0.00
2.00
4.00
6.00
NORMALIZED FREE SURFACE ELEVATION

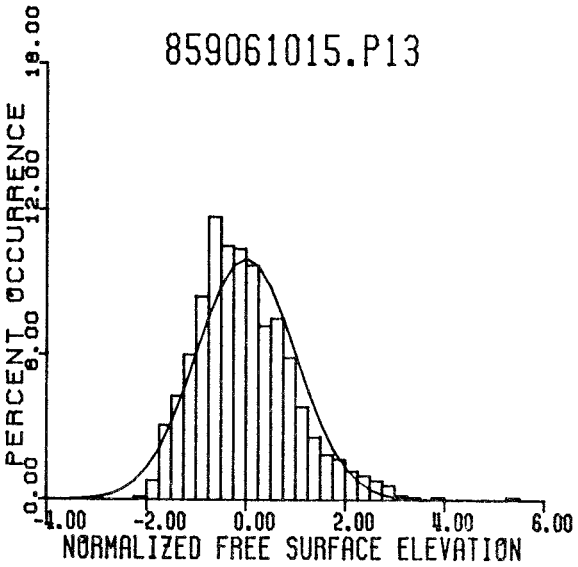
859061015.P13
PERCENT OCCURRENCE
0.00
6.00
12.00
18.00
-4.00
-2.00
0.00
2.00
4.00
6.00
NORMALIZED FREE SURFACE ELEVATION

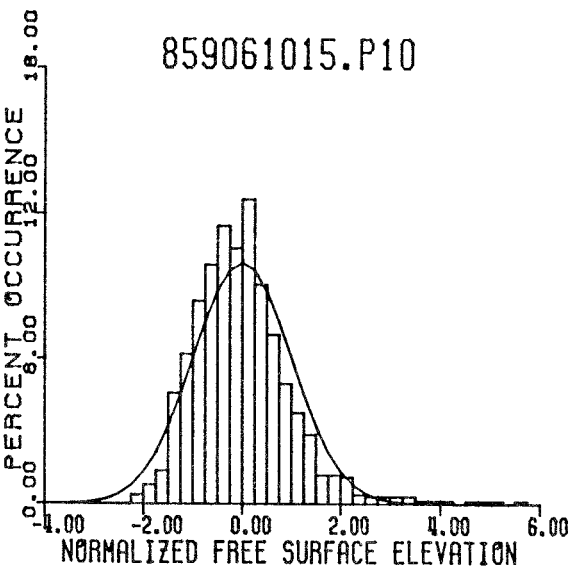
859061015.P10
PERCENT OCCURRENCE
0.00
6.00
12.00
18.00
-4.00
-2.00
0.00
2.00
4.00
6.00
NORMALIZED FREE SURFACE ELEVATION

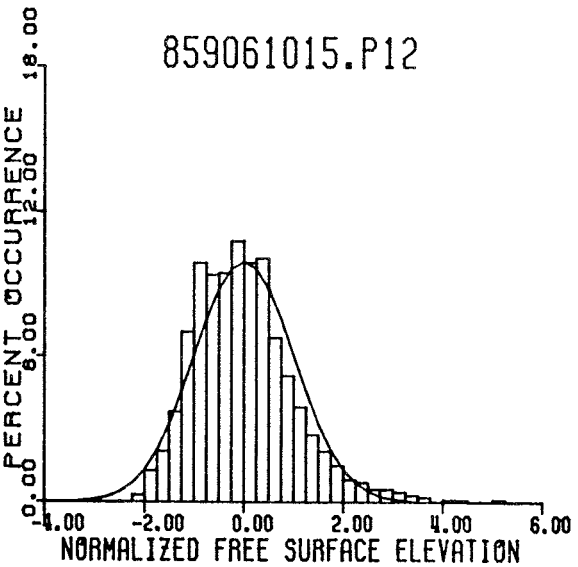
859061015.P12
PERCENT OCCURRENCE
0.00
6.00
12.00
18.00
-4.00
-2.00
0.00
2.00
4.00
6.00
NORMALIZED FREE SURFACE ELEVATION

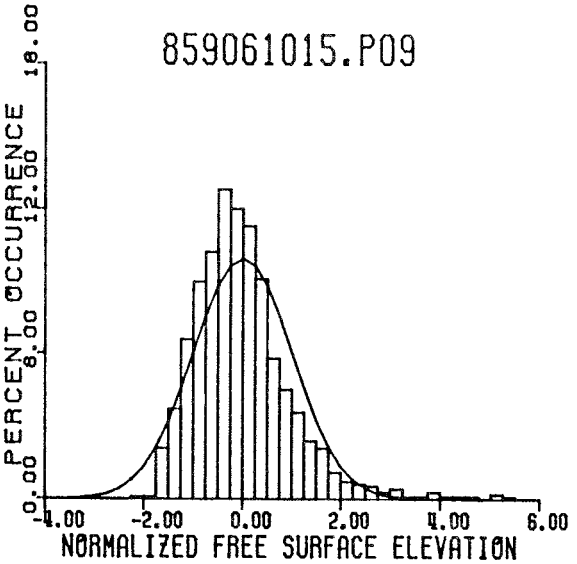
859061015.P09
PERCENT OCCURRENCE
0.00
6.00
12.00
18.00
-4.00
-2.00
0.00
2.00
4.00
6.00
NORMALIZED FREE SURFACE ELEVATION

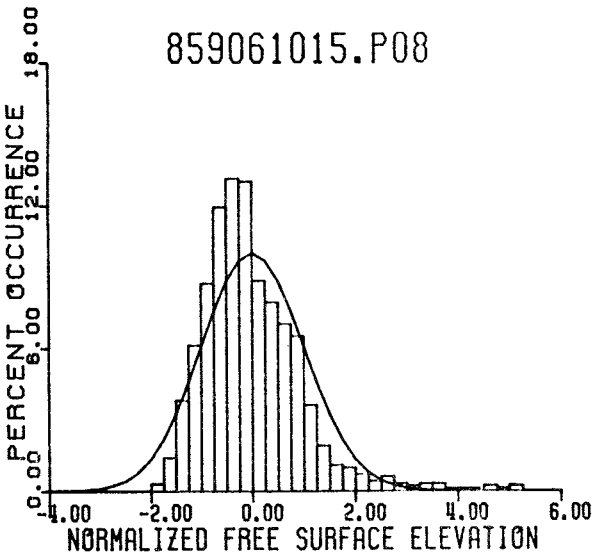
859061015.P08
PERCENT OCCURRENCE
0.00
6.00
12.00
18.00
-4.00
-2.00
0.00
2.00
4.00
6.00
NORMALIZED FREE SURFACE ELEVATION

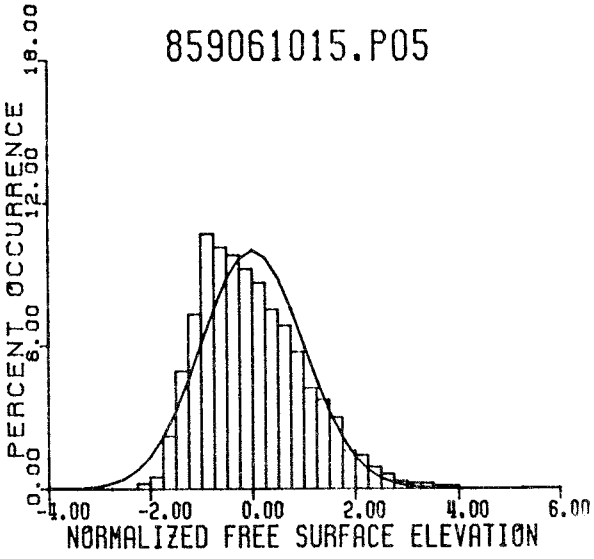
859061015.P05
PERCENT OCCURRENCE
0.00
6.00
12.00
18.00
-4.00
-2.00
0.00
2.00
4.00
6.00
NORMALIZED FREE SURFACE ELEVATION

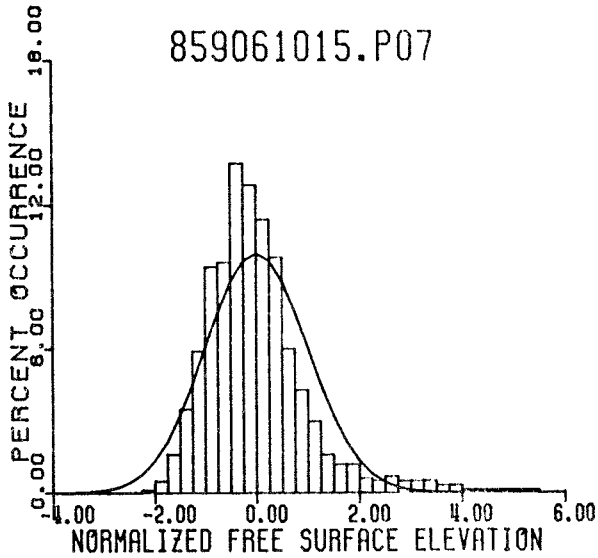
859061015.P07
PERCENT OCCURRENCE
0.00
6.00
12.00
18.00
-4.00
-2.00
0.00
2.00
4.00
6.00
NORMALIZED FREE SURFACE ELEVATION

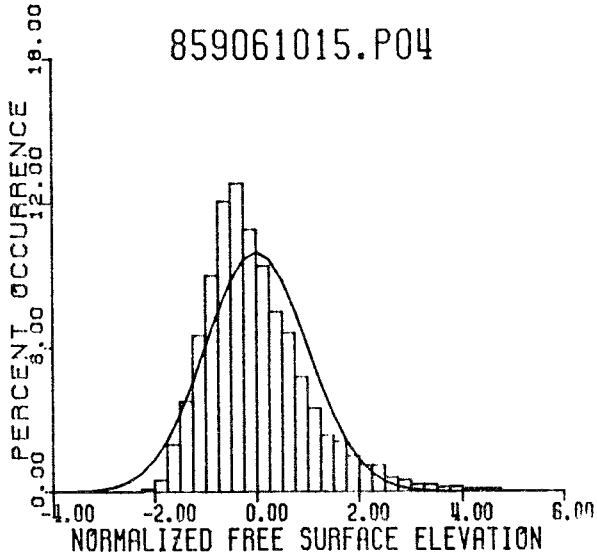
859061015.P04
PERCENT OCCURRENCE
0.00
6.00
12.00
18.00
-4.00
-2.00
0.00
2.00
4.00
6.00
NORMALIZED FREE SURFACE ELEVATION

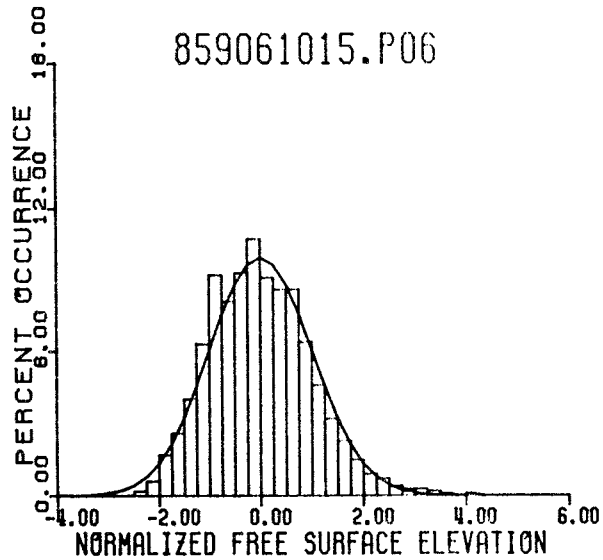
859061015.P06
PERCENT OCCURRENCE
0.00
6.00
12.00
18.00
-4.00
-2.00
0.00
2.00
4.00
6.00
NORMALIZED FREE SURFACE ELEVATION

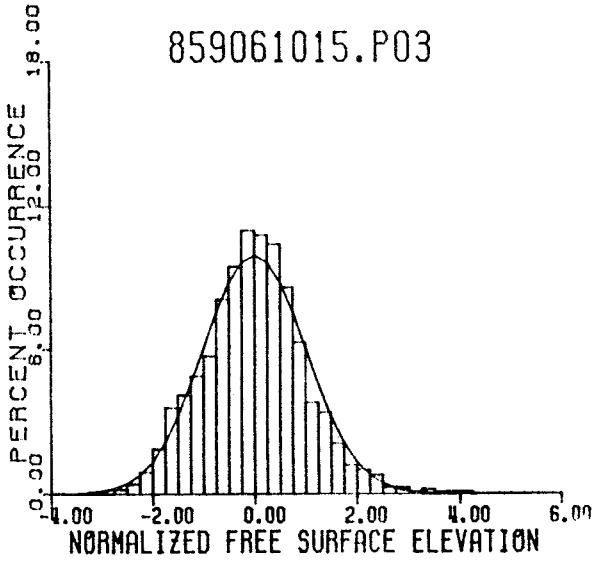
859061015.P03
PERCENT OCCURRENCE
0.00
6.00
12.00
18.00
-4.00
-2.00
0.00
2.00
4.00
6.00
NORMALIZED FREE SURFACE ELEVATION

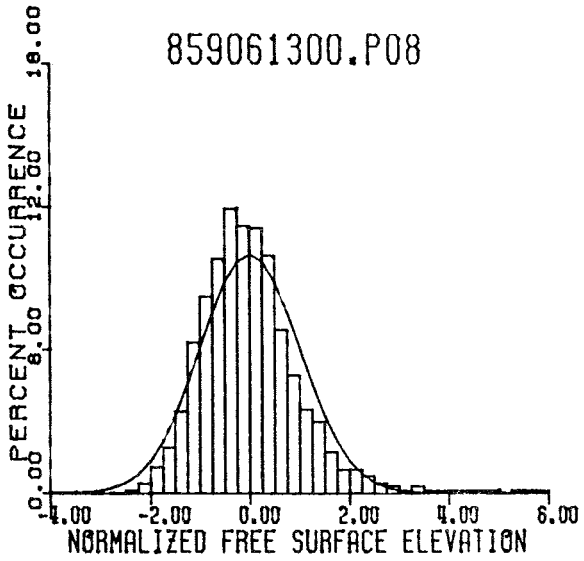
859061300.P08
PERCENT OCCURRENCE
0.00
6.00
12.00
18.00
-4.00
-2.00
0.00
2.00
4.00
6.00
NORMALIZED FREE SURFACE ELEVATION

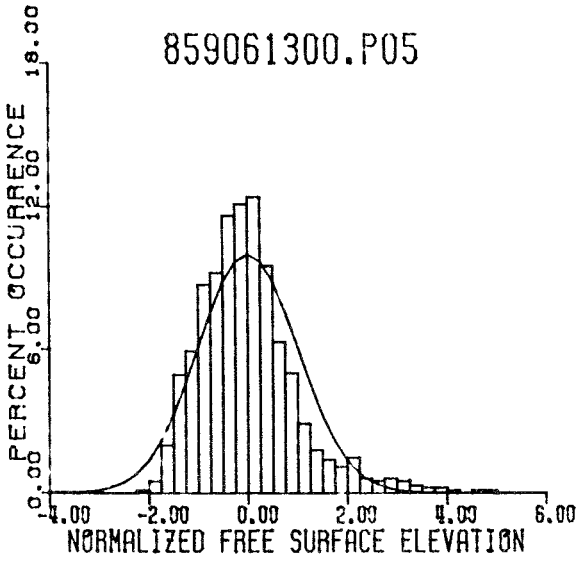
859061300.P05
PERCENT OCCURRENCE
0.00
6.00
12.00
18.00
-4.00
-2.00
0.00
2.00
4.00
6.00
NORMALIZED FREE SURFACE ELEVATION

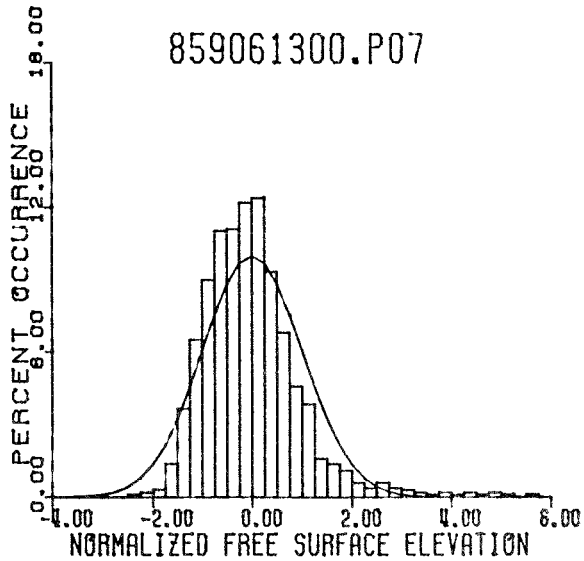
859061300.P07
PERCENT OCCURRENCE
0.00
6.00
12.00
18.00
-4.00
-2.00
0.00
2.00
4.00
6.00
NORMALIZED FREE SURFACE ELEVATION

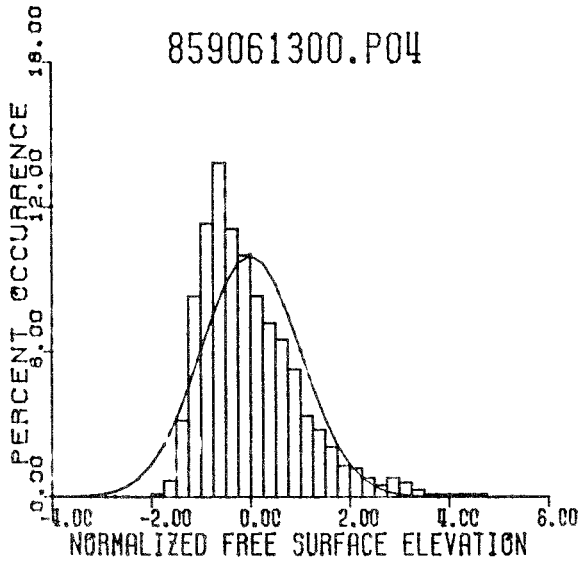
859061300.P04
PERCENT OCCURRENCE
0.00
6.00
12.00
18.00
-4.00
-2.00
0.00
2.00
4.00
6.00
NORMALIZED FREE SURFACE ELEVATION

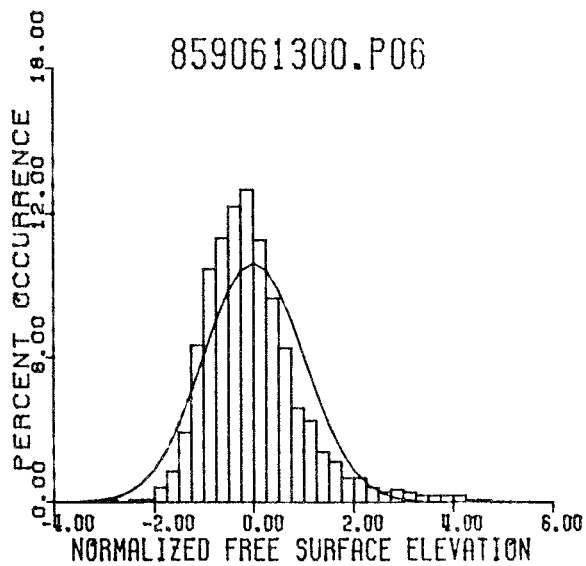
859061300.P06
PERCENT OCCURRENCE
0.00
6.00
12.00
18.00
-4.00
-2.00
0.00
2.00
4.00
6.00
NORMALIZED FREE SURFACE ELEVATION

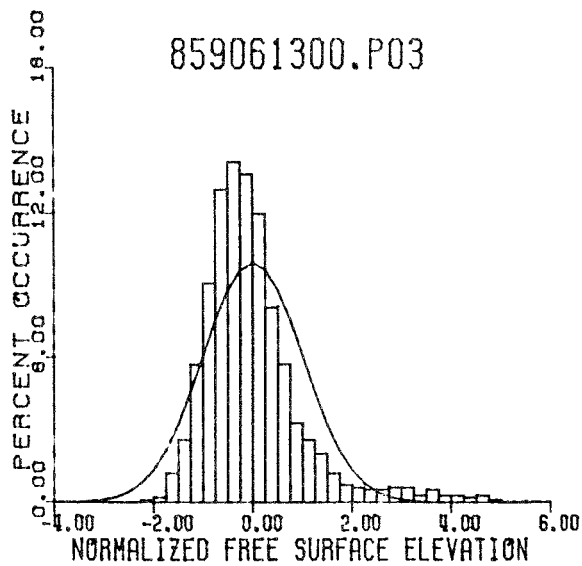
859061300.P03
PERCENT OCCURRENCE
0.00
6.00
12.00
18.00
-4.00
-2.00
0.00
2.00
4.00
6.00
NORMALIZED FREE SURFACE ELEVATION

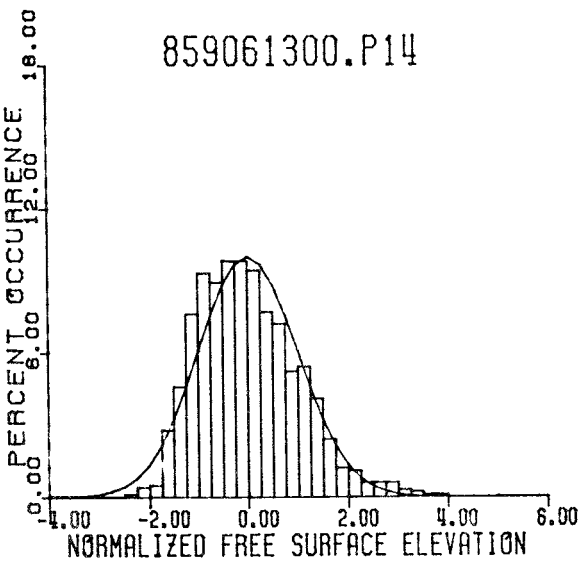
859061300.P14
PERCENT OCCURRENCE
0.00
6.00
12.00
18.00
-4.00
-2.00
0.00
2.00
4.00
6.00
NORMALIZED FREE SURFACE ELEVATION

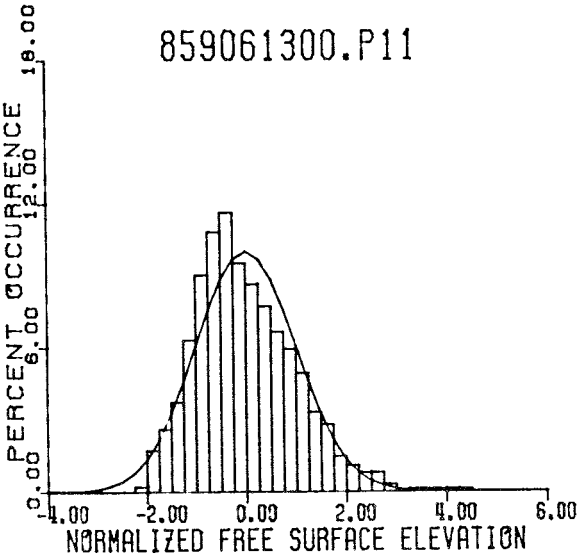
859061300.P11
PERCENT OCCURRENCE
0.00
6.00
12.00
18.00
-4.00
-2.00
0.00
2.00
4.00
6.00
NORMALIZED FREE SURFACE ELEVATION

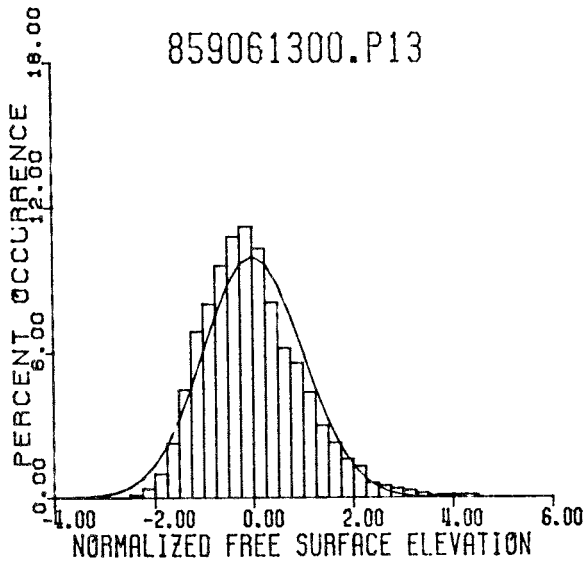
859061300.P13
PERCENT OCCURRENCE
0.00
6.00
12.00
18.00
-4.00
-2.00
0.00
2.00
4.00
6.00
NORMALIZED FREE SURFACE ELEVATION

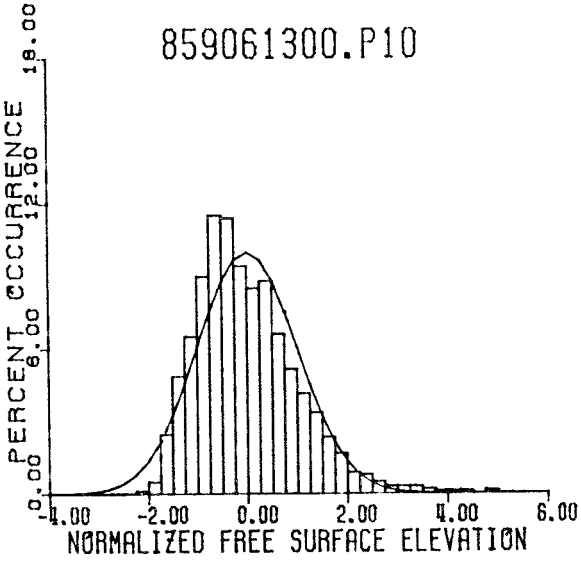
859061300.P10
PERCENT OCCURRENCE
0.00
6.00
12.00
18.00
-4.00
-2.00
0.00
2.00
4.00
6.00
NORMALIZED FREE SURFACE ELEVATION

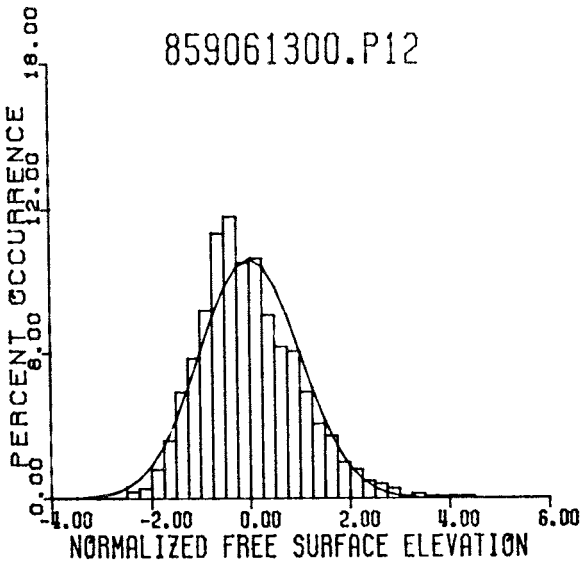
859061300.P12
PERCENT OCCURRENCE
0.00
6.00
12.00
18.00
-4.00
-2.00
0.00
2.00
4.00
6.00
NORMALIZED FREE SURFACE ELEVATION

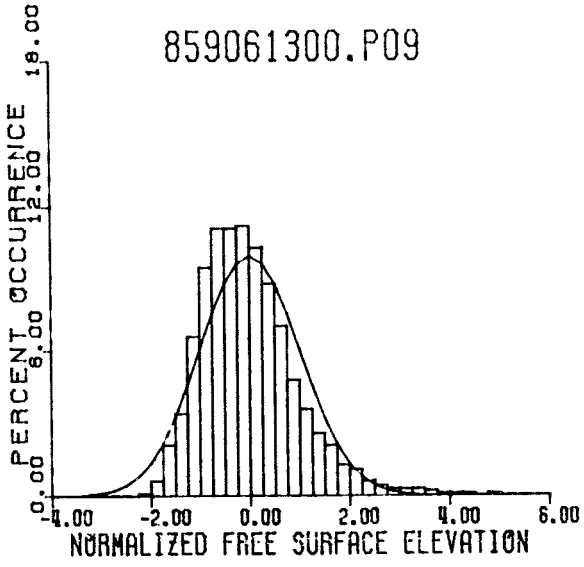
859061300.P09
PERCENT OCCURRENCE
0.00
6.00
12.00
18.00
-4.00
-2.00
0.00
2.00
4.00
6.00
NORMALIZED FREE SURFACE ELEVATION

APPENDIX D: WAVE HEIGHT AND PERIOD DISTRIBUTIONS

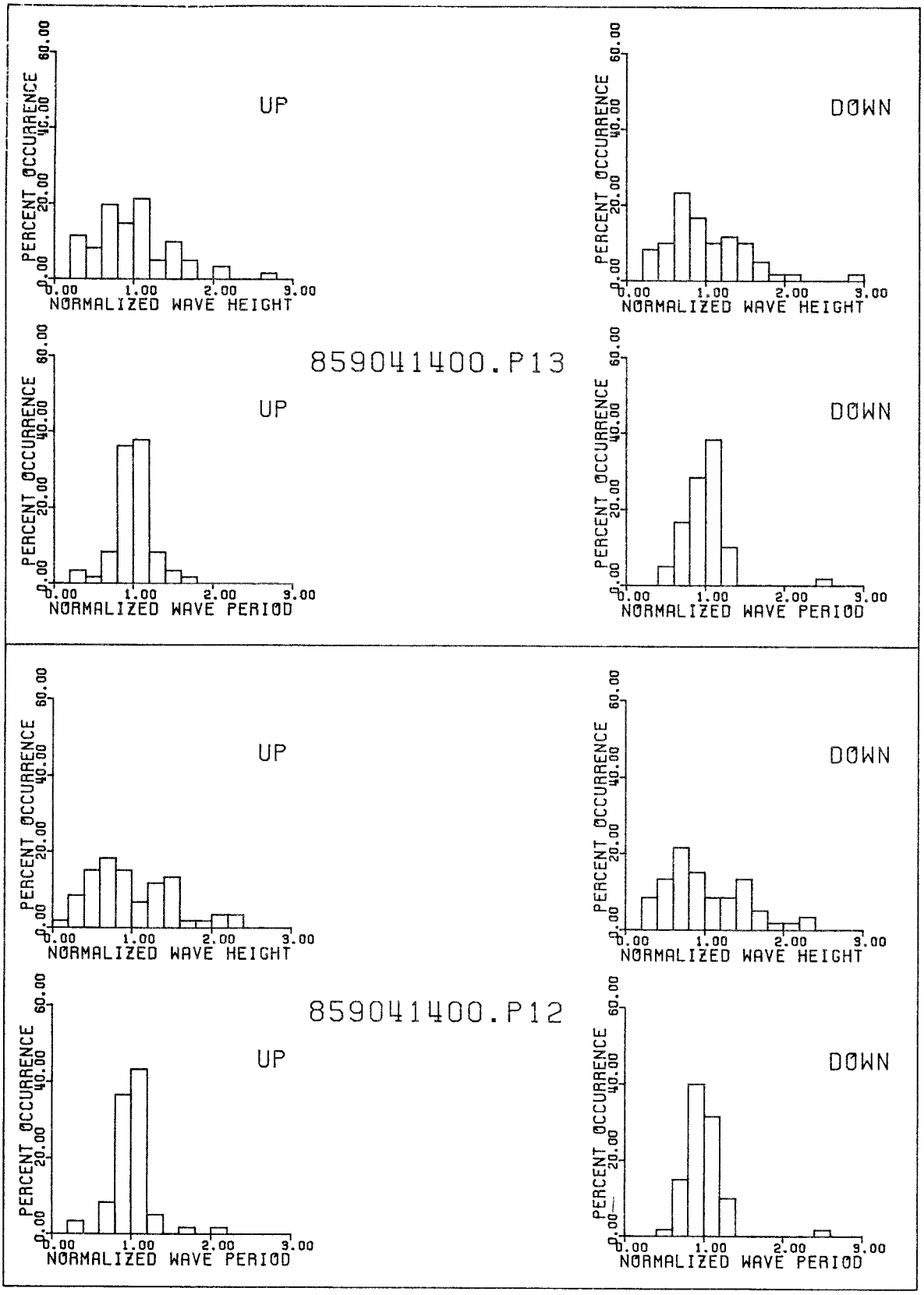
UP
DOWN
PERCENT OCCURRENCE
NORMALIZED WAVE HEIGHT
859041400.P13
UP
DOWN
PERCENT OCCURRENCE
NORMALIZED WAVE PERIOD
UP
DOWN
PERCENT OCCURRENCE
NORMALIZED WAVE HEIGHT
859041400.P12
UP
DOWN
PERCENT OCCURRENCE
NORMALIZED WAVE PERIOD

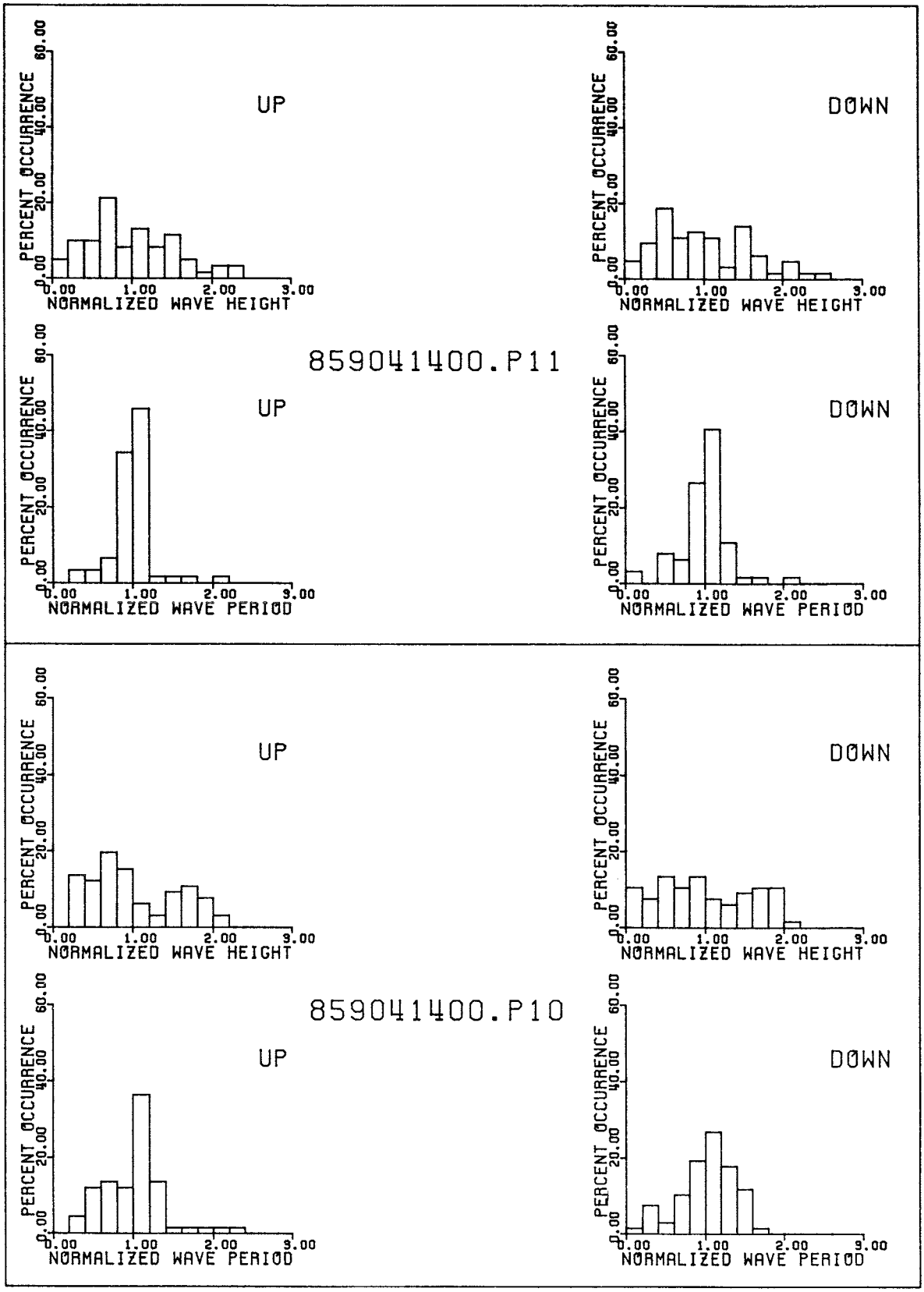
UP
DOWN
PERCENT OCCURRENCE
NORMALIZED WAVE HEIGHT
859041400.P11
UP
DOWN
PERCENT OCCURRENCE
NORMALIZED WAVE PERIOD
UP
DOWN
PERCENT OCCURRENCE
NORMALIZED WAVE HEIGHT
859041400.P10
UP
DOWN
PERCENT OCCURRENCE
NORMALIZED WAVE PERIOD

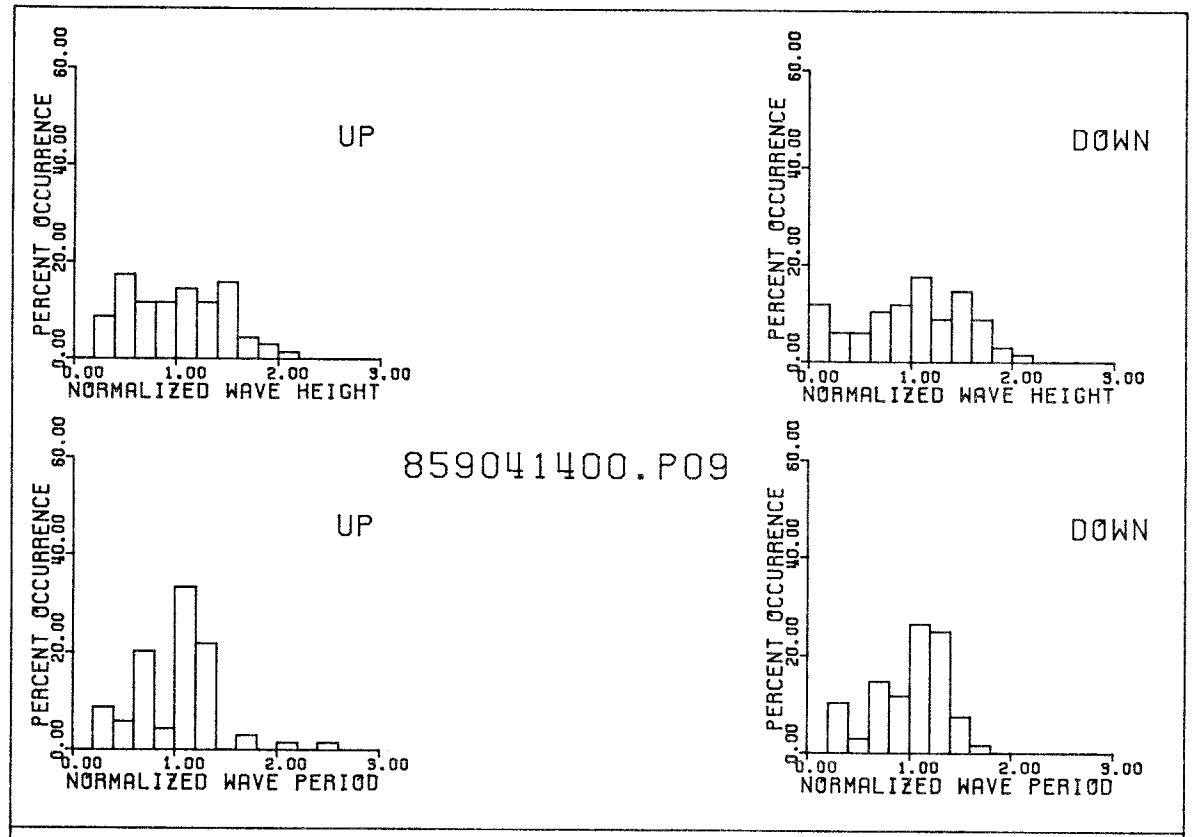
UP
DOWN
PERCENT OCCURRENCE
NORMALIZED WAVE HEIGHT
859041400.P09
UP
DOWN
PERCENT OCCURRENCE
NORMALIZED WAVE PERIOD

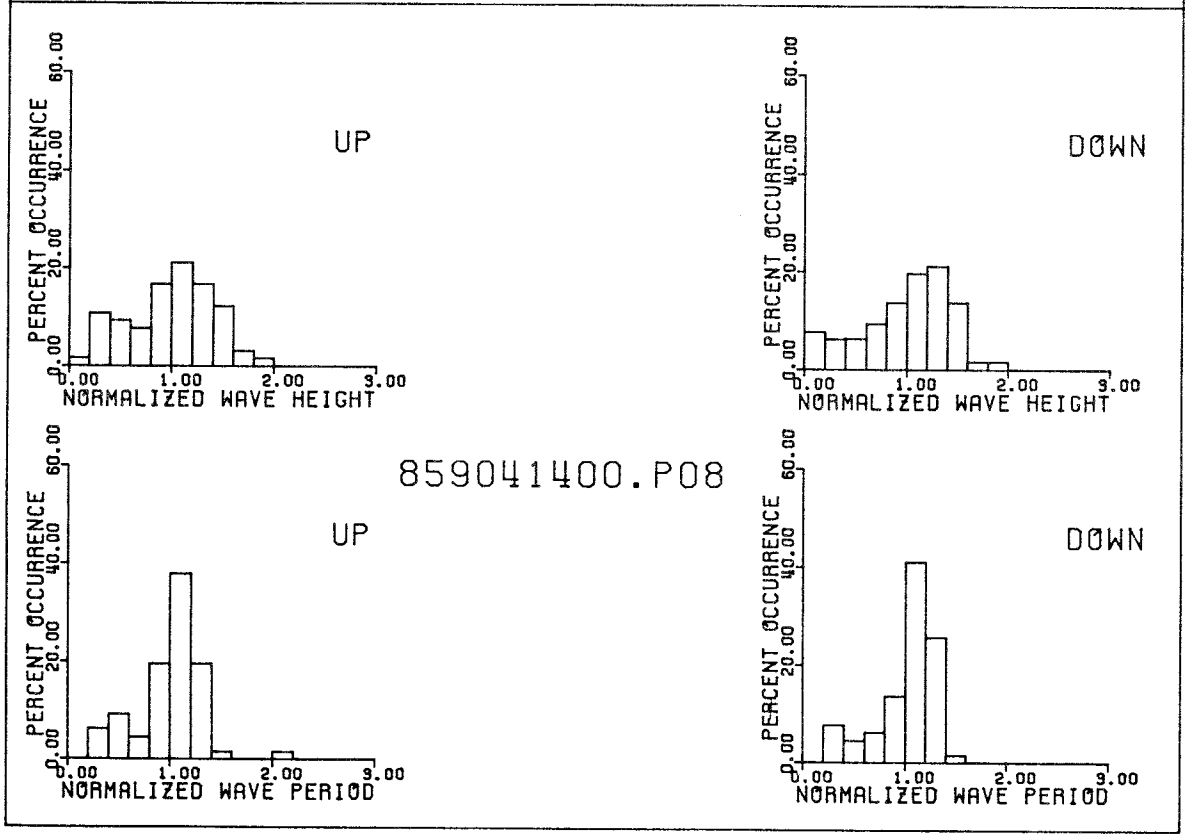
UP
DOWN
PERCENT OCCURRENCE
NORMALIZED WAVE HEIGHT
859041400.P08
UP
DOWN
PERCENT OCCURRENCE
NORMALIZED WAVE PERIOD

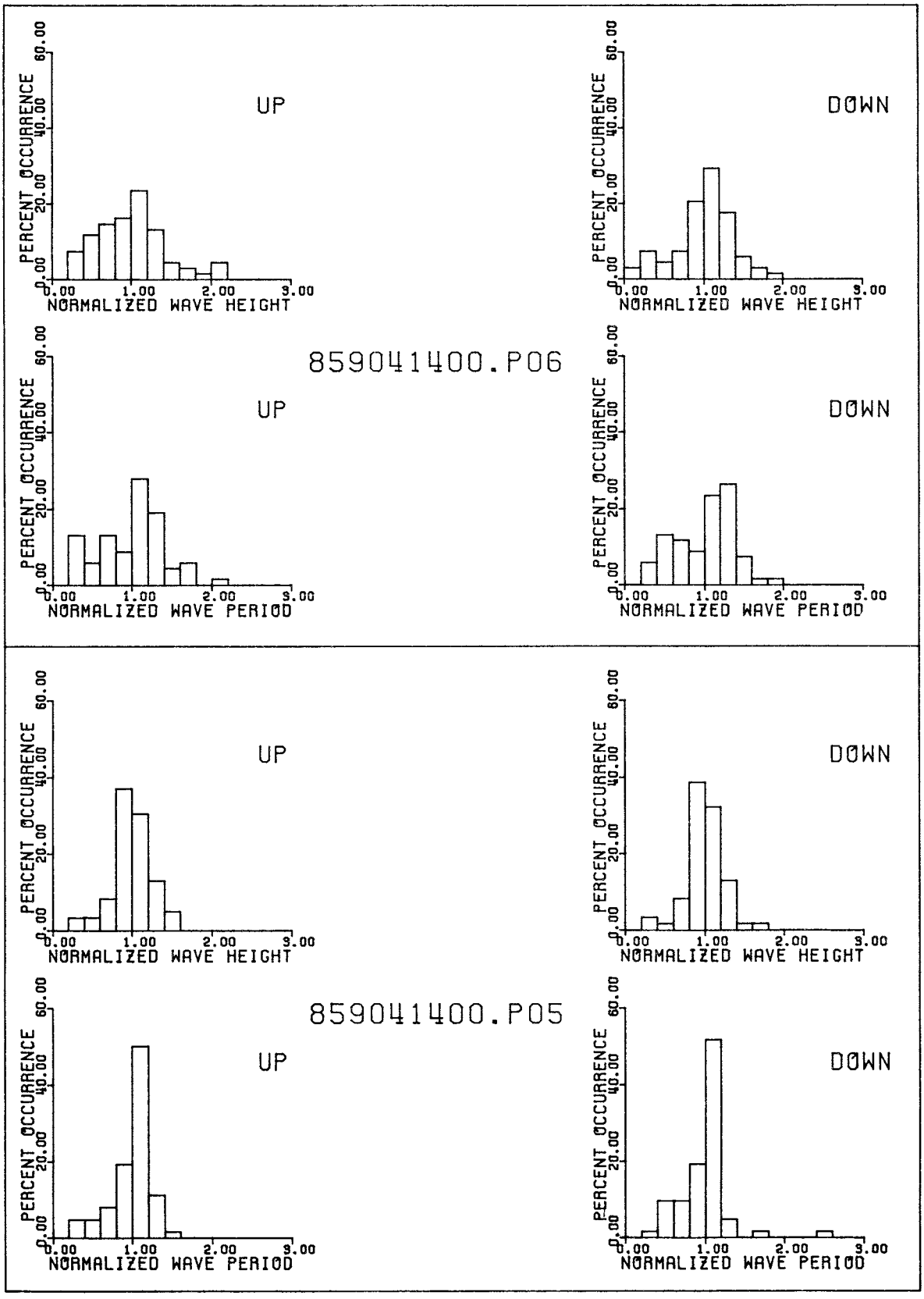
UP
DOWN
PERCENT OCCURRENCE
NORMALIZED WAVE HEIGHT
859041400.P06
UP
DOWN
PERCENT OCCURRENCE
NORMALIZED WAVE PERIOD
UP
DOWN
PERCENT OCCURRENCE
NORMALIZED WAVE HEIGHT
859041400.P05
UP
DOWN
PERCENT OCCURRENCE
NORMALIZED WAVE PERIOD

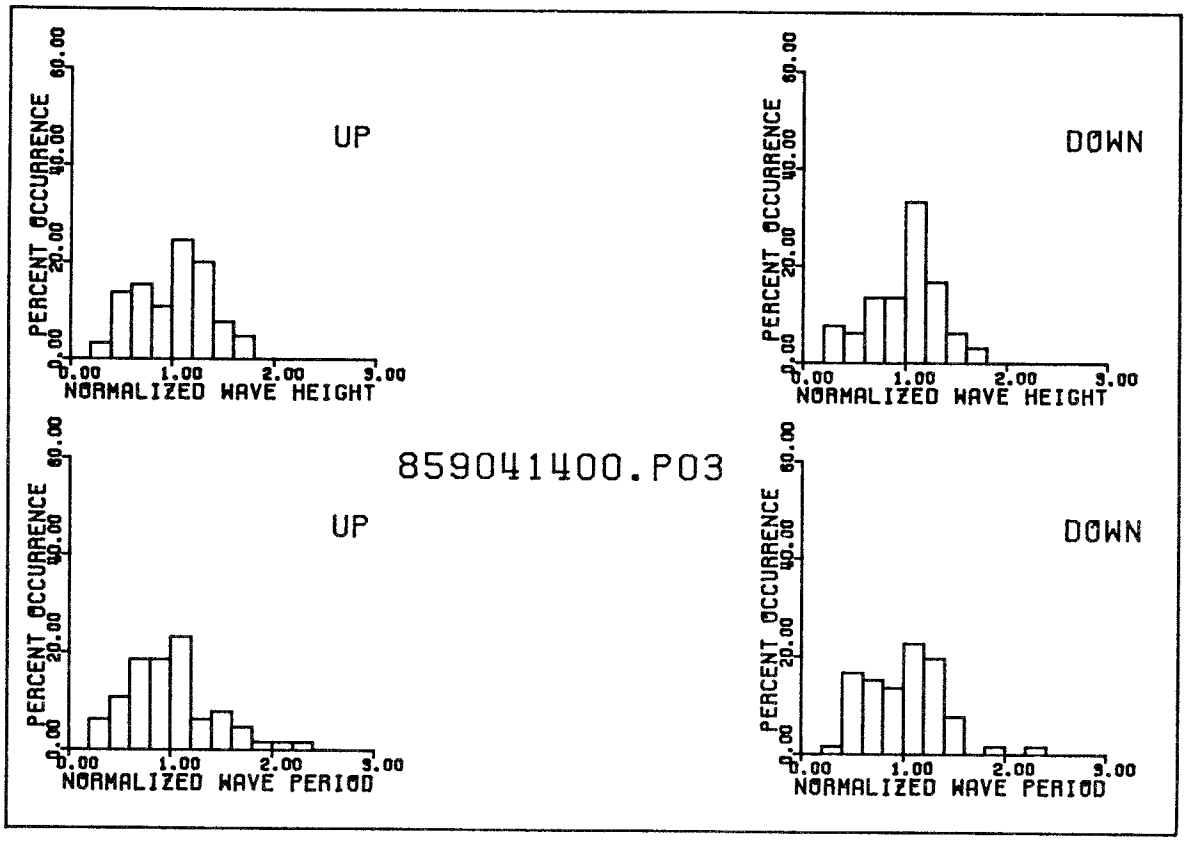
UP
DOWN
859041400.P03
UP
DOWN
PERCENT OCCURRENCE
0.00
20.00
40.00
60.00
0.00
1.00
2.00
3.00
NORMALIZED WAVE HEIGHT
NORMALIZED WAVE PERIOD

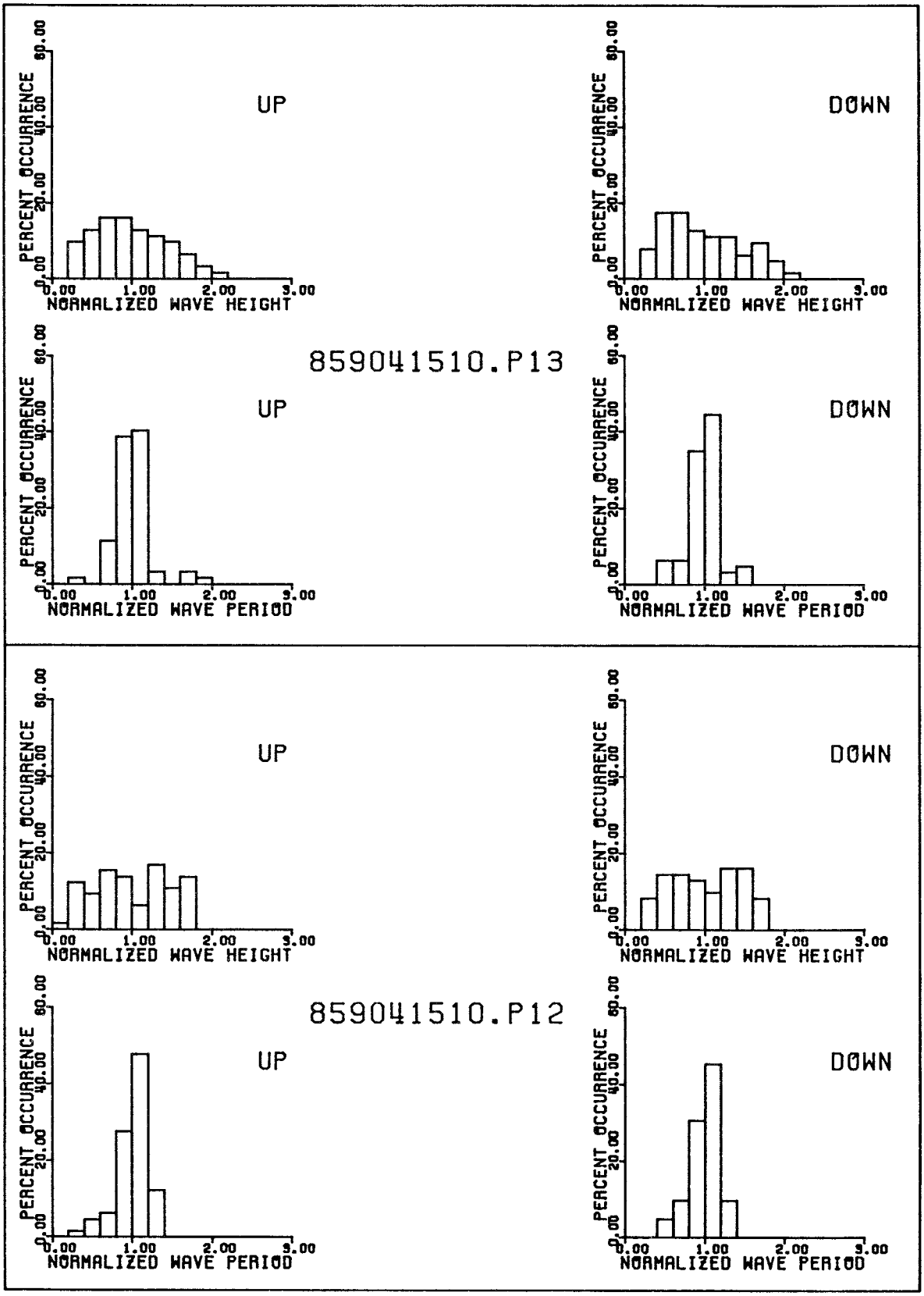
UP
DØWN
PERCENT ØCCURRENCE
NORMALIZED WAVE HEIGHT
859041510.P13
NORMALIZED WAVE PERIØD
859041510.P12
0.00
1.00
2.00
3.00
0.00
20.00
40.00
60.00

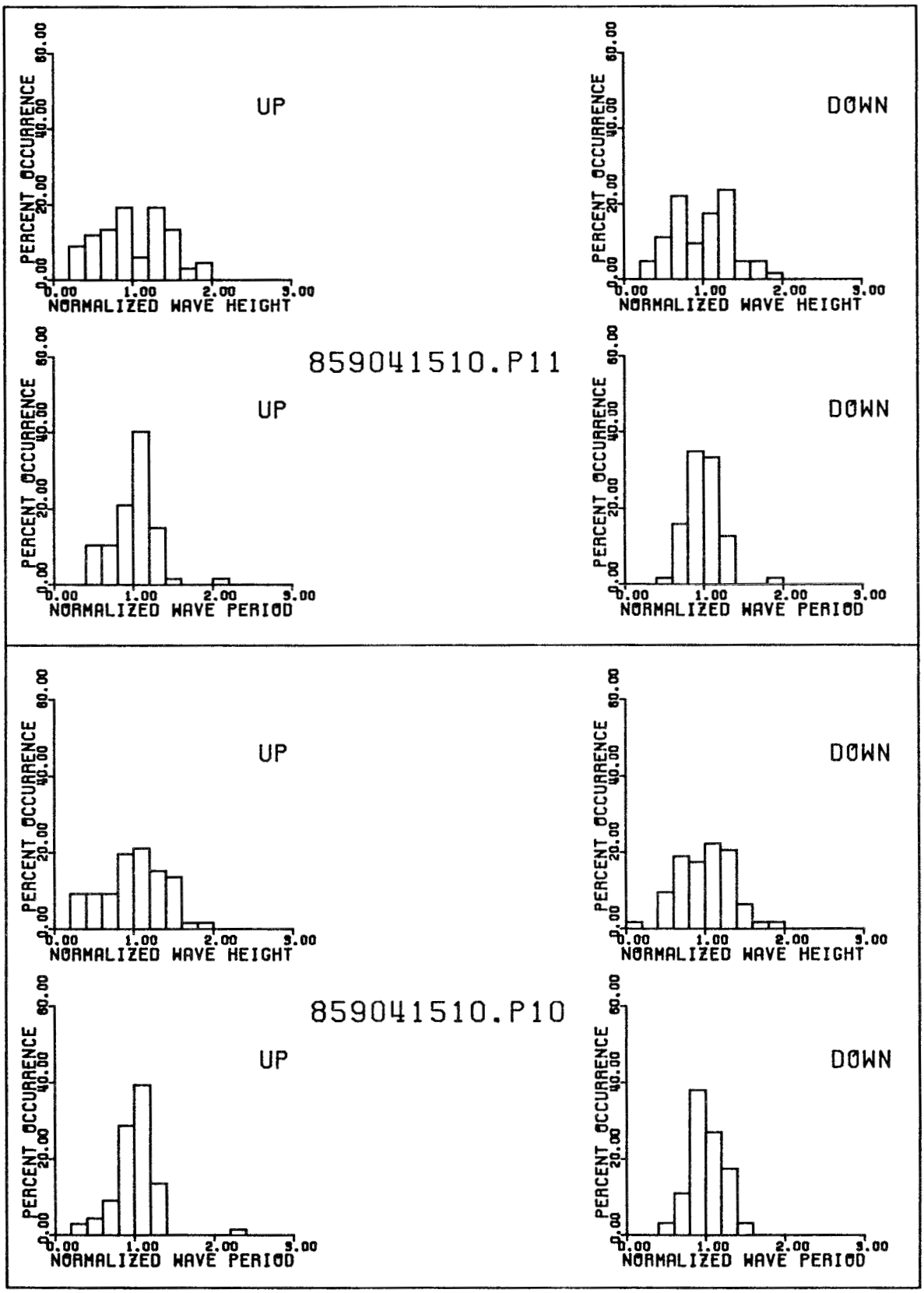
UP
DOWN
PERCENT OCCURRENCE
NORMALIZED WAVE HEIGHT
859041510.P11
UP
DOWN
PERCENT OCCURRENCE
NORMALIZED WAVE PERIOD
UP
DOWN
PERCENT OCCURRENCE
NORMALIZED WAVE HEIGHT
859041510.P10
UP
DOWN
PERCENT OCCURRENCE
NORMALIZED WAVE PERIOD

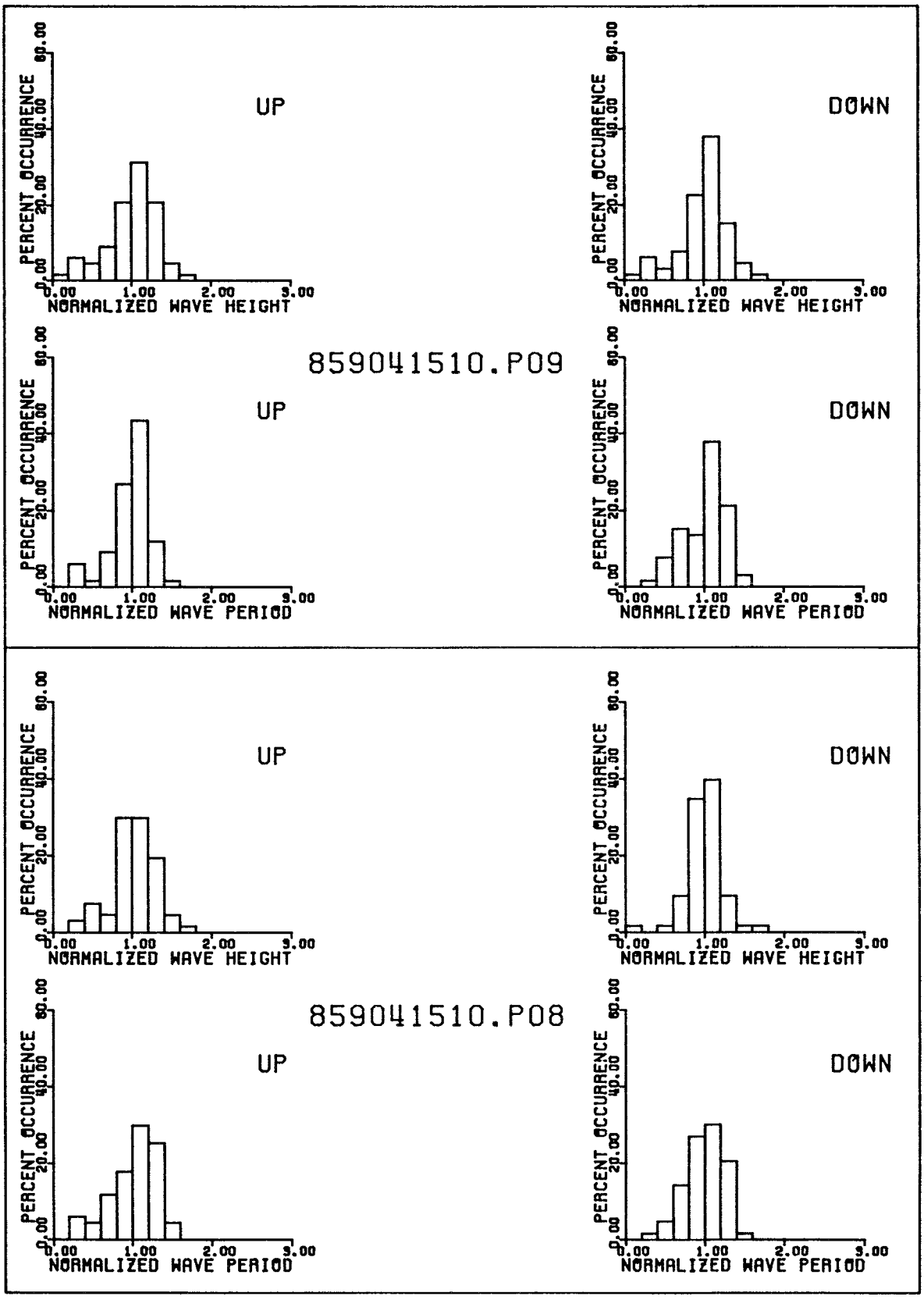
UP
DOWN
PERCENT OCCURRENCE
NORMALIZED WAVE HEIGHT
859041510.P09
UP
DOWN
PERCENT OCCURRENCE
NORMALIZED WAVE PERIOD
UP
DOWN
PERCENT OCCURRENCE
NORMALIZED WAVE HEIGHT
859041510.P08
UP
DOWN
PERCENT OCCURRENCE
NORMALIZED WAVE PERIOD

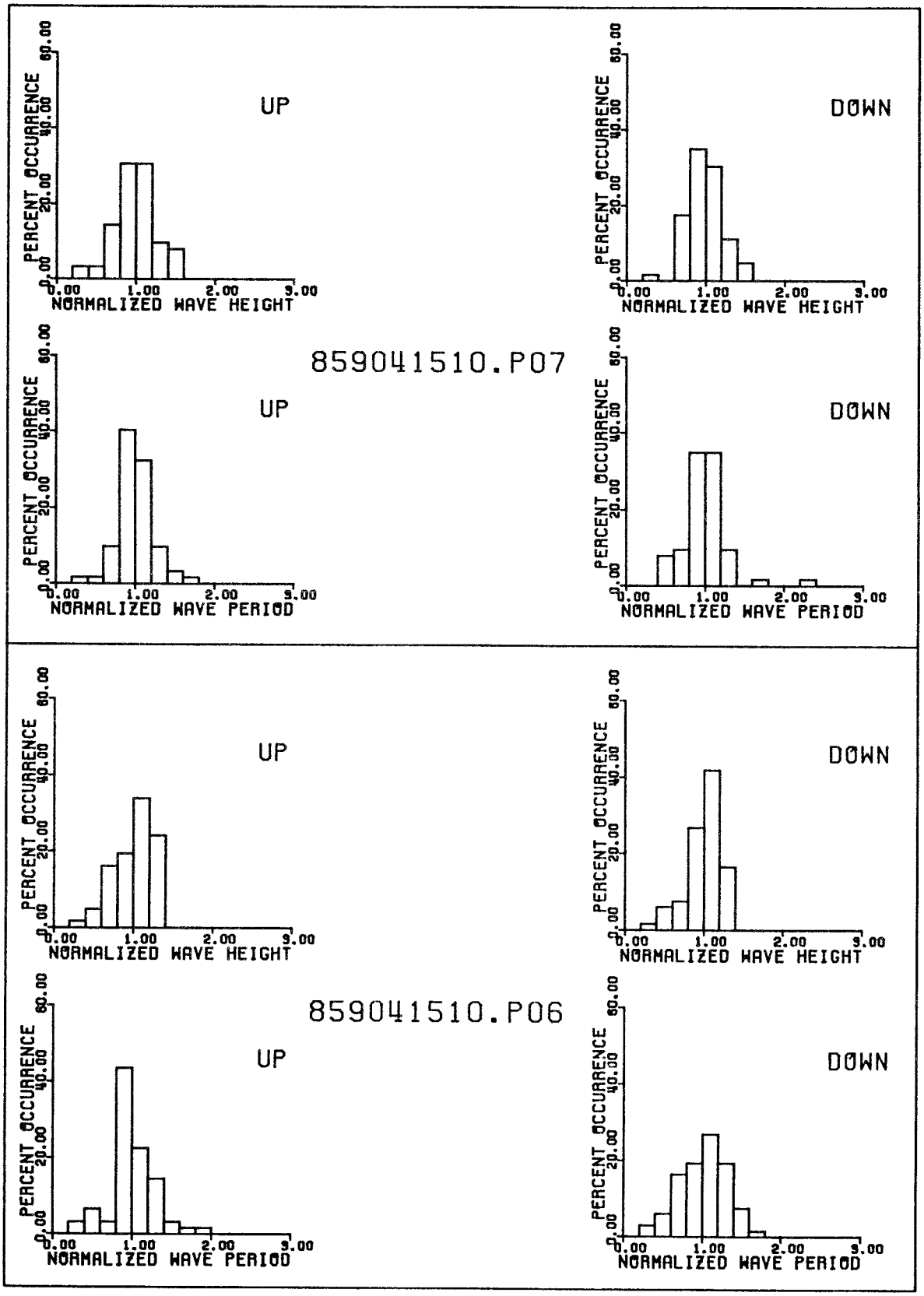
UP
DOWN
PERCENT OCCURRENCE
NORMALIZED WAVE HEIGHT
859041510.P07
UP
DOWN
PERCENT OCCURRENCE
NORMALIZED WAVE PERIOD
UP
DOWN
PERCENT OCCURRENCE
NORMALIZED WAVE HEIGHT
859041510.P06
UP
DOWN
PERCENT OCCURRENCE
NORMALIZED WAVE PERIOD

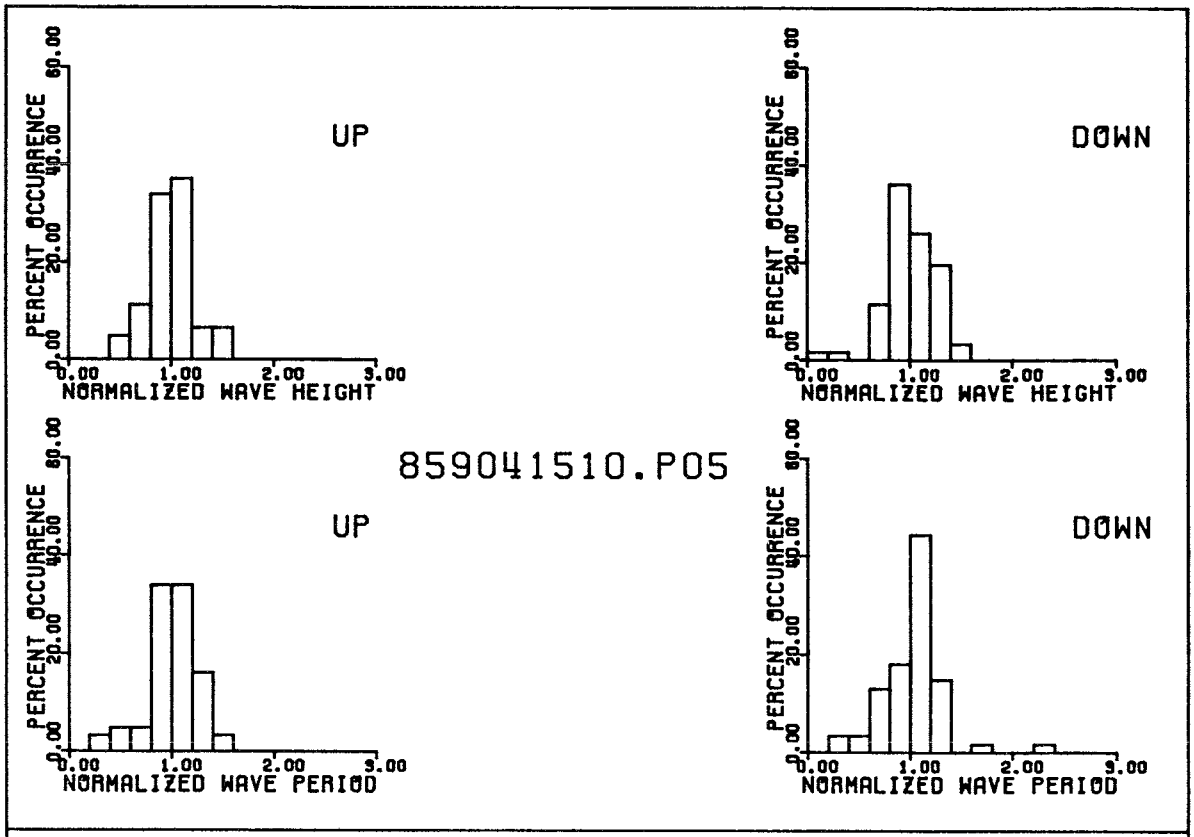
UP
DOWN
PERCENT OCCURRENCE
NORMALIZED WAVE HEIGHT
859041510.P05
UP
DOWN
PERCENT OCCURRENCE
NORMALIZED WAVE PERIOD

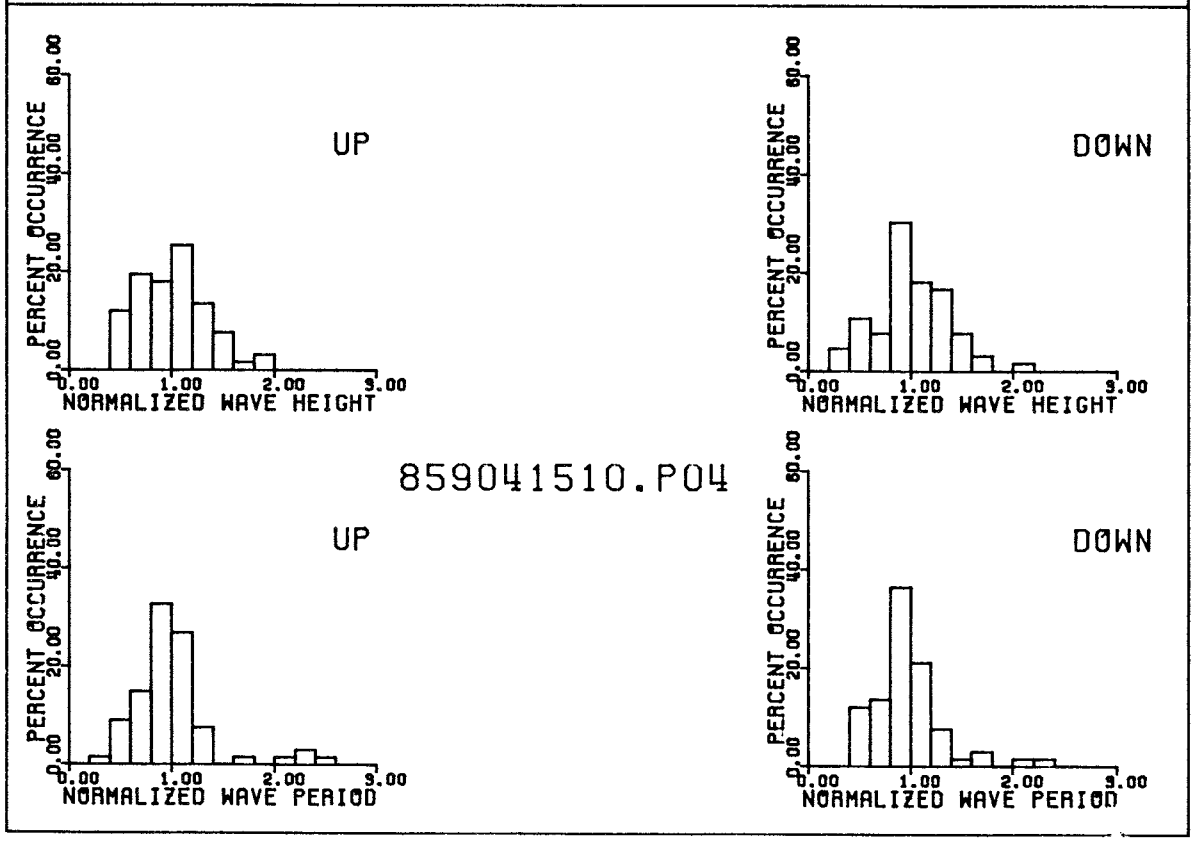
UP
DOWN
PERCENT OCCURRENCE
NORMALIZED WAVE HEIGHT
859041510.P04
UP
DOWN
PERCENT OCCURRENCE
NORMALIZED WAVE PERIOD

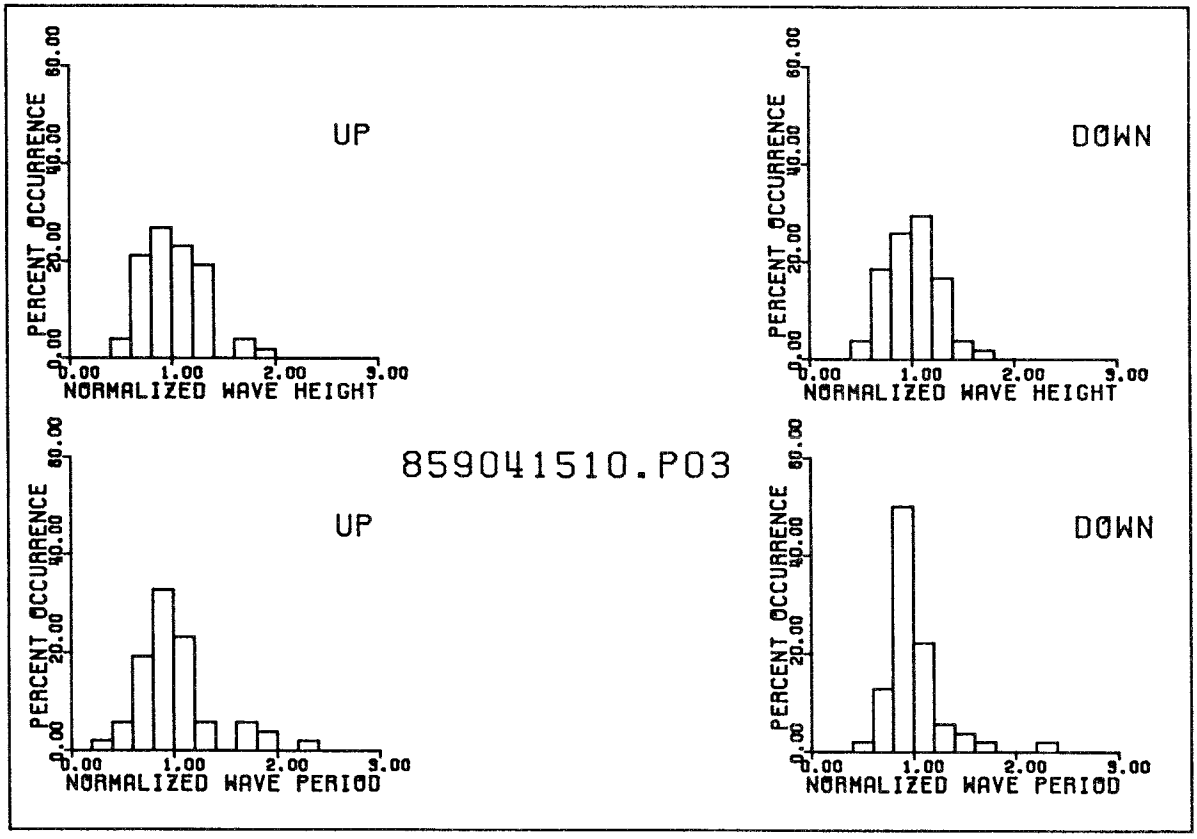
UP
DOWN
859041510.P03
UP
DOWN
PERCENT OCCURRENCE
NORMALIZED WAVE HEIGHT
NORMALIZED WAVE PERIOD
0.00
1.00
2.00
3.00
20.00
40.00
60.00

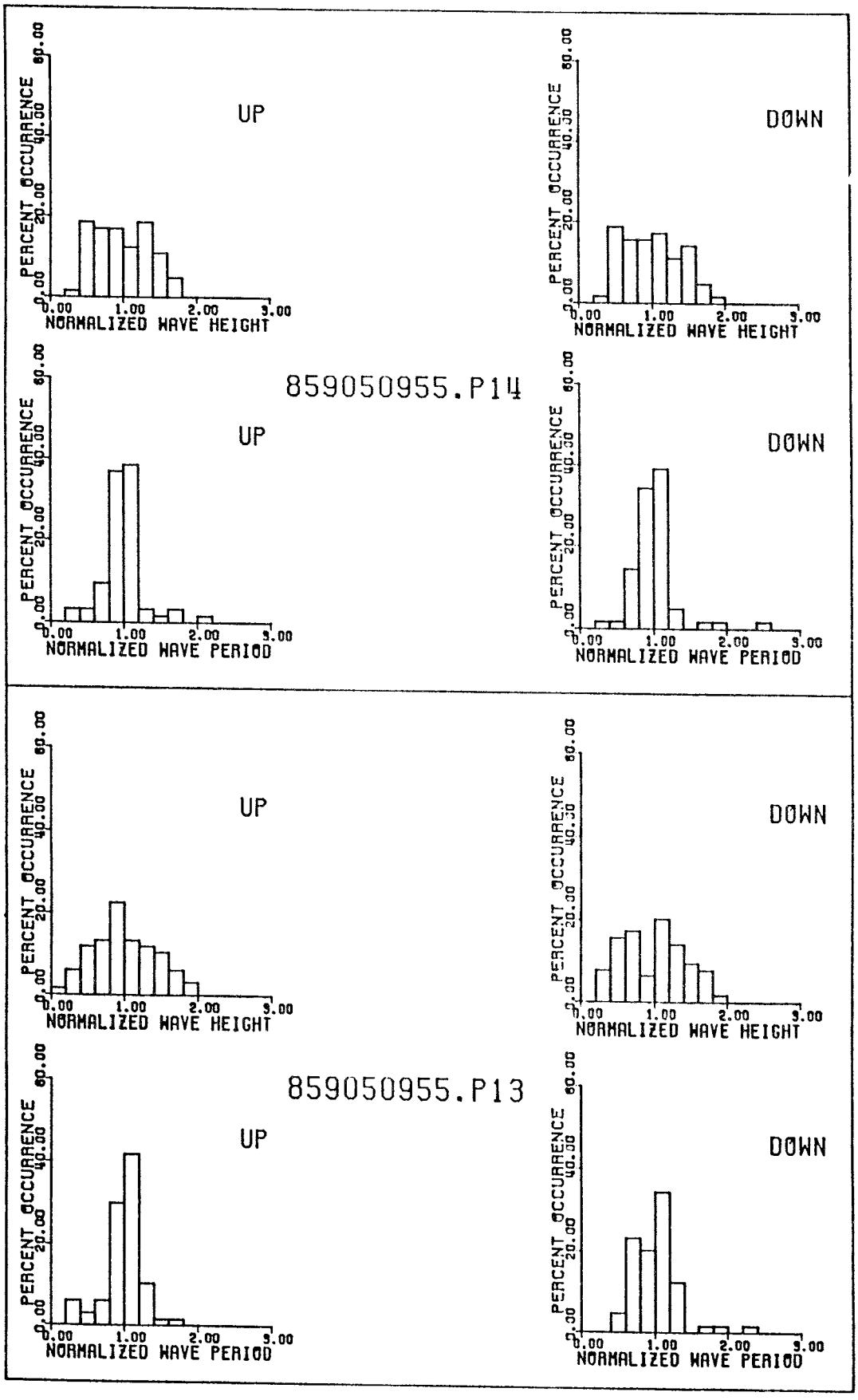
UP
DOWN
PERCENT OCCURRENCE
NORMALIZED WAVE HEIGHT
859050955.P14
UP
DOWN
PERCENT OCCURRENCE
NORMALIZED WAVE PERIOD
UP
DOWN
PERCENT OCCURRENCE
NORMALIZED WAVE HEIGHT
859050955.P13
UP
DOWN
PERCENT OCCURRENCE
NORMALIZED WAVE PERIOD

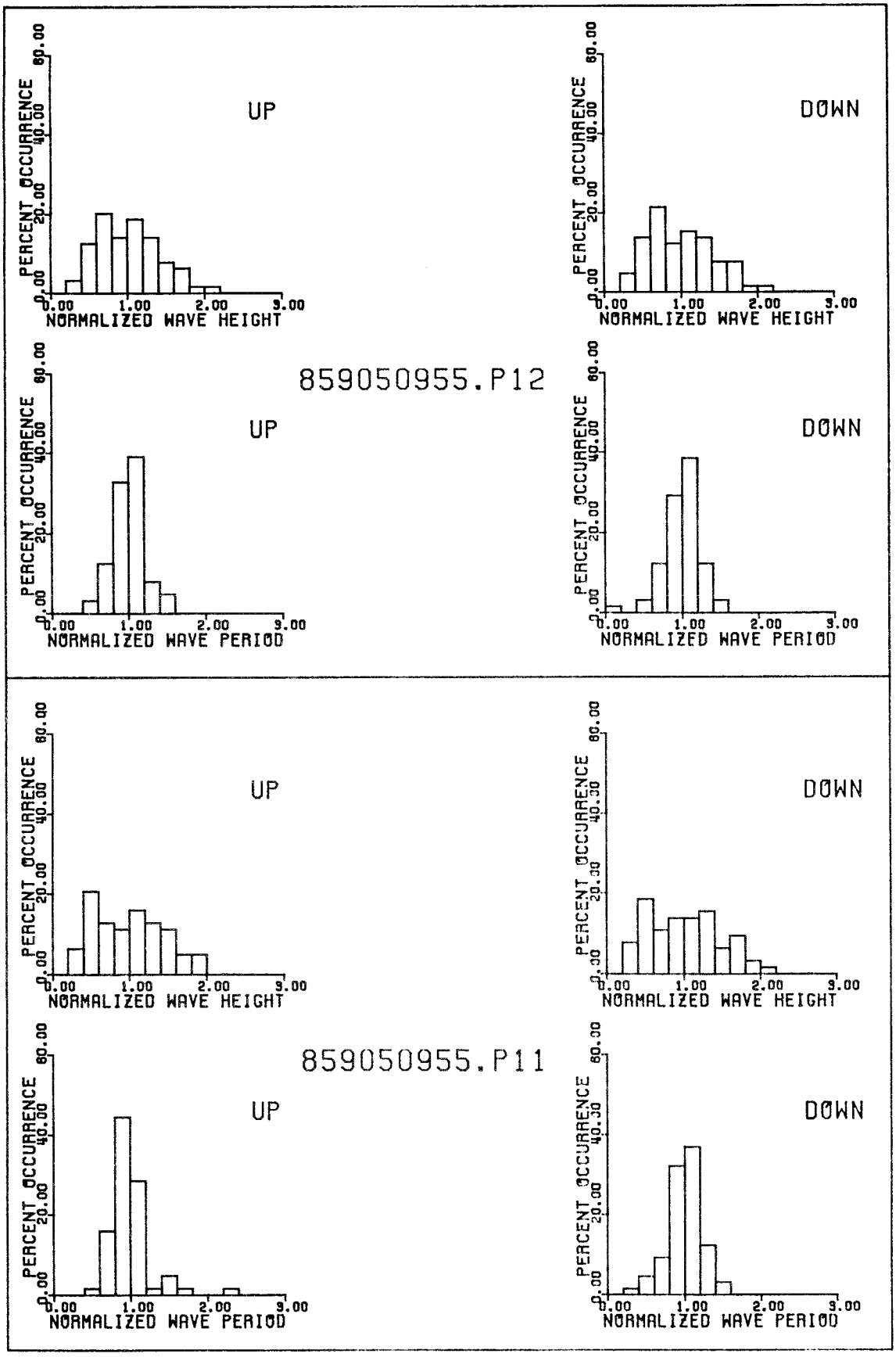
UP
DOWN
PERCENT OCCURRENCE
NORMALIZED WAVE HEIGHT
859050955.P12
UP
DOWN
PERCENT OCCURRENCE
NORMALIZED WAVE PERIOD
UP
DOWN
PERCENT OCCURRENCE
NORMALIZED WAVE HEIGHT
859050955.P11
UP
DOWN
PERCENT OCCURRENCE
NORMALIZED WAVE PERIOD

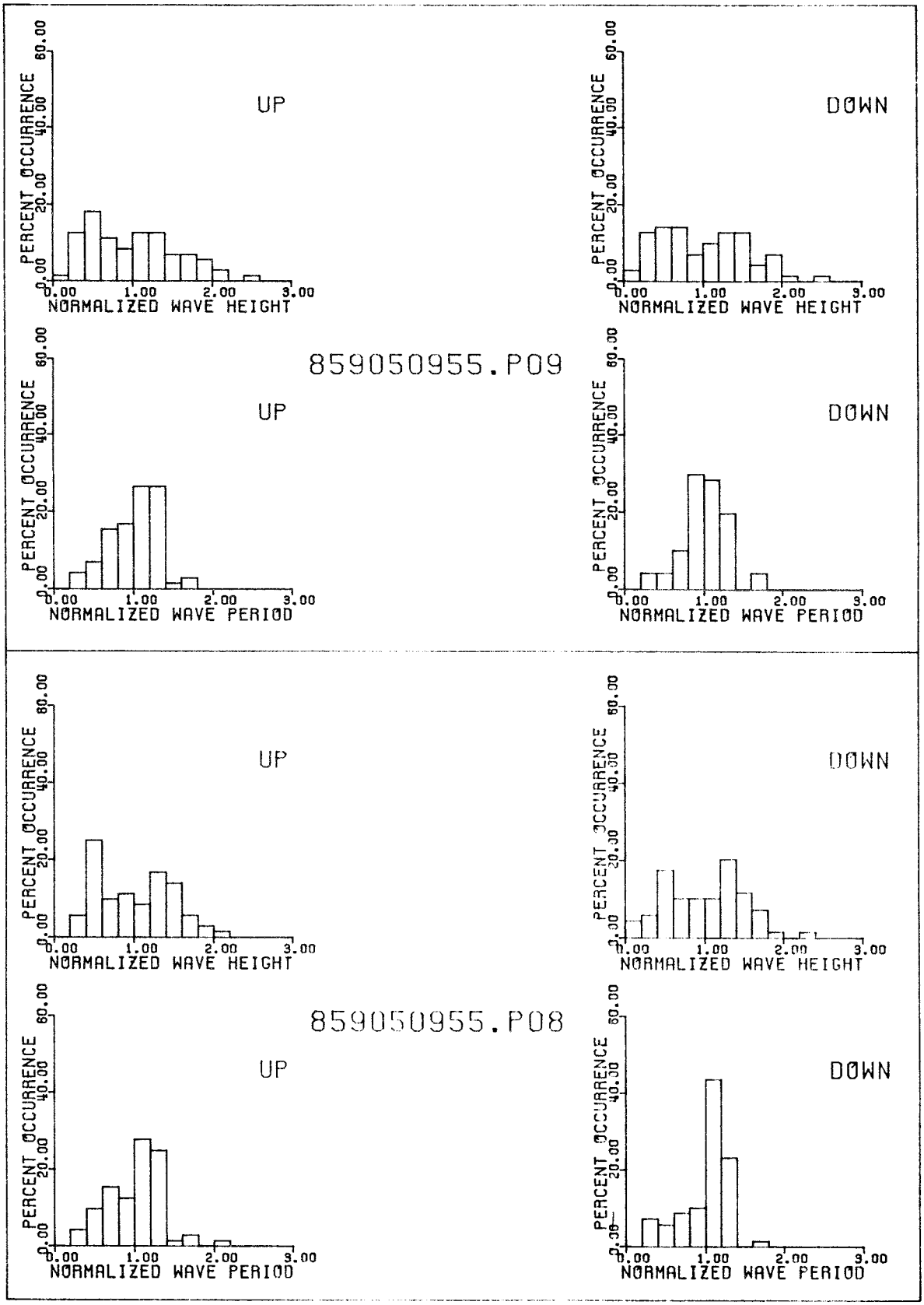
UP
DOWN
PERCENT OCCURRENCE
NORMALIZED WAVE HEIGHT
859050955.P09
UP
DOWN
PERCENT OCCURRENCE
NORMALIZED WAVE PERIOD
UP
DOWN
PERCENT OCCURRENCE
NORMALIZED WAVE HEIGHT
859050955.P08
UP
DOWN
PERCENT OCCURRENCE
NORMALIZED WAVE PERIOD

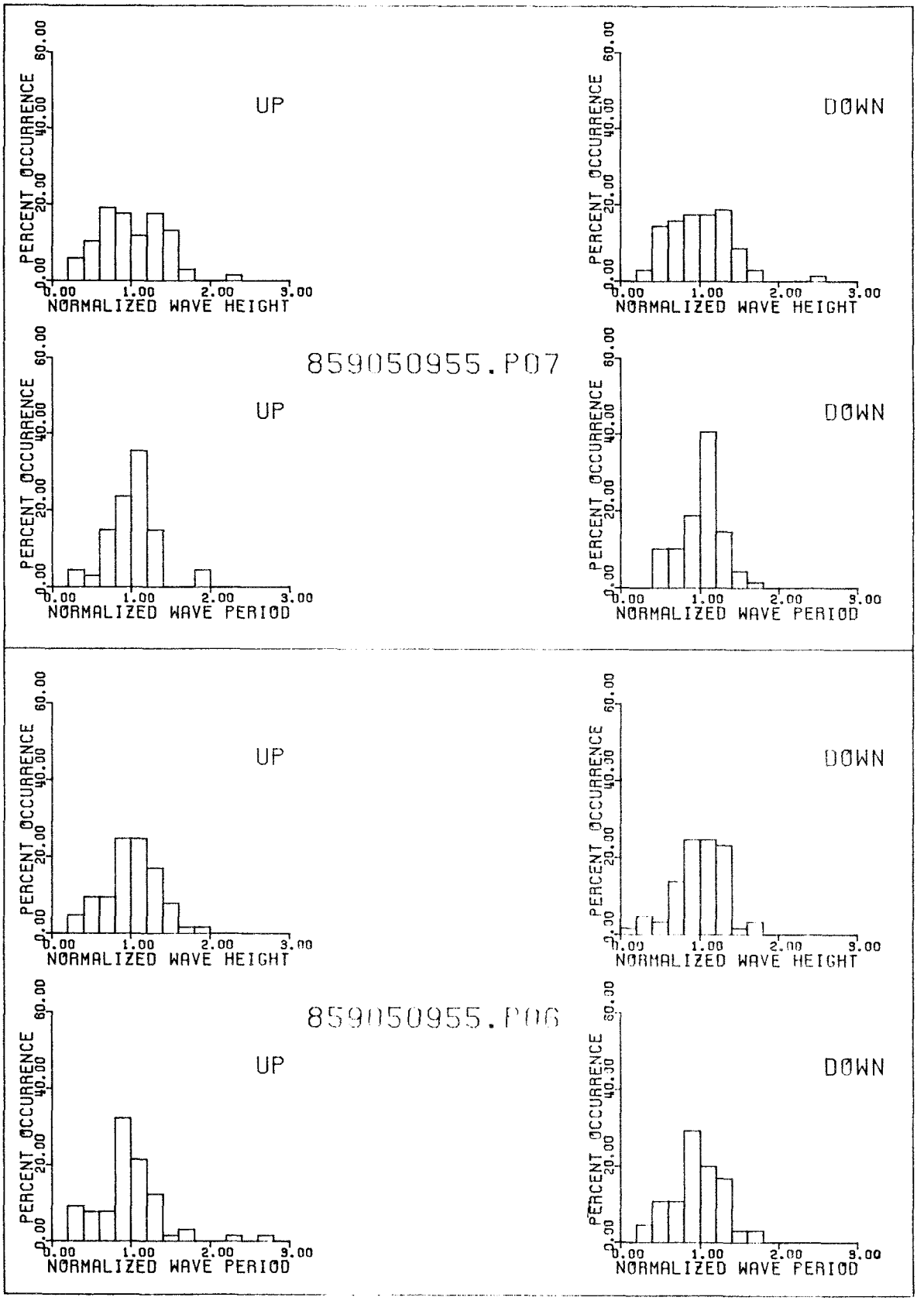
UP
DOWN
PERCENT OCCURRENCE
NORMALIZED WAVE HEIGHT
859050955.P07
UP
DOWN
PERCENT OCCURRENCE
NORMALIZED WAVE PERIOD
UP
DOWN
PERCENT OCCURRENCE
NORMALIZED WAVE HEIGHT
859050955.P06
UP
DOWN
PERCENT OCCURRENCE
NORMALIZED WAVE PERIOD

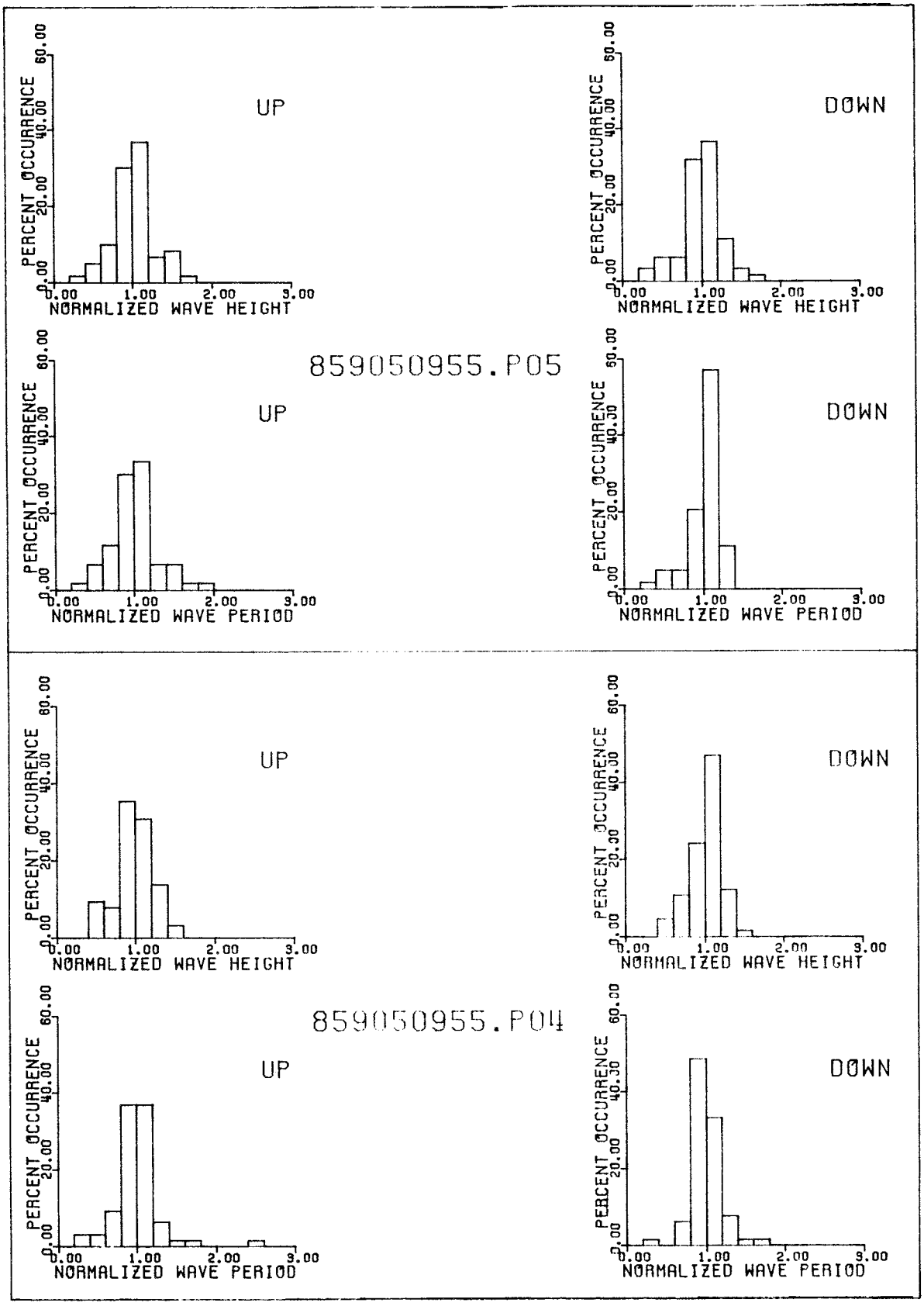
UP
DOWN
PERCENT OCCURRENCE
NORMALIZED WAVE HEIGHT
859050955.P05
UP
DOWN
PERCENT OCCURRENCE
NORMALIZED WAVE PERIOD
UP
DOWN
PERCENT OCCURRENCE
NORMALIZED WAVE HEIGHT
859050955.P04
UP
DOWN
PERCENT OCCURRENCE
NORMALIZED WAVE PERIOD

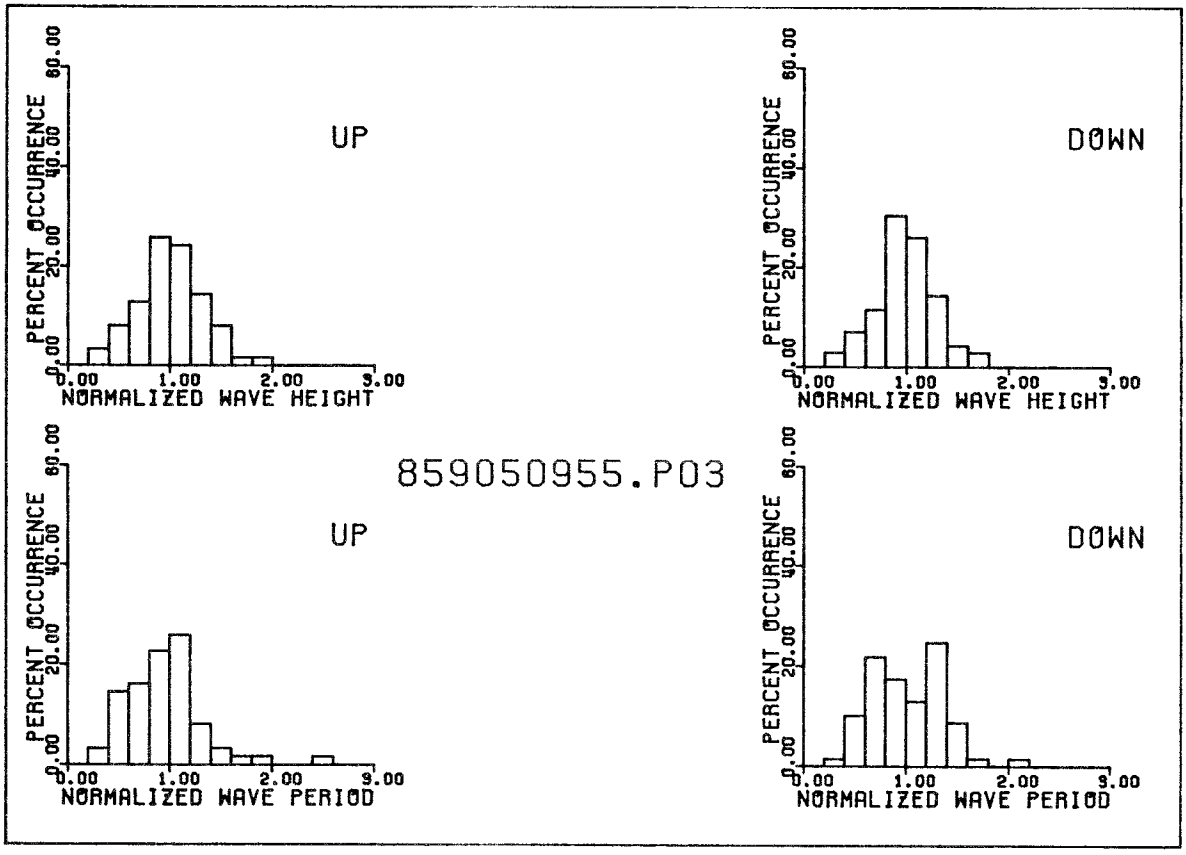
UP
DOWN
859050955.P03
UP
DOWN
PERCENT OCCURRENCE
0.00
20.00
40.00
60.00
0.00
1.00
2.00
3.00
NORMALIZED WAVE HEIGHT
NORMALIZED WAVE PERIOD

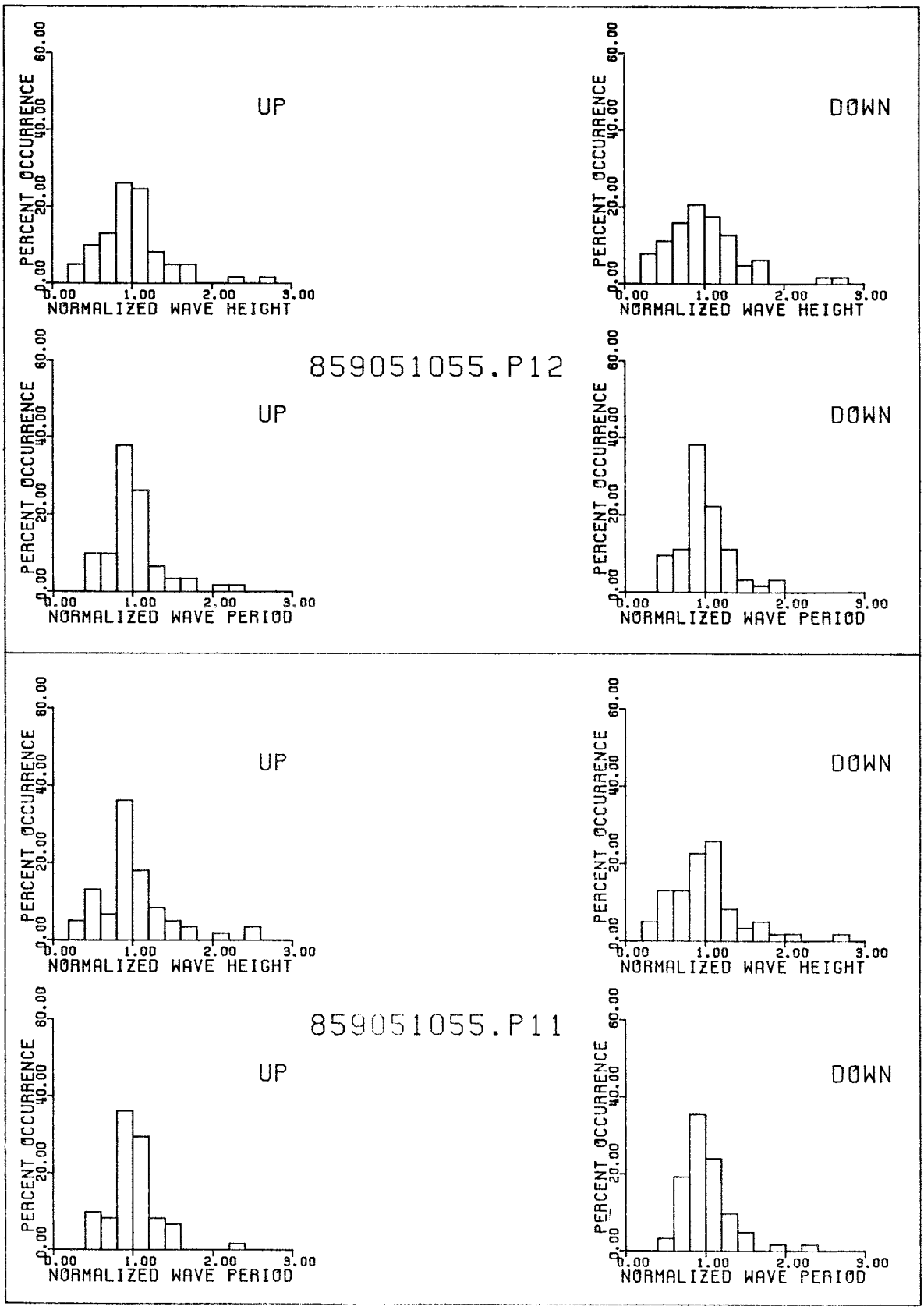
UP
DOWN
PERCENT OCCURRENCE
NORMALIZED WAVE HEIGHT
859051055.P12
UP
DOWN
PERCENT OCCURRENCE
NORMALIZED WAVE PERIOD
UP
DOWN
PERCENT OCCURRENCE
NORMALIZED WAVE HEIGHT
859051055.P11
UP
DOWN
PERCENT OCCURRENCE
NORMALIZED WAVE PERIOD

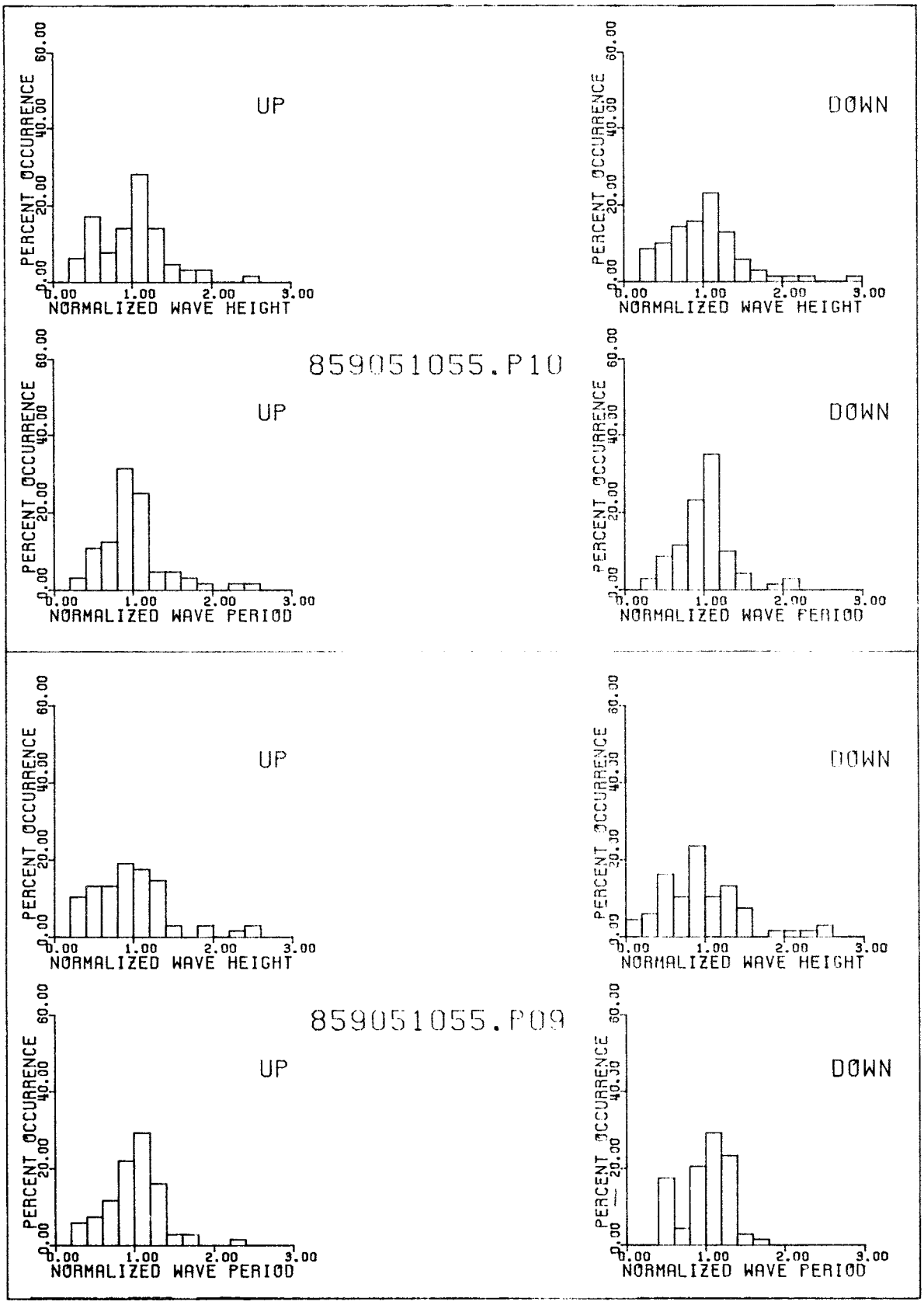
UP
DOWN
PERCENT OCCURRENCE
NORMALIZED WAVE HEIGHT
859051055.P10
UP
DOWN
PERCENT OCCURRENCE
NORMALIZED WAVE PERIOD
UP
DOWN
PERCENT OCCURRENCE
NORMALIZED WAVE HEIGHT
859051055.P09
UP
DOWN
PERCENT OCCURRENCE
NORMALIZED WAVE PERIOD

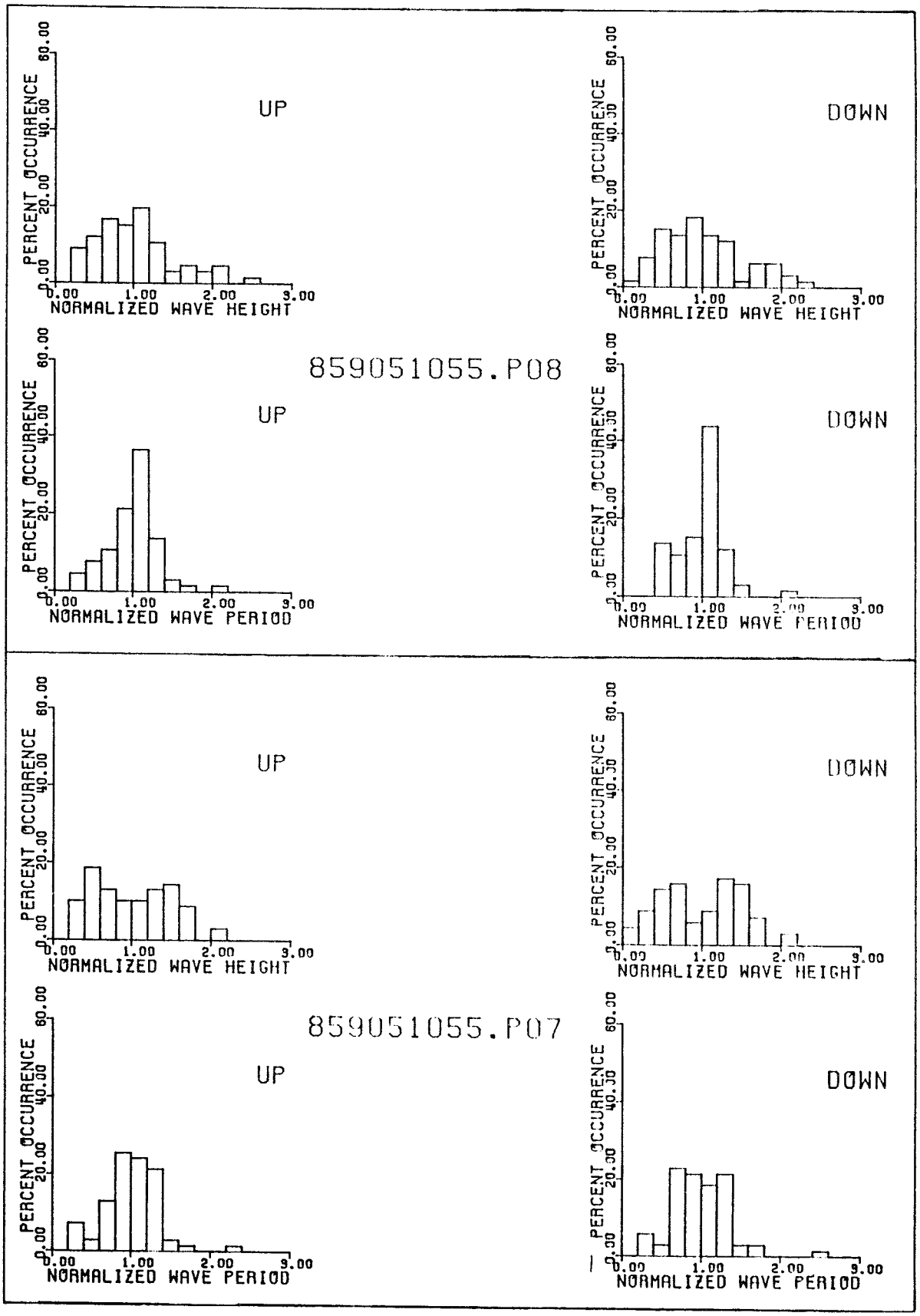
UP
DOWN
PERCENT OCCURRENCE
NORMALIZED WAVE HEIGHT
859051055.P08
UP
DOWN
PERCENT OCCURRENCE
NORMALIZED WAVE PERIOD
UP
DOWN
PERCENT OCCURRENCE
NORMALIZED WAVE HEIGHT
859051055.P07
UP
DOWN
PERCENT OCCURRENCE
NORMALIZED WAVE PERIOD

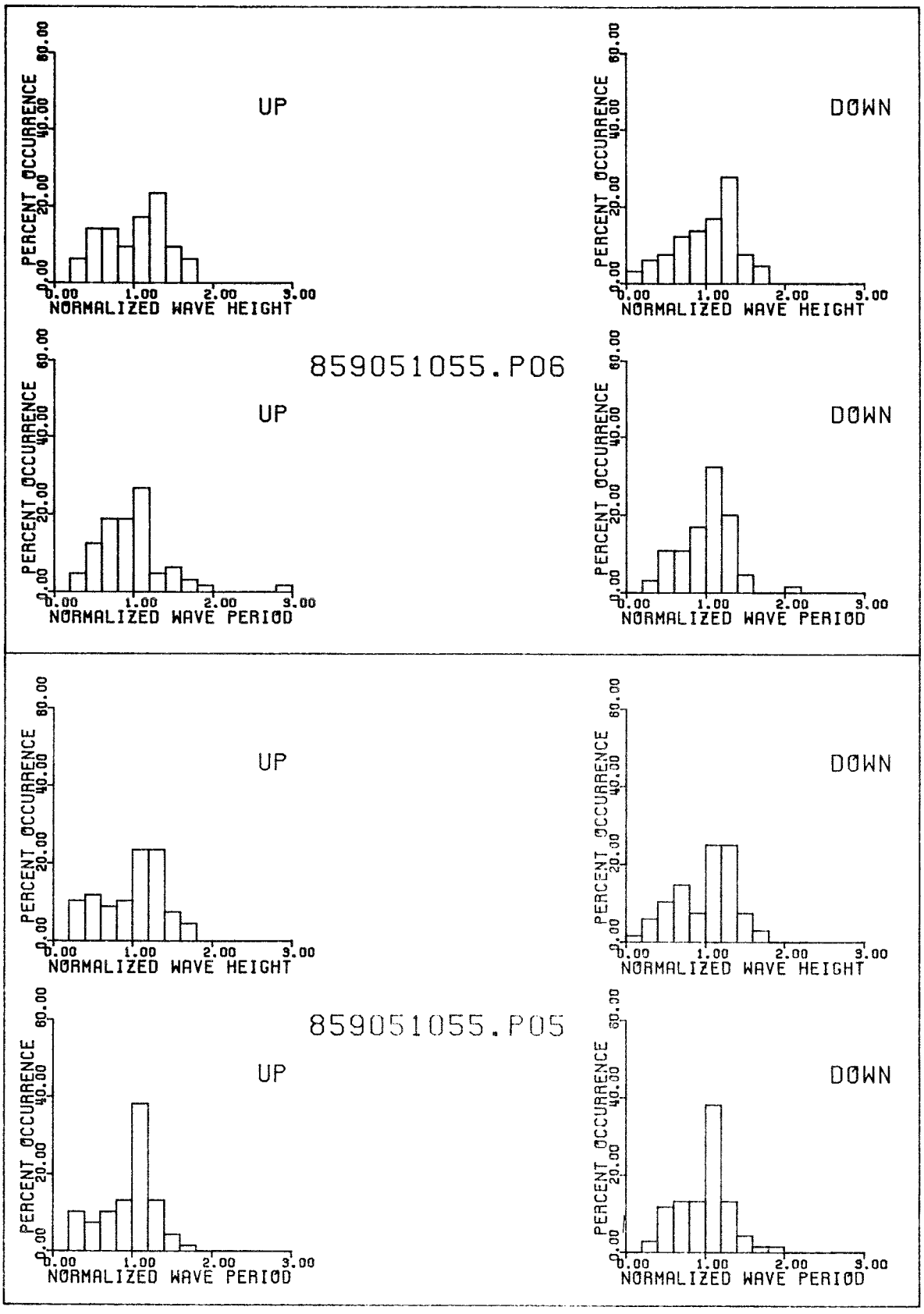
UP
DOWN
PERCENT OCCURRENCE
NORMALIZED WAVE HEIGHT
859051055.P06
UP
DOWN
PERCENT OCCURRENCE
NORMALIZED WAVE PERIOD
UP
DOWN
PERCENT OCCURRENCE
NORMALIZED WAVE HEIGHT
859051055.P05
UP
DOWN
PERCENT OCCURRENCE
NORMALIZED WAVE PERIOD
0.00
1.00
2.00
3.00
20.00
40.00
60.00

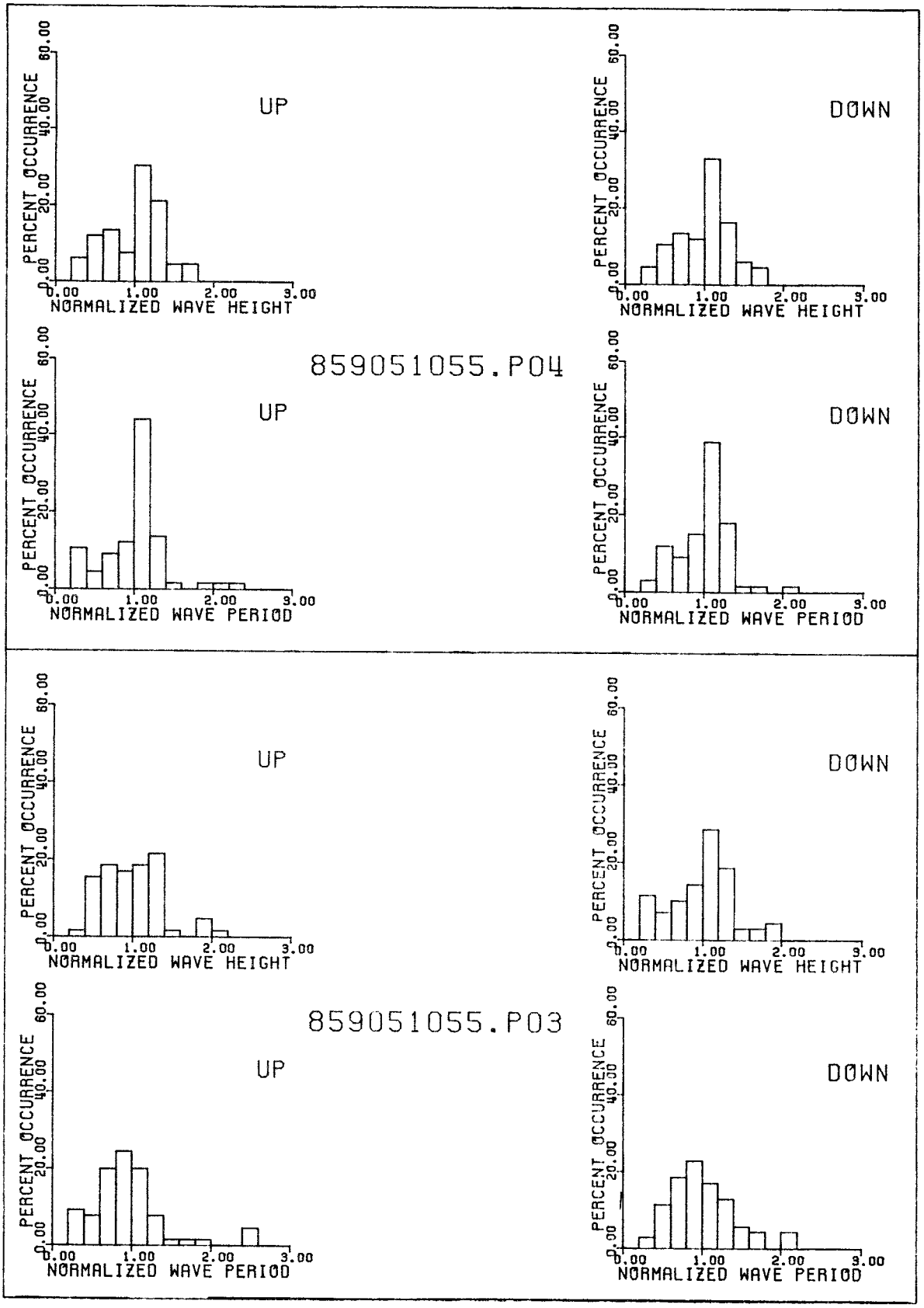
UP
DOWN
PERCENT OCCURRENCE
0.00
20.00
40.00
60.00
0.00
1.00
2.00
3.00
NORMALIZED WAVE HEIGHT
859051055.P04
UP
DOWN
NORMALIZED WAVE PERIOD
UP
DOWN
NORMALIZED WAVE HEIGHT
859051055.P03
UP
DOWN
NORMALIZED WAVE PERIOD

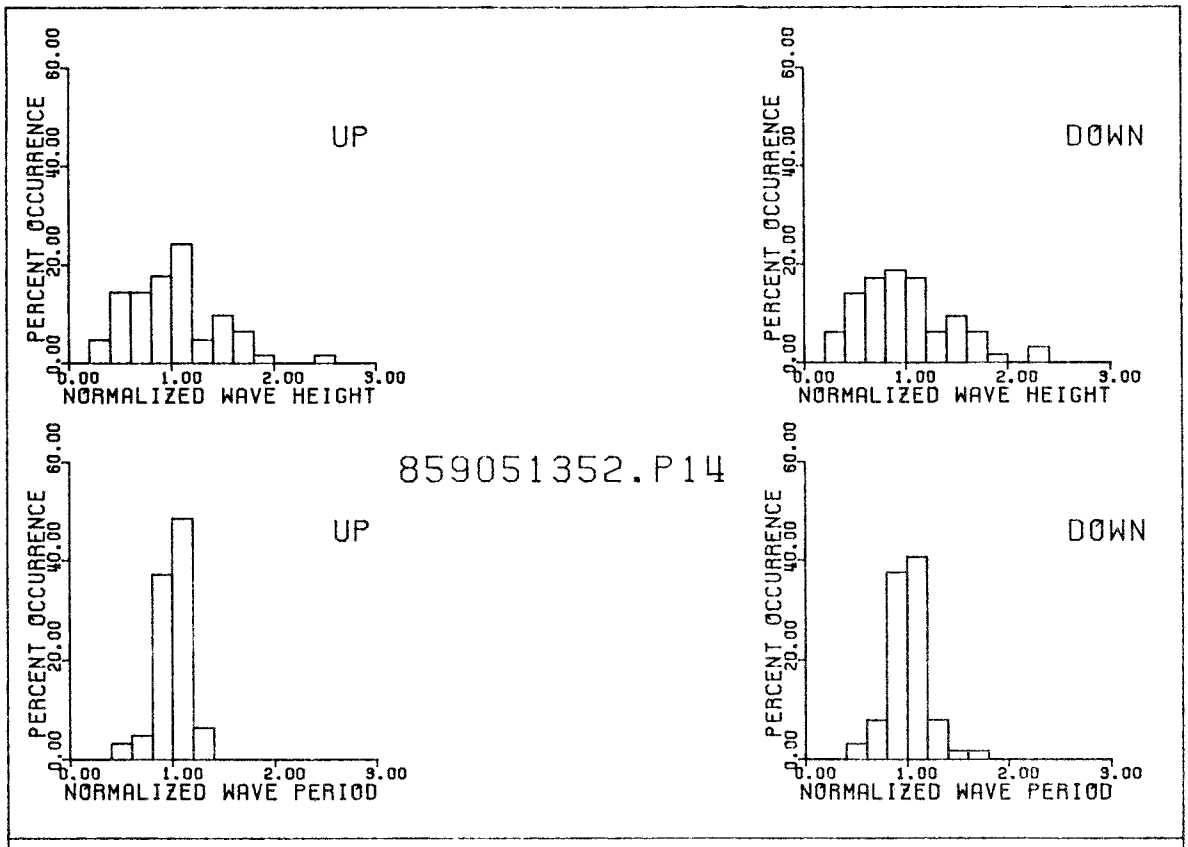
UP
DOWN
PERCENT OCCURRENCE
0.00
20.00
40.00
60.00
0.00
1.00
2.00
3.00
NORMALIZED WAVE HEIGHT
859051352.P14
UP
DOWN
NORMALIZED WAVE PERIOD

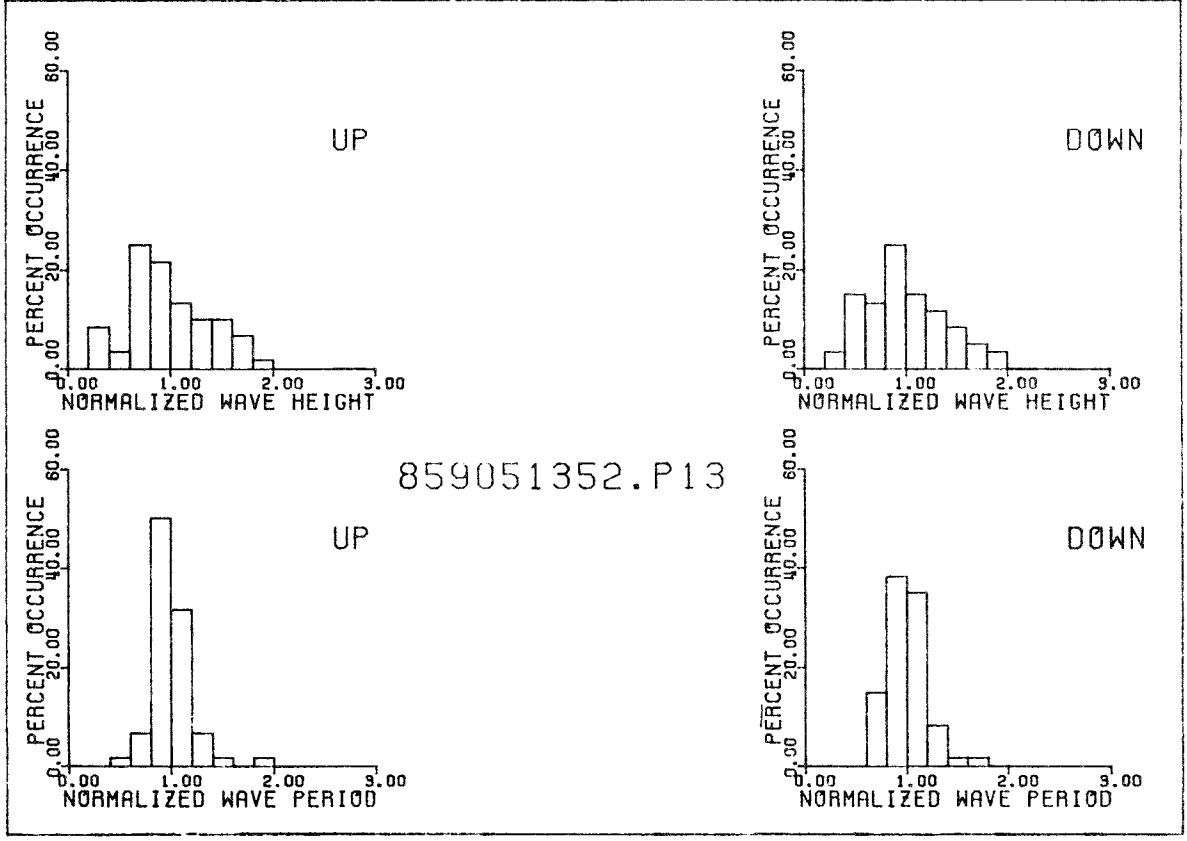
UP
DOWN
PERCENT OCCURRENCE
0.00
20.00
40.00
60.00
0.00
1.00
2.00
3.00
NORMALIZED WAVE HEIGHT
859051352.P13
UP
DOWN
NORMALIZED WAVE PERIOD

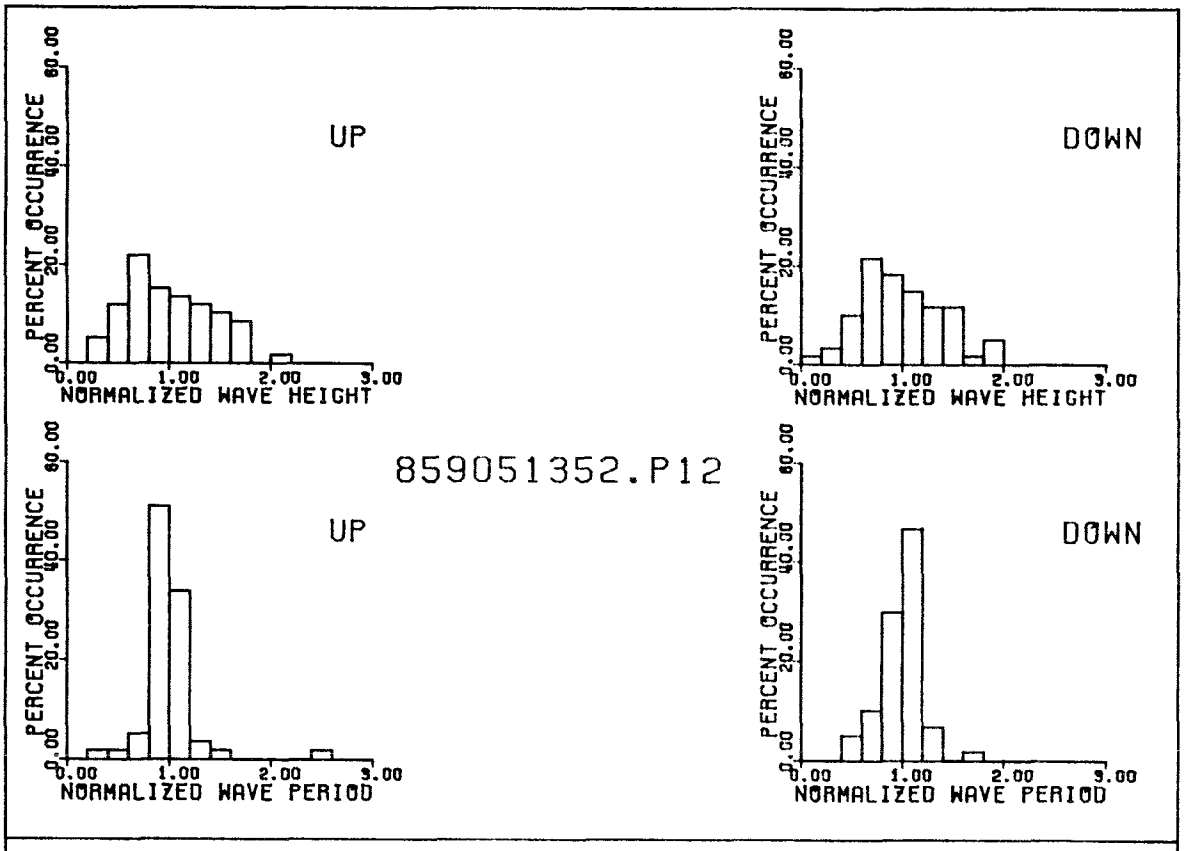
UP
DOWN
PERCENT OCCURRENCE
NORMALIZED WAVE HEIGHT
859051352.P12
UP
DOWN
PERCENT OCCURRENCE
NORMALIZED WAVE PERIOD

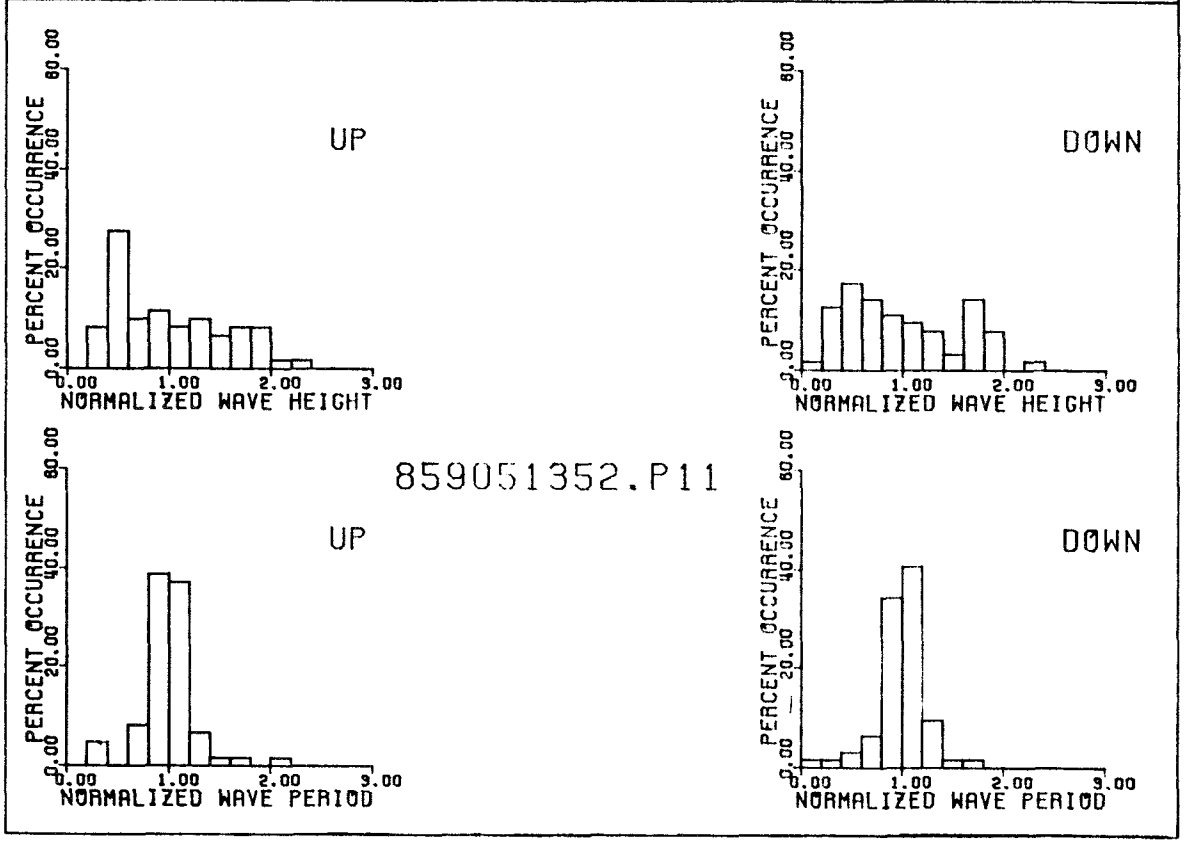
UP
DOWN
PERCENT OCCURRENCE
NORMALIZED WAVE HEIGHT
859051352.P11
UP
DOWN
PERCENT OCCURRENCE
NORMALIZED WAVE PERIOD

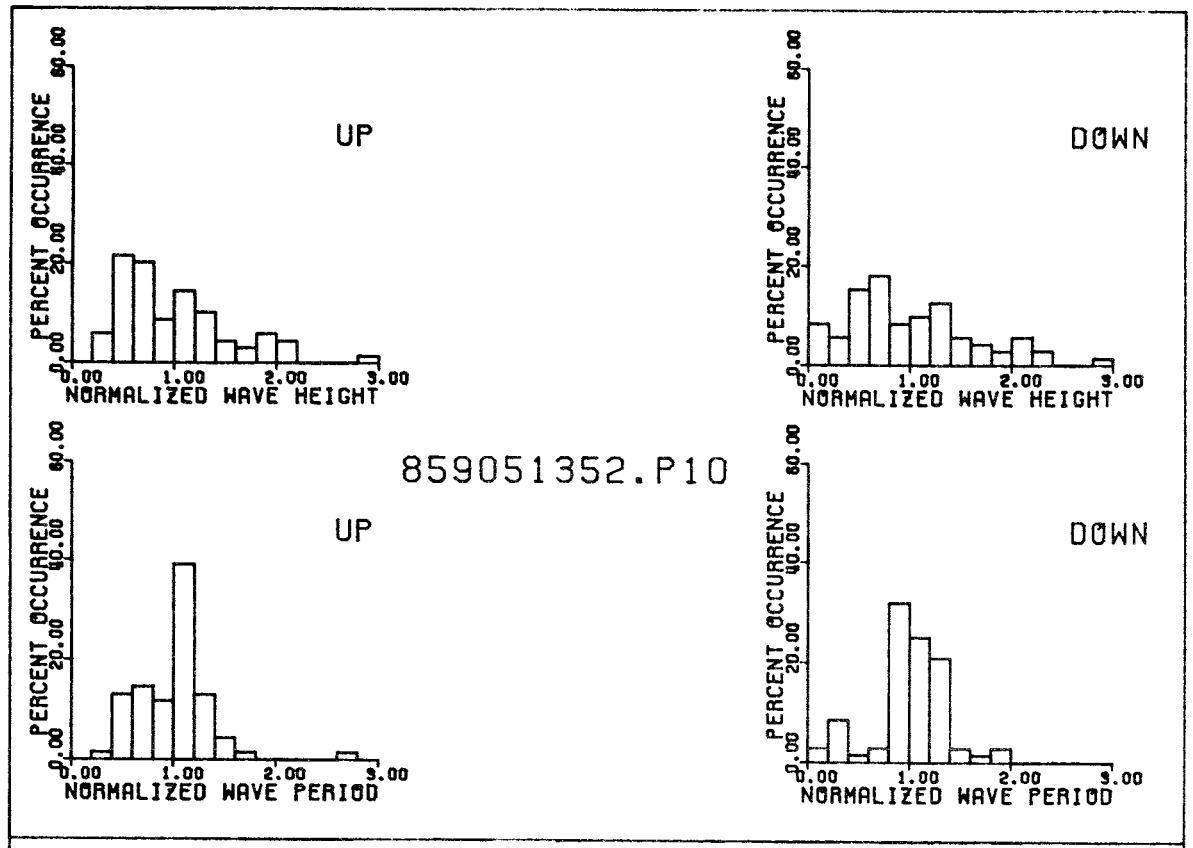
UP
DOWN
PERCENT OCCURRENCE
NORMALIZED WAVE HEIGHT
859051352.P10
UP
DOWN
PERCENT OCCURRENCE
NORMALIZED WAVE PERIOD

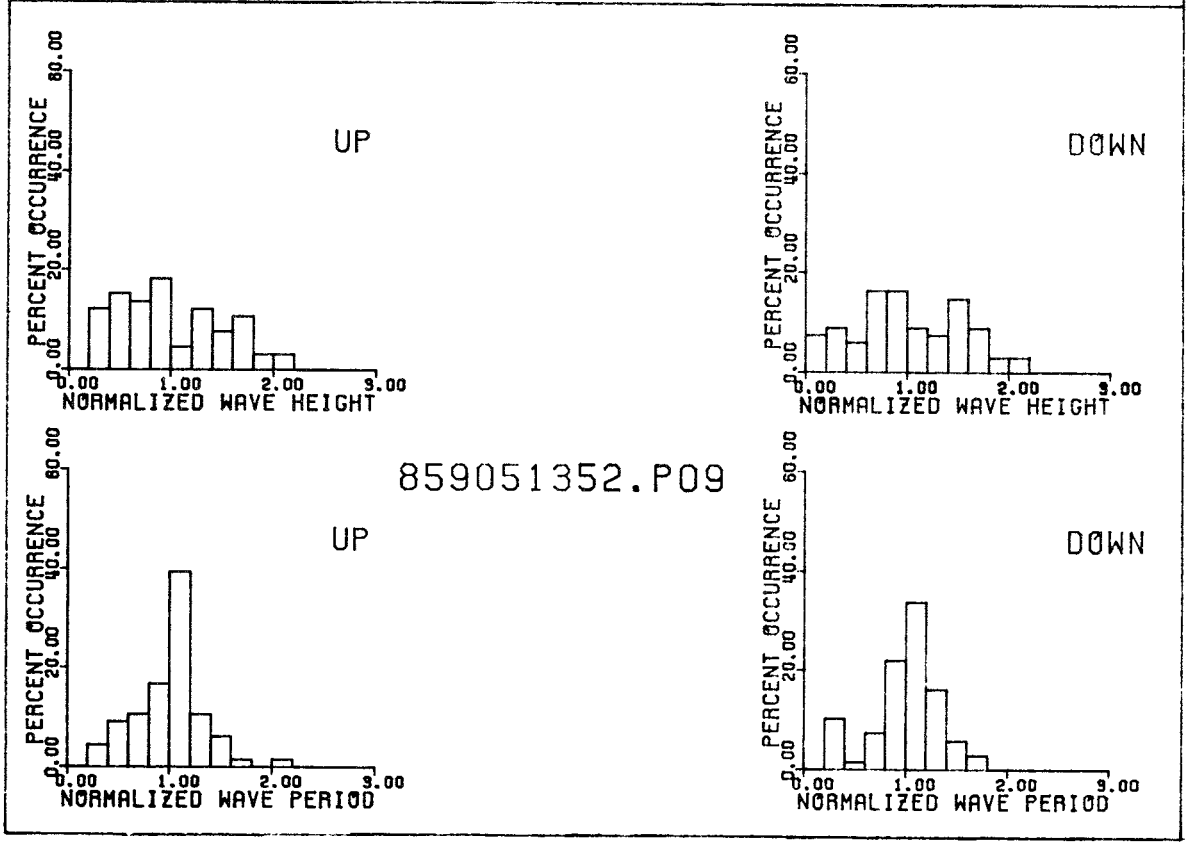
UP
DOWN
PERCENT OCCURRENCE
NORMALIZED WAVE HEIGHT
859051352.P09
UP
DOWN
PERCENT OCCURRENCE
NORMALIZED WAVE PERIOD

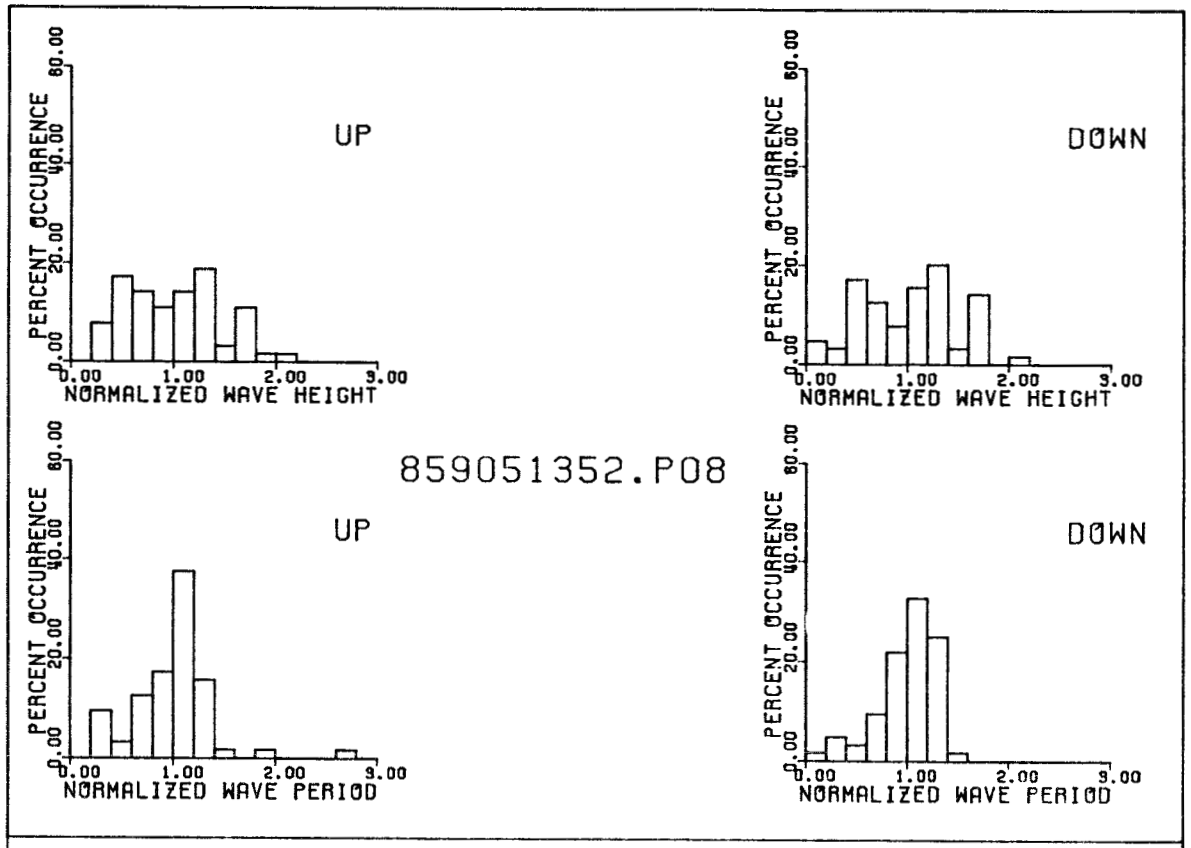
UP
DOWN
PERCENT OCCURRENCE
NORMALIZED WAVE HEIGHT
859051352.P08
UP
DOWN
PERCENT OCCURRENCE
NORMALIZED WAVE PERIOD

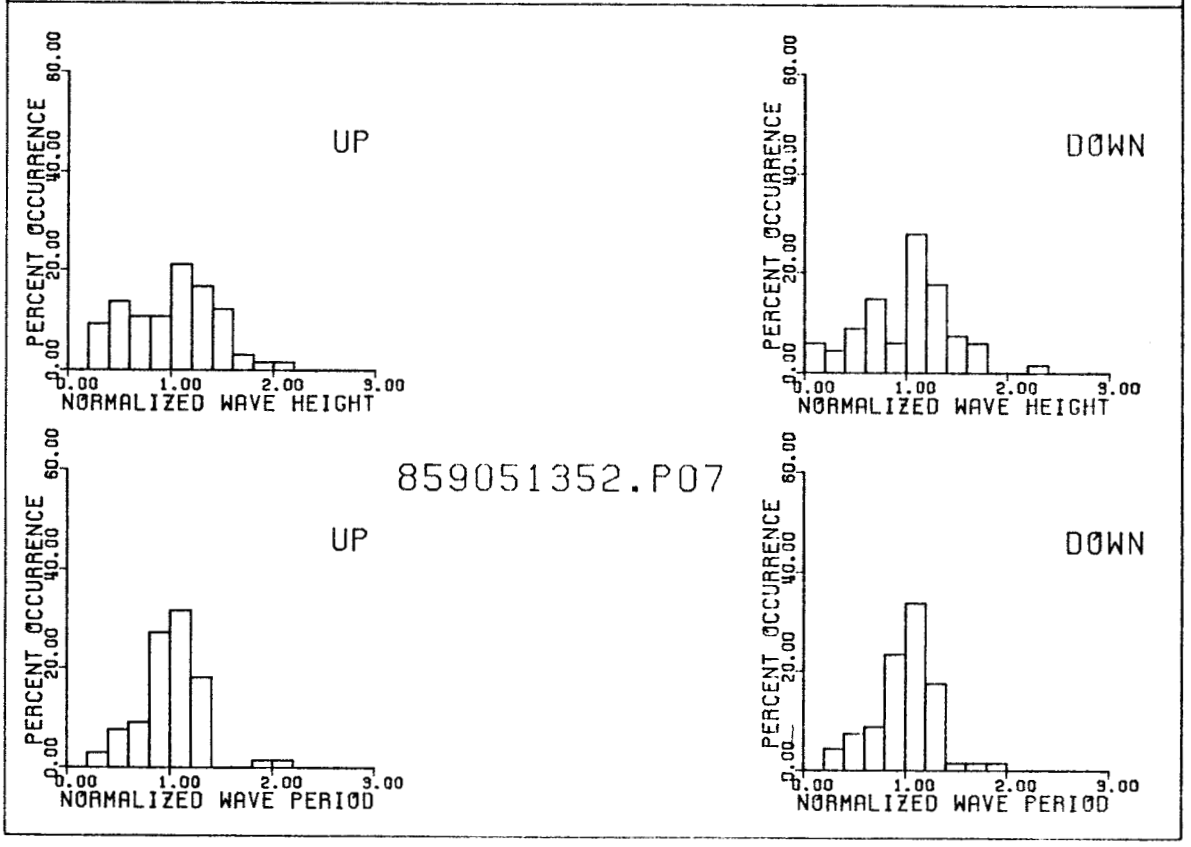
UP
DOWN
PERCENT OCCURRENCE
NORMALIZED WAVE HEIGHT
859051352.P07
UP
DOWN
PERCENT OCCURRENCE
NORMALIZED WAVE PERIOD

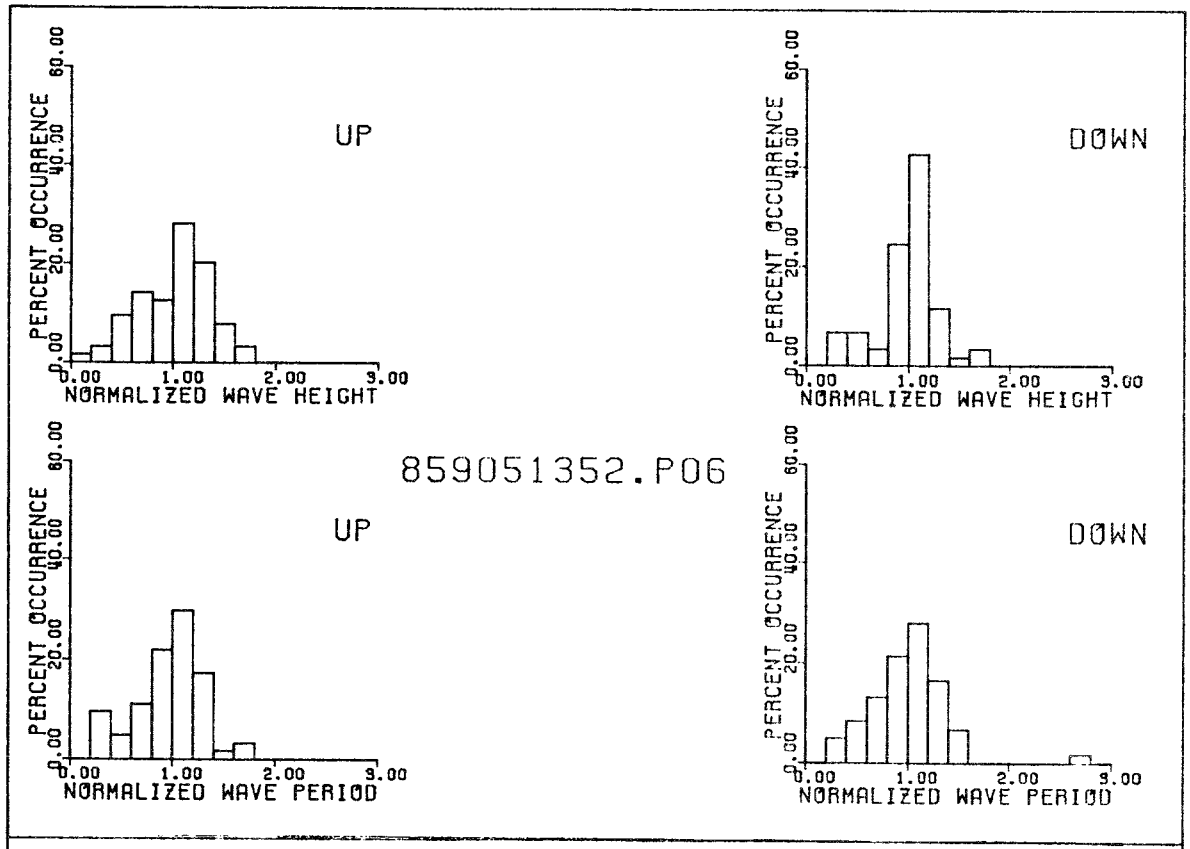
UP
DOWN
PERCENT OCCURRENCE
NORMALIZED WAVE HEIGHT
859051352.P06
UP
DOWN
PERCENT OCCURRENCE
NORMALIZED WAVE PERIOD

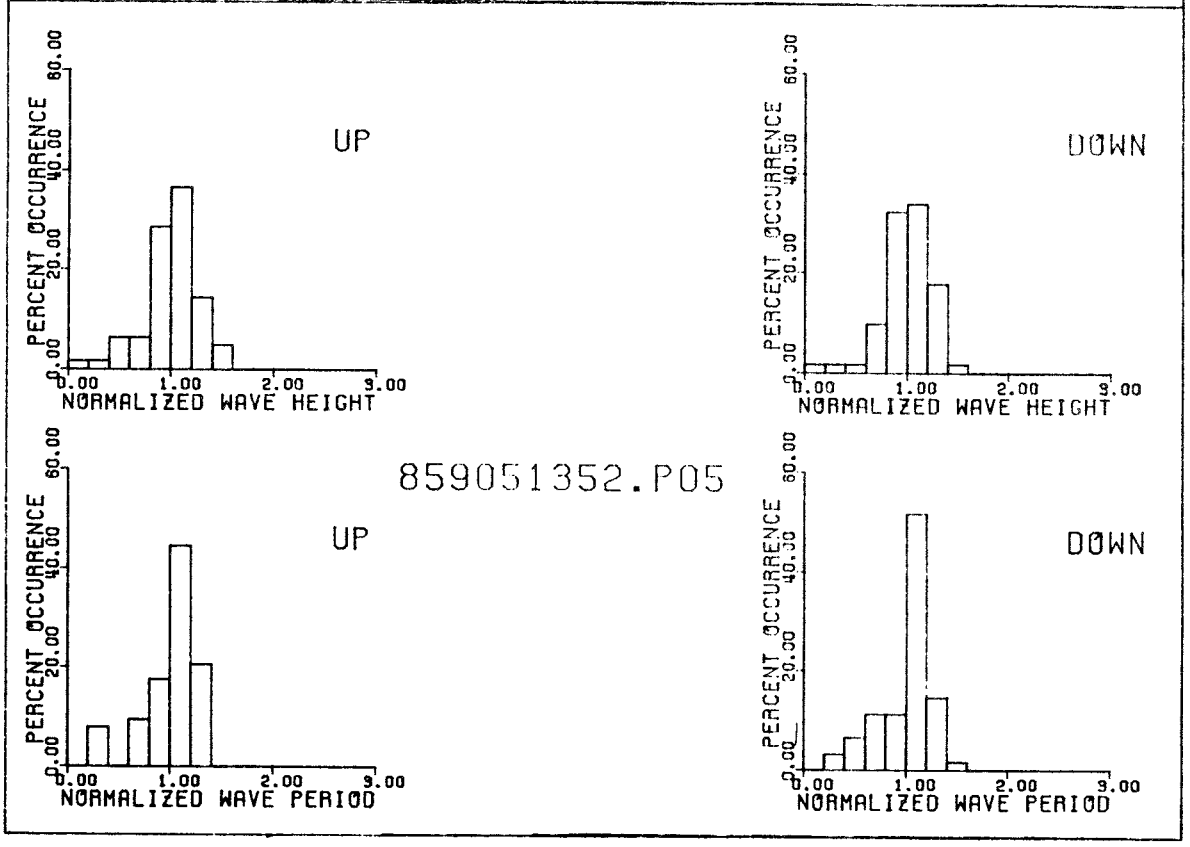
UP
DOWN
PERCENT OCCURRENCE
NORMALIZED WAVE HEIGHT
859051352.P05
UP
DOWN
PERCENT OCCURRENCE
NORMALIZED WAVE PERIOD

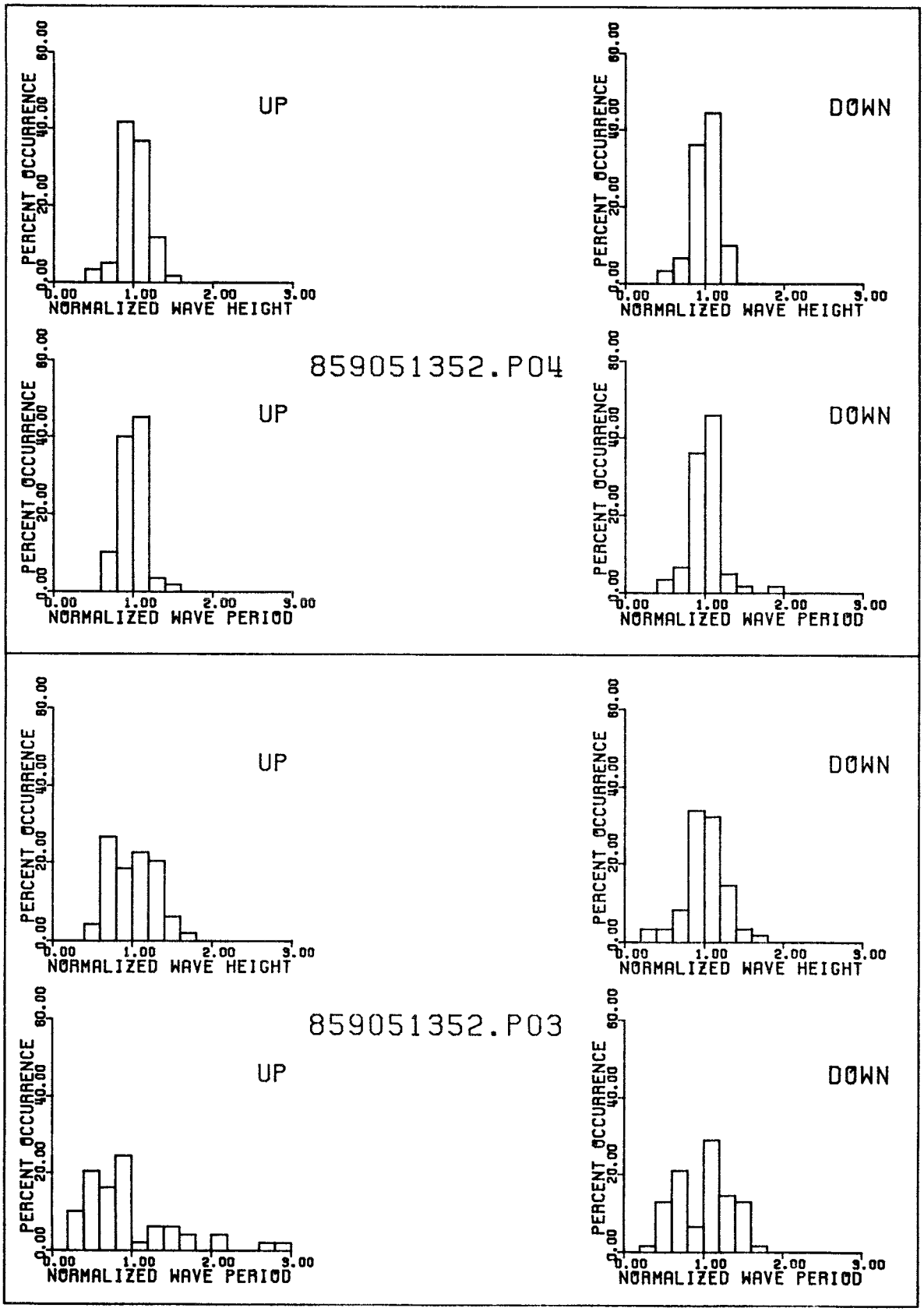
UP
DOWN
859051352.P04
UP
DOWN
859051352.P03
UP
DOWN
PERCENT OCCURRENCE
NORMALIZED WAVE HEIGHT
NORMALIZED WAVE PERIOD
0.00
20.00
40.00
60.00
1.00
2.00
3.00

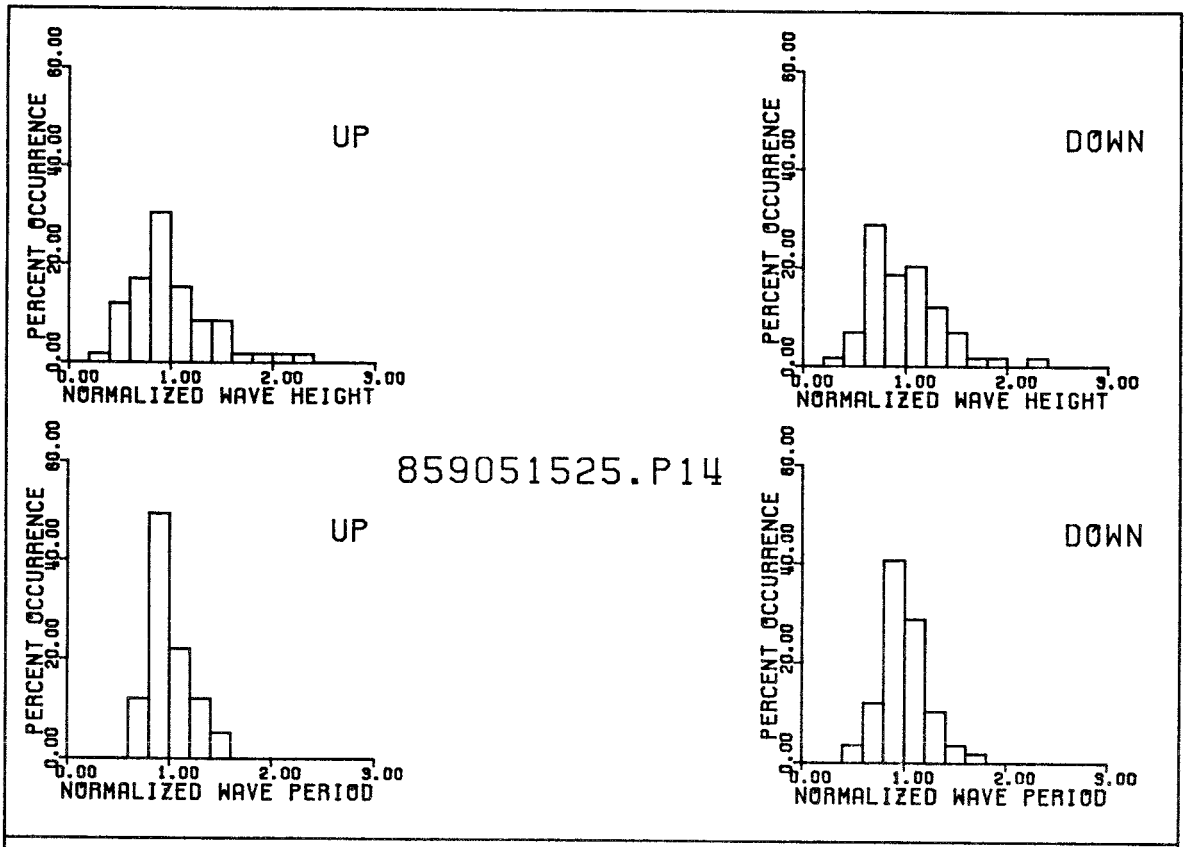
UP
DOWN
PERCENT OCCURRENCE
NORMALIZED WAVE HEIGHT
859051525.P14
UP
DOWN
PERCENT OCCURRENCE
NORMALIZED WAVE PERIOD

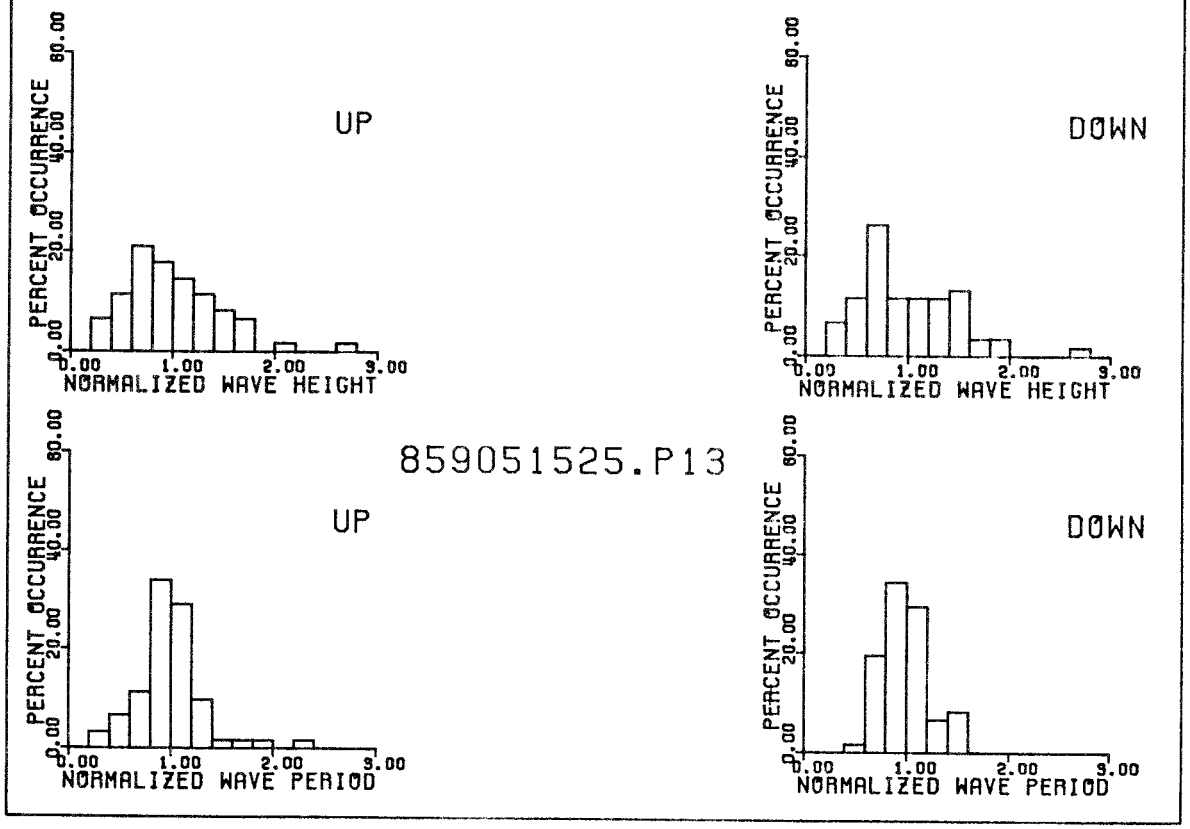
UP
DOWN
PERCENT OCCURRENCE
NORMALIZED WAVE HEIGHT
859051525.P13
UP
DOWN
PERCENT OCCURRENCE
NORMALIZED WAVE PERIOD

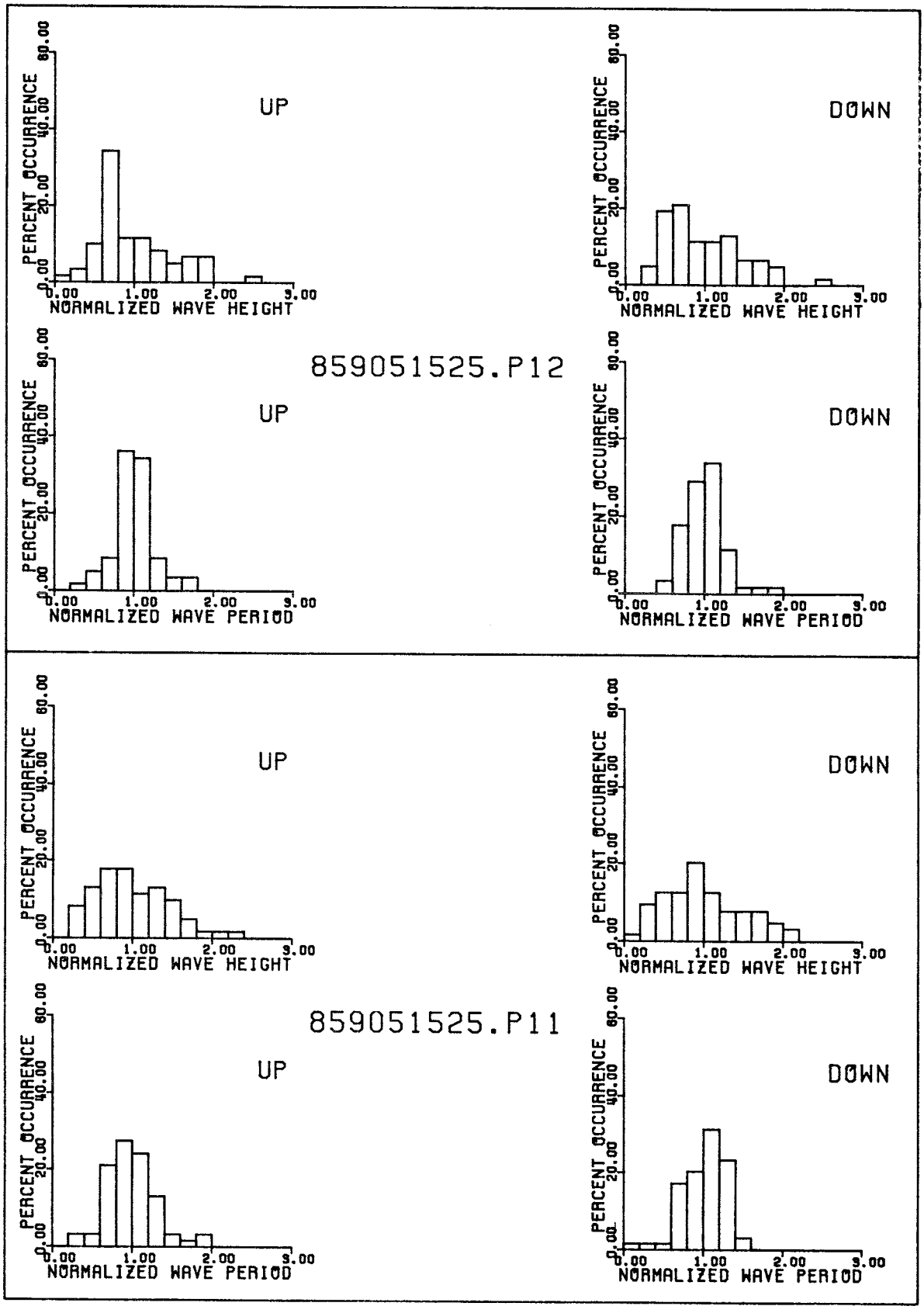
UP
DOWN
PERCENT OCCURRENCE
NORMALIZED WAVE HEIGHT
859051525.P12
UP
DOWN
PERCENT OCCURRENCE
NORMALIZED WAVE PERIOD
UP
DOWN
PERCENT OCCURRENCE
NORMALIZED WAVE HEIGHT
859051525.P11
UP
DOWN
PERCENT OCCURRENCE
NORMALIZED WAVE PERIOD

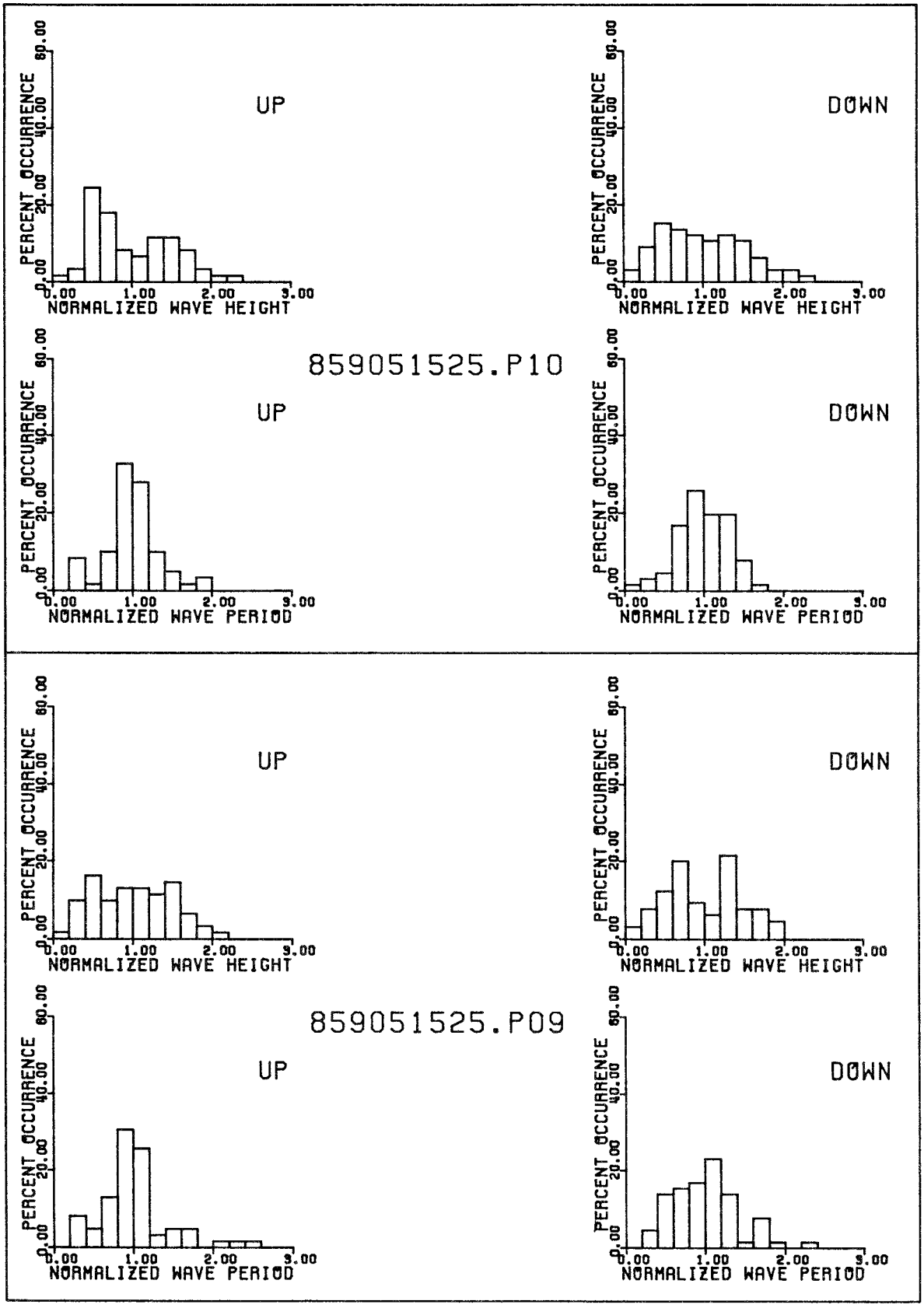
UP
DOWN
PERCENT OCCURRENCE
NORMALIZED WAVE HEIGHT
859051525.P10
UP
DOWN
PERCENT OCCURRENCE
NORMALIZED WAVE PERIOD
UP
DOWN
PERCENT OCCURRENCE
NORMALIZED WAVE HEIGHT
859051525.P09
UP
DOWN
PERCENT OCCURRENCE
NORMALIZED WAVE PERIOD

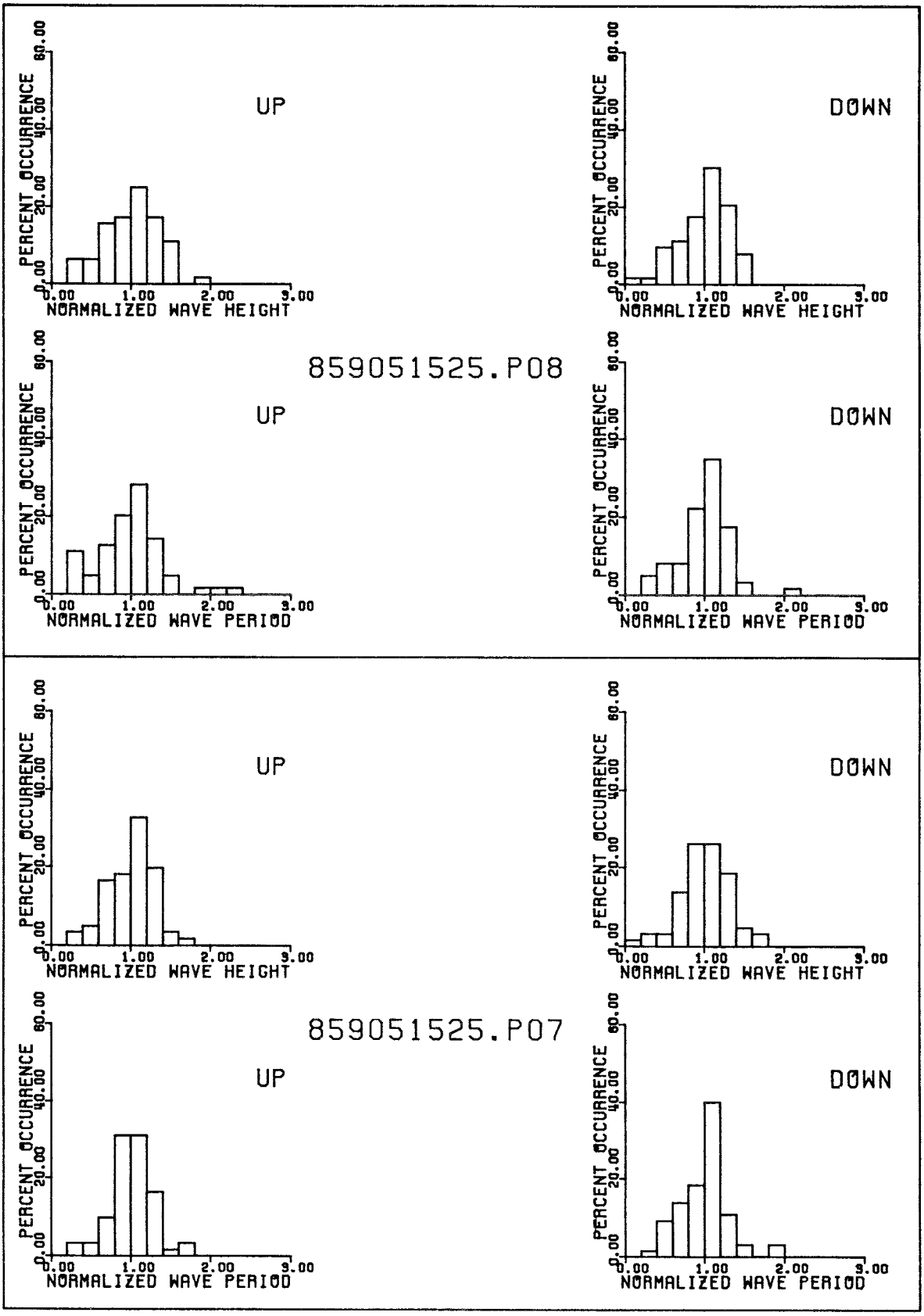
UP
DOWN
859051525.P08
UP
DOWN
859051525.P07
UP
DOWN
PERCENT OCCURRENCE
NORMALIZED WAVE HEIGHT
NORMALIZED WAVE PERIOD
0.00
20.00
40.00
60.00
1.00
2.00
3.00

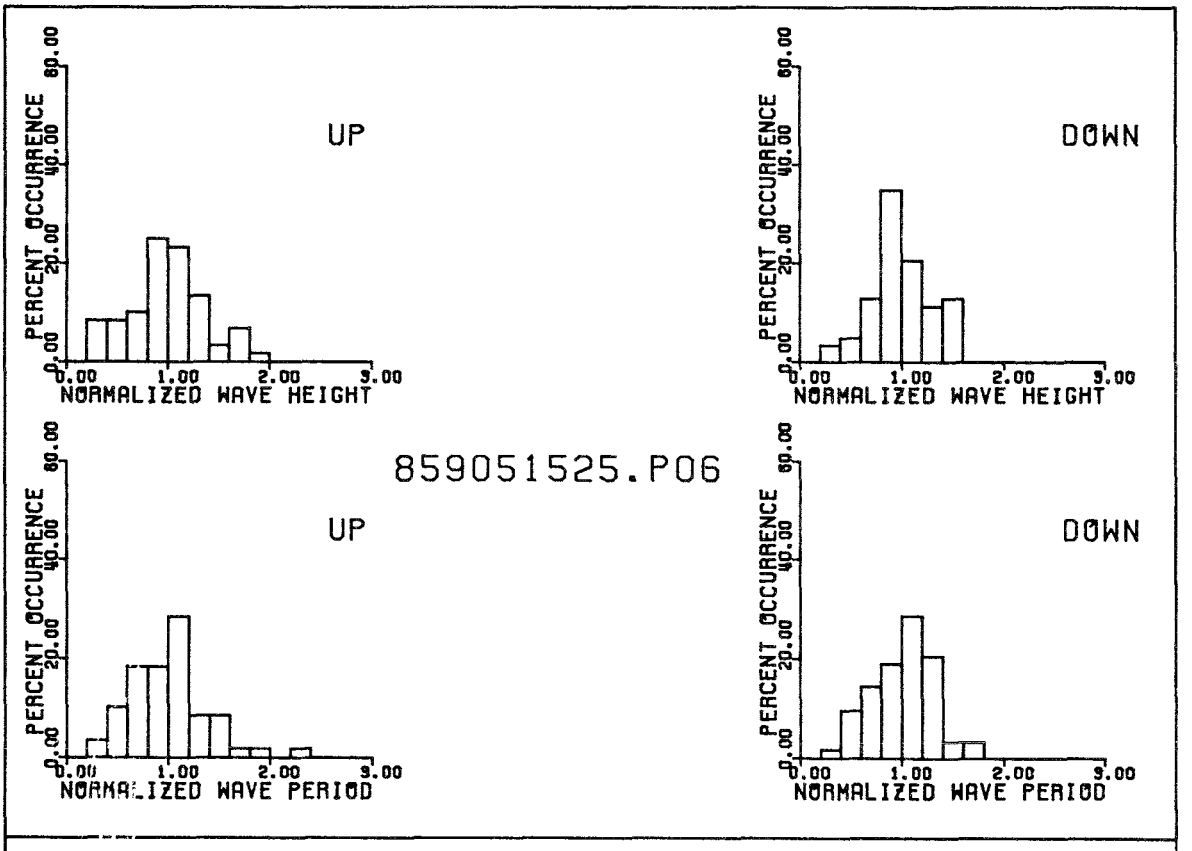
UP
DOWN
PERCENT OCCURRENCE
NORMALIZED WAVE HEIGHT
859051525.P06
UP
DOWN
PERCENT OCCURRENCE
NORMALIZED WAVE PERIOD
0.00
1.00
2.00
3.00
0.00
20.00
40.00
60.00

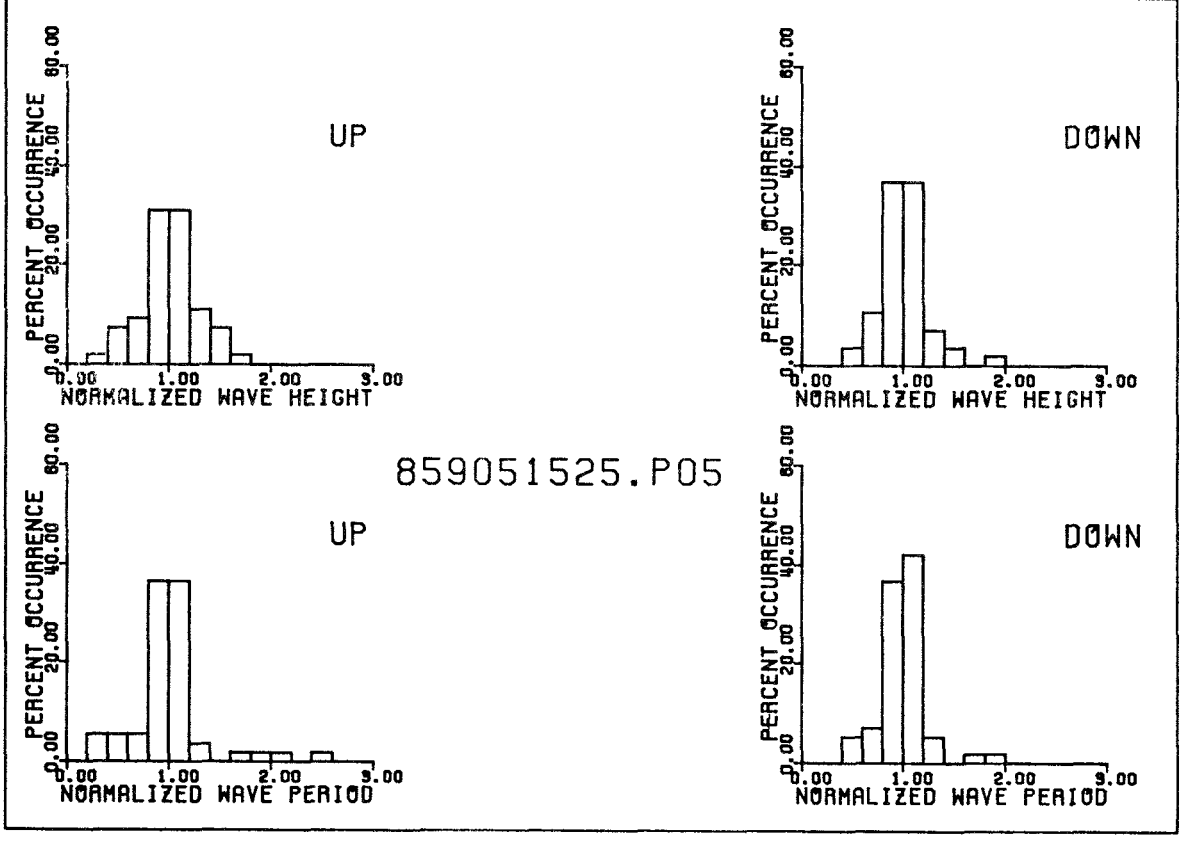
UP
DOWN
PERCENT OCCURRENCE
NORMALIZED WAVE HEIGHT
859051525.P05
UP
DOWN
PERCENT OCCURRENCE
NORMALIZED WAVE PERIOD
0.00
1.00
2.00
3.00
0.00
20.00
40.00
60.00

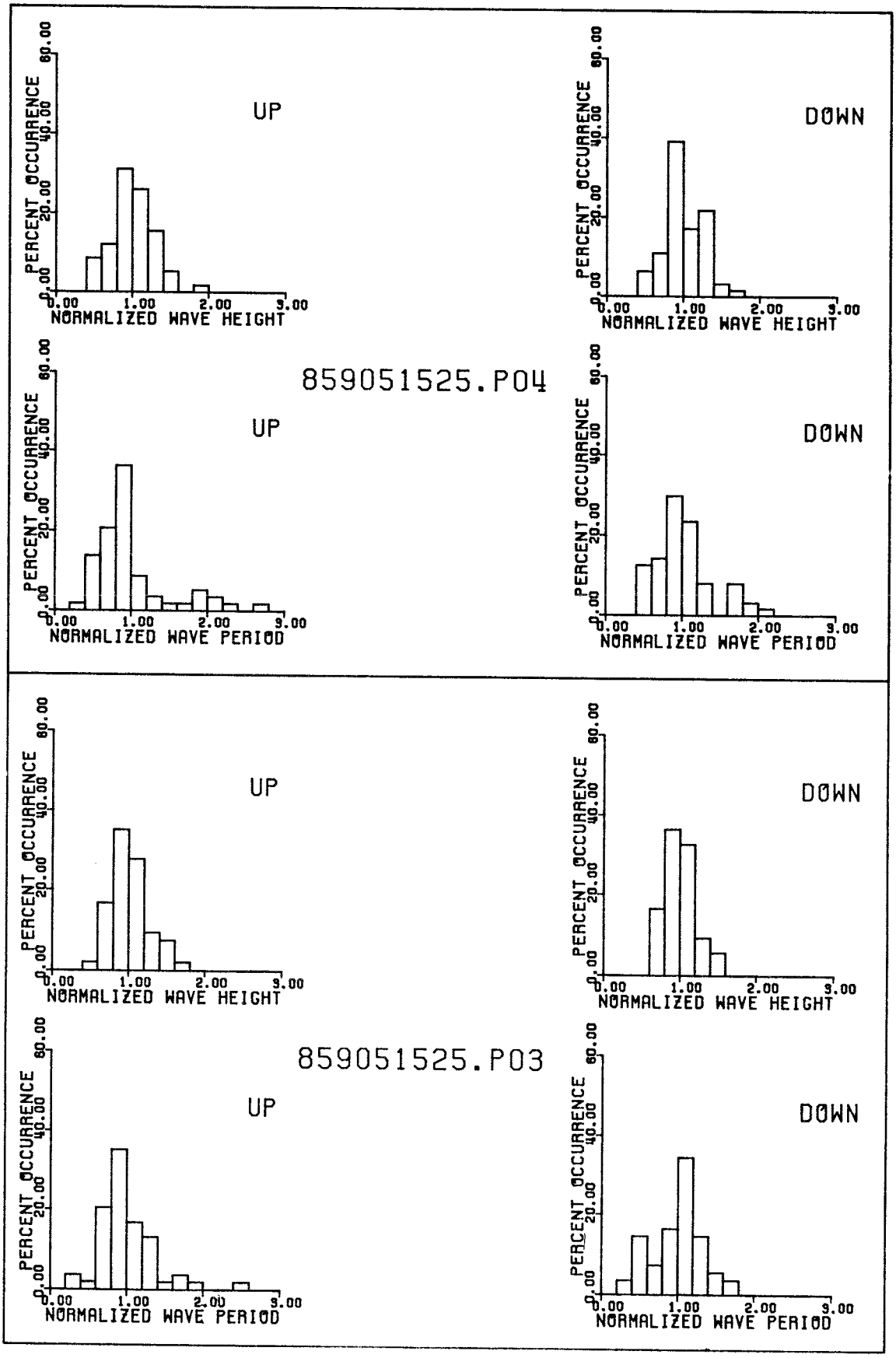
UP
DOWN
PERCENT OCCURRENCE
NORMALIZED WAVE HEIGHT
859051525.P04
UP
DOWN
PERCENT OCCURRENCE
NORMALIZED WAVE PERIOD
UP
DOWN
PERCENT OCCURRENCE
NORMALIZED WAVE HEIGHT
859051525.P03
UP
DOWN
PERCENT OCCURRENCE
NORMALIZED WAVE PERIOD
0.00
20.00
40.00
60.00
1.00
2.00
3.00

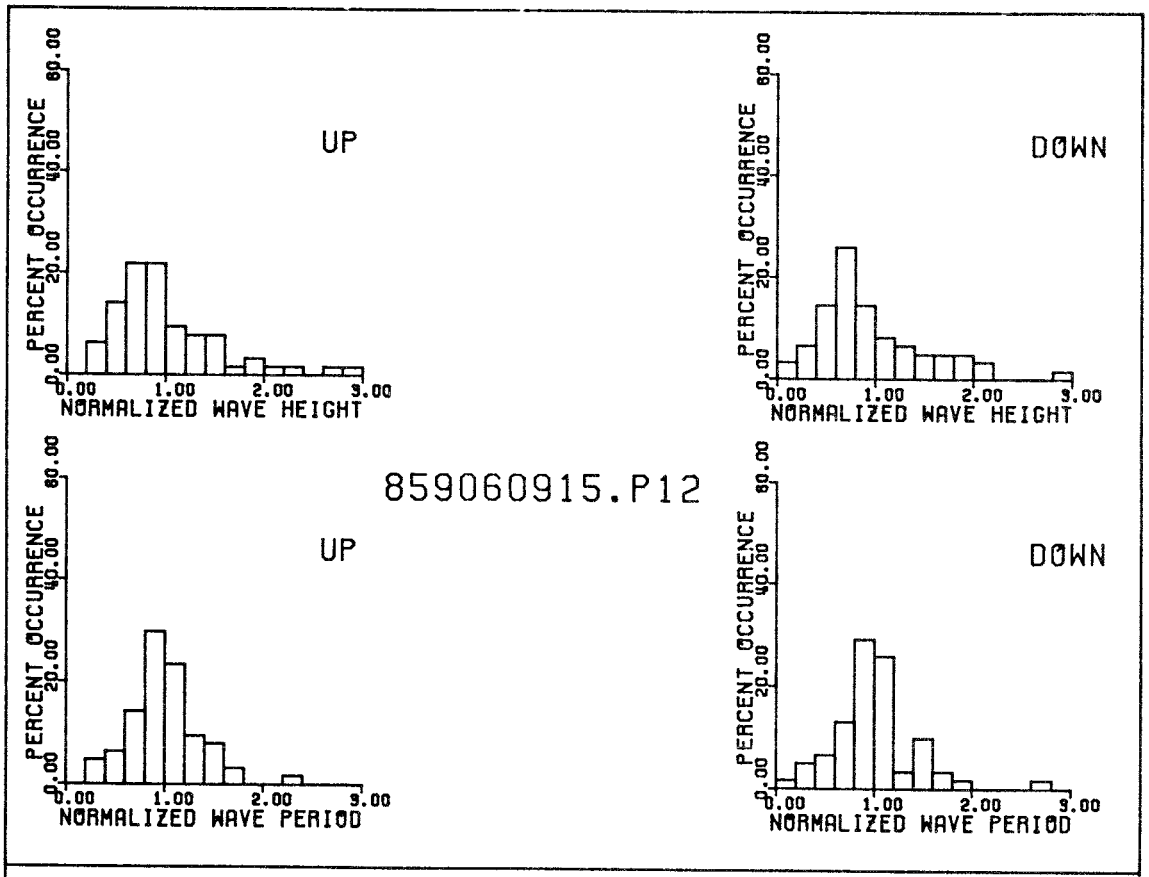
UP
DOWN
PERCENT OCCURRENCE
NORMALIZED WAVE HEIGHT
859060915.P12
UP
DOWN
PERCENT OCCURRENCE
NORMALIZED WAVE PERIOD

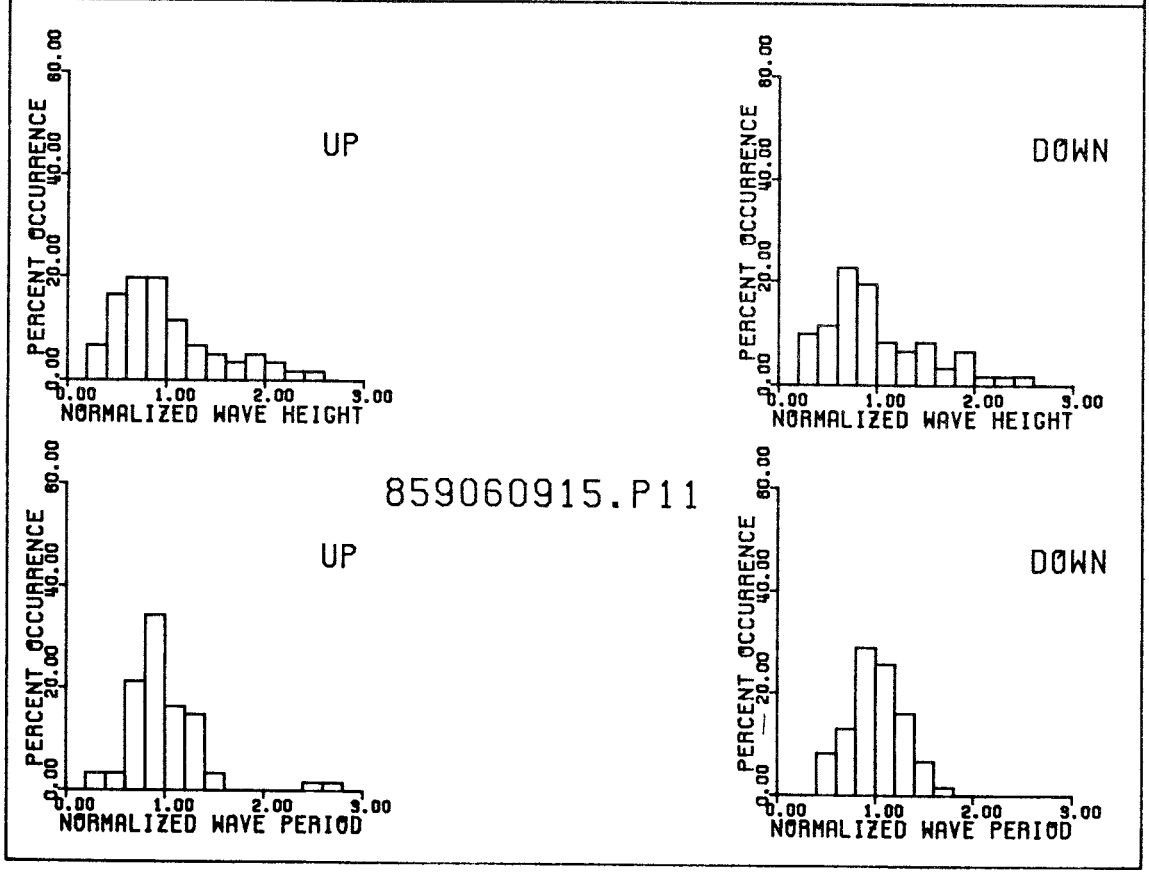
UP
DOWN
PERCENT OCCURRENCE
NORMALIZED WAVE HEIGHT
859060915.P11
UP
DOWN
PERCENT OCCURRENCE
NORMALIZED WAVE PERIOD

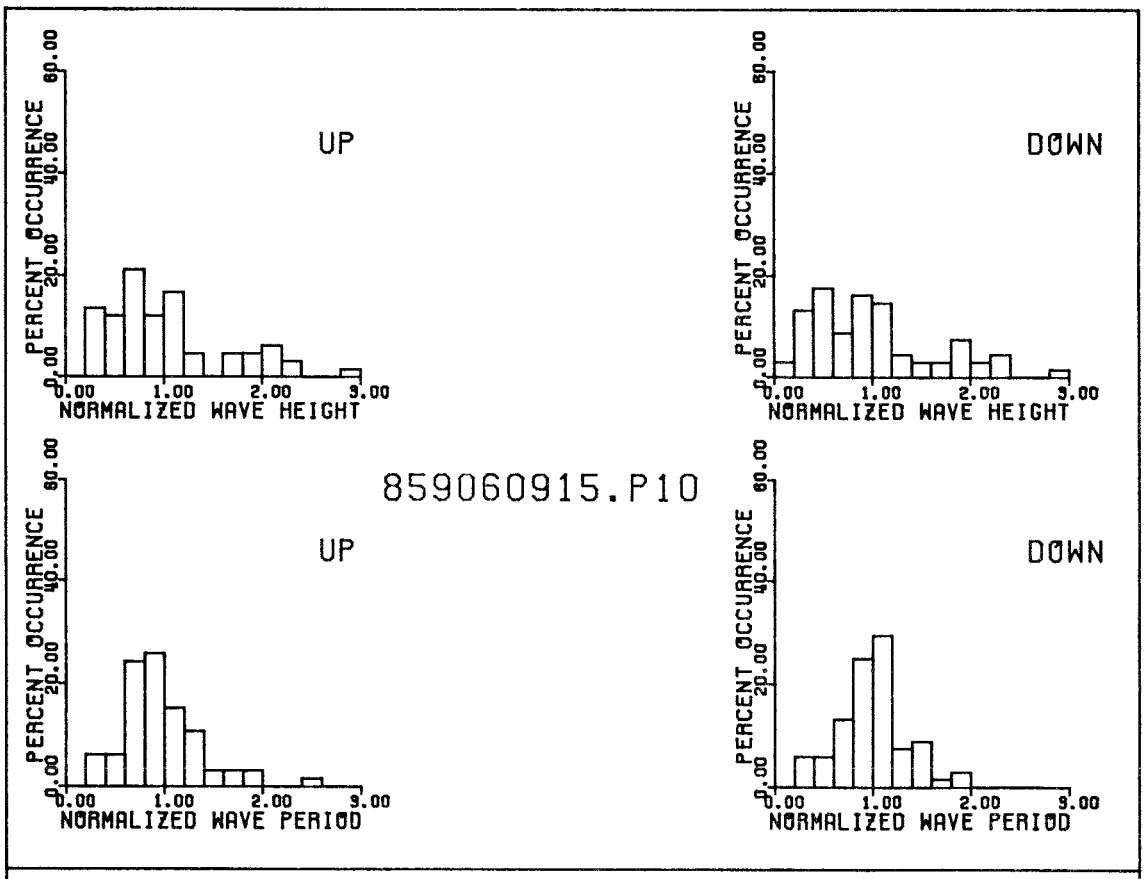
UP
DOWN
PERCENT OCCURRENCE
0.00
20.00
40.00
60.00
0.00
1.00
2.00
3.00
NORMALIZED WAVE HEIGHT
859060915.P10
UP
DOWN
PERCENT OCCURRENCE
NORMALIZED WAVE PERIOD

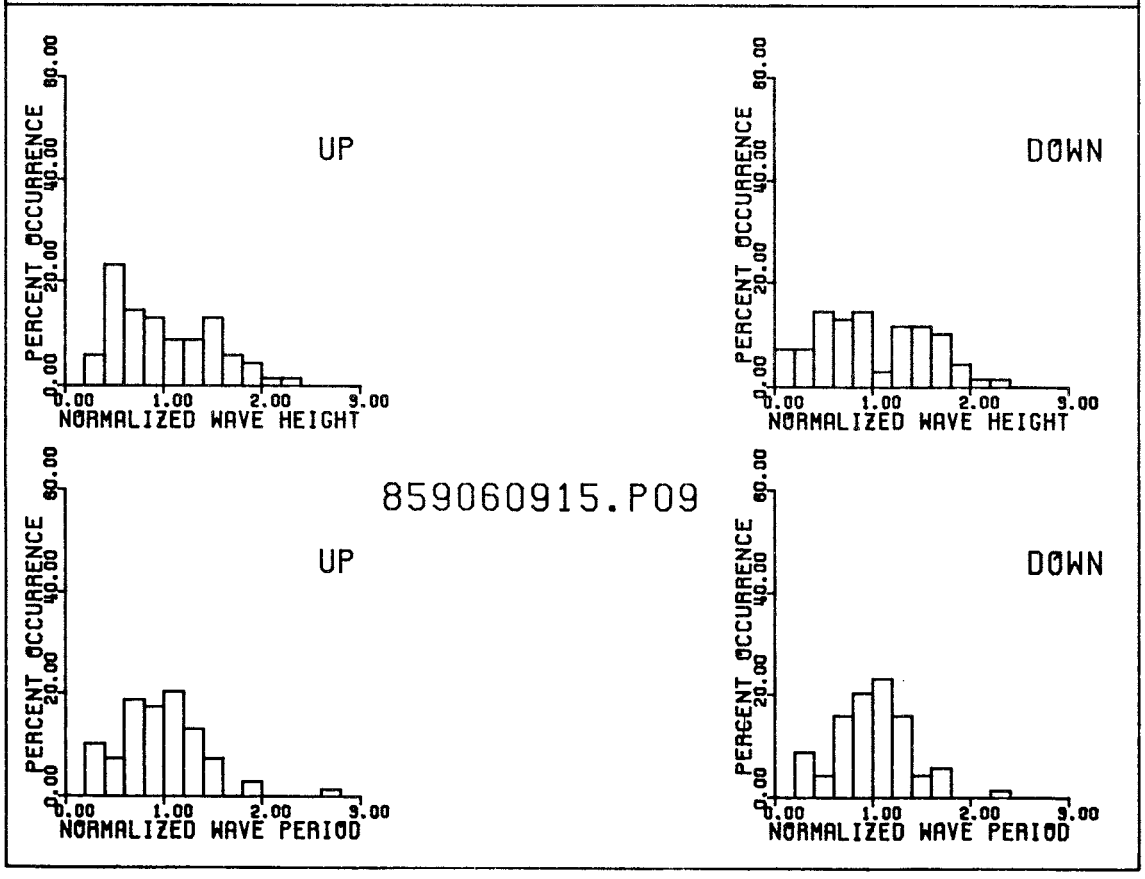
UP
DOWN
PERCENT OCCURRENCE
0.00
20.00
40.00
60.00
0.00
1.00
2.00
3.00
NORMALIZED WAVE HEIGHT
859060915.P09
UP
DOWN
PERCENT OCCURRENCE
NORMALIZED WAVE PERIOD

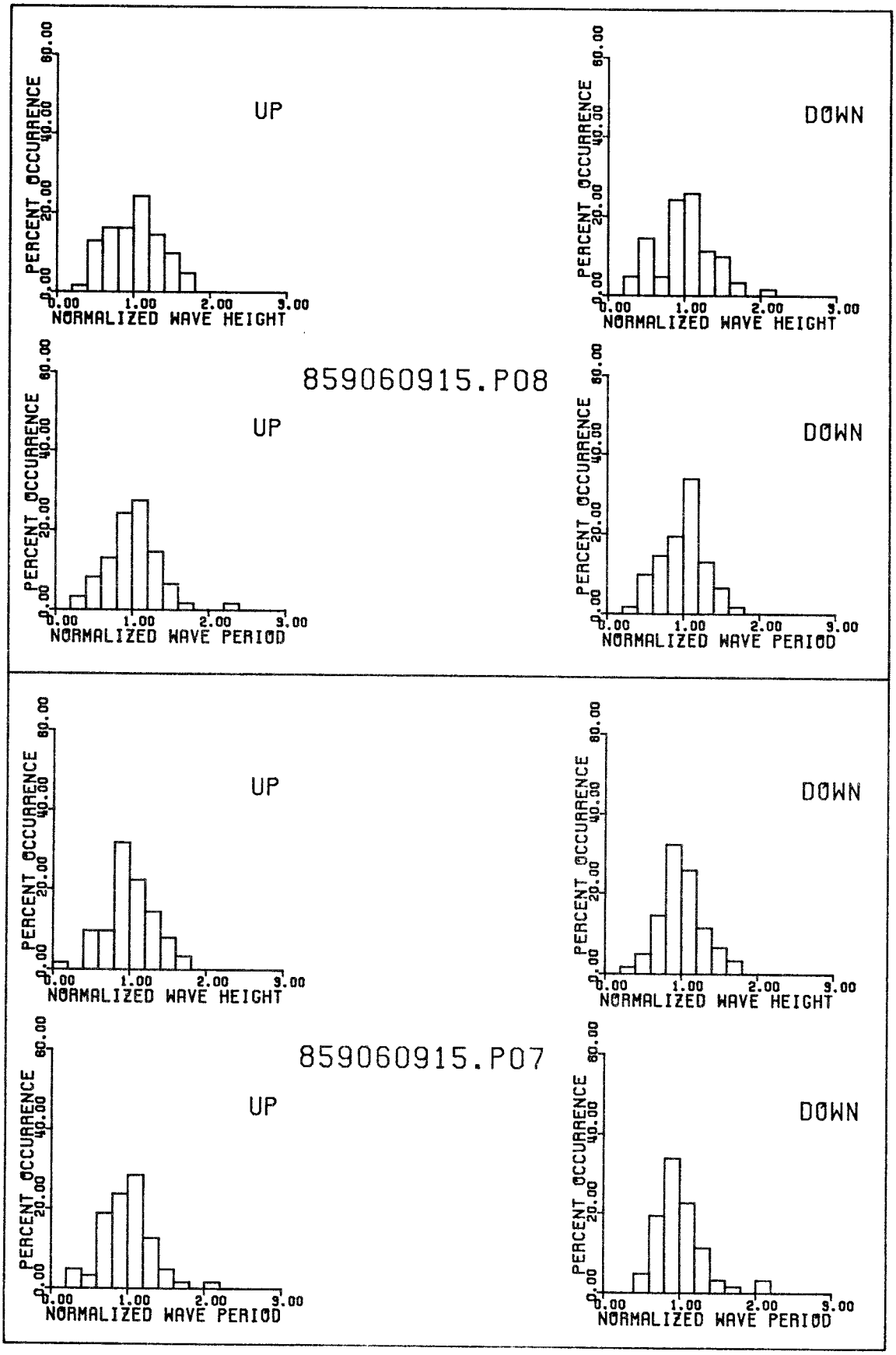
UP
DOWN
PERCENT OCCURRENCE
NORMALIZED WAVE HEIGHT
859060915.P08
UP
DOWN
PERCENT OCCURRENCE
NORMALIZED WAVE PERIOD
UP
DOWN
PERCENT OCCURRENCE
NORMALIZED WAVE HEIGHT
859060915.P07
UP
DOWN
PERCENT OCCURRENCE
NORMALIZED WAVE PERIOD

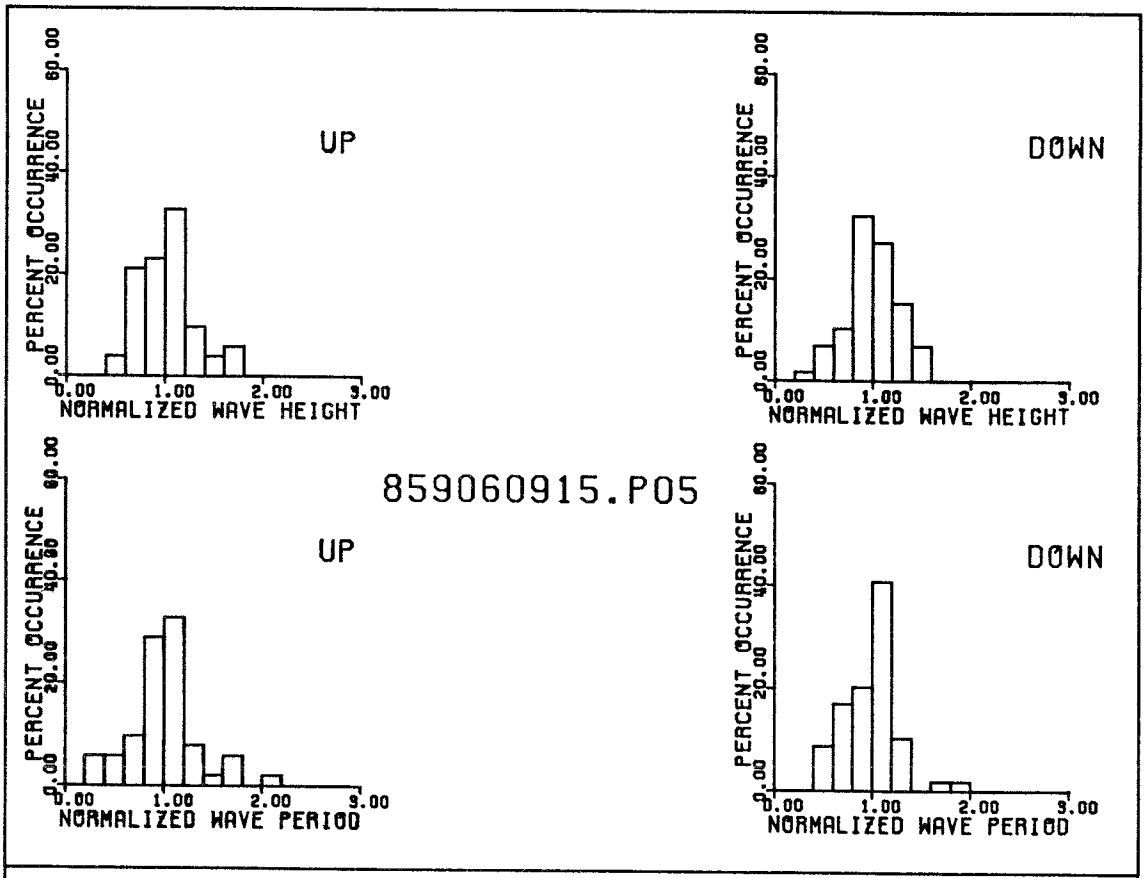
UP
DOWN
PERCENT OCCURRENCE
NORMALIZED WAVE HEIGHT
859060915.P05
UP
DOWN
PERCENT OCCURRENCE
NORMALIZED WAVE PERIOD

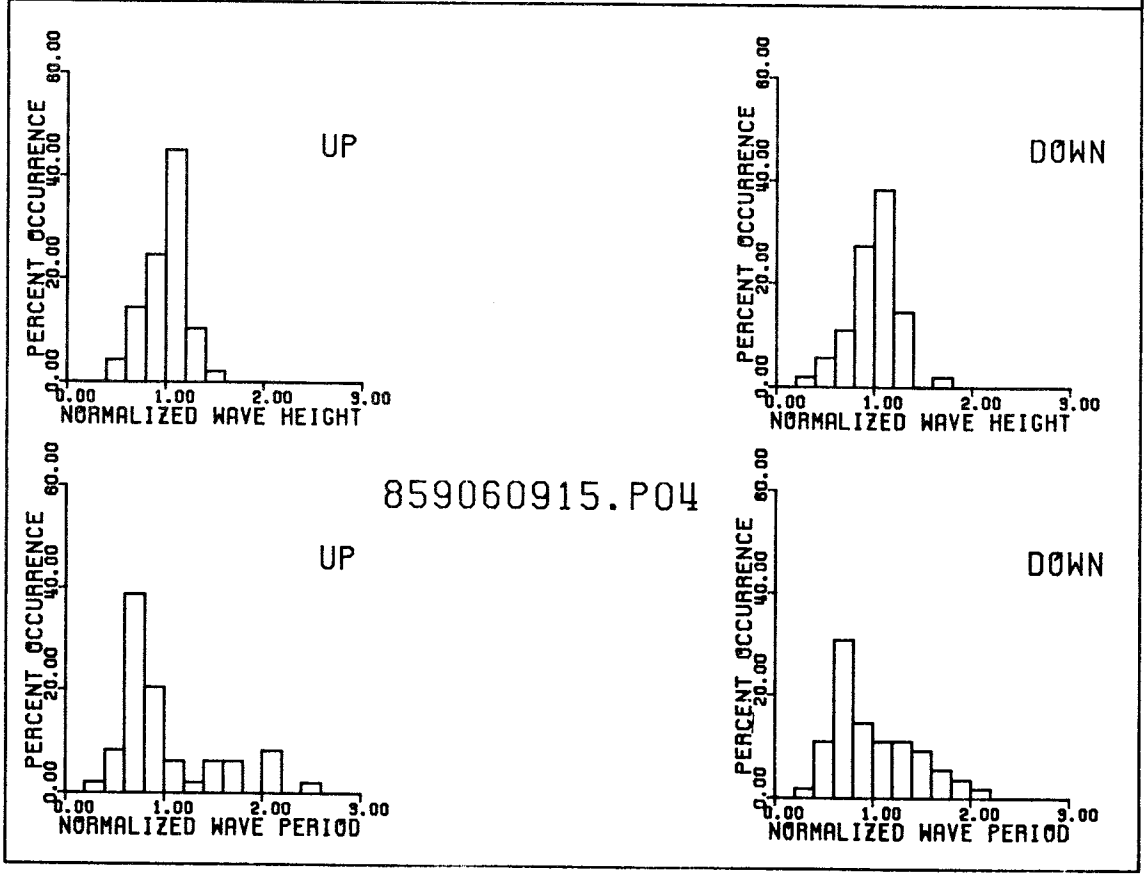
UP
DOWN
PERCENT OCCURRENCE
NORMALIZED WAVE HEIGHT
859060915.P04
UP
DOWN
PERCENT OCCURRENCE
NORMALIZED WAVE PERIOD

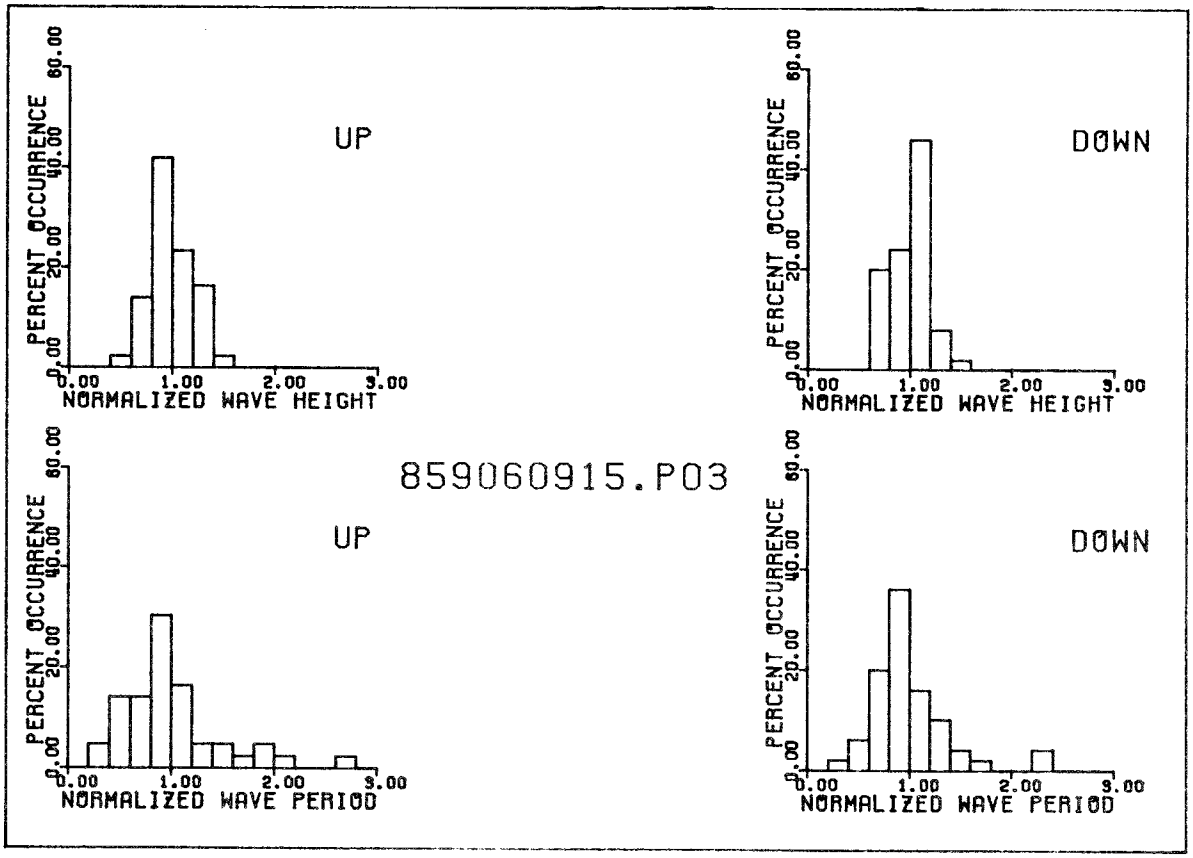
UP
DOWN
859060915.P03
UP
DOWN
PERCENT OCCURRENCE
0.00
20.00
40.00
60.00
0.00
1.00
2.00
3.00
NORMALIZED WAVE HEIGHT
NORMALIZED WAVE PERIOD

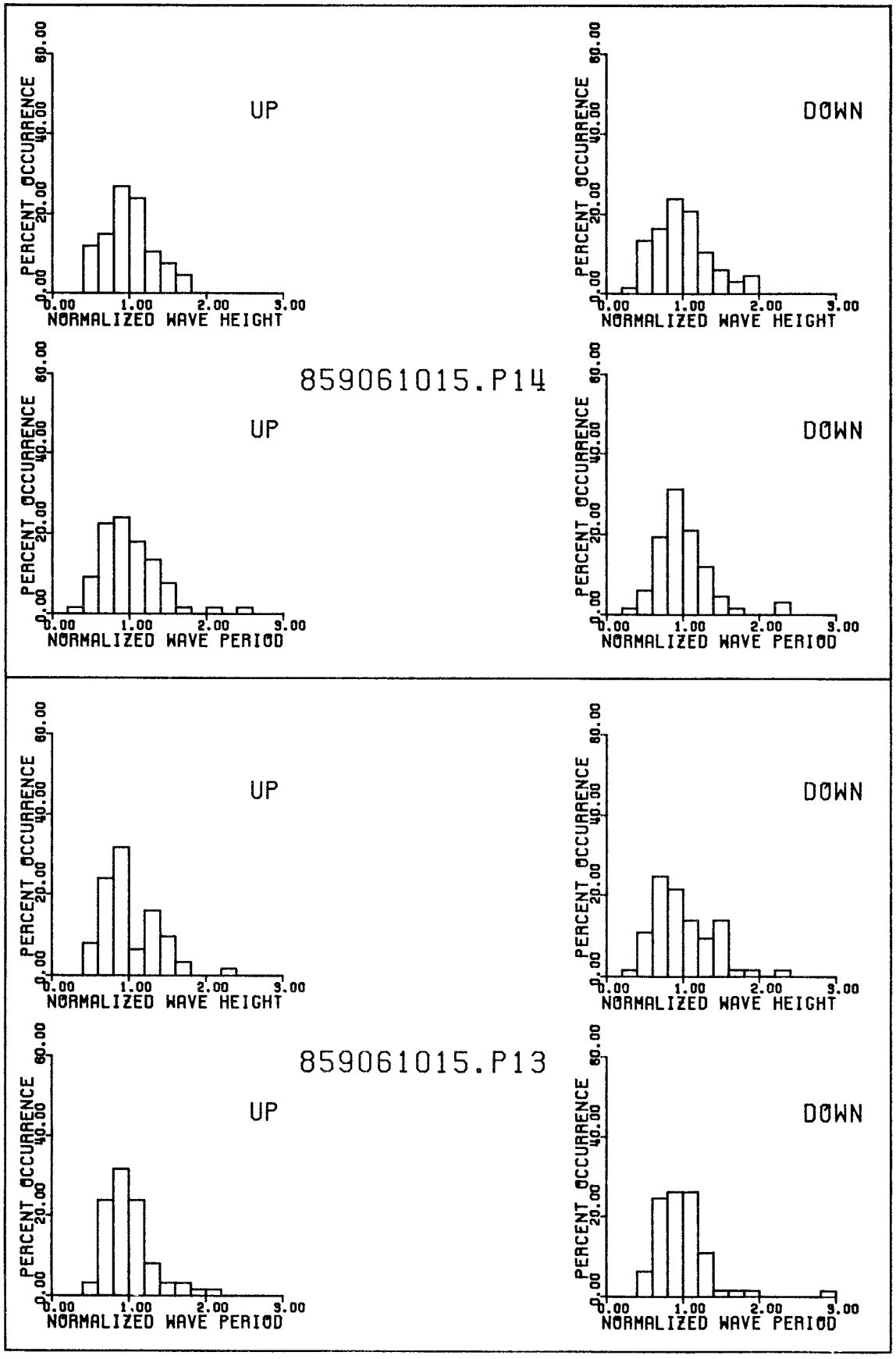
UP
DOWN
PERCENT OCCURRENCE
NORMALIZED WAVE HEIGHT
859061015.P14
UP
DOWN
PERCENT OCCURRENCE
NORMALIZED WAVE PERIOD
UP
DOWN
PERCENT OCCURRENCE
NORMALIZED WAVE HEIGHT
859061015.P13
UP
DOWN
PERCENT OCCURRENCE
NORMALIZED WAVE PERIOD

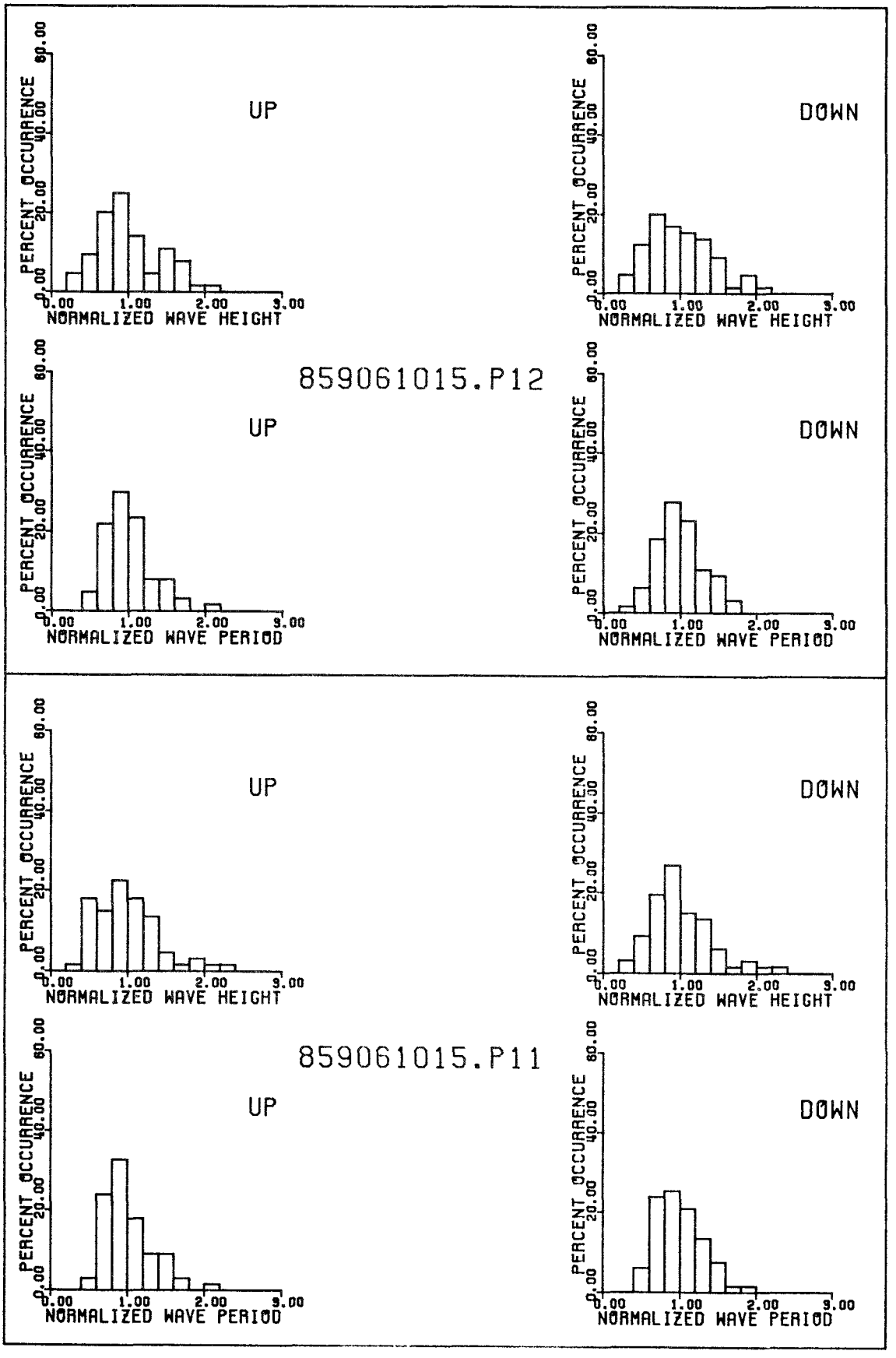
UP
DOWN
PERCENT OCCURRENCE
0.00
20.00
40.00
60.00
0.00
1.00
2.00
3.00
NORMALIZED WAVE HEIGHT
859061015.P12
UP
DOWN
NORMALIZED WAVE PERIOD
UP
DOWN
NORMALIZED WAVE HEIGHT
859061015.P11
UP
DOWN
NORMALIZED WAVE PERIOD

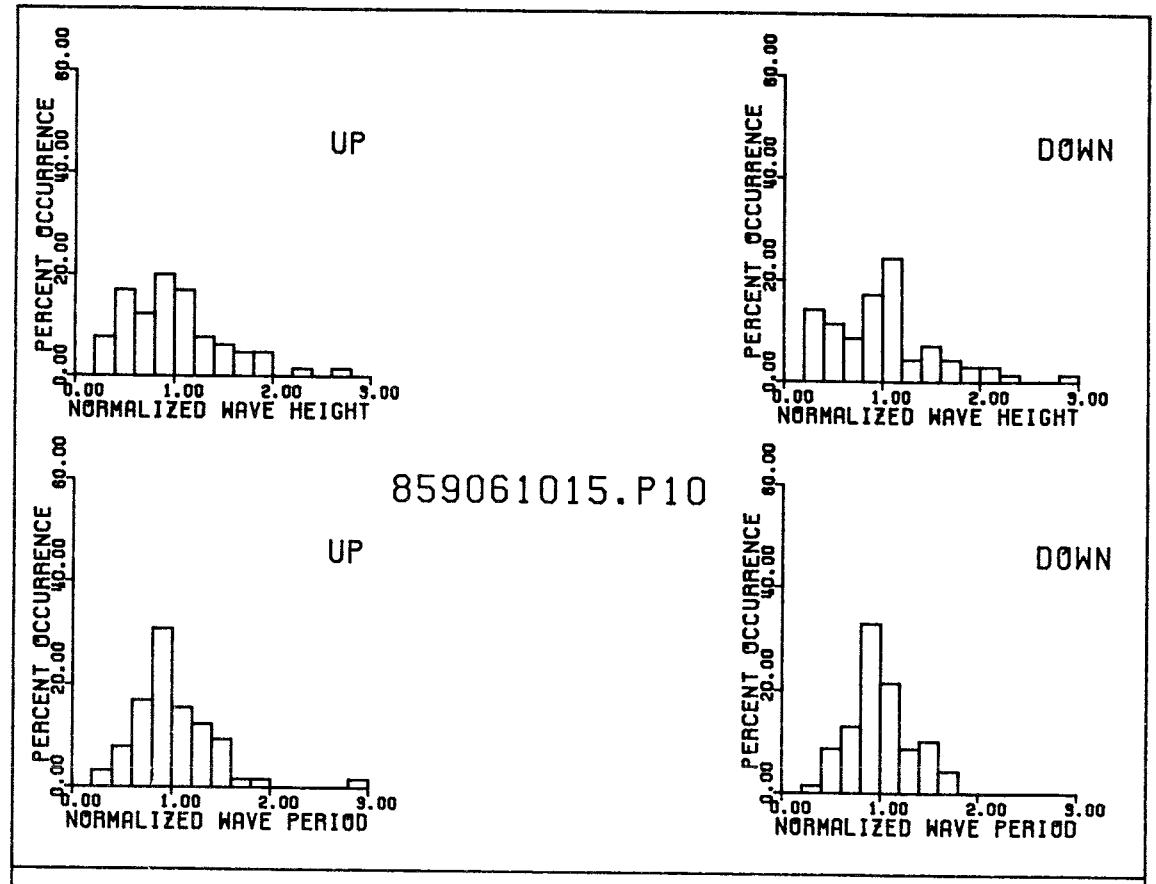
UP
DOWN
PERCENT OCCURRENCE
NORMALIZED WAVE HEIGHT
859061015.P10
UP
DOWN
PERCENT OCCURRENCE
NORMALIZED WAVE PERIOD

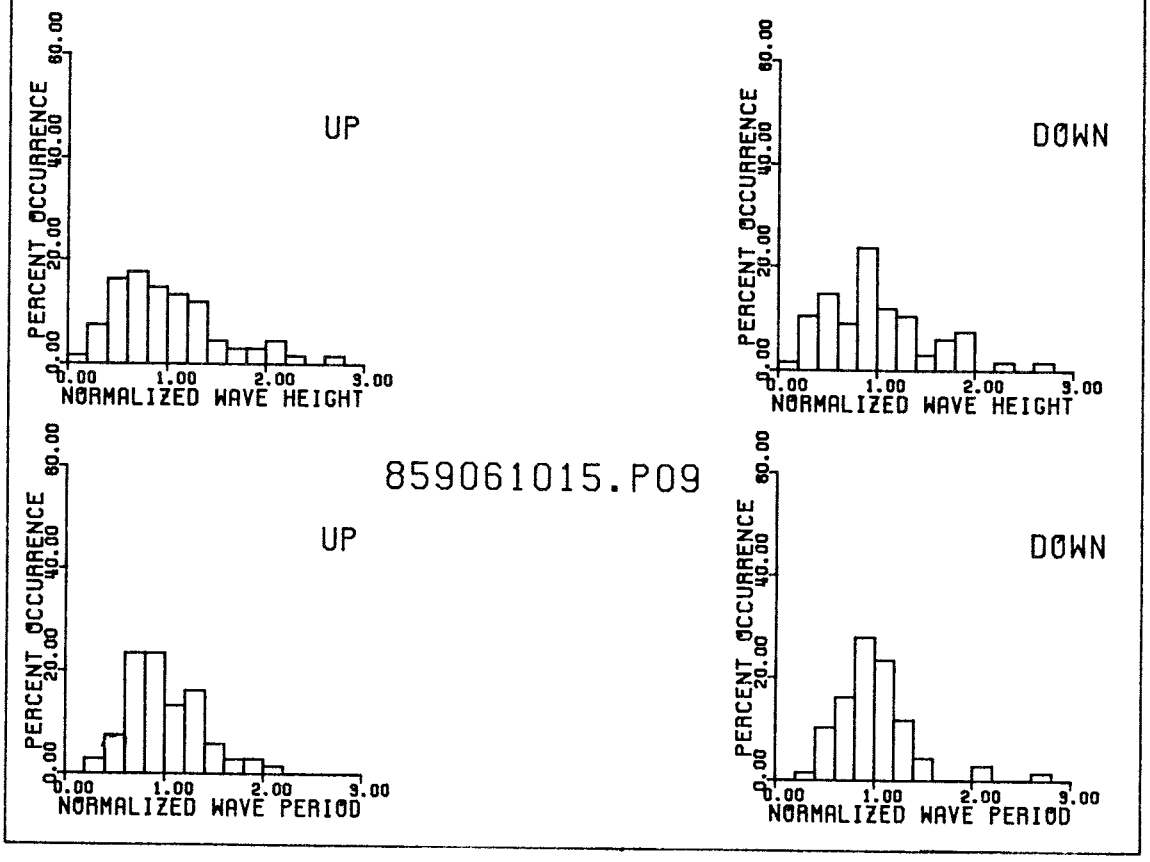
UP
DOWN
PERCENT OCCURRENCE
NORMALIZED WAVE HEIGHT
859061015.P09
UP
DOWN
PERCENT OCCURRENCE
NORMALIZED WAVE PERIOD

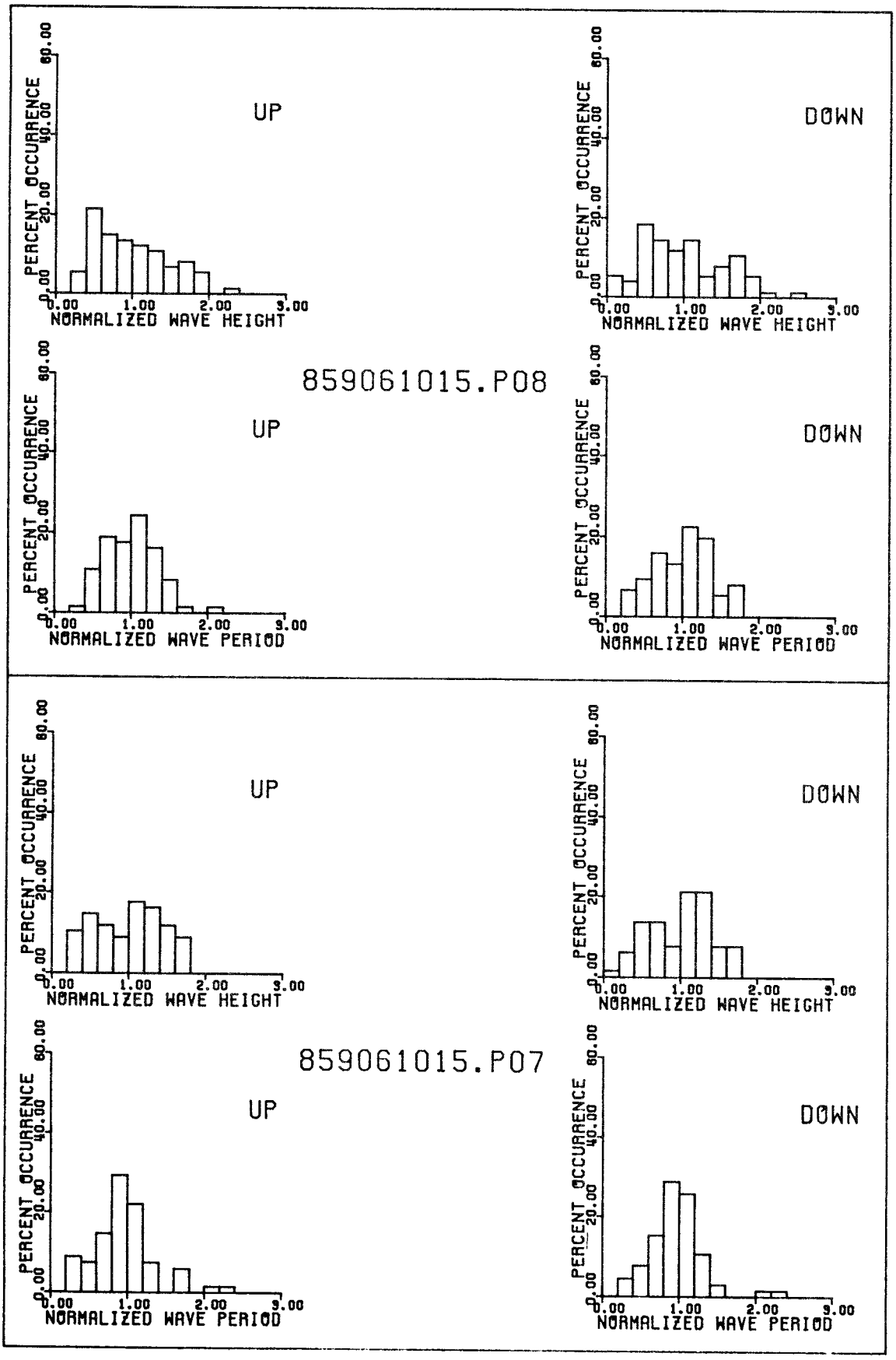
UP
DOWN
PERCENT OCCURRENCE
NORMALIZED WAVE HEIGHT
859061015.P08
UP
DOWN
PERCENT OCCURRENCE
NORMALIZED WAVE PERIOD
UP
DOWN
PERCENT OCCURRENCE
NORMALIZED WAVE HEIGHT
859061015.P07
UP
DOWN
PERCENT OCCURRENCE
NORMALIZED WAVE PERIOD

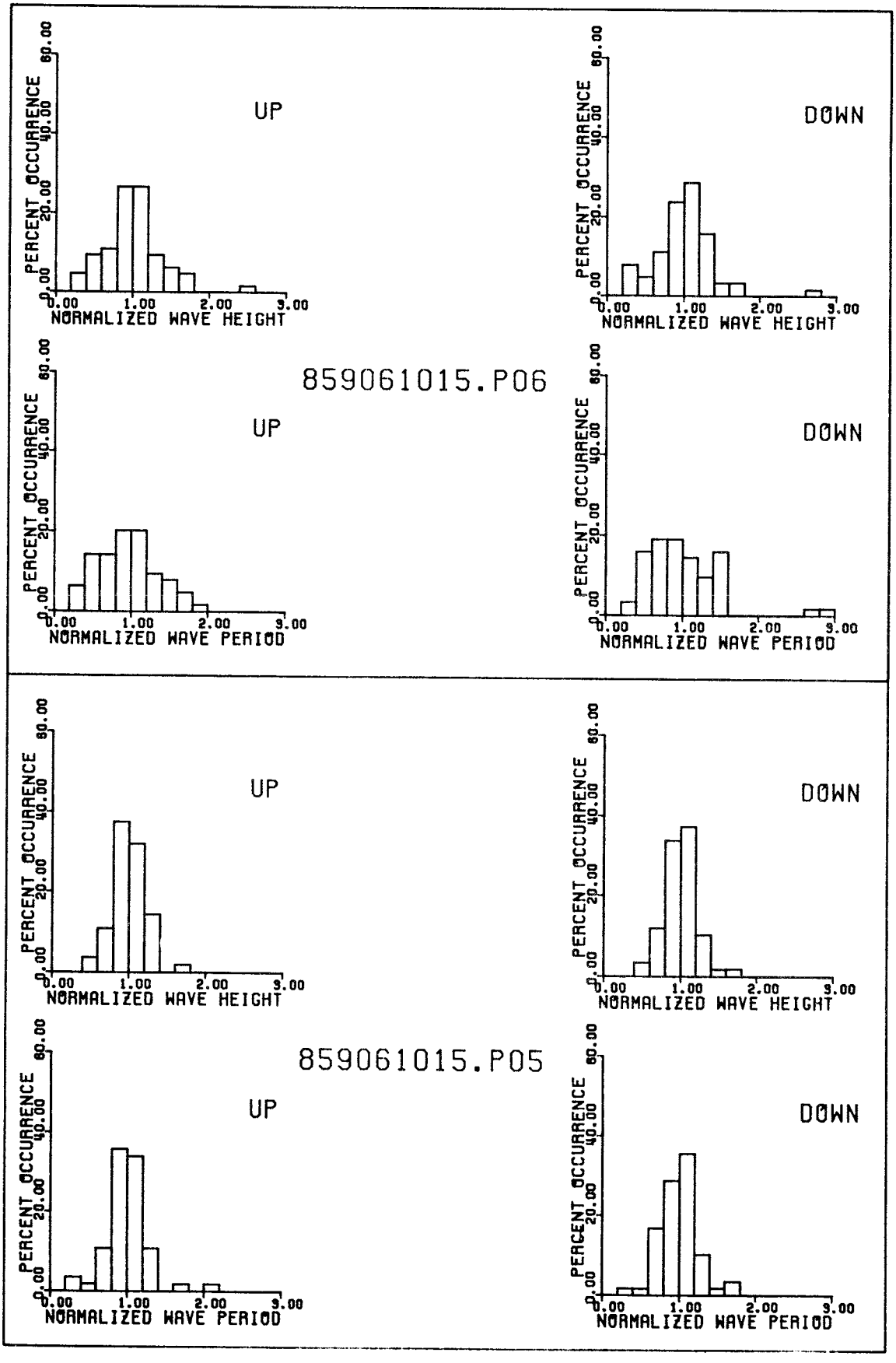
UP
DOWN
859061015.P06
UP
DOWN
859061015.P05
UP
DOWN
PERCENT OCCURRENCE
NORMALIZED WAVE HEIGHT
NORMALIZED WAVE PERIOD
0.00
20.00
40.00
60.00
1.00
2.00
3.00

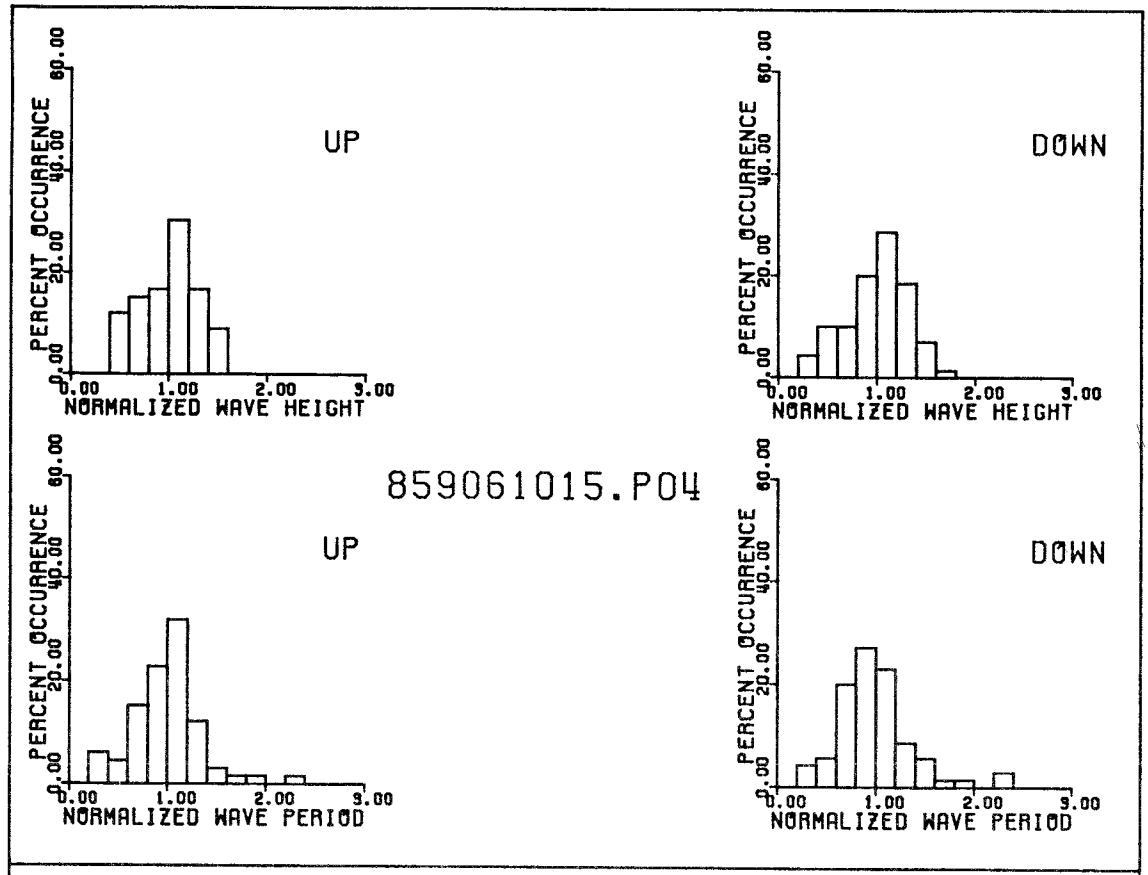
UP
DOWN
PERCENT OCCURRENCE
0.00
20.00
40.00
60.00
0.00
1.00
2.00
3.00
NORMALIZED WAVE HEIGHT
859061015.P04
UP
DOWN
NORMALIZED WAVE PERIOD

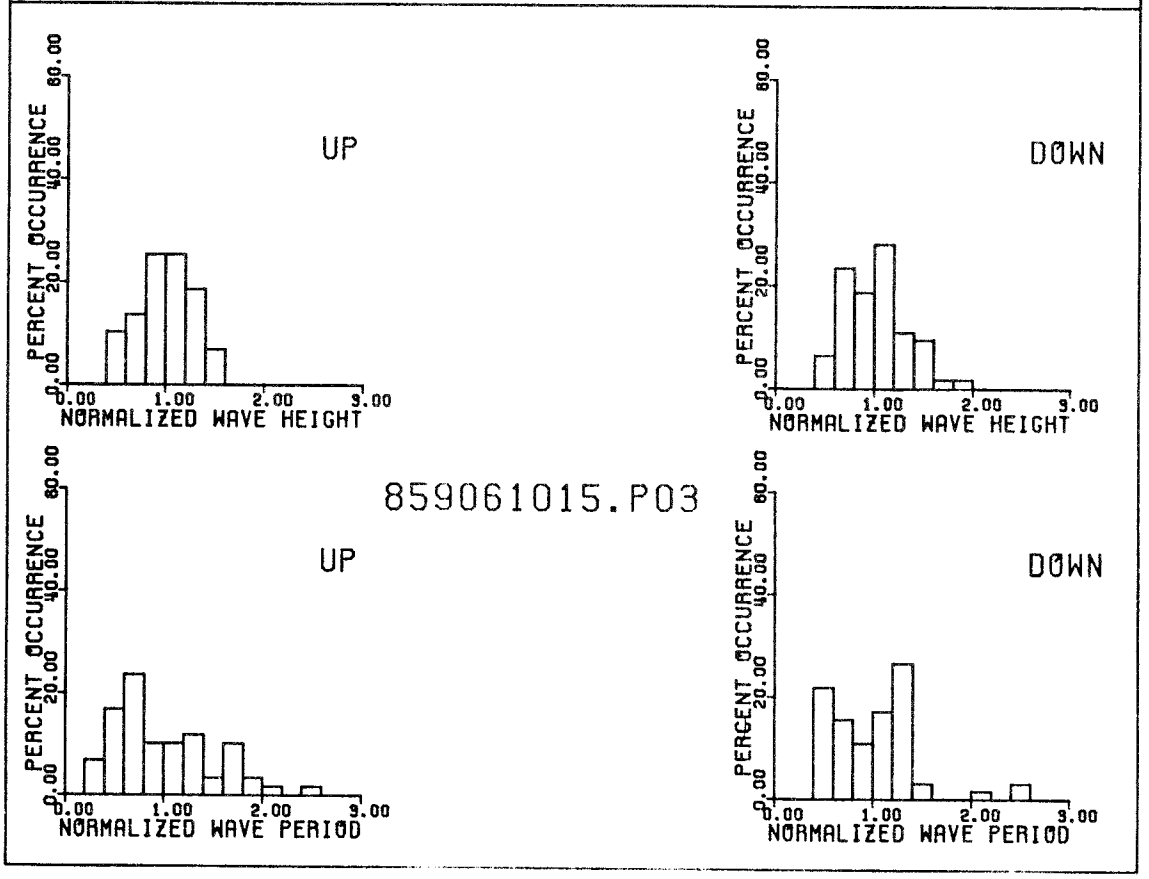
UP
DOWN
PERCENT OCCURRENCE
0.00
20.00
40.00
60.00
0.00
1.00
2.00
3.00
NORMALIZED WAVE HEIGHT
859061015.P03
UP
DOWN
NORMALIZED WAVE PERIOD

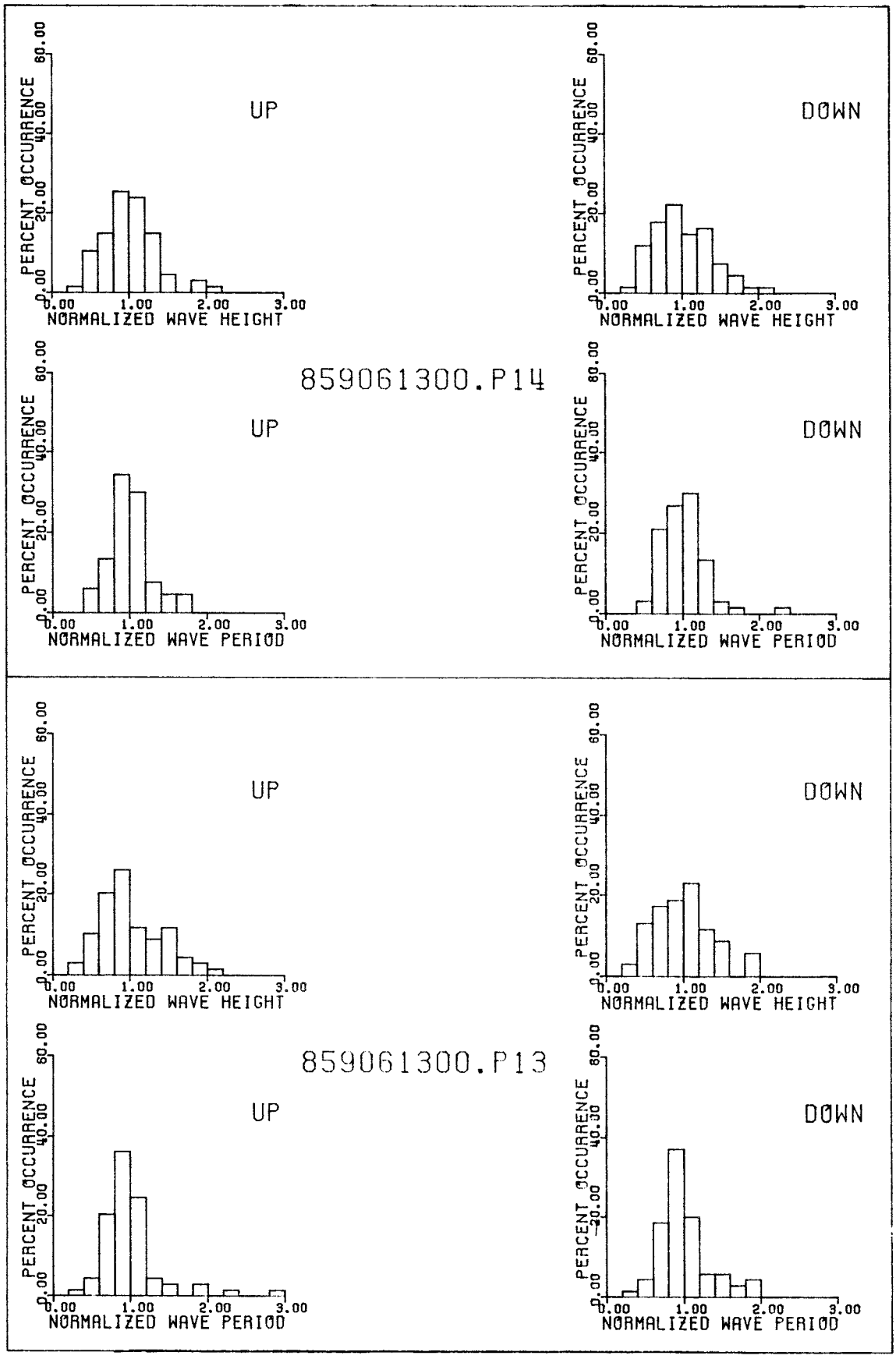
UP
DOWN
PERCENT OCCURRENCE
NORMALIZED WAVE HEIGHT
859061300.P14
UP
DOWN
PERCENT OCCURRENCE
NORMALIZED WAVE PERIOD
UP
DOWN
PERCENT OCCURRENCE
NORMALIZED WAVE HEIGHT
859061300.P13
UP
DOWN
PERCENT OCCURRENCE
NORMALIZED WAVE PERIOD

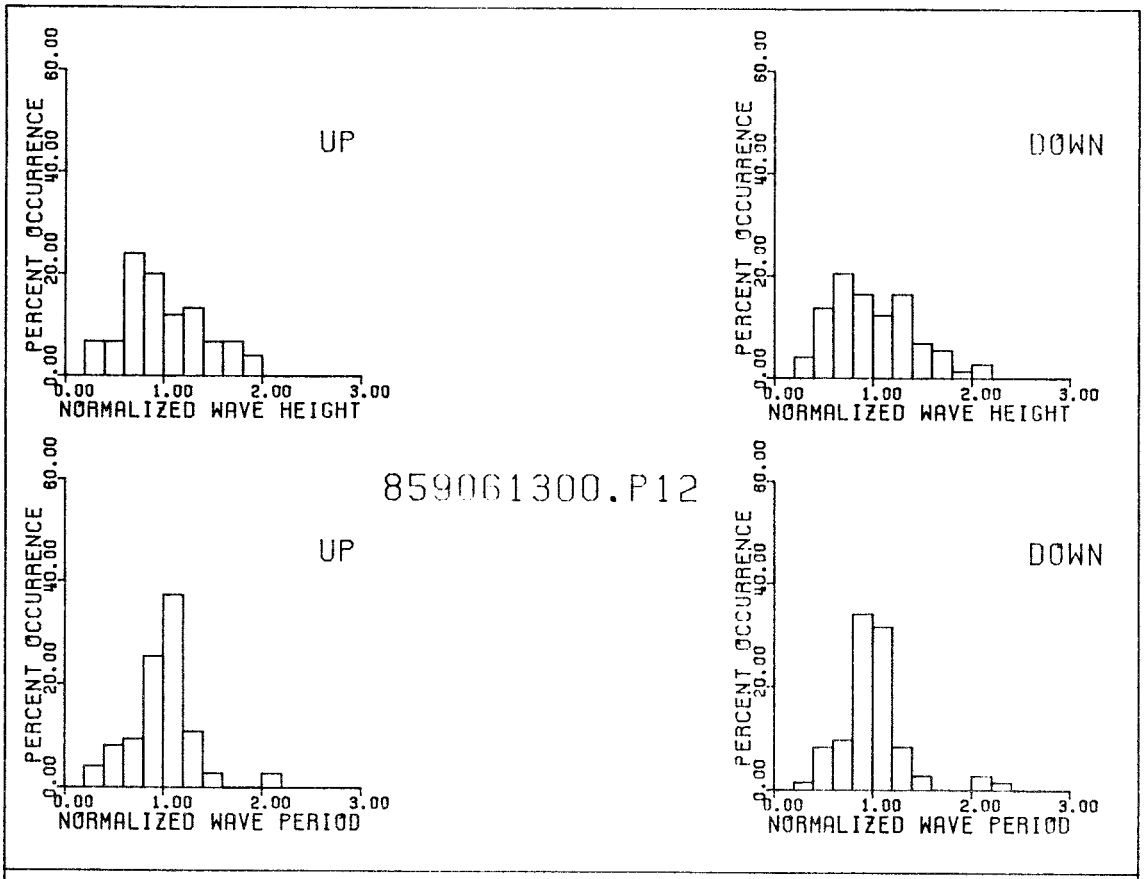
UP
DOWN
PERCENT OCCURRENCE
NORMALIZED WAVE HEIGHT
859061300.P12
UP
DOWN
PERCENT OCCURRENCE
NORMALIZED WAVE PERIOD

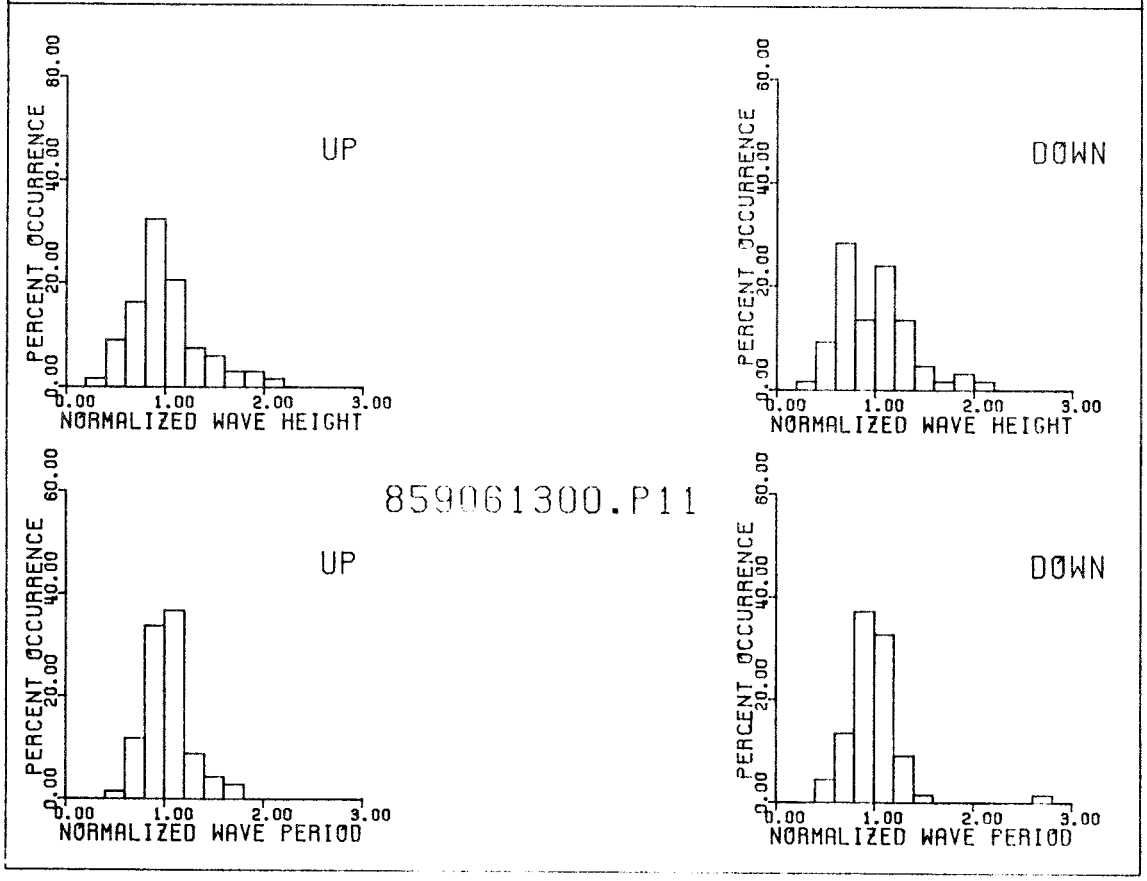
UP
DOWN
PERCENT OCCURRENCE
NORMALIZED WAVE HEIGHT
859061300.P11
UP
DOWN
PERCENT OCCURRENCE
NORMALIZED WAVE PERIOD

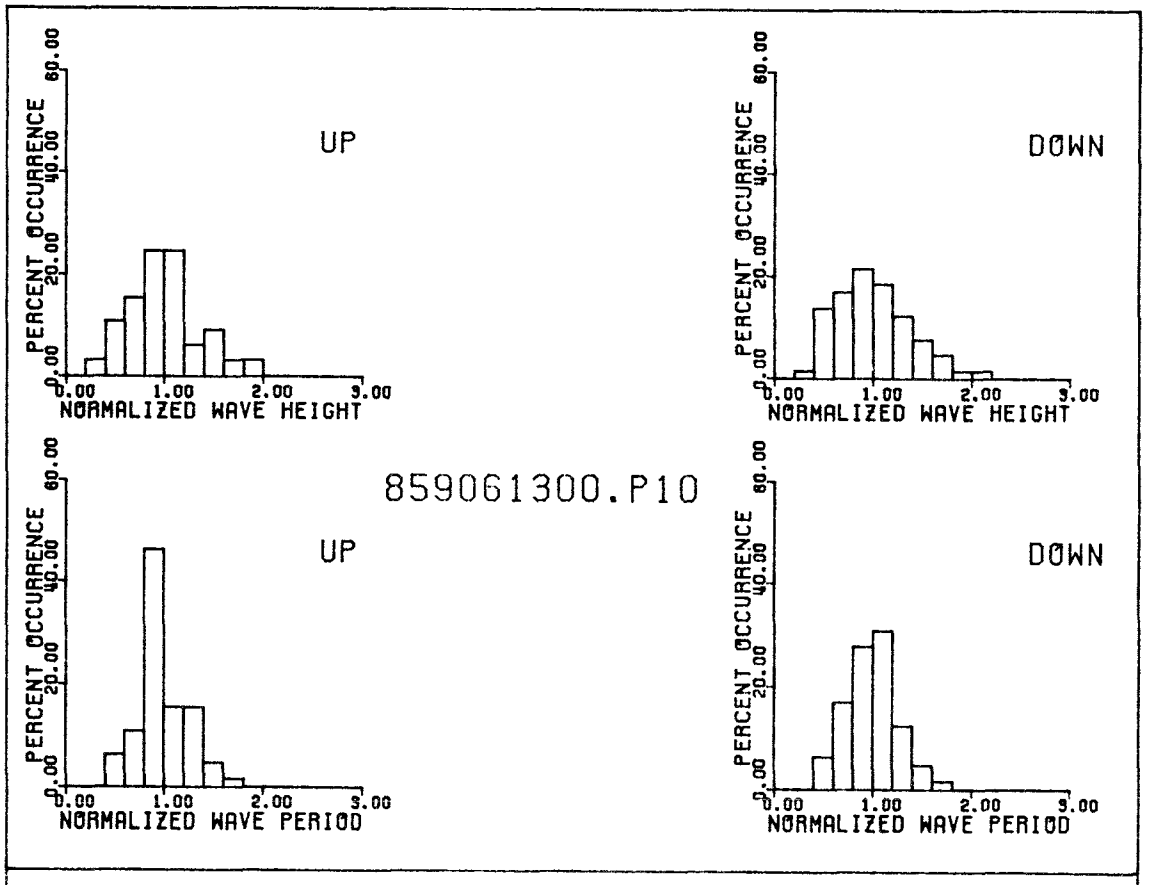
UP
DOWN
PERCENT OCCURRENCE
NORMALIZED WAVE HEIGHT
859061300.P10
UP
DOWN
PERCENT OCCURRENCE
NORMALIZED WAVE PERIOD

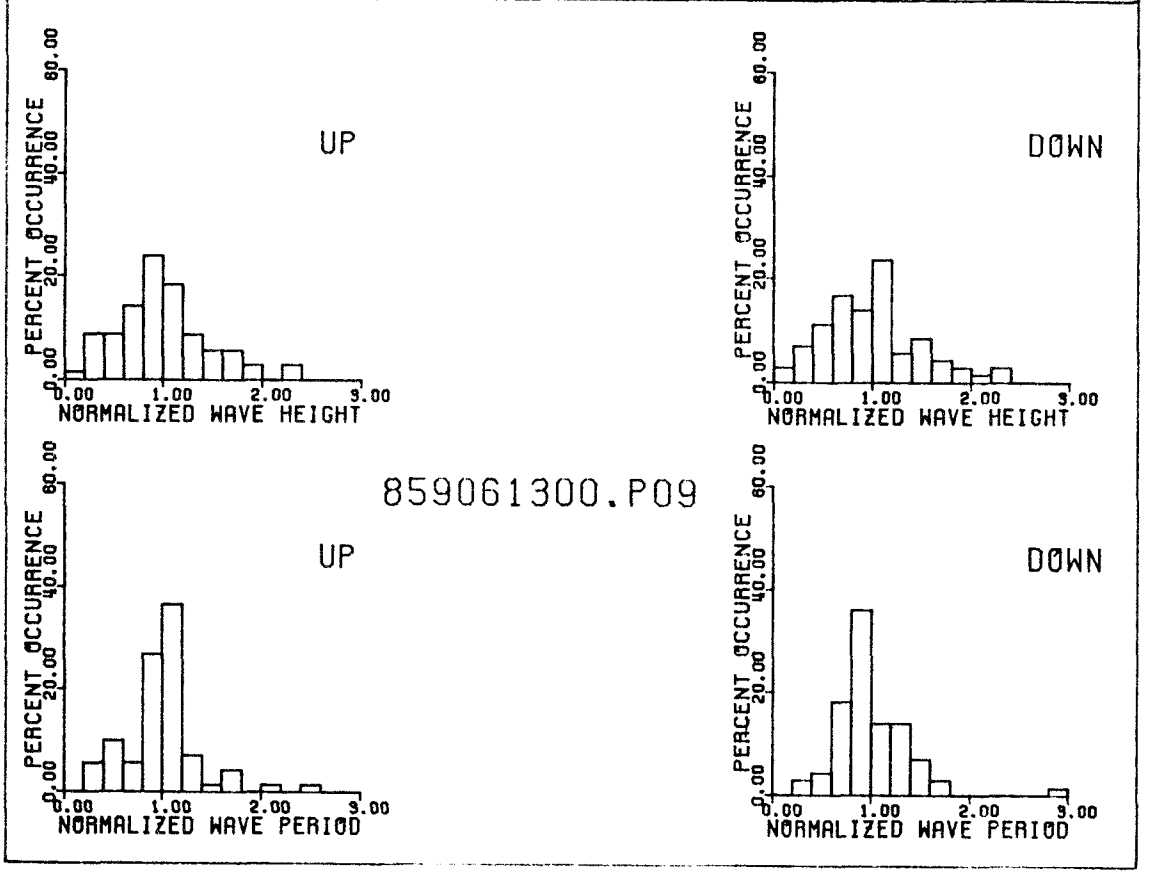
UP
DOWN
PERCENT OCCURRENCE
NORMALIZED WAVE HEIGHT
859061300.P09
UP
DOWN
PERCENT OCCURRENCE
NORMALIZED WAVE PERIOD

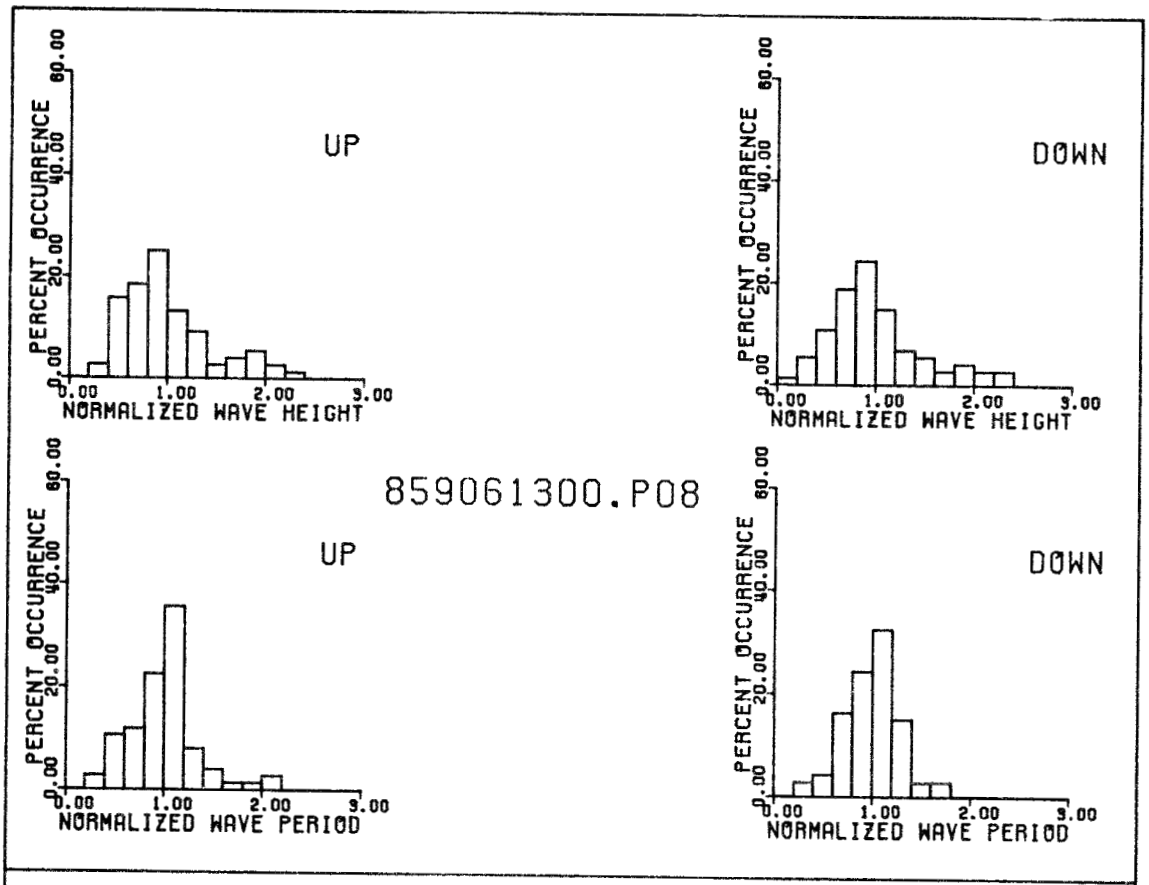
UP
DOWN
PERCENT OCCURRENCE
0.00
20.00
40.00
60.00
0.00
1.00
2.00
3.00
NORMALIZED WAVE HEIGHT
859061300.P08
UP
DOWN
NORMALIZED WAVE PERIOD

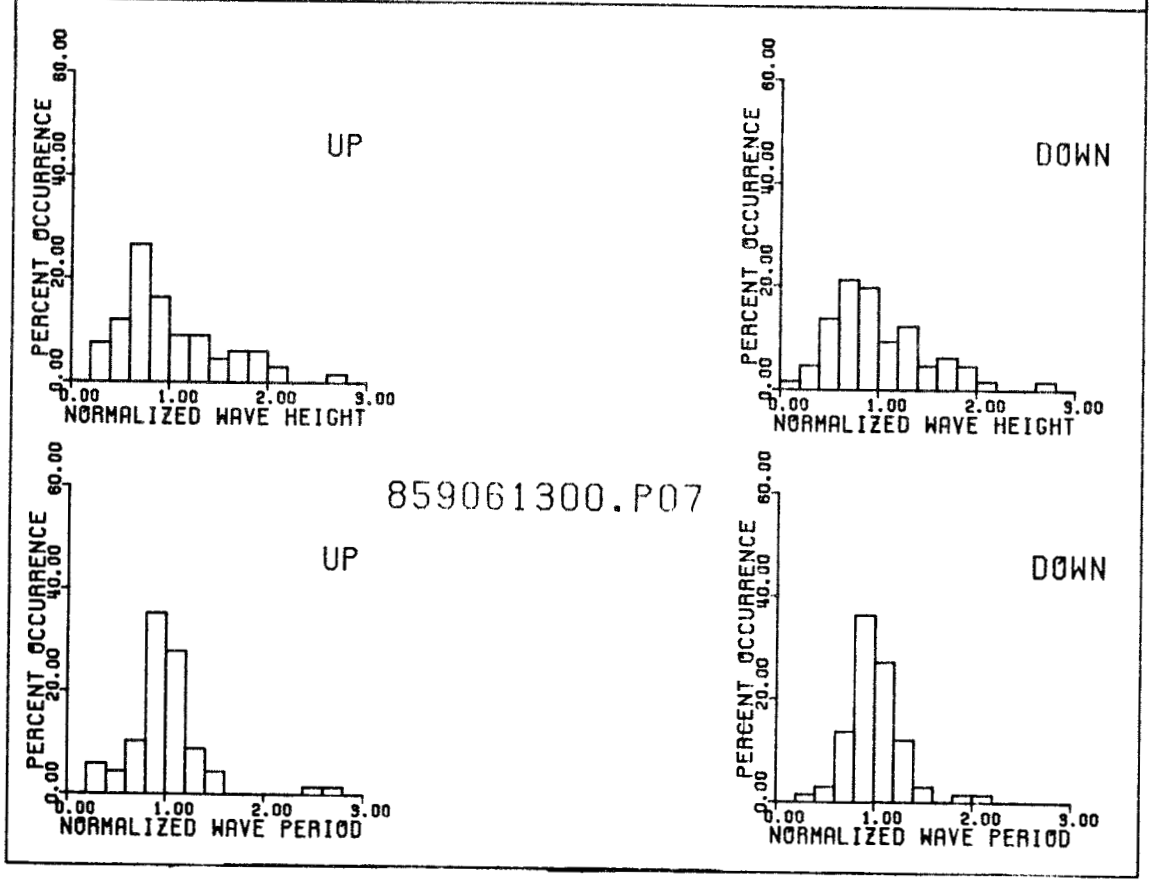
UP
DOWN
PERCENT OCCURRENCE
0.00
20.00
40.00
60.00
0.00
1.00
2.00
3.00
NORMALIZED WAVE HEIGHT
859061300.P07
UP
DOWN
NORMALIZED WAVE PERIOD

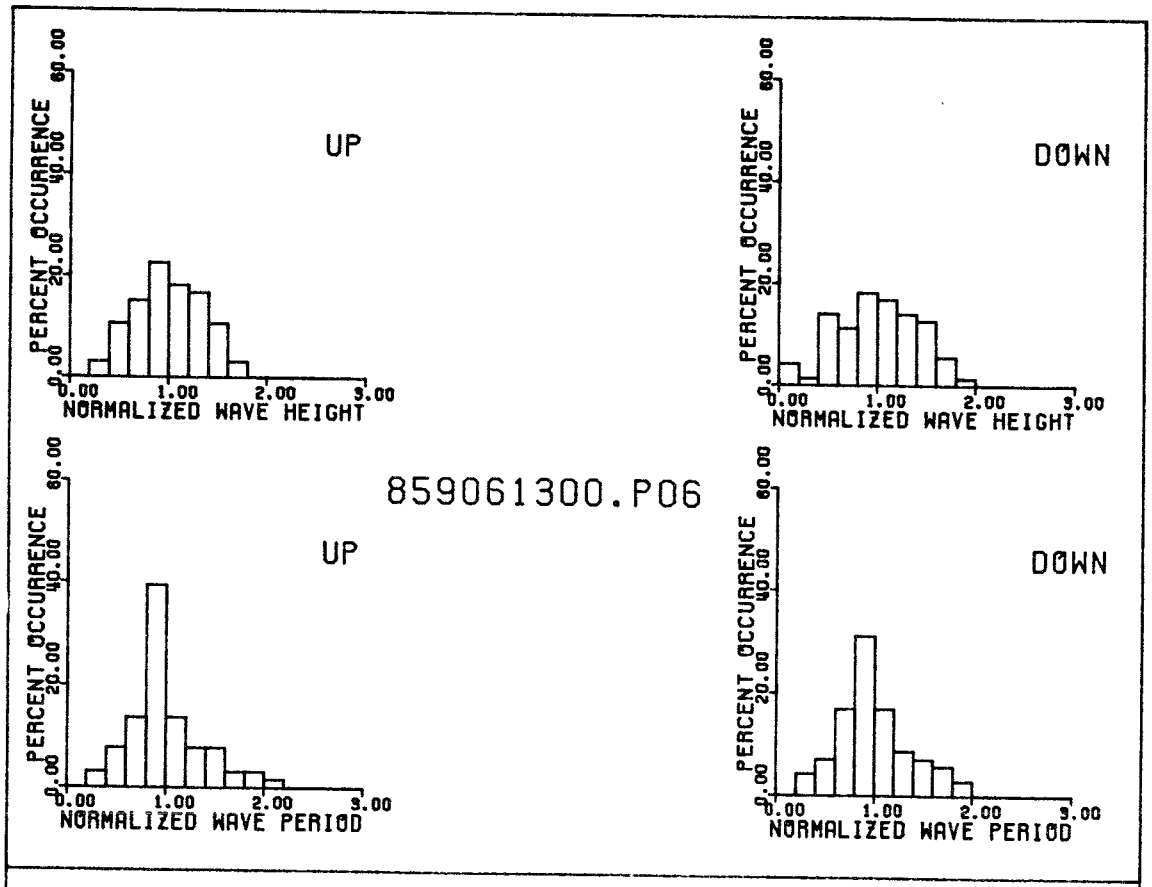
UP
DOWN
PERCENT OCCURRENCE
NORMALIZED WAVE HEIGHT
859061300.P06
UP
DOWN
PERCENT OCCURRENCE
NORMALIZED WAVE PERIOD

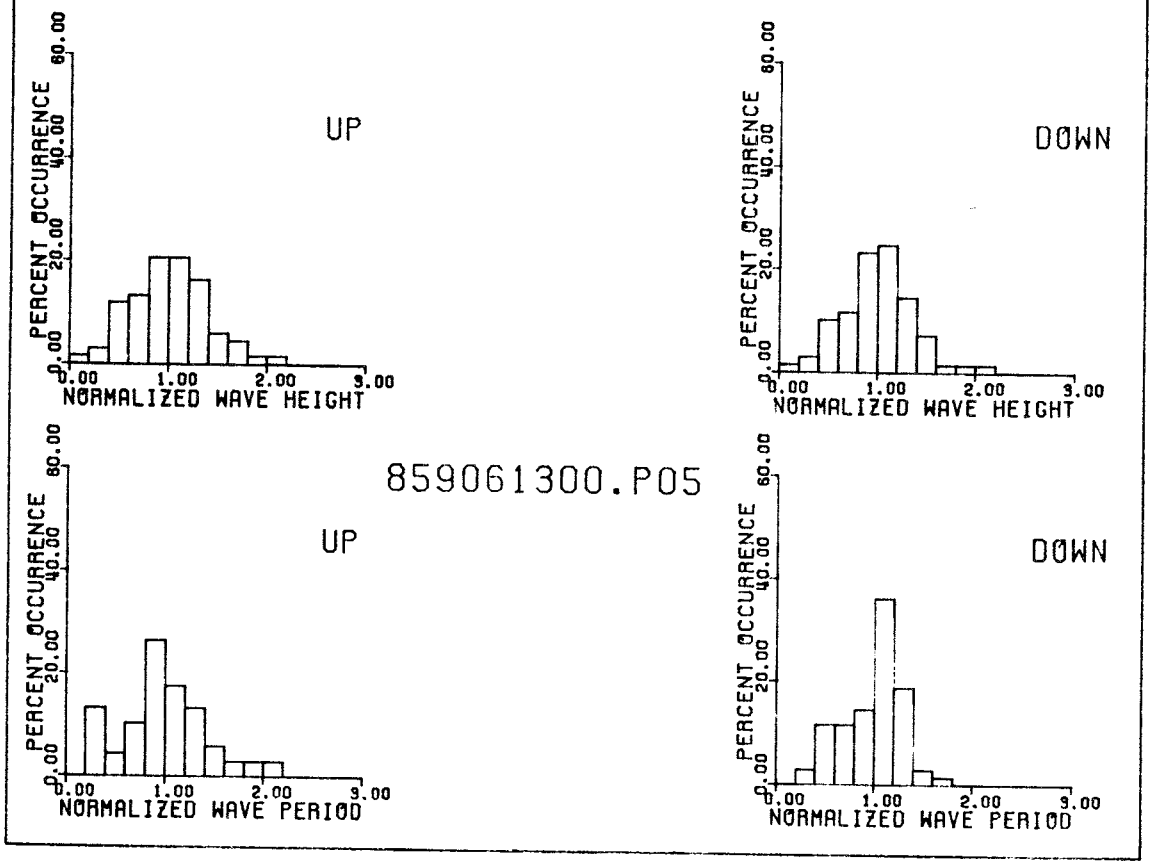
UP
DOWN
PERCENT OCCURRENCE
NORMALIZED WAVE HEIGHT
859061300.P05
UP
DOWN
PERCENT OCCURRENCE
NORMALIZED WAVE PERIOD

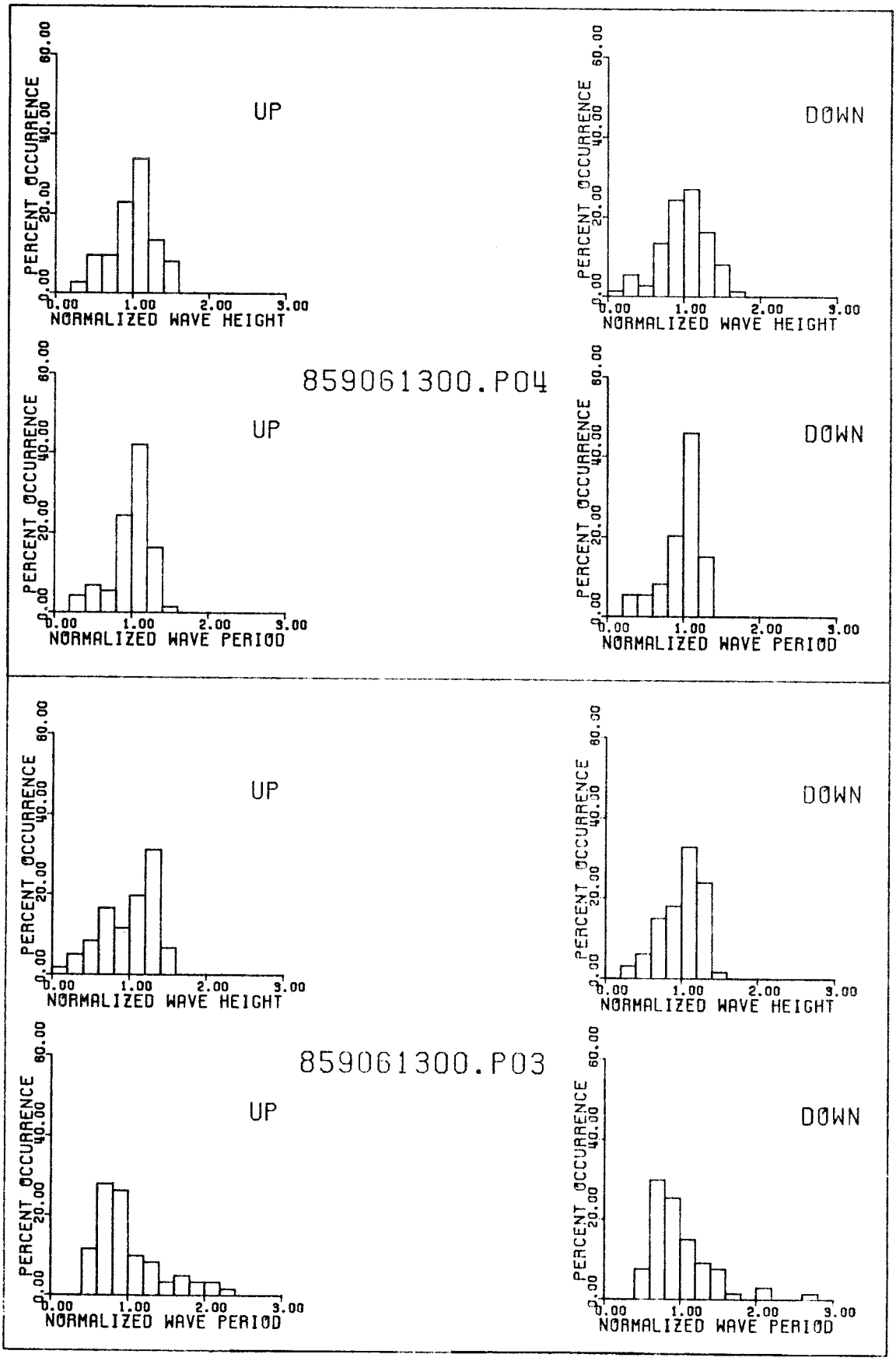
UP
DOWN
PERCENT OCCURRENCE
NORMALIZED WAVE HEIGHT
859061300.P04
UP
DOWN
PERCENT OCCURRENCE
NORMALIZED WAVE PERIOD
UP
DOWN
PERCENT OCCURRENCE
NORMALIZED WAVE HEIGHT
859061300.P03
UP
DOWN
PERCENT OCCURRENCE
NORMALIZED WAVE PERIOD